FRONTIERS OF PHYSICS

REVIEW ARTICLE
Volume 18 / Issue 4 / 44601 / 2023

Heavy flavour physics and CP violation at LHCb: A ten-year review

Shanzhen Chen[1], Yiming Li[1,†], Wenbin Qian[2], Zhihong Shen[3], Yuehong Xie[4], Zhenwei Yang[3], Liming Zhang[5], Yanxi Zhang[3]

1 Institute of High Energy Physics, Chinese Academy of Sciences, Beijing 100049, China
2 University of Chinese Academy of Sciences, Beijing 100049, China
3 State Key Laboratory of Nuclear Physics and Technology & School of Physics, Peking University, Beijing 100871, China
4 Key Laboratory of Quark and Lepton Physics of Ministry of Education & Institute of Particle Physics, Central China Normal University, Wuhan 430079, China
5 Department of Engineering Physics & Center for High Energy Physics, Tsinghua University, Beijing 100084, China
Corresponding author. E-mail: †liyiming@ihep.ac.cn
Received November 7, 2022; accepted December 8, 2022

ABSTRACT

Heavy flavour physics provides excellent opportunities to indirectly search for new physics at very high energy scales and to study hadron properties for deep understanding of the strong interaction. The LHCb experiment has been playing a leading role in the study of heavy flavour physics since the start of the LHC operations about ten years ago, and made a range of high-precision measurements and unexpected discoveries, which may have far-reaching implications on the field of particle physics. This review highlights a selection of the most influential physics results on CP violation, rare decays, and heavy flavour production and spectroscopy obtained by LHCb using the data collected during the first two operation periods of the LHC. The upgrade plan of LHCb and the physics prospects are also briefly discussed.

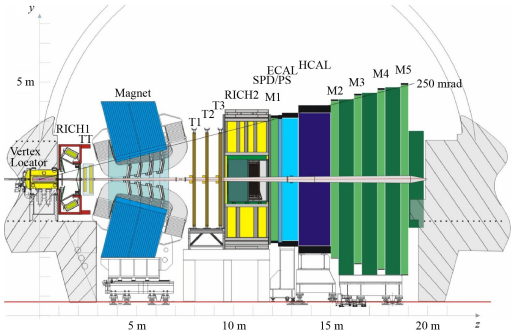

Keywords LHCb, flavour physics, CP vioation

Contents

Higher Education Press

arXiv: 2111.14360
https://doi.org/10.1007/s11467-022-1247-1

1 Introduction

With the discovery of the Higgs boson at the Large Hadron Collider (LHC) in 2012 [1–3], all fundamental particles expected in the Standard Model (SM) of particle physics are found and the SM is finally completed. The SM has achieved tremendous success in explaining experimental results in high-energy physics. However, there are still many key questions that are not answered in the SM, such as the mechanism to generate the matter-antimatter asymmetry in the Universe, the origin of the three generations of fermions and their mixing, and the nature of dark matter and dark energy. It is commonly believed that new physics (NP) beyond the SM should exist at or above the TeV energy scale. Flavour physics can provide a unique approach to indirectly probe NP at energy scales far above TeV via precision study of charge-parity (CP) violation and rare phenomena, complementary to the direct search for new particles and interactions at the energy frontier. Flavour physics also serves as a natural laboratory to test quantum chromodynamics (QCD), the theory of the strong interaction, via measurements of hadron production and spectroscopy. The Large Hadron Collider beauty (LHCb) experiment has been playing a leading role in the study of heavy-flavour physics since the start of the LHC, and has made a series of discoveries and improvements in CP violation, rare decays, and hadron production and spectroscopy. This review aims to present a selection of the high-impact physics results on the above subjects from the LHCb experiment, and to briefly discuss the prospects. Due to the limited space, not all interesting results can be covered here. For a complete list of all LHCb physics results, please refer to the official LHCb summary [4].

The LHCb detector [5] is optimised for the study of the decays of heavy-flavour hadrons, i.e., hadrons containing heavy quarks (b or c quarks, often collectively referred to as Q). In proton–proton (pp) collisions at LHC energies, the $b\bar{b}$ pairs are produced dominantly through the gluon fusion process $gg \to b\bar{b}$. Due to the large Lorentz boost along the proton beam in the laboratory frame, the b and $\bar{b}$ quarks generated in a pair are highly correlated in their momentum directions, either both in the forward region or both in the backward region in the majority of cases. In order to take advantage of this characteristic of the $b\bar{b}$ pair at the LHC, the LHCb detector is designed to have a forward geometry as shown in Fig. 1 to cover the forward region of pp collisions. The flavour of the b-hadron under study can usually be tagged by the other b-hadron that is also inside the LHCb acceptance. This enhances the potential of the LHCb experiment in the study of CP violation and mixing with B^0 and B_s^0 decays.

Excellent vertex and momentum resolution, particle identification etc. are key ingredients for flavour physics measurements at hadron colliders. A silicon vertex locator (VELO) surrounding the pp collision region is used to precisely determine the primary interaction vertices (PVs) and the displaced secondary/tertiary vertices (SVs/TVs) formed by the decay products of heavy-flavour hadrons. The VELO system offers decay time measurements with a typical resolution better than 50 fs, thus allows the LHCb experiment to make precision measurement of hadron lifetimes and resolve the fast B_s^0–$\bar{B}_s^0$ oscillation, which has a period of about 350 fs. The clear separation of SVs from PVs also allows for substantial suppression of the combinatorial background, which is extremely high in pp collisions. In addition to the VELO, the LHCb tracking system includes also four trackers, namely the TT and T1-T3 stations, located upstream and downstream of the dipole magnet, respectively. Together with a magnet that has a bending power of 4 Tm, the tracking system provides precise measurements of the momenta of charged particles. The momentum resolution ($\Delta p/p$) is typically 0.5% for low momentum tracks and 1.0% for track momentum up to 200 GeV/c. The mass resolution for b-hadrons can be as good as 8 MeV/c^2, precise enough to distinguish decays of B^0 and B_s^0 mesons to the same final state.

There are two ring-imaging Cherenkov detectors (RICH1 and RICH2) used to identify charged hadrons in the momentum range $p \in (2, 100)$ GeV/c. The RICH detectors are very powerful at suppressing misidentification background for b-hadron decays to final states containing charged kaons, pions or protons. The muon system provides excellent muon identification and is essential for reconstruction of decays with muons in the final states. The electromagnetic calorimeter is used for

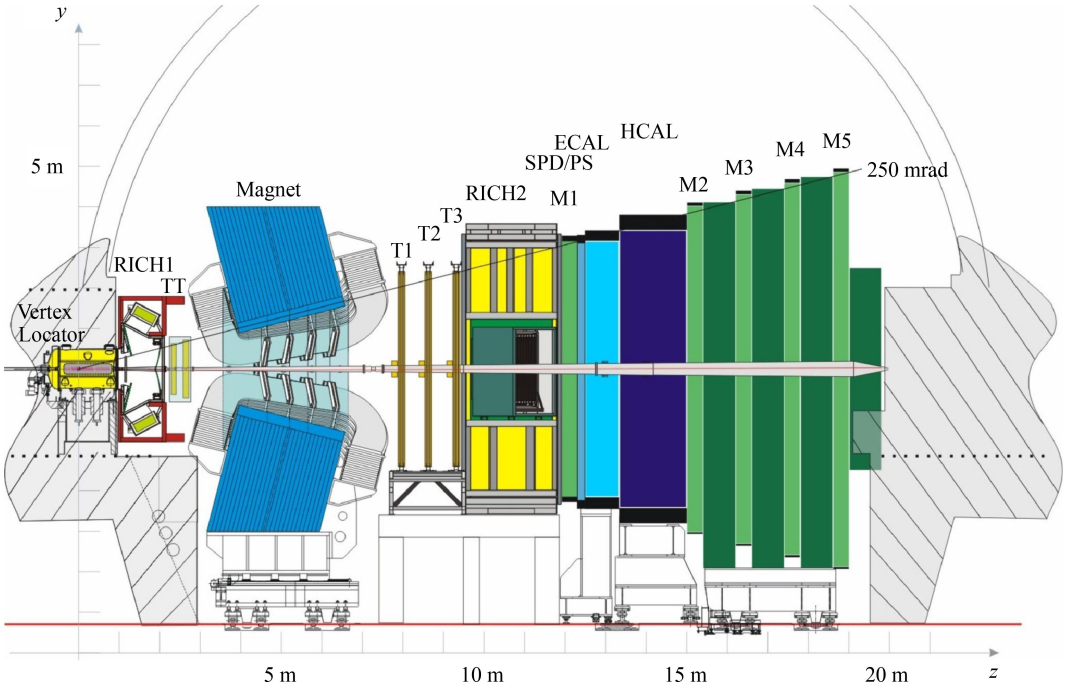

Fig. 1 Layout of the LHCb detector [5].

photon and electron reconstruction and identification. Together with the hadronic calorimeter, it also provides information for event trigger.

The trigger system is crucial for the success of the LHCb experiment. The hardware trigger at the first level reduces the data rate from 40 MHz down to 1 MHz, at which point the flexible software-based trigger takes over to further reduce the rate to around 12 kHz for offline processing and analysis. The ability to sustain such large rates enables the LHCb experiment to trigger with high efficiency on decay processes across a wide range of final states and to provide large data samples for study of exclusive rare decay modes as well as for inclusive data mining. Of particular importance is the LHCb muon trigger, which allows events containing one muon or two muons to be selected with greater than 95% efficiency. This is ideal for studying b-hadron decays to J/ψ or $\psi(2S)$ mesons that further decay to $\mu^+\mu^-$ pairs and semileptonic decays into muons. Meanwhile, there are also highly efficient triggers that are purely based on the multi-body topology of the final state hadrons. These triggers are important for reconstructing decays of heavy-quark hadrons to final states without muons.

The LHCb experiment collected a data sample corresponding to an integrated luminosity of 3 fb^{-1} in pp collisions at centre-of-mass energies $\sqrt{s} = 7$ and 8 TeV from 2011 to 2012 (Run 1), and another sample of 6 fb^{-1} at $\sqrt{s} = 13$ TeV from 2015 to 2018 (Run 2). Results discussed in this review are based on either full Run 1 and Run 2 data samples or a subset. Since the cross-sections for c- and b-quark production in pp collisions at 13 TeV are about twice of the cross-sections at 7 and 8 TeV [6–12], and the trigger scheme for Run 2 has also been improved compared with Run 1, the number of recorded charm and beauty decays available for physics analysis is more than four times higher in the Run 2 data than in Run 1 data. In total, more than 10^{11} b-hadrons and 10^{12} c-hadrons have been produced within the LHCb detector acceptance. The typical trigger and selection efficiencies are of the order of 10^{-3} to 10^{-2} for decays only to charged particles and 10^{-4} to 10^{-3} for decays to final states involving photons, π^0, Λ^0 or K^0_S particles. The enormous b- and c-hadron samples form the basis of precision measurements of CP violation, exploration of rare decays, and searches for new hadrons.

This review is structured as follows, with each section covering a different subject. Recent results of heavy-flavour production and spectroscopy are shown in Section 2. For heavy-flavour production, recent results of associated production and the studies in heavy-ion collisions are shown; for spectroscopy, the results of conventional hadrons and exotic hadrons are summarised. Section 3 discusses rare B-hadron decays. The results on purely leptonic B-meson decays, semileptonic $b\to s\ell^+\ell^-$ decays, and radiative $b\to s\gamma$ decays are shown.[1)] Some puzzling results in angular distributions and lepton flavour universality tests are discussed in details. Section 4 presents the latest results on CP violation in the beauty sector. Emphasis is put on the progresses that have been made for precision test of the Cabibbo–Kobayashi–Maskawa (CKM) mechanism, such

[1)] Charge conjugation is implied throughout unless stated otherwise.

as significant improvement in the determination of the parameters γ, β, β_s, V_{ub}, V_{cb}, and $\Delta m_{s/d}$. Section 5 provides recent results of CP violation in the charm sector, including those for charm mixing and the observation of CP violation in D^0 decays. The final section provides a picture of the LHCb upgrade, as well as a brief summary of the content in this review. The main goals and modifications to the detector in Upgrade I and Upgrade II are introduced, and the prospects of some key measurements are presented.

2 Heavy-flavour production and spectroscopy

Rich information on QCD dynamics can be deciphered from measurements of heavy-flavour production [13–49] and studies of heavy-flavour spectroscopy [50–71]. The mass of a heavy quark, which is much larger than the nonperturbative QCD scale $\Lambda_{\rm QCD}$, provides an energy scale that allows for perturbative calculation of heavy-quark production. The production of heavy quark pairs, $Q\overline{Q}$, is predominantly in the initial stage of the collision, thus can be used to probe properties of the colliding system and the possibly created QCD medium [72, 73]. The presence of heavy quark(s) also provides practical benefits for theoretical and experimental studies of spectroscopy. Heavy quarks are approximately nonrelativistic in hadrons, which makes it possible to simplify theoretical calculations. The large mass and the weak decay of heavy-flavour hadrons offer essential features, such as decay products with high transverse momentum, $p_{\rm T}$, and vertices displaced from the PVs, which can be exploited to reject the huge QCD background at hadron colliders.

As discussed in Section 1, the excellent performance of the LHCb detector, owing to the dedicated design for heavy-flavour hadrons, enables LHCb to make great achievements in the study of heavy-flavour production and spectroscopy, e.g., the observation of pentaquark states and the doubly charmed baryon Ξ_{cc}^{++}. In this section, relevant results from the LHCb experiment are reviewed, with a focus on recent developments.

2.1 Production

A summary of LHCb production measurements for open heavy-flavour hadrons, heavy quarkonia and pairs of heavy-flavour hadrons at LHCb [7, 9–11, 74–119] are listed in Table 1. Inclusive hadroproduction of open heavy-flavour hadrons (H_Q) factorises into three components in perturbative QCD (pQCD) calculations: the parton distribution function (PDF) in the two initial projectiles $f_{i,j}$, the parton level cross-section $\sigma_{ij\to Q+X}$ of a heavy-quark Q production, and the heavy-quark fragmentation function $D_{Q\to H_Q}$ [120]. Differential cross-section for H_Q production in A–B collisions is expressed as

$$\mathrm{d}\sigma_{AB\to H_Q} = \sum_{i,j}(f_i^A \otimes f_j^B) \otimes \mathrm{d}\sigma_{ij\to Q+X} \otimes D_{Q\to H_Q}, \tag{1}$$

where the indices i, j run over all possible parton species, and at LHC energies heavy-flavour production is dominated by gluons. The PDF and fragmentation function include nonperturbative effects, and can be determined from a global fit of available data [14, 120]. The results of open charm and beauty production at LHCb are consistent with pQCD models, for example the calculation based on fixed-order plus next-to-leading logs (FONLL) [121]. It turns out that the LHCb results on charm and beauty cross-sections have a better precision than theoretical calculations [11, 100, 105], and can be used to reduce the uncertainties on gluon PDF, in particular in the small Bjorken-x region, $x \lesssim 10^{-5}$ [122].

For quarkonium production, assumptions have to be put on how heavy-quark pairs, $Q\overline{Q}$, produced with various possible colour, spin and parity configurations, transform into specific colourless quarkonia [127–130]. Cross-section measurements favour calculations using the

Table 1 LHCb measurements of production cross-sections (or ratios) for various heavy hadrons in pp and pPb collisions at different centre-of-mass energies.

System	$\sqrt{s_{(NN)}}$ [TeV]			
	5 (2.76)	7	8 (8.16)	13
pp	J/ψ [84], Υ [88], D [100]	η_c [91], J/ψ [7], $\chi_{c1}(3872)$ [78], $\chi_c/J/\psi$ [77], χ_{c2}/χ_{c1} [76, 86], $\psi(2S)$ [81, 111], Υ [79, 97], χ_{b2}/χ_{b1} [92, 93], D, Λ_c^+ [9], B [80, 85, 105, 117], Λ_b^0 [89, 96], Ξ_b [109], B_c^+ [83], $J/\psi J/\psi$ [75], ΥD [98], $J/\psi D, DD, D\overline{D}^0$ [82]	η_c [91], J/ψ [95], χ_{b2}/χ_{b1} [92, 93], $\chi_{c1}(3872)/\psi(2S)$ [116], $\chi_{c1}(3872)$ [119], Υ [95, 97], B_s^0/B^0 [117], Λ_b^0 [96], Ξ_b [109], ΥD [98], B_c^+ [94]	η_c [112], J/ψ [10, 102], $\chi_{c1}(3872)$ [119], $\psi(2S)$ [111], Υ [106], D [11], Ξ_{cc}^{++} [114], B^+ [105], Ξ_b [109], B_c^+ [113], B_s^0/B^0 [117], $J/\psi J/\psi$ [101]
pPb	J/ψ [87], $\psi(2S)$ [99], Υ [90], D^0 [104], Λ_c^+ [107]		J/ψ [103], Υ [108], D^0 [74], B^+, B^0, Λ_b^0 [110], χ_{c2}/χ_{c1} [118], $DD, D\overline{D}^0$ [115]	

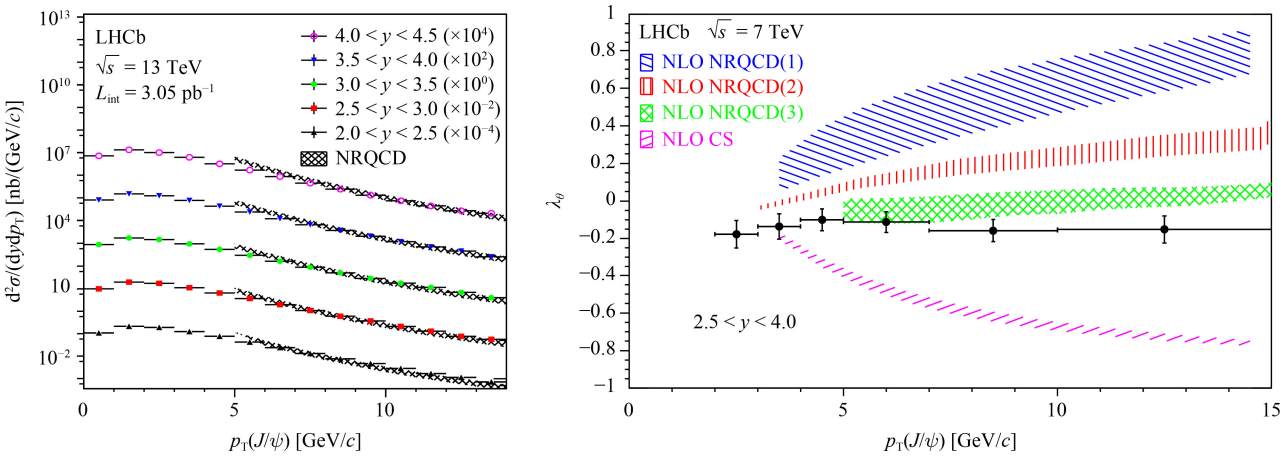

Fig. 2 (Left) Differential cross-section of J/ψ in pp collisions at $\sqrt{s} = 13$ TeV, reproduced from Ref. [10]. (Right) J/ψ polarisation in pp collisions at $\sqrt{s} = 7$ TeV, reproduced from Ref. [123]. The measurements are compared with NRQCD [124–126] and colour singlet calculations [125].

nonrelativistic QCD (NRQCD) framework [131], as shown on the left of Fig. 2, for J/ψ production in pp collisions at $\sqrt{s} = 13$ TeV. The NRQCD framework introduces long distance matrix elements (LDMEs) as model parameters [132] to account for transition probabilities from heavy-quark pairs to quarkonia. LDMEs are assumed to be independent of quarkonium production environments and kinematics, and are fixed by matching the predicted p_T spectrum to data. The polarisation of heavy quarkonia is another observable sensitive to the $Q\overline{Q}$ production mechanism and LDMEs. Inconsistencies are observed between LHCb data and theoretical calculations on the ψ and Υ polarisations [123, 133, 134]. Only a level of 10% or smaller polarisation is observed in the LHCb acceptance, in contrast to a dominant transverse polarisation predicted by NRQCD [124–126]. The measurement of J/ψ polarisation is shown on the right of Fig. 2. Even though the discrepancy can be reduced by tuning the LDMEs, a coherent description of production cross-section and polarisation is still a difficult theoretical problem [26, 31, 126, 135–140]. If only the $Q\overline{Q}$ state that has the same quantum number as the final quarkonium is considered, the NRQCD framework reduces to the colour singlet model, which underestimates production cross-sections [125] and disagrees with data on ψ and Υ polarisations [123, 133, 134].

2.1.1 Associated production

Recent LHCb production measurements focus on associated production of multiple heavy flavours and quantities probing properties of QCD matter. Associated heavy-flavour production provides an approach to study the multiple parton interactions (MPIs). MPIs are sensitive to correlations between partons in space, momentum, flavour, colour, spin etc. inside the colliding projectiles [141–146]. Usually in an MPI process these correlations are assumed to be absent initially such that each parton-scattering is independent from each other, and then consistency checks are performed to verify this assumption. Under this assumption, the cross-section for associated production of ab through a double-parton-scattering (DPS) process is related to the single inclusive production of a and b as [141]

$$\sigma^{ab} = \kappa \frac{\sigma^a \sigma^b}{\sigma_{\text{eff}}}, \tag{2}$$

where κ is a symmetry factor with $\kappa = 1$ if $a \neq b$ and the effective cross-section σ_{eff} is assumed to be universal. Heavy-quark fragmentations in MPIs are implied to be identical to that in inclusive production defined in Eq. (2). In particular, the kinematics of a and b is uncorrelated and each of them is similar to that in single particle inclusive production. Besides MPI, the single parton scattering (SPS) is also able to generate associated production, but in SPS the final-state kinematics is correlated. This difference between DPS and SPS is used to identify DPS. Studies of DPS include measurements of the σ_{eff} parameter and tests of its universality for different states, and investigations of kinematic correlations between a and b. One example of correlation variables is the relative azimuthal angle $\Delta\phi$ between a and b and to infer the correlations between colliding partons. For DPS production $\Delta\phi$ distribution is approximately flat, while in SPS events a concentration at $\Delta\phi \sim 0$ or π is expected.

Measurements of associated production in pp collisions are made at LHCb for two open charm hadrons [82], a heavy quarkonium plus an open charm [82, 98], and double J/ψ mesons [101]. To subtract the SPS contribution from data, one usually relies on theoretical inputs for cross-sections of SPS or fits to data using templates of correlation variables built for both SPS and DPS production. Note that theoretical uncertainties are still

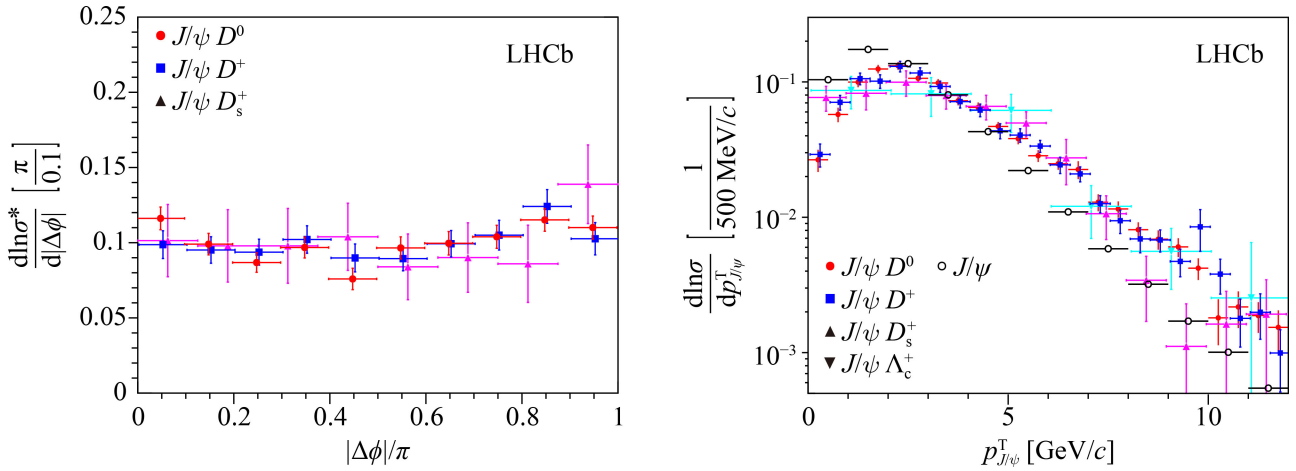

Fig. 3 (Left) Distribution of relative azimuthal angle, $\Delta\phi$, between J/ψ and D mesons in pair production, showing flat behaviour. (Right) the p_T distribution of J/ψ mesons in $J/\psi D$ pair production, compared with that in inclusive production (shown in black open circle) [7]. Reproduced from Ref. [82].

much larger than experimental ones for these measurements.

For some associated production, SPS is estimated or assumed to be negligible, resulting in a sample of approximately pure DPS events. In this case the $\sigma_{\rm eff}$ parameter measured using Eq. (2) is around 15 mb for $J/\psi D$ and ΥD production, independent of the D species and collision centre-of-mass energies [82, 98]. The results are similar to those extracted using multi-jet production at Tevatron [147]. However, the values obtained using same-sign DD pairs are around 20 mb, and that for $J/\psi J/\psi$ pairs is about 7 mb [101]. The former are consistently higher than the value of 15 mb [82], while the latter is significantly lower. Higher values of $\sigma_{\rm eff}$ for $J/\psi J/\psi$ production are obtained if a fraction of SPS is subtracted. The SPS fraction is estimated to be between 20% and 40% depending on the choice of control variables and input templates for SPS and DPS distributions [101]. The smaller $\sigma_{\rm eff}$ measurement for $J/\psi J/\psi$ pairs confirms previous observations by D0, CMS and ATLAS experiments for quarkonium pairs [148–150].

For correlation variables, as shown on the left of Fig. 3, the $\Delta\phi$ distributions of $J/\psi D$ events are reasonably flat [82], consistent with the DPS production in which J/ψ and D kinematics is uncorrelated. This observation is a sign of dominant or pure DPS contribution for $J/\psi D$ samples. For same-sign DD production, the correlation variables also favour DPS dominance [82].

The p_T distribution of each hadron in the pair production is also studied. For DPS events, it is expected to be similar to that in single inclusive production. For ΥD samples, both the Υ and the D meson have a p_T distribution similar to that in single inclusive production [98]. The same conclusion holds for the p_T distribution of D mesons in $J/\psi D$ events. However, the p_T of J/ψ mesons in $J/\psi D$ events is significantly harder than that in inclusive production, indicated by the right of Fig. 3. For the same-sign DD production, the p_T distribution of D mesons is also significantly harder than that in single inclusive D production, but are similar to those in opposite-sign $D\bar{D}^0$ samples [82]. This result is inconsistent with the observation in correlation variables, which hints at a dominant DPS (SPS) contribution in the same-sign (opposite-sign) pair production. Note that for associated production of DD pairs, the p_T distribution of D mesons is similar for different D species, indicating that charm hadron fragmentations are not modified, so that the unexpected p_T distribution is not due to the fragmentation process. A detailed theoretical calculation on $J/\psi D$ production was performed recently to understand the problem, but a solid conclusion is not available yet [146].

2.1.2 Production in pPb collisions

Charm pair production is also studied in pPb collisions of a center-of-mass energy per nucleon pair $\sqrt{s_{\rm NN}} = 8.16$ TeV [115]. The DPS cross-section in pPb collisions is expected to scale with three times of the Pb mass number ($A_{\rm Pb} = 208$) with respect to that in pp data at the same $\sqrt{s_{\rm NN}}$, rather than a simple scale factor of $A_{\rm Pb}$, when nuclear matter effects are not considered [151]. The A-scaling is relevant for SPS production in the absence of nuclear matter effects [151]. In the end DPS production has a factor of three enhancement compared with SPS. The cross-section ratio between same-sign DD and opposite-sign $D\overline{D}$ signals is measured to be around three times of that in pp collisions [115]. The result is in favour of the expected factor-three enhancement. The parameter $\sigma_{\rm eff}$ is measured with $J/\psi D$ and same-sign DD production as shown on the left of Fig. 4, for the positive rapidity region, which corresponds to the Pb-beam

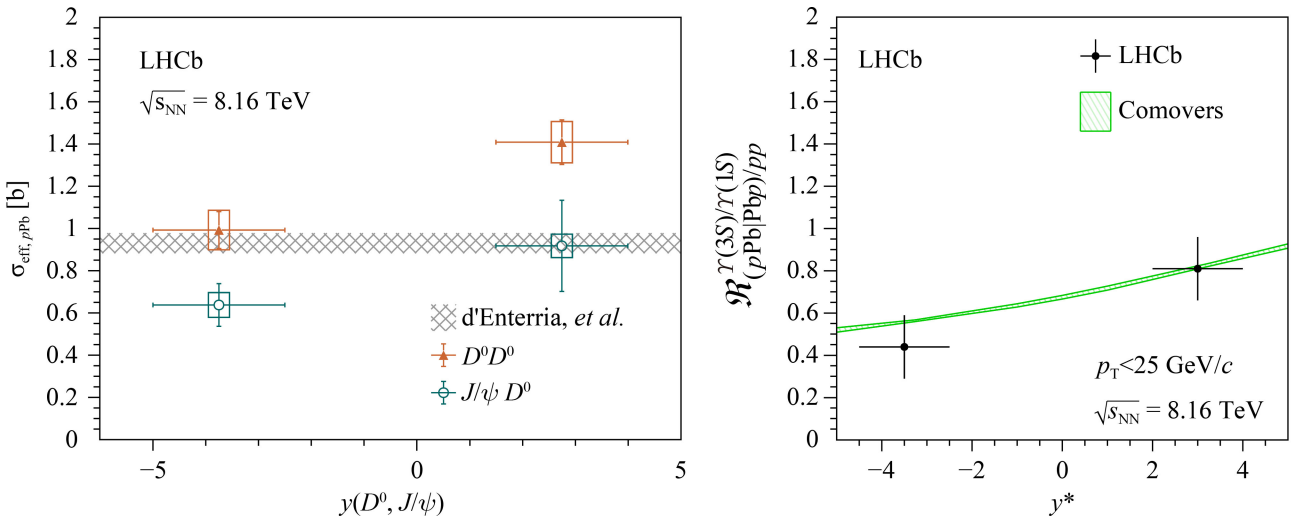

Fig. 4 (Left) The parameter $\sigma_{\rm eff}$ measured in pPb collisions at $\sqrt{s_{\rm NN}} = 8.16$ TeV using (green) $J/\psi D^0$ and (brown) D^0D^0 production for (positive rapidity) p beam and (negative rapidity) Pb-beam direction, reproduced from Ref. [115]. The prediction shown in shaded area is from Ref. [152]. (Right) The ratio of cross-sections between $\Upsilon(3S)$ and $\Upsilon(1S)$ over that in pp data at $\sqrt{s_{\rm NN}} = 8$ TeV, reproduced from Ref. [108], is compared with the comovers model [153]. The rapidities are defined in the rest frame of two colliding nucleons with respect to proton-beam direction.

direction (high Bjorken-x of Pb nucleus), and the negative rapidity region, which corresponds to the p-beam direction (low Bjorken-x of Pb nucleus). The measurements show that, similar to the results in pp data, the $\sigma_{\rm eff}$ parameter for $J/\psi D$ production is about 30% smaller than that for same-sign DD production. Besides, the results in negative rapidity hint at smaller values than those in positive rapidity for both $J/\psi D$ and DD pair production. It may be a sign of universality violation of $\sigma_{\rm eff}$. This will be explored with better precision in Run 3 heavy-ion collision data, where ten times more luminosity is expected to be collected.

Besides the enhancement of DPS production, heavy nuclear collisions have many more new phenomena compared with pp collisions, collectively called nuclear matter effects. Presence of nuclear matter effects in pPb collisions could modify the PDF, or reduce parton energies or dissociate heavy quarkonia, which can be probed using heavy-flavour production in pPb data compared with the $A_{\rm Pb}$ scaled pp cross-section [154–156]. Measurements of D^0 and B^+ production in pPb data suggest heavy-quark production in the p-beam direction is significantly suppressed compared with the $A_{\rm Pb}$ scaling, by about 30%, while the production in Pb-beam direction approximately scales with $A_{\rm Pb}$ [104, 110]. The results are consistent with modifications of the gluon PDF in a Pb nucleus compared with that in a free nucleon. The LHCb measurements are found to be able to reduce the gluon PDF uncertainties in the Pb nucleus by about a factor of three compared with the commonly used nuclear PDF sets [157]. A new precise measurement of D^0 production in pPb shows that the magnitude of the D^0 suppression in p beam direction over that in Pb-beam direction, i.e., the forward-backward ratio $R_{\rm FB}$, increases significantly at high $p_{\rm T}(D^0)$ and seems to reach unity at $p_{\rm T}(D^0) > 8$ GeV/c [74]. However according to predictions using the nuclear PDF, the $R_{\rm FB}$ is about 70%, almost independent of $p_{\rm T}(D^0)$. The observed trend of $R_{\rm FB}$ for D^0 may be caused by the parton energy loss effect which alters heavy-flavour kinematic distribution, whose impact is reduced at high $p_{\rm T}$ [158], otherwise the result will require a modification of current knowledge of the nuclear PDF.

Measurement of J/ψ production in pPb data shows a similar trend of suppression compared with open heavy-flavour hadrons [87, 103], suggesting that they suffer from a common influence by nuclear matter effects. However, the result for $\psi(2S)$ in pPb data suggests a stronger suppression compared with J/ψ, in particularly in the Pb-beam direction [99]. Similarly, the $\Upsilon(3S)$ meson is measured to be more suppressed compared with $\Upsilon(1S)$ [108], as shown on the right of Fig. 4. The stronger suppression for excited quarkonium cannot be explained using the nuclear PDF modification or the parton energy loss effect. The comover model introducing final state interactions between a heavy quarkonium and comoving particles is able to explain data [153]. The comovers effect is stronger in events of higher occupancy and for particles with larger sizes, such that it is more pronounced in Pb-beam direction and for excited states, reducing their yields more significantly than for the ground state in the p-beam direction $A_{\rm Pb}$. The comovers mechanism also exists in pp collisions, and is probed using heavy quarkonium production. The cross-section ratio between prompt $\chi_{c1}(3872)$ and $\psi(2S)$ mesons is measured to decrease with the increase of the number of

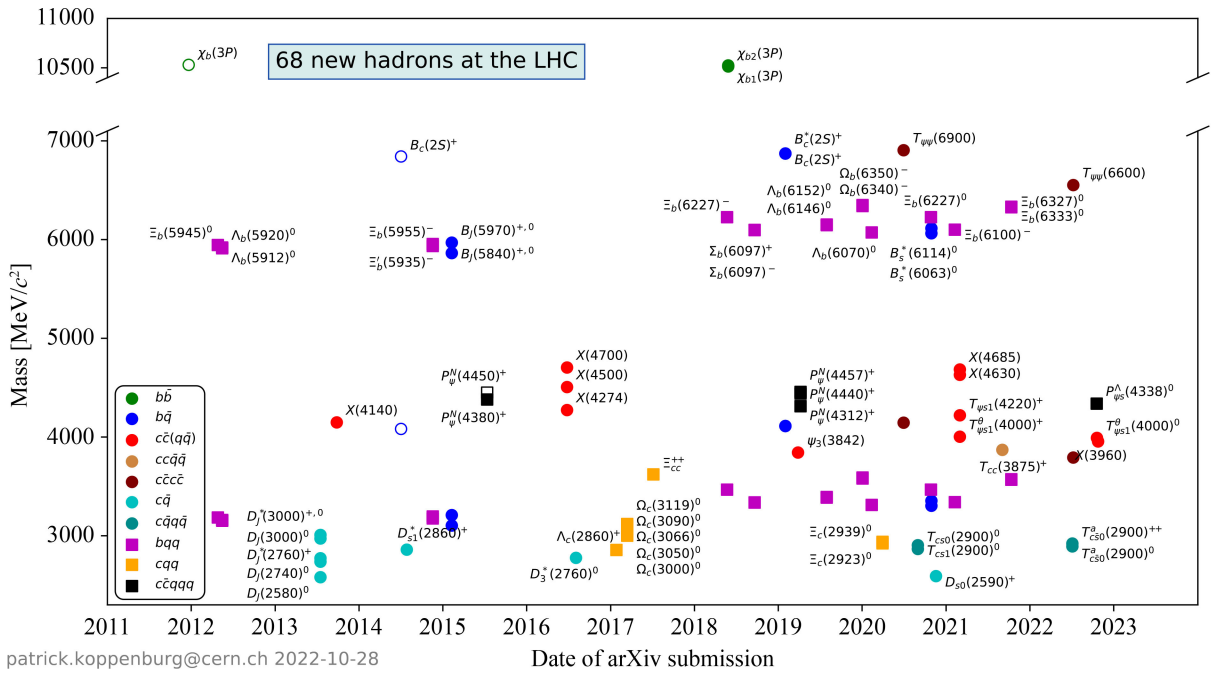

Fig. 5 New hadrons that are discovered by the LHC experiments, reproduced from [170].

reconstructed tracks in the vertex detector [116]. It suggests that the $\chi_{c1}(3872)$ state has a larger size or a smaller binding energy compared with the $\psi(2S)$ meson, and is consistent with a component of $D^{*0}\overline{D}^0 + \overline{D}^{*0}D^0$ hadron molecule in the $\chi_{c1}(3872)$ wave function [159, 160]. The same measurement in pPb data feasible in LHC Run 3 period would be very important to confirm this result.

In the near future, new data will provide enough statistics for associated production of triple heavy flavours and heavy quarkonium pairs beyond $J/\psi J/\psi$, which help to further understand MPI and heavy quarkonium production mechanism [141]. Concerning studies of nuclear matter effects using heavy-flavour production, a rich program is foreseen in Run 3, including measurements probing the DPS enhancement, the modification of nuclear PDF and heavy-quark fragmentation and the heavy quarkonium dissociation mechanism.

2.2 Spectroscopy

The strong interaction confines quarks (and/or gluons) to form various colour-singlet hadrons that are accessible experimentally. This confinement phenomenon is nonperturbative and is not fully understood yet from the current QCD theory. In analogy to photon spectroscopy in atomic physics, hadron spectroscopy provides a way to understand dynamics of QCD at low energies. Hadrons composed of a quark and an antiquark are called mesons, those of three quarks are called baryons, and those composed of more than three quarks are usually referred to as exotic hadrons. Existence of exotic hadrons have been predicted since the birth of the quark model and their properties are reexamined by refined theoretical approaches in the past decades [161–169]. The past years witnessed the observations of a plethora of new conventional and exotic hadrons containing heavy quarks and LHCb is one of the leading players in the field. Figure 5 displays the 68 new hadrons that are discovered by the LHC experiments, and most of them by LHCb.

2.2.1 Conventional hadrons

LHCb have filled many gaps in conventional heavy meson and baryon spectra. This section will focus on more recent highlights in baryon spectroscopy and discovery of doubly heavy hadrons. Though not discussed in detail, it should not be ignored that multiple excited beauty [171, 172] and charm [173] mesons are observed in high energy pp collisions by LHCb. Moreover, the beauty hadron decay is an ideal place to study excited charm hadron as $b\to c$ is the dominant transition of the b quark. Among the many new charm mesons discovered in B decay at LHCb [174–176], an interesting example is a new excited D_s^+ meson, $D_s(2590)^+$, consistent with the radial excited state $D_s(2^1S_0)^+$. Its mass and width will help to understand the excitation spectrum of D_s^+ mesons which are found to be not fully consistent with the quark model predictions [177–182].

Classification of heavy baryons. Following the heavy-quark symmetry, baryons with a heavy quark Q are organised into multiplets according to quantum configurations of the two light quarks [183–199]. The

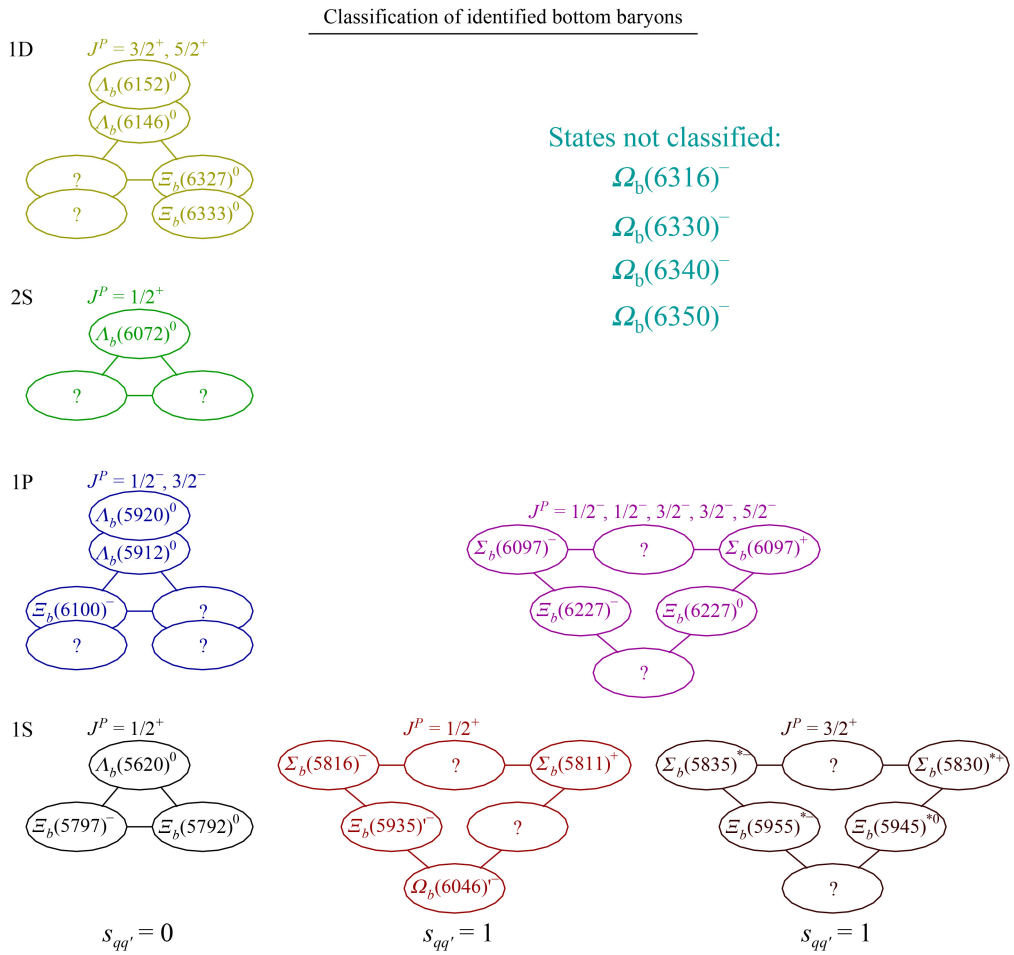

Fig. 6 Experimentally identified bottom baryons, grouped according to spin and flavour symmetry of the light quarks as well as the excitation between the light quark system and b quark. The assignments of quantum numbers are based on measured properties and relevant predictions. Note that for recently discovered states their J^P need confirmation and the assignments of excited Ω_b are not certain, though they likely have $J^P = 1^-$. In the figure, $1P$ excitation of flavour symmetric bottom baryons are gathered into a single multiplet (shown in purple). Only λ mode radial and orbital angular momentum excitation are considered. Missing states are marked as question marks in the figure. The notation $s_{qq'}$ indicates the total spin of the light quark system.

total wave function including flavour (F), spin ($s_{qq'}$) and orbital angular momentum ($l_{qq'}$) must be symmetric for the two light quarks qq' to form an antisymmetric state together with their antisymmetric colour configuration. Baryons with $l_{qq'} = s_{qq'} = 0$ (antisymmetric in spin space) have a spin-parity of $J^P = 1/2^+$, and are grouped into a multiplet of three flavour-antisymmetric states for each heavy quark Q. While baryons with $s_{qq'} = 1, l_{qq'} = 0$ (symmetric in spin space) have $J^P = 1/2^+$ or $J^P = 3/2^+$, and form a multiplet of six flavour-symmetric states for each J^P. These three different multiplets are shown in the bottom row of Fig. 6. Orbital and radial excitation can happen inside the two light quarks (ρ-mode) or between Q and the qq' system (λ-mode). The parity of a baryon is determined to be $P = (-1)^{l_\rho + l_\lambda}$, where $l_\rho \equiv l_{qq'}$, and l_λ is the orbital angular momentum between the Q and qq'. Beauty and charm baryons with $l_\lambda = l_{qq'} = s_{qq'} = 0$ decay weakly and have been well established. However a chart of their excited states are far from being complete. As a matter of fact only a few low lying states are observed, in particularly for beauty baryons as can be seen in Fig. 6. Up to date no sign of ρ-mode states have been identified experimentally, probably because they are too wide (hundreds of MeV) to be resolved from underlying background.

Charm baryons. In the invariant mass spectrum of $\Xi_c^+ K^-$ hadrons shown on the left of Fig. 7, LHCb observed five states whose quark contents are considered to be css: $\Omega_c(3000)^0$, $\Omega_c(3050)^0$, $\Omega_c(3066)^0$, $\Omega_c(3090)^0$ and $\Omega_c(3119)^0$ [200]. All these states have narrow widths, below 10 MeV, and their mass differences are only tens of MeV. The first four states are confirmed by Belle in e^+e^- collisions [201] and by LHCb in the exclusive $\Omega_b^- \to \Xi_c^+ K^- \pi^-$ decay [202]. The spin assignments of the

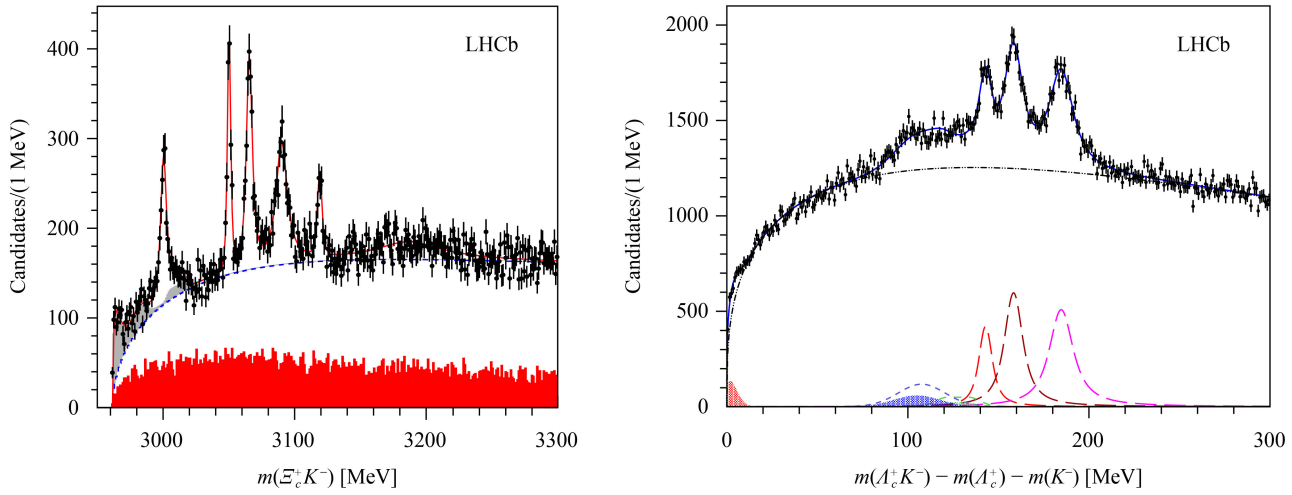

Fig. 7 (Left) Invariant mass distribution of $\Xi_c^+K^-$, overlaid with the fit including five narrow Ω_c states, reproduced from Ref. [200]. (Right) Invariant mass distribution of $\Lambda_c^+K^-$, overlaid with the fit including three narrow Ξ_c states (red, brown and purple dashed lines) and partially reconstructed components. Reproduced from Ref. [215].

first four states favour $1/2, 3/2, 3/2, 5/2$, consistent with the expectations for P-wave λ excitation [202]. A determination of their parities will help to make firm conclusions. According to phenomenological models [203–209], one of the five $1P$ states with $l_\rho = 0, l_\lambda = 1$ in the mass region of observed states is missing, and the $\Omega_c(3119)^0$ state may be a $2S$ or D-wave baryon. In the high mass region of LHCb data, a hint of a wide state $\Omega_c(3188)^0$ is present, to be confirmed in future analysis with additional statistics. It is noted that some of these states are considered to be exotic states of quark constituents $cssu\bar{u}/d\bar{d}$ rather than conventional css baryons [210–214].

Similarly, excited Ξ_c^0 states are searched for by LHCb [215] in the $\Lambda_c^+K^-$ invariant mass spectrum shown on the right of Fig. 7. A new state $\Xi_c(2965)^0$ is observed, and the state $\Xi_c(2930)^0$ claimed by the Belle experiment [216] now splits into two structures, $\Xi_c(2923)^0$ and $\Xi_c(2939)^0$. Separation of the $\Xi_c(2923)^0$ and $\Xi_c(2939)^0$ is recently confirmed in B decay by LHCb [217]. The widths of these three states are determined to be around 10 MeV. These states and previously known $\Xi_c(2790)^0$ and $\Xi_c(2815)^0$ lie in the mass region of $1P$ excitation [218–222]. There are in total seven $1P$ Ξ_c^0 states of the λ-excitation. At least two of these $1P$ states are still missing; Besides, a complete and solid matching of these observed states to predicted spectrum is not resolved yet [223].

Bottom baryons. A summary of all bottom baryons with clear experiment evidences are shown in Fig. 6, organised in multiplets of qq' flavour symmetry and λ-mode excitation when possible. The spin-parity quantum numbers for most of these states are not measured, so we rely on theoretical calculations as a guidance to make the classification. Actually, there is not always a consensus on the J^P of each state, in particularly for Ω_b baryons [224–239].

In total, five states have been reported in the $\Lambda_b^0\pi^+\pi^-$ mass spectrum: $\Lambda_b(5912)^0$ and $\Lambda_b(5920)^0$ with widths below 1 MeV [240], $\Lambda_b(6146)^0$ and $\Lambda_b(6152)^0$ with widths of about 2 MeV [241], and $\Lambda_b(6072)^0$ with a width around 70 MeV [242]. Their masses match two $1P$, two $1D$ and $2S$ Λ_b^0 λ-mode excitation respectively, though other assignments are also discussed [243–247]. It is useful to note that intermediate $\Sigma_b^{(*)\pm}(\to\Lambda_b^0\pi^\pm)$ states are found to be present in the $\Lambda_b{}^{*(*)0}\to\Lambda_b^0\pi^+\pi^-$ decays.

The ground $\Sigma_b^\pm$ and $\Sigma_b^{*\pm}$ states were first detected in the $\Lambda_b^0\pi^\pm$ mass spectrum by CDF [248]. In the same final state, two new ones, $\Sigma_b(6097)^+$ and $\Sigma_b(6097)^-$, are observed by LHCb [249], whose widths are about 30 MeV. These two new states belong to the P-wave family, and many more of them are still missing, like for charm baryons.

In analogy, excited Ξ_b states are searched for by the LHC experiments in the $\Xi_b^0\pi^-/\Xi_b^-\pi^+$ spectra. New states close to $\Xi_b\pi$ mass thresholds are observed, which include the low lying Ξ_b^{*0} baryon discovered by CMS [250] and $\Xi_b^{'-}$, Ξ_b^{*-} states discovered by LHCb [251]. The states $\Xi_b^{'-}$ and $\Sigma_b^\pm$ belong to the flavour symmetric multiplet with $s_{qq'} = 1$, $J^P = 1/2^+$, while Ξ_b^{*0}, Ξ_b^{*-} and $\Sigma_b^{*\pm}$ belong to the flavour symmetric multiplet with $s_{qq'} = 1$, $J^P = 3/2^+$. Going to the higher mass region, a state $\Xi_b(6227)^-$, with a width around 20 MeV, is found in both $\Xi_b^0\pi^-$ and $\Lambda_b^0K^-$ final states [252], and its flavour partner $\Xi_b(6227)^0$ is found in the $\Xi_b^-\pi^+$ mass spectrum [253]. They can be matched to P-wave states or a mixture of several P-wave states with masses close to 6227 MeV/c^2. Very recently, two new states $\Xi_b(6327)^0$ and $\Xi_b(6333)^0$, with widths below 2 MeV, are found in the $\Lambda_b^0K^-\pi^+$ mass spectrum [254], consistent with the $1D$ excitation of the Ξ_b^0 baryon. These two states may also be present in the $\Xi_b^0\pi^+\pi^-$ sample as well, demanding a future investigation

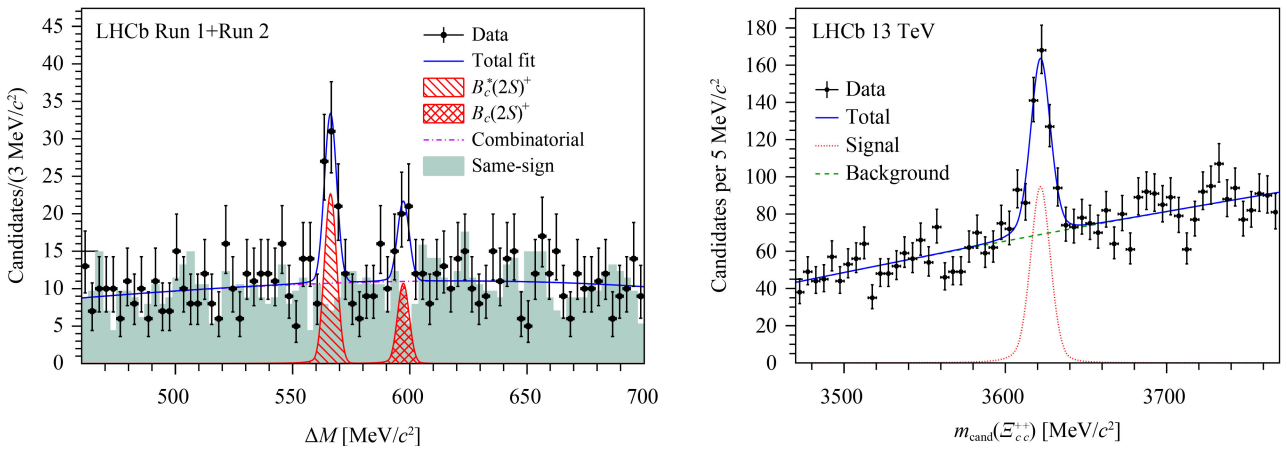

Fig. 8 (Left) Invariant mass distribution of $\Delta M \equiv m_{B_c^+\pi^+\pi^-} - m_{B_c^+}$, overlaid with the fit including two narrow structures, corresponding to $B_c^*(2S)^+$ and $B_c(2S)^+$ repectively, reproduced from Ref. [257]. (Right) Distribution of the reconstructed invariant mass $m_{\rm cand}(\Xi_{cc}^{++}) \equiv m(\Lambda_c^+K^-\pi^+) - m_{\rm cand}(\Lambda_c^+) + m_{\rm PDG}(\Lambda_c^+)$, overlaid with the fit projections. Reproduced from Ref. [258].

of this decay mode by LHCb. In fact, in the $\Xi_b^-\pi^+\pi^-$ spectrum, a $\Xi_b(6100)^-$ state is observed by CMS [255], consistent with the $1P$ excitation of the flavour antisymmetric Ξ_b^- state with $J^P = 3/2^-$. Apparently, the other $1P$ state with $J^P = 1/2^-$ and a mass around 6100 MeV/c^2 is missing. No states with higher masses, for example flavour partners of $\Xi_b(6327)^0$ and $\Xi_b(6333)^0$, are reported by CMS, which may be explained by lower production rate for these states.

Excited Ω_b^- states are searched for in the $\Xi_b^0K^-$ mass spectrum [256]. Four narrow (width < 5 MeV) peaking structures are identified with two of them having significance greater than five standard deviations (5σ), named as $\Omega_b(6340)^-$ and $\Omega_b(6350)^-$ respectively. These states lie in the mass region of P-wave excitation. More statistics in Run 3 will allow for a further investigation of these states.

Doubly heavy hadrons. LHCb has observed a few new hadrons with two heavy quarks. In the final states of $D^0\bar{D}^0$ and D^+D^- mesons produced promptly, a new particle $X(3842)$, with a width of about 3 MeV, is discovered [259]. It is consistent with the spin-3 conventional charmonium $\psi_3(^3D_3)$ with $J^{PC} = 3^{--}$ [260].

As shown on the left of Fig. 8, two narrow structures are detected in the $B_c^+\pi^+\pi^-$ invariant mass spectrum of LHCb data [257]. The left one corresponds to the $B_c^*(2^3S_1)^+ \to B_c^*(1^3S_1)^+\pi^+\pi^-$ decay with the photon in decay of $B_c^*(1^3S_1)^+ \to B_c^+\gamma$ not detected. The peak on the right is consistent with the $B_c(2^1S_0)^+ \to B_c^+\pi^+\pi^-$ decay. Almost in parallel, these two states are independently observed by CMS [261]. As the B_c^+ meson is composed of two heavy quarks, its excitation mass spectroscopy can be calculated using models similar to those applied to heavy quarkonia [262–267] despite their hadroproduction mechanisms are very different [268, 269].

LHCb opens a new era in studies of doubly heavy baryons by observing the Ξ_{cc}^{++} baryon in the $\Xi_{cc}^{++} \to \Lambda_c^+K^-\pi^+\pi^+$ mass spectrum [258], as shown on the right of Fig. 8. This discovery decay mode is predicted to have a relatively large branching fraction [270, 271]. The Ξ_{cc}^{++} state is later confirmed using the $\Xi_{cc}^{++} \to \Xi_c^+\pi^+$ decay [272]. Its lifetime is measured to be about 0.25 ps [273] and its mass is precisely determined to be (3621.55 ± 0.38) MeV/c^2 [273]. Its $SU(3)$ partners, Ξ_{cc}^+ and Ω_{cc}^+, are also searched for by LHCb, but with no sign of observation yet [274–276]. Theoretically, an important question is to understand the mass spectrum of the doubly charm baryons and related systems, which depends on the binding energy between the two heavy quarks [277–289]. The successful discovery of Ξ_{cc}^{++} has triggered wide theoretical work to understand the properties of baryons with more than a heavy quark [290–312]. In addtion, the Ξ_{cc}^{++} baryon mass is used to study the stability of tetraquark states with QQ contents [313, 314] with the assumption that QQ form a heavy diquark [315–319].

2.2.2 Exotic hadrons

Many theoretical efforts have been placed to understand how quarks are combined to form a multi-body system [320–323]. At the same time, more and more new states are observed experimentally which cannot fit into the conventional hadron spectra [54]. As a result, the study on exotic hadrons has been a hot topic for the past decade. New results from LHCb are discussed below.

Tetraquark states. LHCb provides essential information for the understanding of previously known tetraquark states. For example LHCb determined the quantum number of the $X(3872)$ state, first reported by Belle [324], to be $J^{PC} = 1^{++}$ through a full amplitude analysis [325]. LHCb also precisely measured the mass of the $X(3872)$ state (referred to as $\chi_{c1}(3872)$ in Ref. [326]) to be $m_{\chi_{c1}(3872)} - m_{\psi(2S)} = 185.49 \pm 0.06 \pm 0.03$ MeV/c^2 [327,

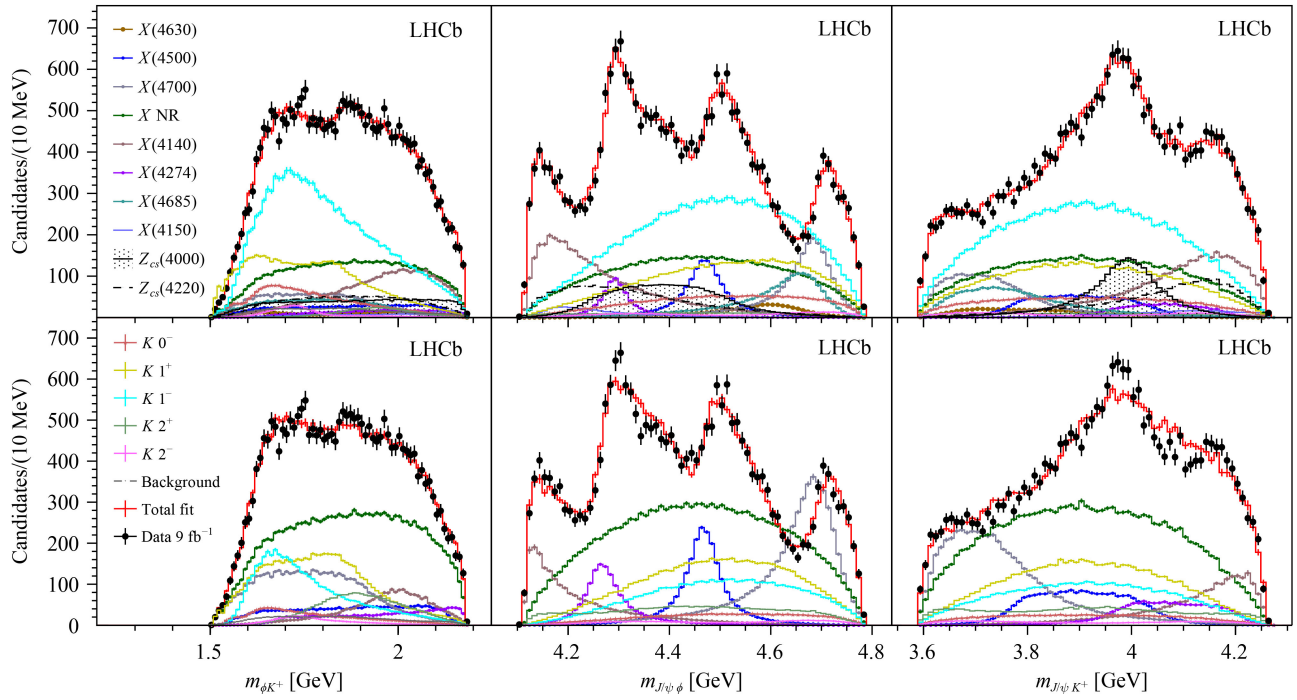

Fig. 9 Distributions of (left) ϕK^+, (middle) $J/\psi\phi$ and (right) $J/\psi K^+$ invariant masses for (black data points) the $B^+\to J/\psi\phi K^+$ candidates compared with (red solid lines) the fit results using (top row) the final model and (bottom row) the model of LHCb Run 1 analysis [401]. reproduced from Ref. [429].

328]. Its Breit–Wigner (BW) width is determined by LHCb to be $\Gamma^{\rm BW}_{\chi_{c1}(3872)} = 0.96^{+0.19}_{-0.18} \pm 0.21$ MeV [327, 328]. Evidence of its decay to $\psi(2S)\gamma$ is found and the branching fraction relative to $J/\psi\gamma$ is measured to $2.46 \pm 0.64 \pm 0.29$ [329], disfavouring a pure $D\overline{D}^*$ molecule intepretation. The ρ^0 and ω contributions are disentangled in its decay to the $J/\psi\pi^+\pi^-$ and a sizeable contribution from ω is confirmed [330]. The $\chi_{c1}(3872)$ state is the mostly studied exotic candidate, and its exotic behaviours include a extremely narrow width, isospin breaking decays and a mass close to the D^*D threshold. Despite all the available information we are still not sure whether it is a compact tetraquark state, a $D^{*0}\overline{D}^0$ hadron molecule, a mixture of $D^{*0}\overline{D}^0$ molecule with a $\chi_{c1}(2P)$ charmonium component or just caused by kinematic rescattering effect [331–373].

The exotic candidate $T^b_{\psi1}(4430)^+$ was first observed by Belle in the $\psi(2S)\pi^-$ mass spectrum in $B^0\to\psi(2S)K^+\pi^-$ decays [374].[2)] An amplitude analysis of the $B^0\to\psi(2S)K^+\pi^-$ decay is performed at LHCb, confirming the existence of the $T^b_{\psi1}(4430)^+$ state and determining it to be consistent with a Breit–Wigner resonance with $J^P = 1^+$ [376]. The quark contents of $T^b_{\psi1}(4430)^+$, $c\overline{c}u\overline{d}$, are the same as the $T^b_{\psi1}(3900)^+$ state observed by the BESIII experiment [377]. Being charged, they are definitely not consistent with conventional charmonia and many phenomenological calculations are performed to explain their internal structure and properties [378–395].

[2)]The exotic hadron naming scheme is used [375].

The $B^+\to J/\psi\phi K^+$ decay is a zoo of exotic hadrons. In 2009, a narrow state $X(4140)$ was reported by CDF in the $J/\psi\phi$ mass spectrum of the $B^+\to J/\psi\phi K^+$ decay [396, 397], and is later confirmed by CMS [398]. The quark contents of the $X(4140)$ state is likely to be $c\overline{c}s\overline{s}$, consistent with an exotic hadron [399, 400], even though excited conventional charmonia may have the chance to decay into $J/\psi\phi$ too. In the amplitude analysis by LHCb using Run 1 data, four exotic candidates $X(4140)$, $X(4274)$, $X(4500)$ and $X(4700)$ are observed [401]. Currently, these X states are considered to be either hadron molecules or compact tetraquark states or high-mass conventional charmonia in various calculations [402–428]. The LHCb analysis is updated recently with a sample that has six times more statistics, in which three more X states are reported [429]. In addition, two $T^+_{\psi s}$ structures are observed in the $J/\psi K^+$ mass spectrum. The mass spectra and fit projections are shown in Fig. 9 and the properties of these exotic candidates are summarised in Table 2. The $T^+_{\psi s}$ states mark the first observation of exotic hadrons with an s quark through beauty decays. It is noted that another $T^+_{\psi s}$ state is reported by BESIII in the final state of $D_s^- D^{*0} + D_s^{*-} D^0$ pairs [430], with a mass and width different from those observed by LHCb. Very recently, evidence of $T^0_{\psi s}$, isopin partner of $T^+_{\psi s}$, is found by LHCb in the $B^+\to J/\psi\phi K^0_S$ decay through a combined amplitude analysis of both $B^+\to J/\psi\phi K^0_S$ and $B^+\to J/\psi\phi K^+$ decays [431]. The masses, widths of these two states and their contributions to the $B\to T_{\psi s}K$ decay

Table 2 Spin-parity, significance, masses, widths, and fit fractions of exotic candidates observed in the $B^+\to J/\psi\phi K^+$ decay by LHCb [429].

Contribution	Significance [$\times\sigma$]	M_0 [MeV]	Γ_0 [MeV]	FF [%]
$X(2^-)$				
$X(4150)$	4.8 (8.7)	$4146\pm18\pm33$	$135\pm28^{+59}_{-30}$	$2.0\pm0.5^{+0.8}_{-1.0}$
$X(1^-)$				
$X(4630)$	5.5 (5.7)	$4626\pm16^{+18}_{-110}$	$174\pm27^{+134}_{-73}$	$2.6\pm0.5^{+2.9}_{-1.5}$
All $X(0^+)$				$20\pm5^{+14}_{-7}$
$X(4500)$	20 (20)	$4474\pm3\pm3$	$77\pm6^{+10}_{-8}$	$5.6\pm0.7^{+2.4}_{-0.6}$
$X(4700)$	17 (18)	$4694\pm4^{+16}_{-3}$	$87\pm8^{+16}_{-6}$	$8.9\pm1.2^{+4.9}_{-1.4}$
All $X(1^+)$				$26\pm3^{+8}_{-10}$
$X(4140)$	13 (16)	$4118\pm11^{+19}_{-36}$	$162\pm21^{+24}_{-49}$	$17\pm3^{+19}_{-6}$
$X(4274)$	18 (18)	$4294\pm4^{+3}_{-6}$	$53\pm5\pm5$	$2.8\pm0.5^{+0.8}_{-0.4}$
$X(4685)$	15 (15)	$4684\pm7^{+13}_{-16}$	$126\pm15^{+37}_{-41}$	$7.2\pm1.0^{+4.0}_{-2.0}$
All $T_{\psi s}(1^+)$				$25\pm5^{+11}_{-12}$
$T_{\psi s}(4000)$	15 (16)	$4003\pm6^{+4}_{-14}$	$131\pm15\pm26$	$9.4\pm2.1\pm3.4$
$T_{\psi s}(4220)$	5.9 (8.4)	$4216\pm24^{+43}_{-30}$	$233\pm52^{+97}_{-73}$	$10\pm4^{+10}_{-7}$

are similar, confirming that they are isospin partners. There should be more states of $c\bar{c}q\bar{s}$ quark contents, and their discovery will definitely help to understand the internal structure of strange tetraquark states [432, 433].

Exotic hadrons are also searched for in open charm final states using fully reconstructed beauty hadron decays. A Dalitz analysis of the $B^+\to D^+D^-K^+$ decay is performed by LHCb [434, 435], and two exotic states, $T_{cs0}(2900)^0$ and $T_{cs1}(2900)^0$, are required to have a good fit to the D^-K^+ invariant mass spectrum. The D^-K^+ invariant-mass distribution and the fit projections are shown in Fig. 10. Their spin-parities are measured to be $J^P=0^+$ and 1^-, and widths to be about 50 MeV and 100 MeV respectively. The quark contents of these X states are $cs\bar{u}\bar{d}$. These two X states contribute up to 35% of the total $B^+\to D^+D^-K^+$ decay branching fraction, a magnitude similar to those of conventional charmonia in the decay. A final state rescattering effect is considered in order to explain such a large branching fraction [436]. In a recent analysis of the $B^0\to\bar{D}^0D_s^+\pi^-$ and $B^+\to D^-D_s^+\pi^+$ decays by LHCb, two new states $T^a_{c\bar{s}0}(2900)^{++/0}$ are observed in the $D_s^+\pi^{+/-}$ systems [437, 438]. The quark contents of these two states are $c\bar{s}d\bar{u}$ and $c\bar{s}u\bar{d}$ respectively. The invariant mass distributions of $D_s^+\pi^-$ and $D_s^+\pi^+$ are shown in Fig. 10 superimposed with the amplitude fit results. The masses and width of these two states are measured to be about 2.9 GeV/c^2 and 0.15 GeV respectively, and they contribute to about 3% of the total $B\to\bar{D}^0D_s^+\pi^-$ decay. The mass of the $T^a_{c\bar{s}0}(2900)$ is consistent with the previously mentioned $T_{cs0}(2900)^0$ discovered in the D^-K^+ final state, but their widths and flavour contents are different. The observation of $X\to Dh$ $(D=D_s^+,D,\ h=\pi,K)$ states in the $B\to D\overline{D}h$ decay opens a new avenue for studies of exotic hadrons composed of four different quark flavours [439–452]. Actually there are more than two dozens of $B\to DDK(\pi)$ decays, and also a few similar decays for b-baryons, and it is promising that more X states will be observed in these decays.

Recently, a Dalitz analysis for the $B^+\to D_s^+D_s^-K^+$ decay was performed by the LHCb collaboration [453, 454]. A near-threshold structure in the $D_s^+D_s^-$ system is observed with a significance larger than 12σ. The $D_s^+D_s^-$ invariant-mass distribution is shown on the top right of Fig. 10. The spin-parity of the $X(3960)$ state is determined to be $J^{PC}=0^{++}$. The $X(3960)$ state is similar to the $\chi_{c0}(3930)$ state in Ref. [326]. If they are the same states, the partial width ratio is measured to be

$$\frac{\Gamma\left(X\to D^+D^-\right)}{\Gamma\left(X\to D_s^+D_s^-\right)}=0.29\pm0.09\pm0.10\pm0.08,$$

where the first uncertainty is statistical, the second systematic, and the third external. The ratio is smaller than unity. Since the creation of $s\bar{s}$ from vacuum is suppressed than $u\bar{u}$ or $d\bar{d}$ and the phase-space factor of $X\to D^+D^-$ is smaller than $X\to D_s^+D_s^-$, the $\Gamma\left(X\to D^+D^-\right)$ is expected to be larger than $\Gamma\left(X\to D_s^+D_s^-\right)$, which is inconsistent with the results from experiment. The inconsistency indicates the exotic nature of the $X(3960)$ states under the assumption of the $X(3960)$ and the $\chi_{c0}(3930)$ being the same states.

Prompt production of di-charm hadrons has been suggested to search for exotic states containing multiple charm quarks [455]. In the invariant mass spectrum of $D^0D^0\pi^+$, shown in Fig. 11, a new structure is observed close to the $D^{*+}D^0$ mass threshold [456, 457]. The structure

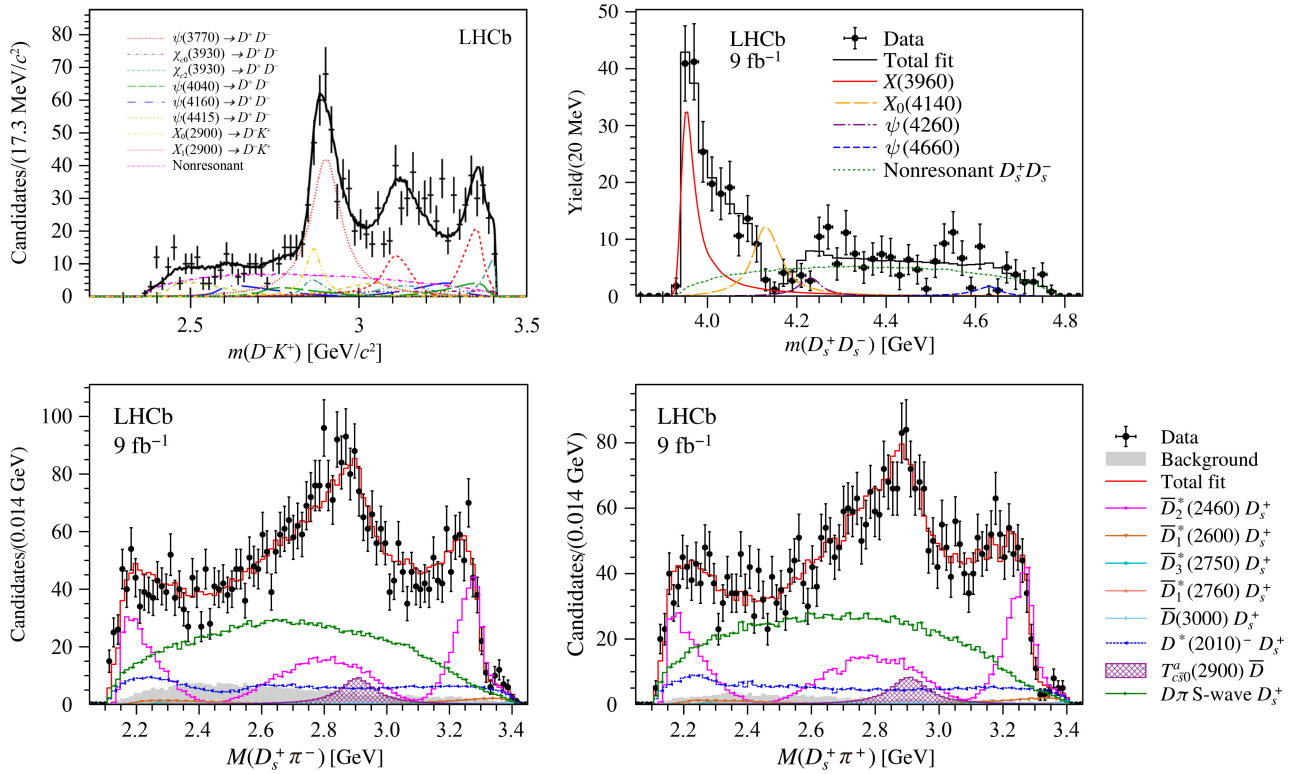

Fig. 10 (Top left) Invariant-mass distribution of D^-K^+ in $B^+\to D^+D^-K^+$ decays in data and the fit projections, reproduced from Ref. [435]. The yellow dot-dashed and red dotted line correspond to $T_{cs0}(2900)^0$ and $T_{cs1}(2900)^0$, respectively, and more details can be found in Ref. [435]. (Top right) The distribution of the invariant mass of the $D_s^+D_s^-$ system in the $B^+\to D_s^+D_s^-K^+$ decay. A near-threshold structure, denoted as $X(3960)$, is marked in red [453]. The distribution of the invariant mass of (bottom left) the $D_s^+\pi^-$ pair in the $B^0\to\bar{D}^0D_s^+\pi^-$ and (bottom right) $D_s^+\pi^+$ system in the $B^+\to D^-D_s^+\pi^+$ decay [438].

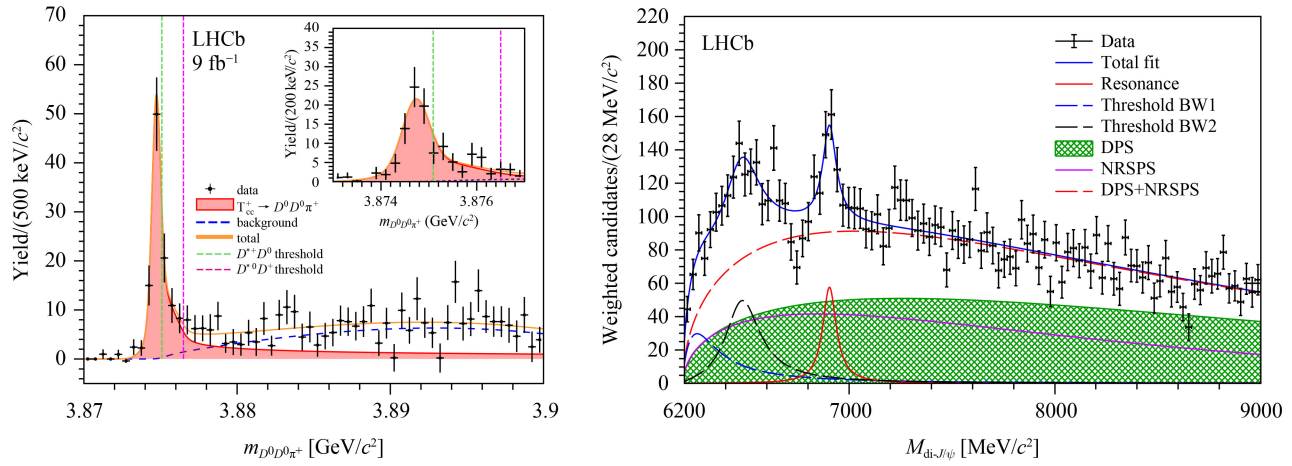

Fig. 11 (Left) Distribution of $D^0D^0\pi^+$ invariant mass overlaid with fit projections. The contribution of the non-D^0 background has been statistically subtracted. Vertical dashed lines show the $D^{*+}D^0$ and $D^{*0}D^+$ mass thresholds respectively for a comparison, reproduced from Ref. [457]. (Right) Invariant mass distribution of the combination of two J/ψ mesons overlaid with fit projections, reproduced from Ref. [487]. The fit model does not contain interference between any components.

is measured to be consistent with the ground state of a T_{cc}^+ isoscalar tetraquark, with $J^P=1^+$ and quark contents $cc\bar{u}\bar{d}$. Its Breit-Wigner mass is measured to be $-273\pm61\pm5^{+11}_{-14}$ keV/c^2 below $m_{D^{*+}}+m_{D^0}$, and its Breit-Wigner width is $\Gamma_{\mathrm{BW}}=410\pm165\pm43^{+18}_{-38}$ keV. The same state also appears in the D^0D^0 and D^0D^+ mass spectra, with a π^+, π^0 or γ in the $T_{cc}^+\to D^0D^0\pi^+$, $T_{cc}^+\to D^0D^+\pi^0$ or $T_{cc}^+\to D^0D^+\gamma$ decays undetected, respectively. Dedicated

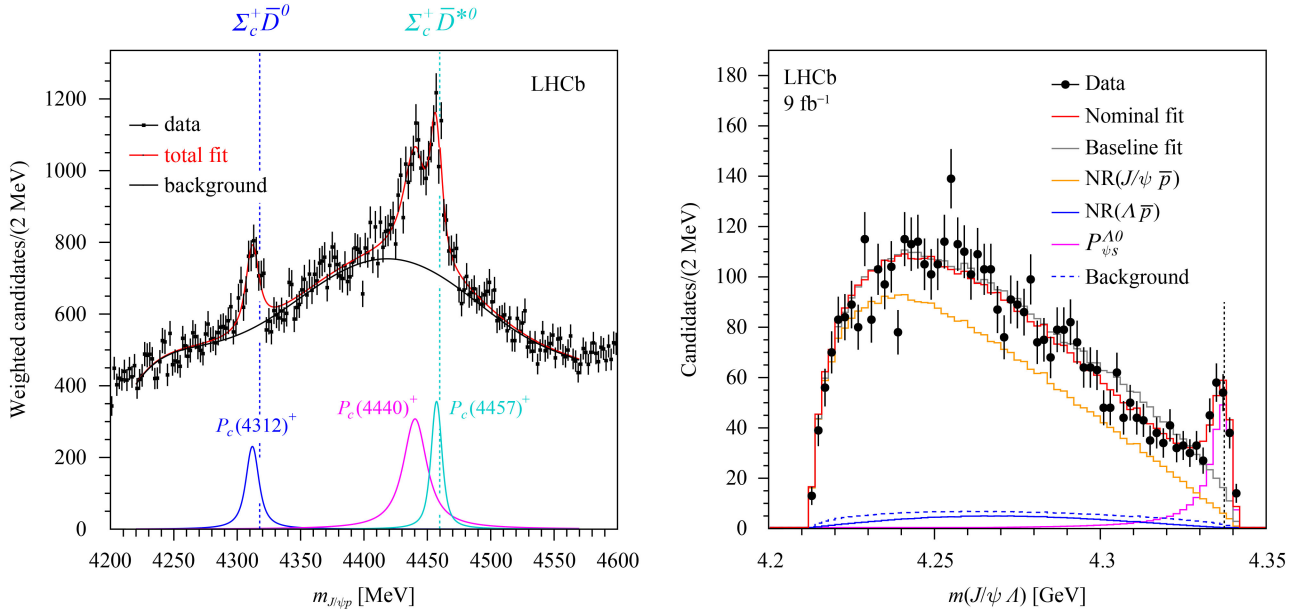

Fig. 12 (Left) Invariant mass distribution of $J/\psi p$ in the $\Lambda_b^0 \to J/\psi p K^-$ decay fitted with three BW functions plus polynomial background, reproduced from Ref. [487]. The vertical lines mark the $\Sigma_c^+\bar{D}^0$ and the $\Sigma_c^+\bar{D}^{*0}$ mass thresholds respectively. (Right) Invariant mass distribution of the $J/\psi\Lambda$ system in the $\Xi_b \to J/\psi\Lambda K^-$ decay overlaid with fit projections, reproduced from Ref. [564].

studies of the T_{cc}^+ resonance lineshape are performed using a unitarised Breit–Wigner distribution, considering T_{cc}^+ decays in $D^0D^0\pi^+, D^0D^+\pi^0$ and $D^0D^0\gamma$ final states. The pole mass of the resonance in this advanced model is measured to be $-360 \pm 4^{+4}_{-0}$ keV/c^2 below $m_{D^*} + m_{D^0}$, and the pole width is $\Gamma_{\text{pole}} = -48 \pm 2^{+0}_{-14}$ keV. This extremely narrow width has attracted many theoretical interests [458–463]. The T_{cc}^+ state is the first observed tetraquark candidates with two heavy quarks of the same flavour. Many theoretical models have been applied to explain the existence and structure of such a tetraquark state with a large fraction of them favouring a $D^{*+}D^0$ hadron molecule interpretation [464–486].

In addition to two open charm final states, di-J/ψ mass spectrum of prompt production is also studied using full LHCb data [487]. Two peaking structures are observed in the mass range $6.2 < m_{J/\psi J/\psi} < 7.4$ GeV/c^2, where fully charmed tetraquark states are predicted [488–512]. The first structure (referred to as the threshold peak) covers the range between 6.2 and 6.6 GeV/c^2 close to the di-J/ψ mass threshold, and the other one sits at 6.9 GeV/c^2, as shown on the left of Fig. 11. The di-J/ψ mass spectrum is modelled with a combination of BW functions for the two peaking structures and empirical smooth functions for SPS, DPS production of nonpeaking background. When no interference between BW and SPS is applied, the threshold structure can be described by two BW functions and the one at 6.9 GeV/c^2 is well described by a BW. The narrow structure, denoted as $T_{\psi\psi}(6900)$, is measured to have a mass of $m_{T_{\psi\psi}(6900)} = 6905 \pm 11 \pm 7$ MeV/c^2 and a width of $\Gamma_{T_{\psi\psi}(6900)} = 80 \pm 19 \pm 33$ MeV. Interpretations of the threshold peak using feed-

Table 3 Detection decay channels, experimental significance, masses and widths of pentaquark states reported by LHCb.

State	Decays	Significance [σ]	Mass [MeV/c^2]	Width [MeV]
$P_\psi^N(4312)^+$	$J/\psi p$	7.3σ	$4311.9 \pm 0.7^{+6.8}_{-0.6}$	$9.8 \pm 2.7^{+\ 3.7}_{-\ 4.5}$
$P_\psi^N(4440)^+$	$J/\psi p$	5.4σ	$4440.3 \pm 1.3^{+4.1}_{-4.7}$	$20.6 \pm 4.9^{+\ 8.7}_{-10.1}$
$P_\psi^N(4457)^+$	$J/\psi p$	5.4σ	$4457.3 \pm 0.6^{+4.1}_{-1.7}$	$0.53 \pm 2.0^{+\ 5.7}_{-\ 1.9}$
$P_\psi^N(4337)^+$	$J/\psi p$	3.1σ	$4337\ ^{+\ 7}_{-\ 4} \pm 2$	$29\ ^{+\ 26}_{-\ 12} \pm 14$
$P_{\psi s}^\Lambda(4459)^0$	$J/\psi\Lambda$	3.1σ	$4458.8 \pm 2.9^{+4.7}_{-1.1}$	$17.3 \pm 6.5^{+\ 8.0}_{-\ 5.7}$
$P_{\psi s}^\Lambda(4338)^0$	$J/\psi\Lambda$	$> 15\sigma$	$4338.2 \pm 0.7 \pm 0.4$	$7.0 \pm 1.2 \pm 1.3$

down decays from excited quarkonium pairs are also possible. For various fit models without any interference, the dip around 6.8 GeV/c^2 cannot be well described. Advance fit studies are performed introducing interference between SPS and resonant structures. In one such fit, two BW functions are considered: a broad BW interfering with SPS used to describe the threshold structure, and a stand-alone narrow one used to model the 6.9 GeV/c^2 peak. This new model could fit well the overall spectrum, and the broad structure is now measured to have a mass around 6.7 GeV/c^2 and a width of about 0.3 GeV, while the $T_{\psi\psi}(6900)$ structure has a mass consistent with the no-interference fit model, but its width becomes about twice larger. As the fit results for the broad structure is not stable in different models, its nature is not fully resolved and more data are needed to provide better information. The $T_{\psi\psi}(6900)$ and higher resonances have been recently confirmed by CMS [513] and ATLAS [514]. The $T_{\psi\psi}(6900)$ state is consistent with a genuine fully charmed tetraquark, however, in some models possible origins due to rescatterings of multiple charmonia or dibaryon molecules etc. are also discussed [515–551]. Other fully heavy tetraquarks, such as $b\bar{b}c\bar{c}$ and $b\bar{b}b\bar{b}$, can be searched for in $\Upsilon J/\psi$ and $\Upsilon\Upsilon$ or similar final states, however current limited data are estimated to have small sensitivities for these states, demanding the increased luminosity in LHCb upgrades.

Pentaquark states. Following the successful discoveries of tetraquarks with $Q\overline{Q}$ contents, pentaquark states with $Q\overline{Q}$ were predicted, in the form of either meson-baryon hadron molecules or compact five-quark hadrons [552–555]. Since 2015, several pentaquark candidates are found in LHCb, as summarised in Table 3. The first observation of them is made in $J/\psi p$ final states in $\Lambda_b^0\to J/\psi pK^-$ decays through an amplitude analysis of Run 1 data [556]. Two states were reported, $P_\psi^N(4380)^+$ and $P_\psi^N(4450)^+$, and their evidence is also found in the $\Lambda_b^0\to J/\psi p\pi^-$ decays with a similar amplitude study [557]. A model-independent moment analysis of the $\Lambda_b^0\to J/\psi pK^-$ decay concludes that contributions of $J/\psi p$ exotics are essential, since only allowing $\Lambda^*\to pK^-$ resonances in the decay are not sufficient to describe data [558]. With full LHCb data, an amplitude analysis of $\Lambda_b^0\to J/\psi pK^-$ decays becomes computationally very difficult. On the other hand, benefiting from the high statistics, one dimensional $J/\psi p$ mass spectrum is investigated to look for narrow pentaquark states [559]. In this new analysis, the $P_\psi^N(4450)^+$ structure is found to consist of two narrow overlapping peaks $P_\psi^N(4440)^+$ and $P_\psi^N(4457)^+$, and a new structure $P_\psi^N(4312)^+$ is observed. It is noted that the $P_\psi^N(4312)^+$ and $P_\psi^N(4457)^+$ states are close to the $\Sigma_c^+\bar{D}^0$ and $\Sigma_c^+\bar{D}^{*0}$ mass thresholds respectively, as shown in Fig. 12 making them ideal candidates of meson-baryon molecules. Recently, LHCb reported the evidence of a new pentaquark state, $P_\psi^N(4337)^+$, in the $J/\psi p(\bar{p})$ mass spectrum of $B_s^0\to J/\psi p\bar{p}$ decays [560]. This possible state is different from those observed in Λ_b^0 decays, making beauty meson decays a new place to search for pentaquarks.

Pentaquark candidates with strangeness are predicted in the $\Xi_b^-\to J/\psi\Lambda K^-$ decay [561, 562], which is an analogy of the $\Lambda_b^0\to J/\psi pK^-$ channel by replacing the d quark by the s quark. An amplitude analysis of the $\Xi_b^-\to J/\psi\Lambda K^-$ decay is performed using full LHCb data, resulting in the evidence of a new state, $P_{\psi s}^\Lambda(4459)^0$, in the $J/\psi\Lambda$ mass spectrum, with quark contents, $c\bar{c}uds$. Its mass is measured to be $4458.8\pm2.9^{+4.7}_{-1.1}$ MeV/c^2 and width to be $17.3\pm6.5^{+8.0}_{-5.7}$ MeV [563]. According to the prediction in Ref. [561], there are two Ξ_cD^* hadron molecules with masses within a few MeV/c^2 around the observed structure. If the $P_{\psi s}^\Lambda(4459)^0$ structure is found to be composed of two nearby states with LHCb upgrade data, it will be a strong proof of the molecular interpretation of such states. Recently, an amplitude analysis of the $B^-\to J/\psi\Lambda\overline{p}$ was performed [564]. A narrow structure in the $J/\psi\Lambda$ system, denoted as $P_{\psi s}^\Lambda(4338)^0$, is observed with high significance, which is consistent with pentaquark state with strangeness. The invariant-mass distribution of the $J/\psi\Lambda$ system is shown in Fig. 12. The mass and width of the state are measured to be $4338.2\pm0.7\pm0.4$ MeV and $7.0\pm1.2\pm1.3$ MeV, respectively, where the first uncertainty is statistical and the second systematic. The spin-parity of the state is determined to be $J^P=\frac{1}{2}^-$.

Observations of pentaquark states with heavy-quark contents have triggered many studies from theorists, with the purpose of understanding their nature. In general, these states are considered to either be compact tetraquarks, hadronic molecules or simple bumps due to kinematic rescatterings [565–638]. Measurements of their J^P and production properties, and finding their flavour partners will shed light on the problem. However, it is likely that debates on the nature of exotic hadrons will continue before we have a complete and coherent theory to explain all of them. In the past years, phenomenology models on the hadron spectroscopy evolved quickly and some patterns have been revealed, for example, dynamics close to two-hadron mass thresholds [639]. Besides, lattice QCD simulations have improved in computational performances and application scopes substantially over the years and will play more and more important roles in our understanding of low-energy QCD [640–646]. Hopefully, one day we can predict low energy QCD phenomena as precise as other parts of the SM.

3 Rare beauty hadron decays

By rare decays we mainly refer to flavour-changing-neutral-current (FCNC) processes, which are highly suppressed in the SM by the Glashow–Iliopoulos–Maiani (GIM) mechanism [647]. Rare decays of hadrons could receive significant contributions from new particles or new interactions beyond the SM. Precision measurements of their properties play a special role in search of physics beyond the SM.

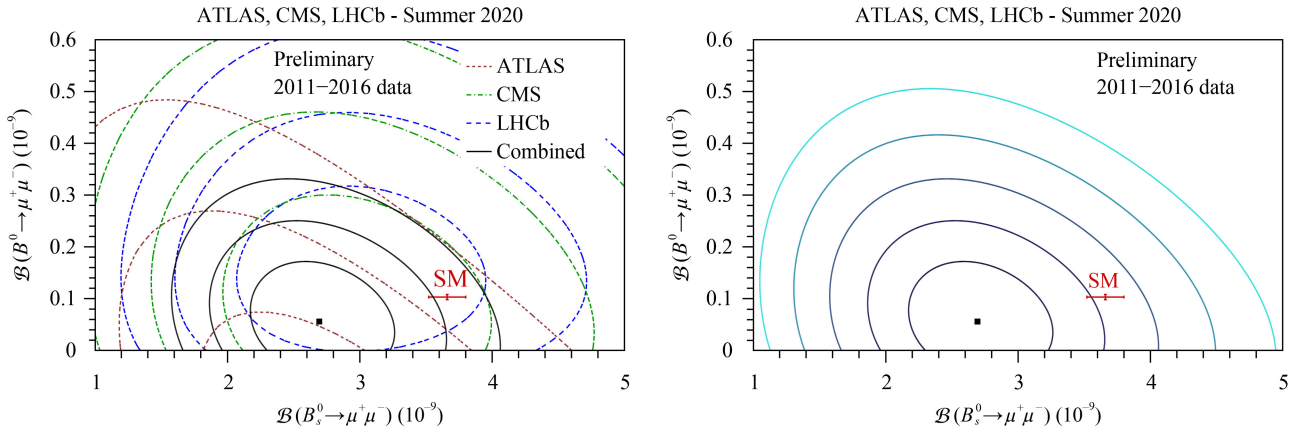

Fig. 13 (Left) Likelihood contours in the $\mathcal{B}(B^0\to\mu^+\mu^-)$–$\mathcal{B}(B_s^0\to\mu^+\mu^-)$ plane corresponding to $-2\Delta\ln L = 2.3$, 6.2 and 11.8, for ATLAS, CMS and LHCb experiments and the combination. (Right) Likelihood contours for the combination corresponding to $-2\Delta\ln L = 2.3$, 6.2, 11.8, 19.3 and 30.2. The data sets used were collected from 2011 to 2016. Reproduced from Refs. [660].

The LHCb collaboration has given priority to the study of FCNC $b\to s$ transitions, focusing on theoretically clean observables such as decay rates of purely leptonic B-meson decays, angular coefficients in $b\to s\ell^+\ell^-$ decays, and ratio of decay rates between $b\to s\ell^+\ell^-$ processes with different lepton flavours. Analyses of pp collision data collected in the Run 1 and Run 2 periods have already led to some very important and interesting findings, including but not limited to the first observation of the purely leptonic decay $B_s^0\to\mu^+\mu^-$, anomalous angular distribution in the decay $B^0\to K^{*0}\mu^+\mu^-$, and intriguing results from extensive tests of lepton flavour universality in $B\to K^{(*)}\ell^+\ell^-$ decays.

3.1 Effective field theory for $b\to s$ transitions

The effective Hamiltonian describing the quark-level $b\to s$ transitions is given by [648–654]

$$H_{\rm eff}(b\to s) = -\frac{4G_F}{\sqrt{2}}V_{tb}V_{ts}^*\sum_{i=1}^{10}C_i\mathcal{O}_i, \tag{3}$$

with $\mathcal{O}_i$ denoting the local operators in the SM and C_i indicating the corresponding Wilson coefficients. Of particular interest is the electromagnetic dipole operator corresponding to penguin diagrams mediated by photons,

$$\mathcal{O}_7 = \frac{e}{16\pi^2}m_b(\bar{s}\sigma_{\mu\nu}P_Rb)F^{\mu\nu}, \tag{4}$$

and semileptonic operators corresponding to loop diagrams mediated by Z^0 or $W^\pm$ bosons,

$$\begin{aligned}\mathcal{O}_9 &= \frac{e^2}{16\pi^2}(\bar{s}\gamma_\mu P_Lb)(\bar{\ell}\gamma^\mu\ell),\\ \mathcal{O}_{10} &= \frac{e^2}{16\pi^2}(\bar{s}\gamma_\mu P_Lb)(\bar{\ell}\gamma^\mu\gamma_5\ell),\end{aligned} \tag{5}$$

where $P_L = (1-\gamma_5)/2$ and $P_R = (1+\gamma_5)/2$. Contribution from physics beyond the SM can either alter the values of the Wilson coefficients and/or give rise to new operators that are absent or highly suppressed in the SM, such as the scalar and pseudo-scalar operators

$$\mathcal{O}_S = \frac{e^2}{16\pi^2}(\bar{s}P_Lb)(\bar{\ell}\ell),\ \mathcal{O}_P = \frac{e^2}{16\pi^2}(\bar{s}P_Lb)(\bar{\ell}\gamma_5\ell)\ , \tag{6}$$

and the chirality-flipped operators $\mathcal{O}'_{7,8,9,10,S,P}$, which are obtained by changing $P_{L(R)}$ to $P_{R(L)}$ in $\mathcal{O}_{7,8,9,10,S,P}$.

The Wilson coefficients $C_7^{(\prime)}$ can be probed in radiative b-hadron decays such as $B_s^0\to\phi\gamma$ and $\Lambda_b^0\to\Lambda\gamma$, $C_{9,10}^{(\prime)}$ probed in semileptonic decays such as $B^0\to K^+\ell^+\ell^-$ and $B^+\to K^{*0}\ell^+\ell^-$, and $C_{S,P}^{(\prime)}$ probed in purely leptonic decays such as $B_s^0\to\ell^+\ell^-$. Recent LHCb results on $b\to s$ transitions are summarised in the remainder of this section.

3.2 Purely leptonic B meson decays

The decays $B_{(s)}^0\to\ell^+\ell^-(\ell=\mu,e)$ are among the most interesting probes of new physics. They are theoretically clean and are expected to be extremely rare in the SM due to helicity suppression in addition to the FCNC loop suppression. Their branching fractions in the SM are precisely predicted to be [655]

$$\begin{aligned}\mathcal{B}(B_s^0\to\mu^+\mu^-) &= (3.66\pm0.14)\times10^{-9},\\ \mathcal{B}(B^0\to\mu^+\mu^-) &= (1.03\pm0.05)\times10^{-10},\\ \mathcal{B}(B_s^0\to e^+e^-) &= (8.60\pm0.36)\times10^{-14},\\ \mathcal{B}(B^0\to e^+e^-) &= (2.41\pm0.13)\times10^{-15}.\end{aligned} \tag{7}$$

Note the $B^0\to\ell^+\ell^-$ decays proceed via $b\to d$ transitions, thus are further suppressed with respect to the $B_s^0\to\ell^+\ell^-$ decays by a factor of $|V_{td}/V_{ts}|^2\sim\lambda^2$. The decay rates of $B_{(s)}^0\to\ell^+\ell^-$ processes are highly sensitive to (pseudo-) scalar interactions beyond the SM.

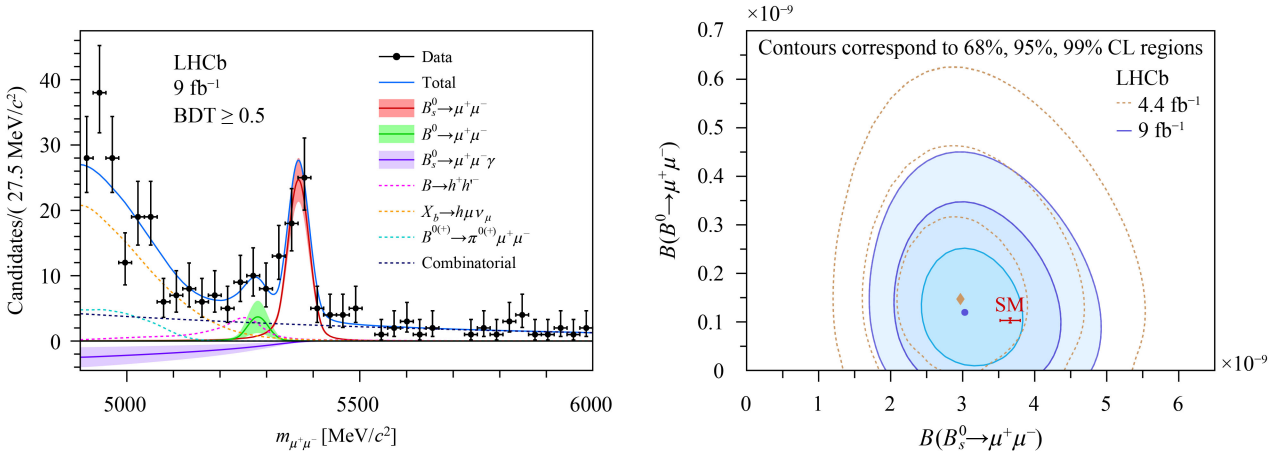

Fig. 14 (Left) Invariant mass distribution of the selected $B^0_{(s)}\to\mu^+\mu^-$ candidates with output of the used multivariate classifier above 0.5, superimposed with the fit result. (Right) Confidence intervals in the plane of the branching fractions of $B^0_s\to\mu^+\mu^-$ and $B^0\to\mu^+\mu^-$. The data sets used for the blue solid (brown dotted) contours were collected from 2011 to 2018 (2016). Reproduced from Refs. [661, 662].

A joint analysis of data from the LHCb and CMS experiments collected in Run 1 led to the observation of the $B^0_s\to\mu^+\mu^-$ decay with a significance exceeding six standard deviations, and determined the branching fraction to be $\mathcal{B}(B^0_s\to\mu^+\mu^-)=(2.8^{+0.7}_{-0.6})\times10^{-9}$ [656]. This result was later updated by LHCb [657] and CMS [658] by adding the 2016 data. The ATLAS collaboration reported an evidence for the decay $B^0_s\to\mu^+\mu^-$ with a significance of 4.6σ using the data collected between 2011 and 2016 [659]. However, no significant signal for the decay $B^0\to\mu^+\mu^-$ has been found by any experiment yet. A combination of the results from ATLAS, CMS and LHCb gives the branching fraction $\mathcal{B}(B^0_s\to\mu^+\mu^-)=(2.69^{+0.37}_{-0.35})\times10^{-9}$, and sets an upper limit of $\mathcal{B}(B^0\to\mu^+\mu^-)<1.9\times10^{-10}$ at 95% confidence level [660]. Figure 13 shows the constraints on $\mathcal{B}(B^0_s\to\mu^+\mu^-)$ and $\mathcal{B}(B^0_s\to\mu^+\mu^-)$ from the three experiments and the combined results, which are compatible with the SM predictions [655] within 2.1 σ. The difference is mainly driven by the ATLAS results, which have an optimal solution outside the physical region and are slightly in tension with the SM predictions.

Very recently, LHCb reported updated results on the $B^0_s\to\mu^+\mu^-$ and $B^0\to\mu^+\mu^-$ decays using all data collected in Run 1 and Run 2. The results are $\mathcal{B}(B^0_s\to\mu^+\mu^-)=(3.09^{+0.46+0.15}_{-0.43-0.11})\times10^{-9}$, $\mathcal{B}(B^0\to\mu^+\mu^-)<2.6\times10^{-10}$ at 95% confidence level [661, 662], which are in good agreement with the SM expectations, as shown in Fig. 14.

In addition to the decay rate, other interesting quantities, such as effective lifetime and CP asymmetry, can also be measured to search for possible non-SM contribution to the decay $B^0_s\to\mu^+\mu^-$ [663]. Pioneering studies of its effective lifetime using all data collected in Run 1 and Run 2 have been performed at LHCb, leading to the result of $\tau^{\rm eff}(B^0_s\to\mu^+\mu^-)=2.07\pm0.29\pm0.03$ ps [661, 662]. As a long-term goal, the effective lifetime and time-dependent CP violation of the decay $B^0_s\to\mu^+\mu^-$ will be fully exploited in LHCb upgrade II, which aims to accumulate a pp collision data sample of 300 fb^{-1} [664].

The decays $B^0_{(s)}\to e^+e^-$ are even rarer than $B^0_{(s)}\to\mu^+\mu^-$ and can provide powerful tests of lepton flavour universality. To date, the searches performed by the CDF and LHCb experiments have found no evidence for either $B^0_s\to e^+e^-$ or $B^0\to e^+e^-$. The most stringent upper limits on their branching fractions are $\mathcal{B}(B^0_s\to e^+e^-)<11.2\times10^{-9}$ and $\mathcal{B}(B^0\to e^+e^-)<3.0\times10^{-9}$ at 95% confidence level set by LHCb [665].

In addition to decays to dileptons, the LHCb experiment has also searched for decays of neutral B mesons to four leptons. A recent search using the full Run 1 and Run 2 data sample found no hint of such decays, and upper limits at 90% confidence level for the nonresonant decays are determined to be $\mathcal{B}(B^0_s\to\mu^+\mu^-\mu^+\mu^-)<8.6\times10^{-10}$ and $\mathcal{B}(B^0\to\mu^+\mu^-\mu^+\mu^-)<1.8\times10^{-10}$ [666]. More stringent limits are set for decays involving the J/ψ resonance or a promptly decaying intermediate scalar particle with a mass of 1 GeV/c^2.

3.3 Semileptonic $b\to s\ell^+\ell^-$ decays

Semileptonic $b\to s\ell^+\ell^-$ decays provide valuable insight into possible non-SM contributions that affect the Wilson coefficients C_9 and C_{10} of the electromagnetic operators. The presence of hadrons in the final state makes the search for new physics in semileptonic decays more complicated than that in purely leptonic decays. The challenges in hadronic form-factor calculations lead to significant uncertainties in the SM predictions of their decay rates. Fortunately, a number of relatively clean observables that are less affected by the form factors

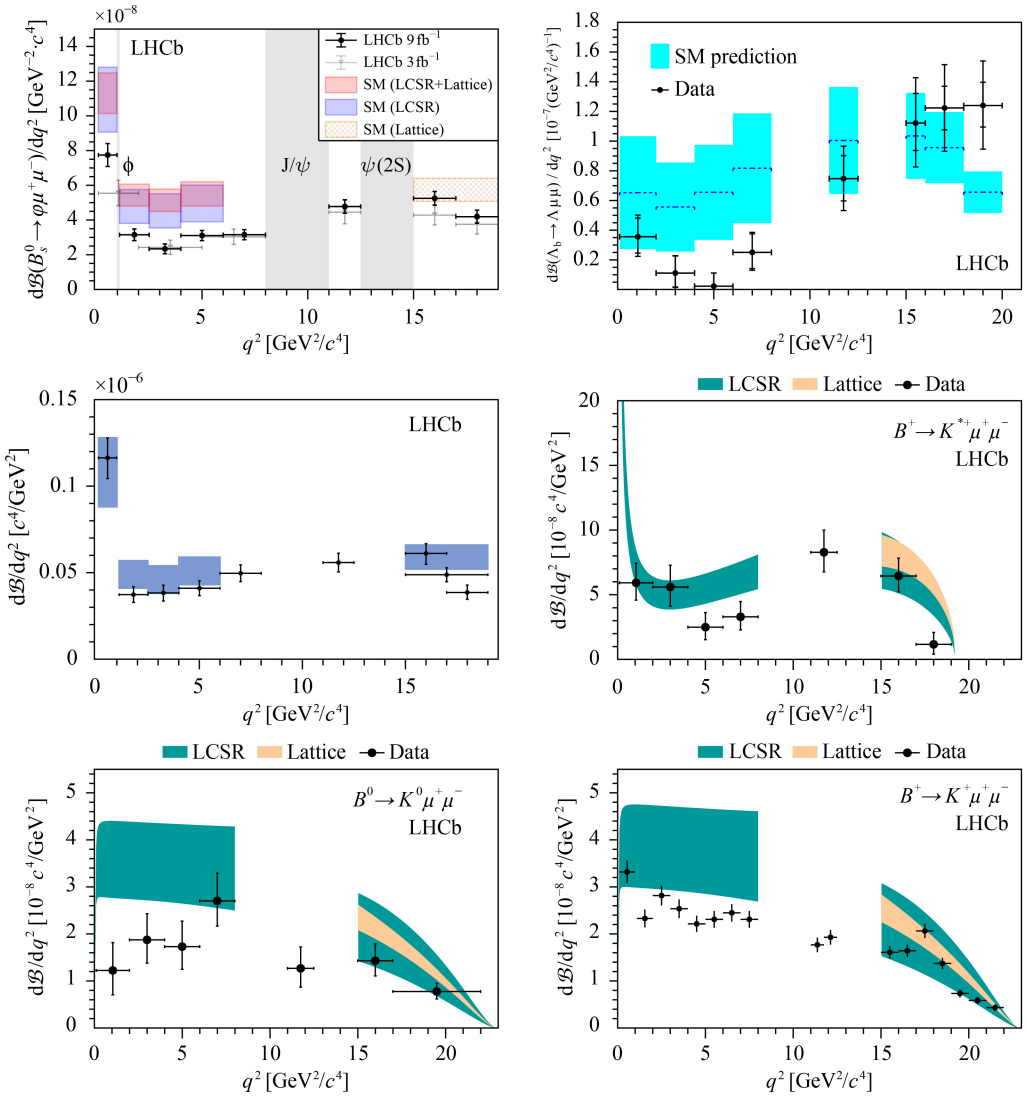

Fig. 15 Top left: Measured $\mathrm{d}\mathcal{B}(B_s^0 \to \phi\mu^+\mu^-)/\mathrm{d}q^2$ [673] overlaid with the SM predictions based on light-cone sum rule calculations [667, 677, 678] at low q^2 and lattice QCD calculations [670, 671] at high q^2; Top right: Measured $\mathrm{d}\mathcal{B}(\Lambda_b^0 \to \Lambda\mu^+\mu^-)/\mathrm{d}q^2$ [674] compared with the SM predictions using form factors from lattice QCD calculations [679]; Middle left: Measured $\mathrm{d}\mathcal{B}(B^0 \to K^{*0}\mu^+\mu^-)/\mathrm{d}q^2$ [675] compared with the SM predictions using form factors from line-cone sum rule and lattice QCD calculations [667, 670]; Middle right, bottom left and bottom right: Measured $\mathrm{d}\mathcal{B}(B^+ \to K^{*+}\mu^+\mu^-)/\mathrm{d}q^2$, $\mathrm{d}\mathcal{B}(B^0 \to K_S^0\mu^+\mu^-)/\mathrm{d}q^2$ and $\mathrm{d}\mathcal{B}(B^+ \to K^+\mu^+\mu^-)/\mathrm{d}q^2$ [676] compared with the SM predictions using form factors from light-cone sum rule and lattice QCD calculations [680, 681].

than the total decay rates have been identified, including some special observables in angular distributions and observables for lepton universality test. A comprehensive study of these observables in a series of $b \to s\ell^+\ell^-$ processes has been pursued by the LHCb collaboration and the results are summarized below.

3.3.1 Differential decay rates with respect to q^2

The differential branching fraction $\mathrm{d}\mathcal{B}/\mathrm{d}q^2$ can be measured in intervals of q^2, the invariant mass squared of the lepton pair, and compared with SM predictions. Calculations of form factors are needed for making the SM predictions. Such calculations are challenging, and require different treatments depending on the q^2 regions. Light-cone sum rule calculations [667–669] and lattice QCD calculations [670, 671] are often used to determine the form factors in low- and high-q^2 regions, respectively.

After measuring the branching fraction of the decay $B_s^0 \to \phi\mu^+\mu^-$ to be about 3σ below the SM expectation value [672], the LHCb experiment further studied its differential branching fraction as a function of q^2. The top left plot in Fig. 15 shows the latest results of $\mathrm{d}\mathcal{B}(B_s^0 \to \phi\mu^+\mu^-)/\mathrm{d}q^2$ obtained using Run 1 data [673], where the J/ψ and $\psi(2S)$ regions are excluded. A puzzle

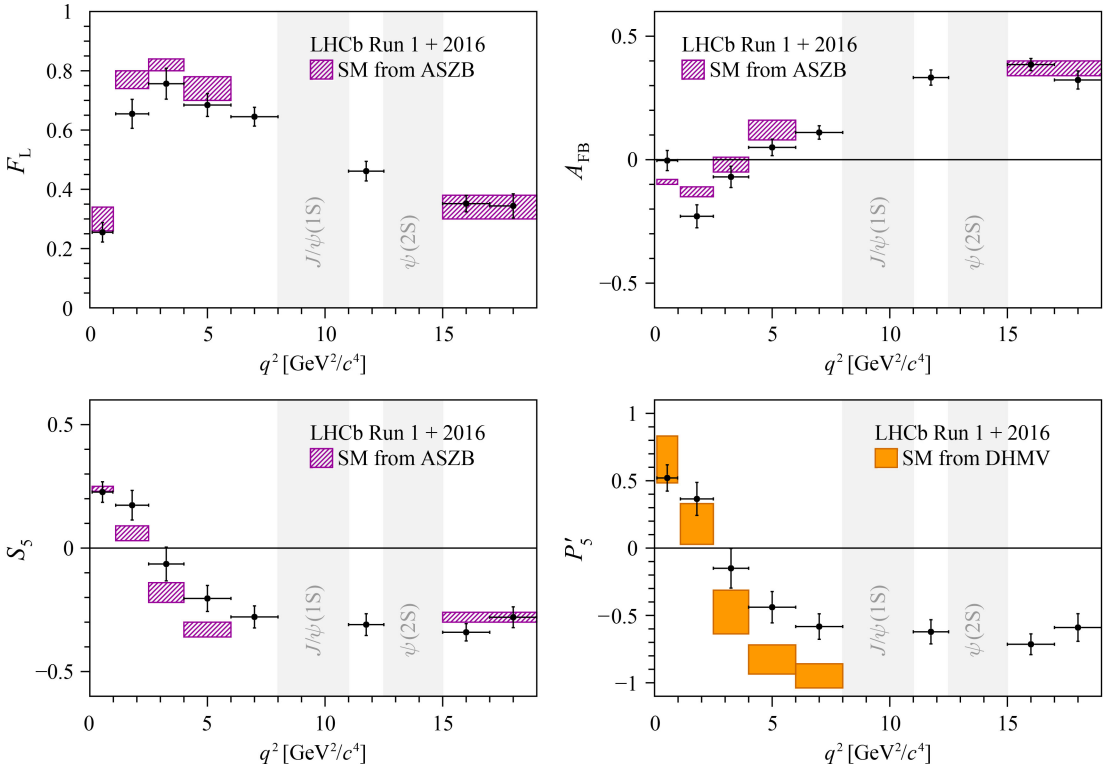

Fig. 16 Results of the observables F_L, A_{FB}, S_5 and P'_5 in bins of q^2, compared with the SM predictions. Reproduced from Ref. [689].

appears in the range $1 < q^2 < 6\,\text{GeV}^2/c^4$. The branching fraction integrated over this range is measured to be $(2.88 \pm 0.22) \times 10^{-8}$. Currently, the most precise SM prediction for this range is $(5.37 \pm 0.66) \times 10^{-8}$, obtained from a combination of light-cone sum rule and lattice QCD calculations. A discrepancy of $3.6\,\sigma$ is observed. Similar patterns are also seen in the LHCb measurements of differential branching fractions in the decays $\Lambda_b^0 \to \Lambda\mu^+\mu^-$ [674], $B^0 \to K^{*0}\mu^+\mu^-$ [675], $B^+ \to K^+\mu^+\mu^-$, $B^0 \to K_S^0\mu^+\mu^-$ and $B^+ \to K^{*+}\mu^+\mu^-$ [676], as shown in Fig. 15.

3.3.2 Angular distributions

Angular distributions in $b \to s\ell^+\ell^-$ decays contain rich information about interference between the SM and non-SM contributions that may not be accessible via decay rates integrated over angular variables. A set of q^2-dependent angular coefficients can be extracted from the angular distributions and used as probes for new physics, which are complementary to branching fractions and $d\mathcal{B}/dq^2$. Based on these coefficients, we can define some theoretically clean observables with reduced dependency on the form factors.

Of particular interest is the angular distribution of the $B^0 \to K^{*0}(\to K^+\pi^-)\,\mu^+\mu^-$ decay, which has been extensively studied by BaBar [682], Belle [683], ATLAS [684], CMS [685] and LHCb [686–689]. Following the definitions in Ref. [651], the CP-averaged angular distribution of the decay $B^0 \to K^{*0}\mu^+\mu^-$ with $K^{*0} \to K^+\pi^-$ is given by

$$\begin{aligned}
&\frac{1}{\mathrm{d}(\Gamma+\bar{\Gamma})/\mathrm{d}q^2}\frac{\mathrm{d}^4(\Gamma+\bar{\Gamma})}{\mathrm{d}q^2\mathrm{d}\vec{\Omega}} \\
&= \frac{9}{32\pi}\Big[\frac{3}{4}(1-F_L)\sin^2\theta_K + F_L\cos^2\theta_K \\
&\quad + \frac{1}{4}(1-F_L)\sin^2\theta_K\cos 2\theta_\ell - F_L\cos^2\theta_K\cos 2\theta_\ell \\
&\quad + S_3\sin^2\theta_K\sin^2\theta_\ell\cos 2\phi + S_4\sin 2\theta_K\sin 2\theta_\ell\cos\phi \\
&\quad + S_5\sin 2\theta_K\sin\theta_\ell\cos\phi + \frac{4}{3}A_{FB}\sin^2\theta_K\cos\theta_\ell \\
&\quad + S_7\sin 2\theta_K\sin\theta_\ell\sin\phi + S_8\sin 2\theta_K\sin 2\theta_\ell\sin\phi \\
&\quad + S_9\sin^2\theta_K\sin^2\theta_\ell\sin 2\phi\Big],
\end{aligned} \tag{8}$$

where $\mathbf{\Omega} = (\cos\theta_K, \cos\theta_\ell, \phi)$, θ_K is the angle between the directions of the K^+ (K^-) and B^0 ($\bar{B}^0$) in the rest frame of the K^{*0} ($\bar{K}^0$) system, θ_ℓ is the angle between the direction of the μ^+ (μ^-) and the opposite direction of the B^0 ($\bar{B}^0$) in the rest frame of the $\mu^+\mu^-$ system, ϕ is the angle between the plane defined by the muon pair and the plane defined by the kaon and pion in the B^0 ($\bar{B}^0$) rest frame. Eight observables can be extracted, including the fraction of the longitudinal polarisation of the K^{*0} meson (F_L), the forward-backward asymmetry of the

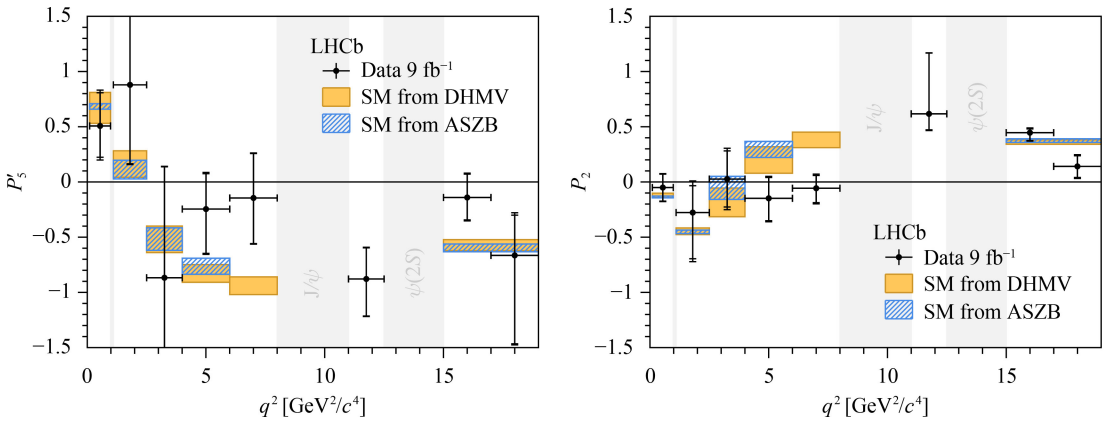

Fig. 17 Results for the observables P_5' and P_2 in $B^+\to K^{*+}\mu^+\mu^-$, compared with SM predictions. Reproduced Ref. [692].

$\mu^+\mu^-$ system ($A_{\rm FB}$), and six other angular coefficients (S_i, $i=3,4,5,7,8,9$). Using the S_i coefficients, new observables less sensitive to form factor uncertainties are defined, such as $P_i'=S_i/\sqrt{F_{\rm L}(1-F_{\rm L})}$ $(i=3,4,5)$ [690].

The latest LHCb results on angular analysis of the $B^0\to K^{*0}\mu^+\mu^-$ decay are obtained using data collected in 2011, 2012 and 2016 [689]. The majority of the angular observables are consistent with the SM predictions [677] based on form factors obtained from a combination of light-cone sum rule calculations [667] for low-q^2 regions and lattice QCD calculations [670, 671] for high-q^2 regions. A clear exception is seen with the robust observable P_5' defined using S_5, as shown in Fig. 16. The measured values of P_5' in the intervals $4.0<q^2<6.0\,{\rm GeV}^2/c^4$ and $6.0<q^2<8.0\,{\rm GeV}^2/c^4$ are found to be higher than the SM predictions [668, 690] by $2.5\,\sigma$ and $2.9\,\sigma$, respectively. These results confirm the discrepancy in P_5' observed in an earlier LHCb analysis with Run 1 data [688]. According to model-independent fits using the FLAVIO software package [691], the overall tension with the SM is increased from $3.0\,\sigma$ to $3.3\,\sigma$. The fits reveal that the current measurements of the angular observables in $B^0\to K^{*0}\mu^+\mu^-$ can be accommodated by shifting the real part of the Wilson coefficient C_9 from its SM value by $0.99^{+0.25}_{-0.21}$ [689].

Recently, LHCb reported results of angular analysis of the $B^+\to K^{*+}(\to K^0_S\pi^+)\mu^+\mu^-$ decay using Run 1 and Run 2 data [692]. A trend of deviations from the SM predictions in P_5', similar to that in the isospin partner decay $B^0\to K^{*0}\mu^+\mu^-$, is shown in the left of Fig. 17. Meanwhile, a large discrepancy in the measurement of $P_2=\frac{2}{3}A_{\rm FB}/(1-F_{\rm L})$ has also been observed in the $6.0<q^2<8.0\,{\rm GeV}^2/c^4$ region, where the measurement deviates from its SM prediction [677, 690] by $3.0\,\sigma$ (Fig. 17 right).

An untagged time-integrated angular analysis of the decay $B^0_s\to\phi\mu^+\mu^-$ has been performed by the LHCb collaboration using data collected in 2011 to 2012 and 2016 to 2018 [693]. In this channel, the same particles (μ^+ and K^+) are used to define the angular variables for both B^0_s and $\bar{B}^0_s$ decays, since the final state is not self-tagging as in the $B^0\to K^{*0}\mu^+\mu^-$ case. With this convention, the coefficients of the terms in the CP-averaged time-integrated angular distributions corresponding to the interference between CP-even (0 or //) and CP-odd ($\perp$ or S) amplitudes are CP asymmetries, $A^{CP}_{\rm FB}$ and $A_{5,8,9}$, rather than the CP-average observables $A_{\rm FB}$ and $S_{5,8,9}$ in Eq.8. These asymmetries can arise from either direct CP violation or nonzero effective mixing phase, with the latter contribution suppressed by the small value of $\Delta\Gamma_s/\Gamma_s$. They are predicted to be close to zero in the SM but has some sensitivity to new physics contributions [694]. The measurements of $A^{CP}_{\rm FB}$ and $A_{5,8,9}$ in intervals of q^2 are shown in Fig. 18, which are consistent with CP invariance. Much more information on CP violation can be obtained from time-dependent angular analysis of tagged $B^0_s\to\phi\mu^+\mu^-$ decays [695], which may become feasible with the huge amount of data that will be collected with the upgraded LHCb detector in the coming data-taking periods.

Angular coefficients in the $B^+\to K^+\mu^+\mu^-$ decay have been measured by LHCb [696] and CMS [697] using Run 1 data. Angular observables in $\Lambda^0_b\to pK^-\mu^+\mu^-$ decays have been determined by LHCb [698] from a moment analysis using data collected between 2011 and 2016. These results are consistent with the SM predictions but limited by statistical uncertainties.

3.3.3 Lepton flavour universality tests

In the SM, the couplings of the three generations of leptons to the electroweak gauge bosons Z^0 and $W^\pm$ are assumed to be identical. This is known as lepton flavour universality (LFU). Under this assumption, processes involving the three flavours of charged leptons, e, μ and τ, have equal rates up to corrections caused by different lepton masses, which can be trivially taken into account. Contributions of new particles or new interactions may lead to violation of LFU, particularly in FCNC processes

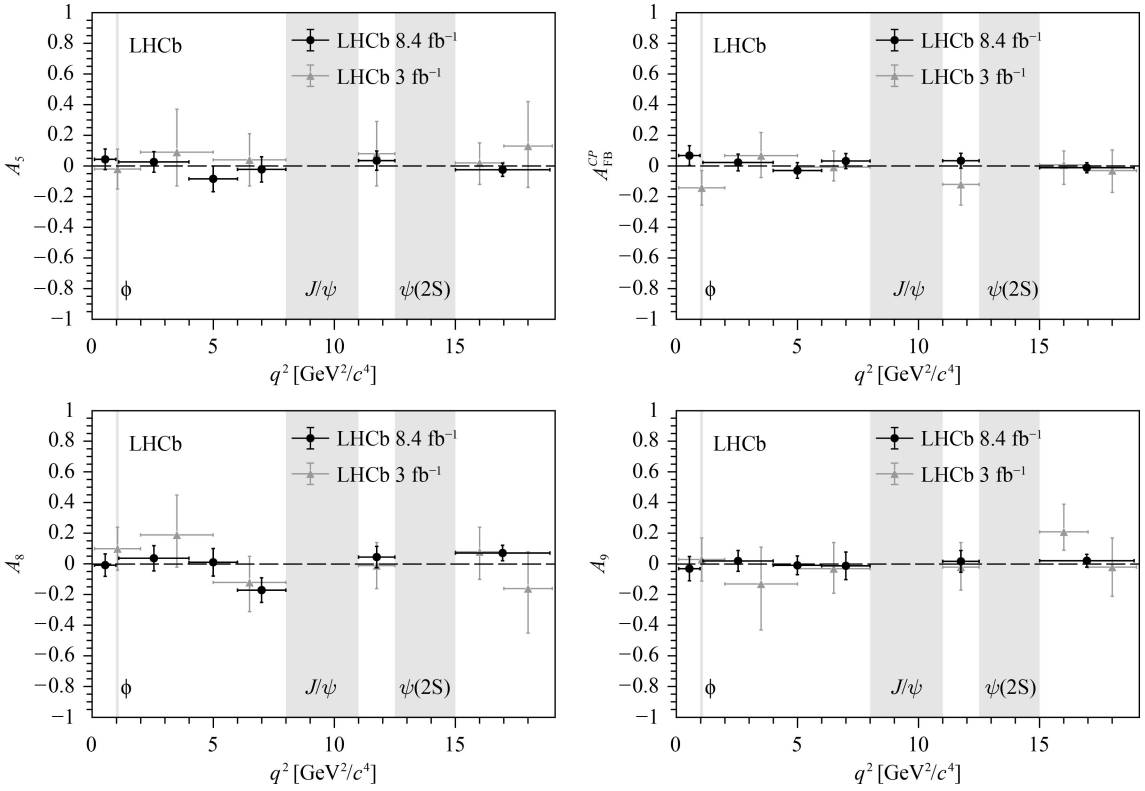

Fig. 18 CP asymmetries $A_{\rm FB}^{CP}$ and $A_{5,8,9}$ in intervals of q^2 in the decay $B_s^0 \to \phi\mu^+\mu^-$ measured using Run 1 and Run 2 data (black) in Run 1 data only (grey). Reproduced from Ref. [693].

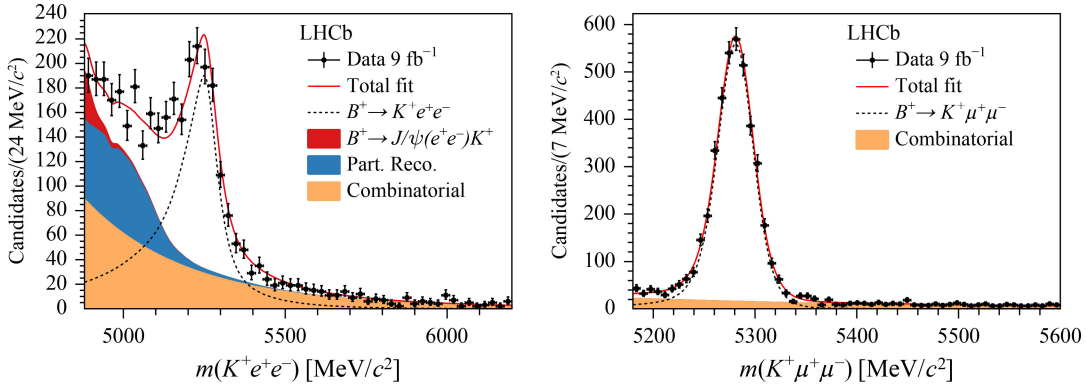

Fig. 19 Invariant mass distributions of the selected (left) $B^+ \to K^+e^+e^-$ and (right) $B^+ \to K^+\mu^+\mu^-$ candidates, superimposed by the fit results. Reproduced from Ref. [703].

such as $b \to s\ell^+\ell^-$ decays. Stringent tests of LFU can be performed by measuring the ratio of the branching fractions between $B \to X\mu^+\mu^-$ and $B \to Xe^+e^-$ decays [699–701] outside the charmonium regions in the dilepton mass spectrum, with X indicating the hadron(s) in the decays. The ratio is denoted by

$$R_X \equiv \frac{\mathcal{B}(B \to X\mu^+\mu^-)}{\mathcal{B}(B \to Xe^+e^-)} . \tag{9}$$

In the SM, R_X is expected to be very close to unity with negligible theoretical uncertainty, due to the small and precisely known difference between the muon and electron masses. On the experimental side, reconstruction of electrons is challenging due to the Bremsstrahlung radiation. The decays $B \to XJ/\psi(\to\mu^+\mu^-)$ and $B \to XJ/\psi(\to e^+e^-)$ are used as control channels for cancellation of systematic uncertainties associated with electron reconstruction. Practically, the ratio R_X is measured using a double-ratio technique following the equation

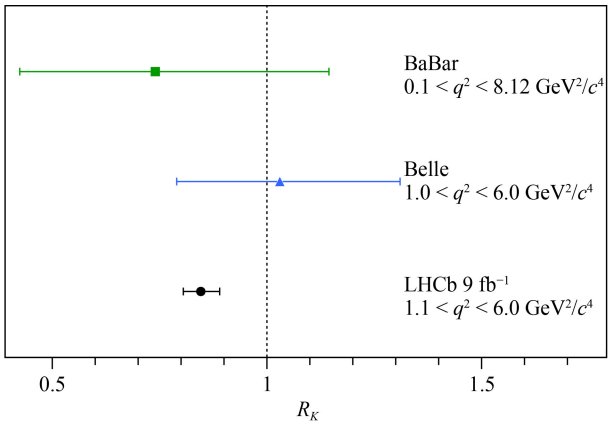

Fig. 20 Comparison of the LHCb R_K result with the measurements by B-factories [707, 708]. The vertical line indicates the SM expected value. Reproduced from Ref. [703].

$$R_X = \frac{\mathcal{B}(B\to X\mu^+\mu^-)/\mathcal{B}(B\to XJ/\psi(\to\mu^+\mu^-))}{\mathcal{B}(B\to Xe^+e^-)/\mathcal{B}(B\to XJ/\psi(\to e^+e^-))}\ , \quad (10)$$

where $\mathcal{B}(B\to XJ/\psi(\to\mu^+\mu^-))/\mathcal{B}(B\to XJ/\psi(\to e^+e^-))$ is known to be very close to unity [326].

The LHCb collaboration previously measured $R_K = 0.846^{+0.060}_{-0.054}\,(\text{stat})^{+0.016}_{-0.014}\,(\text{syst})$ in $B^+\to K^+\ell^+\ell^-$ $(\ell = e,\,\mu)$ decays in the dilepton mass-squared range $1.1 < q^2 < 6.0\,\text{GeV}^2/c^4$ using Run 1 and part of Run 2 data [702]. The result was below the SM expectation [691] by $2.5\,\sigma$. Recently, LHCb updated the R_K measurement using the full Run 1 and Run 2 sample [703]. The mass distributions of the $B^+\to K^+\ell^+\ell^-$ candidates are shown in Fig. 19. The R_K value is measured to be

$$R_K(1.1 < q^2 < 6.0\,\text{GeV}^2/c^4) = 0.846^{+0.042}_{-0.039}\,(\text{stat})^{+0.013}_{-0.012}\,(\text{syst})\ ,$$

which are lower than the SM prediction, 1.00 ± 0.01 [691, 700, 704–706], by $3.1\,\sigma$. A comparison of the LHCb R_K result with the values measured by BaBar [707] and Belle [708] is shown in Fig. 20.

Tests of LFU have also been performed in other $b\to s\ell^+\ell^-$ $(\ell = e,\mu)$ decays. Based on the Run 1 data sample, the LHCb collaboration has determined the ratios of branching fractions of $B^0\to K^{*0}\ell^+\ell^-$ $(\ell = e,\mu)$ decays in two regions of dilepton mass-squared below the J/ψ resonance to be [709]

$$R_{K^{*0}}(0.045 < q^2 < 1.1\,\text{GeV}^2/c^4) = 0.66^{+0.11}_{-0.07}\,(\text{stat}) \pm 0.03\,(\text{syst})\ ,$$
$$R_{K^{*0}}(1.1 < q^2 < 6.0\,\text{GeV}^2/c^4) = 0.69^{+0.11}_{-0.07}\,(\text{stat}) \pm 0.05\,(\text{syst})\ .$$

These results are in tension with the SM predictions [667, 691, 700, 704, 706, 710–713] at the level of $2.1-2.3\,\sigma$ and $2.4-2.5\,\sigma$, respectively. LHCb has also measured

$$R_{pK}(0.1 < q^2 < 6.0\,\text{GeV}^2/c^4) = 0.86^{+0.14}_{-0.11}\,(\text{stat}) \pm 0.05\,(\text{syst})$$

in $\Lambda_b^0\to pK^-\ell^+\ell^-$ $(\ell = e,\mu)$ decays using Run 1 and part of Run 2 data [714].

Very recently, LHCb reported the observation of the decays $B^0\to K^0_S e^+e^-$ and $B^+\to K^{*+}e^+e^-$ and the measurements of LFU observables $R_{K^0_S}$ and $R_{K^{*+}}$ using the full Run 1 and Run 2 data samples [715]. The obtained results of $R_{K^0_S}$ and $R_{K^{*+}}$ are

$$R_{K^0_S}(1.1 < q^2 < 6.0\ \text{GeV}^2/c^4) = 0.66^{+0.20}_{-0.14}\,(\text{stat})^{+0.02}_{-0.04}\,(\text{syst})\ ,$$
$$R_{K^{*+}}(0.045 < q^2 < 6.0\ \text{GeV}^2/c^4) = 0.70^{+0.11}_{-0.07}\,(\text{stat})^{+0.03}_{-0.04}\,(\text{syst})\ ,$$

which are lower than but consistent with the SM predictions at $1.5\,\sigma$ and $1.4\,\sigma$, respectively.

The anomalous results that the LHCb collaboration has obtained in the study of LFU and angular distributions in $b\to s\ell^+\ell^-$ decays are highly interesting but not well understood yet. These results have prompted extensive theoretical studies of potential new physics effects in $b\to s\ell^+\ell^-$ transitions [716–725]. Particularly, new physics scenarios that mainly affect $b\to s\mu^+\mu^-$ transitions are preferred, according to global analysis in the framework of SM effective field theory [718–721, 724, 725].

It should be noted with caution that the current measurements of these rare decays are largely limited by the statistical precision, and the non-trivial background contamination and reconstruction efficiency in $b\to se^+e^-$ decays may also need to be further scrutinized. An improved understanding of FCNC b-hadron decays can be achieved using the huge amount of data that will be recorded following Upgrade I and Upgrade II. This will not only significantly increase the accuracy of the benchmark measurements in $b\to s$ transitions, but also provide great opportunities to explore new observables and new rare decay modes that are currently inaccessible, such as time-dependent observables in $B^0\to K^0_S\mu^+\mu^-$ [726, 727] and $B^0_s\to\phi\mu^+\mu^-$ [695] decays, and lepton universality ratios and angular observables in heavily suppressed $b\to d\ell^+\ell^-$ transitions [728–731].

3.4 Radiative $b\to s\gamma$ decays

The effective Hamiltonian for $b\to s\gamma$ transitions can be approximately written as

$$H_{\text{eff}}(b\to s\gamma) = -\frac{4G_F}{\sqrt{2}}V_{tb}V_{ts}^*(C_7\mathcal{O}_7 + C_7'\mathcal{O}_7'), \quad (11)$$

where only the leading operator $\mathcal{O}_7$ and its chirality-flipped counterpart $\mathcal{O}_7'$ are included. In the SM, the coefficient C_7' is given by $C_7' = \frac{m_s}{m_b}C_7$ due to the chiral $V-A$

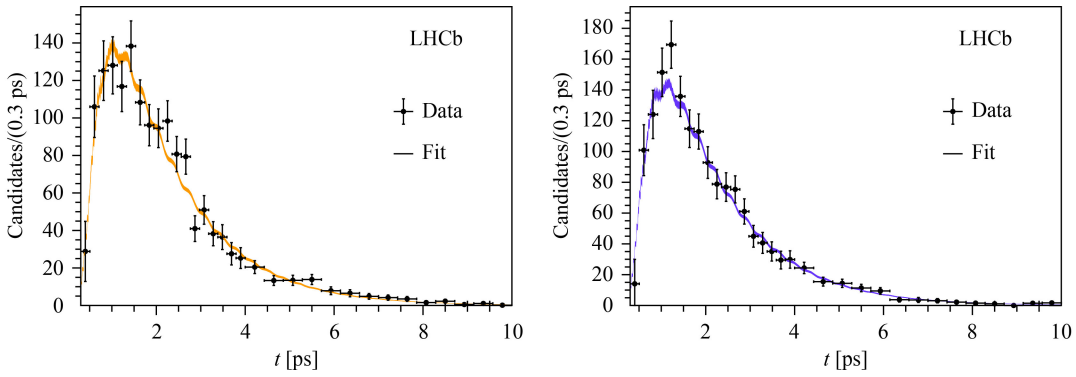

Fig. 21 Decay-time distributions of the tagged (left) $B_s^0 \to \phi\gamma$ and (right) $\bar{B}_s^0 \to \phi\gamma$ candidates, superimposed by the fit projections. Reproduced from Ref. [746].

structure of the weak interaction, where m_s (m_b) indicates the mass of the s (b) quark. Consequently, the photons emitted in radiative b-hadron ($\bar{b}$-hadron) decays are predominantly left-handed (right-handed). Amplitudes with right-handed photons, A_R, are suppressed by the ratio m_s/m_b compared with those with left-handed photons, A_L, but could be enhanced in new physics scenarios with right-handed charged current, such as supersymmetric grand unified theories and left-right symmetric models [732–738].

Rich information on photon polarisation can be obtained from time-dependent analysis of $B_q^0(\bar{B}_q^0) \to f_{\rm CP}\gamma$ decays [732, 739, 740], where $f_{\rm CP}$ is a CP eigenstate with eigenvalue η. The time-dependent decay rates summing over left-handed and right-handed photons are expressed as

$$P(t) = P_0 e^{-\Gamma_q t}\left[\cosh(\Delta\Gamma_q t/2) - A^{\Delta}\sinh(\Delta\Gamma_q t/2) + \xi C\cos(\Delta m_q t) - \xi S\sin(\Delta m_q t)\right] , \tag{12}$$

where ξ takes the value of +1 (−1) for an initial B_q^0 ($\bar{B}_q^0$) meson. The coefficient C quantifies CP violation in the decay. This type of CP violation has been constrained to be small in radiative B meson decays by BaBar, Belle and LHCb [741–743]. Assume no CP violation in the decay for simplicity, it is convenient to write

$$\begin{aligned} &\text{Favoured:}\quad A(\bar{B}_q^0 \to f_{\rm CP}\gamma_L) = a_L e^{i\delta_L} e^{i\phi_L} \\ &\qquad\Rightarrow\ A(B_q^0 \to f_{\rm CP}\gamma_R) = \eta\, a_L e^{i\delta_L} e^{-i\phi_L} , \\ &\text{Suppressed:}\ A(\bar{B}_q^0 \to f_{\rm CP}\gamma_R) = a_R e^{i\delta_R} e^{i\phi_R} \\ &\qquad\Rightarrow\ A(B_q^0 \to f_{\rm CP}\gamma_L) = \eta\, a_R e^{i\delta_R} e^{-i\phi_R} , \end{aligned} \tag{13}$$

where $a_{L(R)}$, $\delta_{L(R)}$ and $\phi_{L(R)}$ are the size, strong phase and weak phase of $A(\bar{B}_q^0 \to f_{\rm CP}\gamma_{L(R)})$, respectively. The terms $\sin(\Delta m_q)$ and $\cosh(\Delta\Gamma_q t/2)$ in Eq. (12) arise from interference of the amplitudes of direct decay, $A(\bar{B}_q^0 \to f_{\rm CP}\gamma_L)$ or $A(B_q^0 \to f_{\rm CP}\gamma_R)$, and the decay via B_q^0-$\bar{B}_q^0$ mixing, $p/qA(B_q^0 \to f_{\rm CP}\gamma_L)$ or $q/pA(\bar{B}_q^0 \to f_{\rm CP}\gamma_R)$. The mixing-induced observables S and A^{Δ} are given by [740]

$$\begin{aligned} S &\approx \frac{2\eta\, r}{1+r^2}\cos(\delta_L - \delta_R)\sin(\phi_q - \phi_L - \phi_R) , \\ A^{\Delta} &\approx \frac{2\eta\, r}{1+r^2}\cos(\delta_L - \delta_R)\cos(\phi_q - \phi_L - \phi_R) , \end{aligned} \tag{14}$$

where $r \equiv |a_R/a_L| \approx |C_7'/C_7|$, ϕ_q is the B_q^0–$\bar{B}_q^0$ mixing phase. The values of S and A^{Δ} are expected to be small in the SM due to the suppression by the ratio $r \approx m_s/m_b$. Since S and A^{Δ} are approximately linearly dependent on r, they are sensitive to even a small increase of right-handed photons.

Currently, the observables S and A^{Δ} are only weakly constrained. The $B^0 \to K_S^0\pi^0\gamma$ decay is a golden channel to study photon polarisation at B factories. The mixing-induced CP asymmetry in this channel has been measured to be $S_{K_S^0\pi^0\gamma} = -0.10 \pm 0.31\,({\rm stat}) \pm 0.07\,({\rm syst})$ [744] and $S_{K_S^0\pi^0\gamma} = -0.78 \pm 0.59\,({\rm stat}) \pm 0.09\,({\rm syst})$ [745] by the Belle and BaBar collaborations, respectively, both consistent with the SM expectation value of roughly $\frac{m_s}{m_b}\sin(2\beta)$. The coefficient of the $\sinh(\Delta\Gamma_d t/2)$ term, A^{Δ}, is inaccessible in B^0 decays due to the tiny value of the B^0 width difference, $\Delta\Gamma_d$.

Reconstruction of $B^0 \to K_S^0\pi^0\gamma$ decays is challenging at the LHCb experiment. Alternatively, LHCb can measure mixing-induced CP violation in $B^0 \to K_S^0\pi^+\pi^-\gamma$ decays through a time-dependent amplitude analysis [664]. A more promising channel to probe right-handed NP is the decay $B_s^0 \to \phi\gamma$. Both S and A^{Δ} can be measured in this channel and they are predicted to be close to zero in the SM [740]:

$$S_{\phi\gamma}({\rm SM}) = 0.000 \pm 0.002 , \quad A_{\phi\gamma}^{\Delta}({\rm SM}) = 0.047 \pm 0.039 .$$

Using data collected in Run 1, the LHCb collaboration studied the tagged time-dependent decay rates of $B_s^0 \to \phi\gamma$, which are shown in Fig. 21. The mixing-induced observables are measured to be [746]

$$\begin{aligned} S_{\phi\gamma} &= 0.43 \pm 0.30\,({\rm stat}) \pm 0.11\,({\rm syst}) , \\ A_{\phi\gamma}^{\Delta} &= -0.67^{+0.37}_{-0.41}\,({\rm stat}) \pm 0.17\,({\rm syst}) , \end{aligned}$$

which are in agreement with the SM expectations.

The $B^0 \to K^{*0} e^+ e^-$ decay in the low-q^2 region offers a powerful probe of right-handed new physics. In the vicinity of the photon pole, the decay amplitudes are dominated by contributions from the electromagnetic Wilson coefficients $C_7^{(\prime)}$. An angular analysis can be performed in a similar way as that in the $B^0 \to K^{*0}\mu^+\mu^-$ case. In the angular distribution, there are two terms arising from interference of the left-handed and right-handed decay amplitudes that are proportional to C_7 and C_7', respectively. For small values of r $(\equiv |C_7'/C_7|)$, the coefficients of these two terms, denoted $A_{\rm T}^{(2)}$ and $A_{\rm T}^{\rm Im}$, are approximately expressed as [738, 747]

$$A_{\rm T}^{(2)} \approx r\,\cos(\phi_L - \phi_R)\,,\ A_{\rm T}^{\rm Im} \approx r\,\sin(\phi_L - \phi_R)\,, \quad (15)$$

where ϕ_L and ϕ_R represent the phases of C_7 and C_7', respectively. Like the mixing-induced observables in $B_s^0 \to \phi\gamma$, $A_{\rm T}^{(2)}$ and $A_{\rm T}^{\rm Im}$ depend approximately linearly on r, thus can provide high sensitivity to right-handed currents in the small r region. Using data collected in Run 1 and Run 2, the LHCb collaboration has measured $A_{\rm T}^{(2)}$ and $A_{\rm T}^{\rm Im}$ to be [748]

$$A_{\rm T}^{(2)} = 0.11 \pm 0.10\,({\rm stat}) \pm 0.02\,({\rm syst})\,,$$
$$A_{\rm T}^{\rm Im} = 0.02 \pm 0.10\,({\rm stat}) \pm 0.01\,({\rm syst})\,.$$

These results are compatible with the following SM predictions calculated using the FLAVIO software package [691]:

$$A_{\rm T}^{(2)}({\rm SM}) = 0.033 \pm 0.020\,,$$
$$A_{\rm T}^{\rm Im}({\rm SM}) = -0.00012 \pm 0.00034\,,$$

and provide the most stringent constraint on the $b \to s\gamma$ photon polarisation.

Photon polarisation in $b \to s\gamma$ transitions can also be probed by exploiting the angular correlations in radiative decays of b baryons or charged b mesons. Since current detection technology cannot distinguish left-handed and right-handed photons, the final states with both left-handed and right-handed photons are summed together. The left-handed amplitude A_L and right-handed amplitude A_R add incoherently in the form of $|A_L|^2 + |A_R|^2$, without any interference. In certain cases, the angular distributions allow for determining a parity violation parameter, $A_{\rm parity}$, which is proportional to the photon polarisation [749, 750],

$$A_{\rm parity} \propto \lambda_\gamma \equiv \frac{|A_L|^2 - |A_R|^2}{|A_L|^2 + |A_R|^2} \approx \frac{1 - r^2}{1 + r^2}\,. \quad (16)$$

This approach is powerful in probing large right-handed currents but has limited sensitivity to any small right-handed component.

The LHCb collaboration observed a significantly non-zero up-down asymmetry of the photons in $B^- \to K^-\pi^+\pi^-\gamma$ decays in the range $m_{K\pi\pi} = [1.1, 1.3]\,{\rm GeV}/c^2$ [751] with respect to the plane defined by the three final-state hadrons in their rest frame. This observation demonstrates that the photons are indeed polarised. However, it is nontrivial to translate the measured asymmetry into a constraint on the polarisation parameter λ_γ, due to currently limited knowledge of the structure and decay dynamics of the intermediate resonances involved in this process. A recent theoretical study pointed out that this $m_{K\pi\pi}$ range is dominated by the $K_1(1270)$ resonance and proposed to exploit the charm decay $D \to K_1 e\nu$ to quantify the hadronic effects in $K_1 \to K^-\pi^+\pi^-$ [752], which can be studied at a future Super τ-charm factory [753].

The baryonic decay $\Lambda_b^0 \to \Lambda\gamma$, observed by the LHCb experiment using data collected in 2016 [754], provides a more convenient way to measure the photon polarisation in $b \to s\gamma$ transitions [755–757]. The angular distribution of this process is given by the differential rate

$$\frac{{\rm d}\Gamma}{{\rm d}\cos\theta_p} \propto 1 - \alpha_\Lambda \lambda_\gamma \cos\theta_p\,, \quad (17)$$

where θ_p is the helicity angle of the proton in the Λ rest frame with respect to the opposite direction of the photon, α_Λ is the decay parameter of the weak process $\Lambda \to p\pi^-$. The photon polarisation parameter has recently been measured to be $\lambda_\gamma = 0.82^{+0.17}_{-0.26}({\rm stat})^{+0.04}_{-0.13}({\rm syst})$ [758] by the LHCb experiment using all data from Run 2 and the average of the decay parameter values of Λ and $\bar{\Lambda}$ measured by BESIII, $\alpha_\Lambda = 0.754 \pm 0.004$ [759]. This result is in agreement with the SM predictions from Refs. [760–762]. The LHCb experiment also searched for the decay $\Xi_b^- \to \Xi^-\gamma$ using Run 2 data and found no signal [763].

3.5 Other rare decays of beauty hadrons

Besides the $b \to s\ell^+\ell^-$ decays discussed above, the LHCb experiment has also performed studies of other rare decay processes of beauty hadrons. These include: lepton-flavour violating decays $B^0 \to K^{*0}\tau^\pm\mu^\mp$ [764], $B^0 \to K^{*0}\mu^\pm e^\mp$ and $B_s^0 \to \phi\mu^\pm e^\mp$ [765], $B^+ \to K^+\mu^-\tau^+$ [766], $B^+ \to K^+\mu^\pm e^\mp$ [767], $B_{(s)}^0 \to \tau^\pm\mu^\mp$ [768], $B_{(a)}^0 \to e^\pm\mu^\mp$ [769]; lepton- and baryon-number violating decays $B_{(s)}^0 \to p\mu^-$ [770]; $b \to d\ell^+\ell^-$ decays $B_s^0 \to K^{*0}\mu^+\mu^-$ [771], $\Lambda_b^0 \to p\pi^-\mu^+\mu^-$ [772], $B^+ \to \pi^+\mu^+\mu^-$ [773]; annihilation-type decays $B^0 \to \phi\mu^+\mu^-$ [774], $B^0 \to J/\psi\phi$ [775]. Due to the limited space, the results of these studies are not included in this review.

4 CP violation in beauty and CKM parameters

CP violation is a necessary condition to explain the matter-dominated universe. While the SM with the CKM mechanism can account for the current experimental results on CP violation, it fails to explain the cosmological

matter–antimatter imbalance. Searching for new sources of CP violation is one of the primary goals of flavour physics. This can be done by overconstraining the CKM matrix using measurements of the matrix elements in many different processes.

The decays of b-hadrons provide a number of key measurements to access the five CKM matrix elements related to the b or t quark. Taking advantages of the intense source of b-hadrons at the LHC and a detector designed to probe CP violation in heavy-flavour decays, the LHCb experiment has been the leading experiment in the field of B physics in the past ten years, and achieved some of the most precise measurements of CP violation and mixing of B mesons. Particularly, the precision of the CKM angle γ is now approaching that of the indirect determination; the CP violation parameter ϕ_s and mixing parameter Δm_s of the B_s^0 system, which are key observables for NP searches, have been pinned down with unprecedented precision.

This section describes the key measurements of the CKM elements in the beauty sector by the LHCb experiment using the data taken in Run 1 and Run 2. The parameters γ, ϕ_s and Δm_s, which have received the most significant improvements, are discussed in detail. Other observables related to CKM global fit will also be discussed briefly while many other interesting topics, such as CP violation in b-baryon decays, are not mentioned.

4.1 CKM angle γ

The angle γ, defined as $\arg[-(V_{ud}V_{ub}^*)/(V_{cd}V_{cb}^*)]$, is one of the key observables related to the CKM matrix. As can be seen from Fig. 29, one of the main limitations of global constraints comes from the angle γ. To be noted, the fits have already included recent γ measurements from LHCb which improves the sensitivity on γ from 14°, established at the era of B-factories, to around 5°. Future improvements on the sensitivities on γ can be foreseen with the upgrade of LHCb and running of the Belle II experiment. In the following sections, we briefly overview the main developments on γ measurements in the past several years from the LHCb experiment.

The direct determination of the angle γ is obtained through interference between $b\to c$ and $b\to u$ tree-level processes, where new physics hardly enters [776]. The hadronic parameters of the system are all determined from experimental data and related theoretical uncertainty is negligible [777]. The direct γ measurements thus serve as key inputs for SM predictions, which can be compared with other NP sensitive measurements to search for physics beyond the SM.

Several methods have been proposed to measure the angle γ, based on the types of D decays. In this paper, when not specified, D means a mixture state of D^0 and $\overline{D}^0$. The GLW method [778, 779] refers to those decays with D into a CP eigenstate or multi-body D decays which can be effectively considered as a CP eigenstate using a CP-even fraction F_+. The ADS method [780] refers to two-body D decays or multi-body D decays where the detailed structures over phase space are considered by introducing a global coherent factor R_D and an effective strong phase δ_D. In this case, the interference happens between $b\to c$ transition, with D decaying into doubly-Cabibbo-suppressed final states, and $b\to u$ transition, with D decaying into Cabibbo favoured final state. The BPGGSZ method [781–783] refers to D decaying into multi-body final state where the phase space is binned to make full use of the statistic power of the decay. In addition, the angle γ can also be extracted from time-dependent CP violation measurements of B_s^0 decays. The measurements from the LHCb experiments with these methods are discussed in detail in the following section.

4.1.1 GLW and ADS measurements

The GLW and ADS channels are usually considered together for their similarities in their final states and experimental treatments. The GLW and ADS measurements have been performed in many decay channels to obtain the best sensitivity on γ. The full list of the measured channels can be found in Ref. [784].

The decay rate of the GLW method is

$$\Gamma(B^-\to D[\to f_{\rm GLW}]h^-) \propto 1 + r_B^2 + 2\kappa_B r_B(2F_+ - 1)\cos(\delta_B - \gamma), \quad (18)$$

where $F_+ = 1(0)$ means a pure CP-even (CP-odd) state while decays with $F_+ = 0.5$ does not have any sensitivity on γ. The value of F_+ can be determined from quantum-coherent data from BESIII and CLEO-c experiments in a model-independent way. For example, the decays $B^-\to DK^-$, $D\to\pi^+\pi^-\pi^0$ and $D\to K^+K^-\pi^0$ have been used to measure the angle γ in LHCb using the measured $F_+^{\pi^+\pi^-\pi^0}$ and $F_+^{K^+K^-\pi^0}$ of 0.973 ± 0.017 and 0.73 ± 0.06, respectively [785]. One can see that almost full sensitivity can be achieved in the $\pi^+\pi^-\pi^0$ channel without considering structures over the phase space while further binning the phase space of $K^+K^-\pi^0$ will help get more sensitivity due to small $F_+^{K^+K^-\pi^0}$. In fact, the amplitude analyses of $D^0\to\pi^+\pi^-\pi^0$ and $D^0\to K^+K^-\pi^0$ channels have both been performed [786–789]. The relative strong phase between $D^0\to\rho^+\pi^-$ and $D^0\to\rho^-\pi^+$ is $(-2.0\pm0.8)°$ while that between $D^0\to K^*(892)^+K^-$ and $D^0\to K^*(892)^-K^+$ is $(-37.0\pm2.9)°$, this is consistent with the fact that $F_+^{\pi^+\pi^-\pi^0}$ is close to 1 and is much larger than $F_+^{K^+K^-\pi^0}$. The parameters r_B and δ_B are the amplitude ratio and phase difference between $b\to u$ and $b\to c$ processes, κ_B is the coherent factor to take into account the sensitivity lost due to contamination of other contributions when the bachelor h is a broad resonant structure, e.g.,

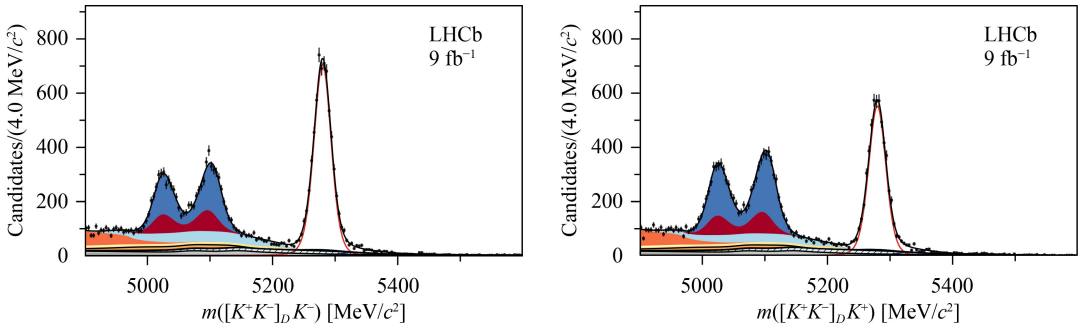

Fig. 22 The invariant mass distributions of $(K^+K^-)_D K^+$ (left) and $(K^+K^-)_D K^-$ (right) from Ref. [792].

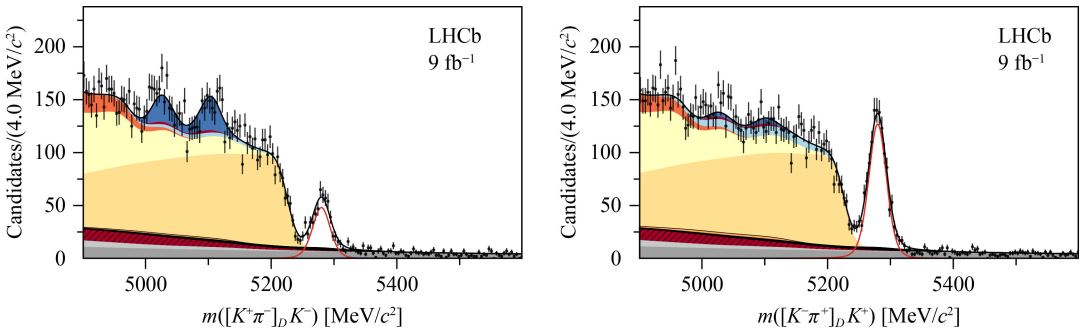

Fig. 23 The invariant mass distributions of $(K^+\pi^-)_D K^+$ (left) and $(\pi^+K^-)_D K^-$ (right) from Ref. [792].

$K^*(892)$. The coherent factor κ_B is obtained based on amplitude models used to describe multi-body B decays. In Eq. (18) only B^- is written; however, it also applies for B^0 decays. The sensitivity of γ is directly linked to the size of r_B and κ_B, larger $r_B \times \kappa_B$ gives better sensitivity on γ. The CP measurements from the GLW channels are only sensitive to $\cos(\delta_B - \gamma)$ which has four-fold ambiguity on determination of angle γ.

In the GLW modes, as D decays into CP eigenstates, in case of no CP violation in D decays, the decay amplitudes and their phases are the same for D^0 and $\overline{D}^0$. However, LHCb has discovered direct CP violation in $D^0 \to K^+K^-$ and $D^0 \to \pi^+\pi^-$ by looking at the difference of CP violation between the two decay channels [790]. This indicates small difference of amplitudes and phases between the two channels, which affects γ determination. Studies [791] show that the effect on γ determination is smaller than 0.5°. The CP violation measured between $D^0 \to K^+K^-$ and $D^0 \to \pi^+\pi^-$ has been considered in the LHCb γ combinations shown later.

Based on Eq. (18), the angle γ can be accessed by measuring the relative decay rate difference for B^+ and B^- mesons. An example of the decay rate difference can be seen directly from the raw yields of the invariant mass distributions of the decays $B^\pm \to D(\to K^+K^-)K^\pm$ as shown in Fig. 22. The figures are from the latest LHCb measurements using 9 fb^{-1} data [792]. By further considering the production asymmetry of B^+ and B^- and detection efficiency difference between K^+ and K^-, the size of the CP violation of the decay can be determined.

The decay rate of the ADS channel has a similar form of

$$\Gamma(B^- \to D[\to f_{\rm ADS}]h^-) \propto r_D^2 + r_B^2 + 2\kappa_B r_B r_D R_D \cos(\delta_D + \delta_B - \gamma), \quad (19)$$

where r_D and δ_D are the average amplitude ratio and phase difference between doubly Cabibbo-suppressed and Cabibbo-favoured D decays. The value of r_D is at similar magnitude as r_B and thus leads to larger CP violation. However, the statistics of the ADS channel is also suppressed. This can be seen from the measurements done by the LHCb experiment using $B^\pm \to (K^\mp\pi^\pm)K^\pm$ decays as show in Fig. 23 [792]. The measurements also have four-fold ambiguity, however, as δ_D is not zero, combining with GLW mode gives two-fold ambiguity on determination of angle γ.

The coherent factor R_D equals to one for two-body final states and is less than one for multi-body final states to take into account dilutions due to different resonant contributions from Cabibbo-favoured and doubly-Cabibbo-suppressed D decays. The values of r_D, R_D and δ_D can also be determined using the quantum-coherent data from BESIII and CLEO-c experiments. For example, the coherent factor of $D^0(\bar{D}^0) \to K^+\pi^+\pi^-\pi^-$, $R_{K3\pi}$ is measured by the two experiments to be $0.43^{+0.17}_{-0.13}$ [793], which is significantly lower than one. Further binning the phase space according to the variation of

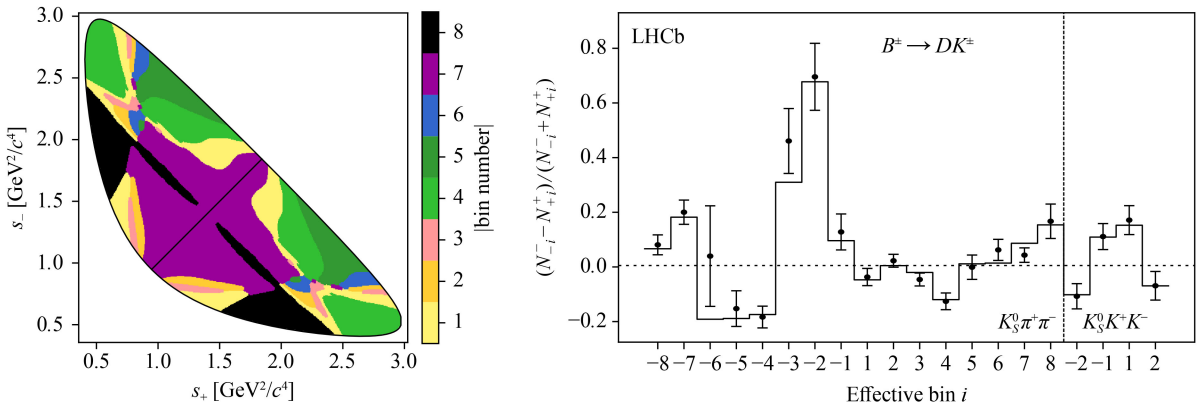

Fig. 24 (Left) Binning scheme of $D\to K^0_S\pi^+\pi^-$ decays used for γ measurements; (right) Observed raw CP asymmetries and the predicted values using obtained CP parameters in different bins [802].

strong phase determined from amplitude analysis can improve the sensitivity on γ [794], and a first measurement using this approach is recently published [795].

The GLW and ADS measurements have been performed by the LHCb experiment with D decaying mainly into charged final states. However, final states with neutral particles are also studied, either by reconstructing the neutral particles π^0 or γ as in recent study of $B^\pm\to Dh^\pm, D\to h^\pm h'^\mp\pi^0$ [796], or in a partially reconstructed method, where π^0 and γ from D^{*0} are not reconstructed [792]. In the second case, the reconstruction efficiency is much higher, however, the sensitivity of γ is limited by the background contributions, especially those from $B^0\to D^{*-}K^+$ decays which has similar lineshapes as signal.

4.1.2 Measurements using the GGSZ method

As has discussed in the above section, for multi-body D decays, if CP even fraction F_+ for self-conjugated decay or coherent factor R for semi-flavour tagged decay is significantly smaller than one, further sensitivity can be achieved by considering the variation of r_D and δ_D over the phase space. One can model the D decays with an amplitude model which provides the information of strong phase δ_D over the phase space. However, this may suffer from large systematic uncertainties due to modelling of amplitude distributions.

An alternative method [782, 783] is to bin the phase space and the effective r^i_D and δ^i_D (or c_i and s_i) in bin i are defined as

$$c_i+is_i\equiv R^i_D e^{i\delta^i_D}\equiv\frac{\int_{\text{bin}i}A_f(p)\overline{A}_f(p)^*\mathrm{d}p}{\sqrt{\int_{\text{bin}i}|A_f(p)|^2\mathrm{d}p}\sqrt{\int_{\text{bin}i}|\overline{A}_f(p)|^2\mathrm{d}p}}. \tag{20}$$

The GGSZ mode refers to decays into self-conjugated final states. BPGGSZ is used when referring to the analysis method using a binned strategy. In the BPGGSZ analysis, c_i and s_i are used instead of effective R_D and δ_D for the benefit of better statistical performance. The values of c_i and s_i can be determined using quantum coherent data collected by BESIII and CLEO-c experiments, where a mixture of D^0 and $\overline{D}^0$ can be achieved from $\psi(3770)\to D^0\overline{D}^0$. As $\psi(3770)$ is a parity-odd state, the D^0 and $\overline{D}^0$ are in quantum-correlated state of $(|D^0\overline{D}^0\rangle-|\overline{D}^0D^0\rangle)/\sqrt{2}$ [797–800]. Using the measured c_i and s_i values, the angle γ and strong parameters r_B and δ_B can be extracted. The method has been applied to $B^-\to DK^-$, $D\to K^0_S\pi^+\pi^-$ and $D\to K^0_S K^+K^-$ decays by LHCb [801, 802], where 16 bins and 4 bins are used according to the statistics of the decays, respectively. In order to optimise the sensitivity, binning schemes are chosen according to the strong phase variation over the Dalitz plot considering possible background contamination and efficiency effects. Symmetry between $K^0_S\pi^+(K^0_SK^+)$ and $K^0_S\pi^-(K^0_SK^-)$ is also used to increase the sensitivity on c_i and s_i. The binning scheme optimised for the $K^0_S\pi^+\pi^-$ decays is shown in Fig. 24 [798, 799].

Each bin of the BPGGSZ method can offer constraints to the angle γ and to the strong parameters r_B and δ_B. The number of measurements is much more than the number of unknown parameters, thus global production asymmetry and detection asymmetry can be treated as fit variables and related systematic uncertainties are reduced. While for the ADS and GLW methods, production asymmetry and detection asymmetry have to be considered using control channels. The measured yield difference in each bin is shown in Fig. 24 for the $K^0_S\pi^+\pi^-$ and $K^0_SK^+K^-$ decays. Clear CP violation can be found. By combining the statistical power of these bins, the angle γ is measured to be $(68.7^{+5.2}_{-5.1})^\circ$ [802].

4.1.3 Multi-body B decays

Similar to multi-body D decays, multi-body B decays

can also be used where r_B and δ_B now is a function of B decay Dalitz plot. However, in this case, one can only use a model to describe different resonant contributions, where some can only be obtained through $b\to c$ process and some can be obtained through both $b\to c$ and $b\to u$ processes and the interference between them gives sensitivity to the angle γ. The measurements have been performed by the LHCb collaboration in $B^0\to DK^+\pi^-$ decays with $D\to K^+K^-(\pi^+\pi^-)$ [803] using 3 fb^{-1} Run 1 data. However, due to limited statistics, the sensitivity on γ is still low. Further measurements with all the data collected by the LHCb experiment will be very interesting.

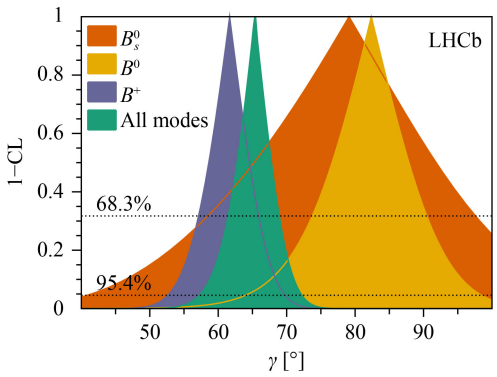

Fig. 25 γ combinations from different B hadrons [784].

4.1.4 Time-dependent B_s^0 decays

The angle γ can be measured through time-dependent B_s^0 and B^0 decays where the weak phases extracted are $(\gamma-2\beta_s)$ and $(\gamma+2\beta)$, respectively. In hadron collider experiments like LHCb, the golden channels are $B_s^0\to D_s^\pm K^\mp$, $B_s^0\to D_s^\pm K^\mp\pi^+\pi^-$ and $B_s^0\to D\phi$ decays. The time-dependent analyses have been performed for the first two channels [804, 805], while only branching fraction has been measured for the $B_s^0\to\overline{D}^0\phi$ decay [806, 807].

As B_s^0 mixing is involved, a time-dependent analysis is needed to extract CP parameters. The time-dependent decay rate of the B_s^0 decay into a final state f is given by

$$\frac{\mathrm{d}\Gamma_{B_s^0\to f}(t)}{\mathrm{d}t}\propto \mathrm{e}^{-\Gamma_s t}\Big[\cosh\left(\frac{\Delta\Gamma_s t}{2}\right)+A_f^{\Delta\Gamma}\sinh\left(\frac{\Delta\Gamma_s t}{2}\right) + C_f\cos(\Delta m_s t)-S_f\sin(\Delta m_s t)\Big], \tag{21}$$

where $\Delta\Gamma_s=\Gamma_{B_L}-\Gamma_{B_H}$ and $\Delta m_s=m_{B_H}-m_{B_L}$ are the decay-width and mass differences between the light (B_L) and heavy (B_H) B_s^0 mass eigenstates and Γ_s is the average B_s^0 decay width. For the decays to the CP-conjugated final states, the CP violation parameters C_f, S_f and $A_f^{\Delta\Gamma}$ are replaced with $C_{\overline{f}}$, $S_{\overline{f}}$ and $A_{\overline{f}}^{\Delta\Gamma}$. These CP violation parameters are related with γ through

$$\begin{aligned}
C_f &= -C_{\overline{f}}=\frac{1-r_B^2}{1+r_B^2},\\
S_f &= \frac{2r_B\sin(\delta_B-(\gamma-2\beta_s))}{1+r_B^2},\\
S_{\overline{f}} &= \frac{-2r_B\sin(\delta_B+(\gamma-2\beta_s))}{1+r_B^2},\\
A_f^{\Delta\Gamma} &= \frac{-2r_B\cos(\delta_B-(\gamma-2\beta_s))}{1+r_B^2},\\
A_{\overline{f}}^{\Delta\Gamma} &= \frac{-2r_B\cos(\delta_B+(\gamma-2\beta_s))}{1+r_B^2}
\end{aligned} \tag{22}$$

following the definitions in Ref. [808]. In the formulae above, we have assumed no CP violation in either the mixing and in the decay amplitude.

The time-dependent CP violation has been measured using 3.0 fb^{-1} and 9.0 fb^{-1} data for $B_s^0\to D_s^\pm K^\mp$ [805] and $B_s^0\to D_s^\pm K^\mp\pi^+\pi^-$ [804], respectively. The measured values of the angle γ, using the world-average value of $-2\beta_s$, are $\gamma=(128^{+17}_{-22})^\circ$ and $\gamma=(44\pm12)^\circ$, respectively (modulo 180°). The $B_s^0\to D_s^\pm K^\mp\pi^+\pi^-$ is complicated due to multiple bachelor particles, and an amplitude analysis is needed. However, as discussed before, multi-body B decays effectively introduce a dilution factor κ, as Eq. (22) have five constraints while together with κ, there are four unknown variables. The measurement is performed in the same paper in a model-independent way, which leads to $\gamma=(44^{+20}_{-13})^\circ$. The sensitivity is worse than model-dependent results as expected.

Sensitivity studies with $B_s^0\to D\phi$ using a time-integrated method has also been performed [809], the expected statistical sensitivity of γ is about $(8-19)^\circ$ using the 9 fb^{-1} pp collision data collected by the LHCb experiment. It is pointed out that additional sensitivity on γ can be achieved using the longitudinal polarised part of $B_s^0\to D^*\phi$ decays with a partially reconstructed technique [807]. Besides, further sensitivities on γ can also be obtained by using other quasi-two-body decays in $B_s^0\to DK^+K^-$ decays [810].

4.1.5 Combination on γ

A combination of the parameter γ was recently performed using all available results of γ measurements from the LHCb experiment [784]. The determination of γ relies on the inputs from charm decays; on the other hand, precise γ measurements and strong parameters of B decays can offer valuable constraints on the charm parameters, which in turn helps constraining the mixing parameters of D^0 mesons. Therefore, the measurements that are sensitive to the charm mixing parameters are also used in the combination. The CKM angle γ and charm mixing parameters are simultaneously determined with significant improvements. Here we focus on the γ

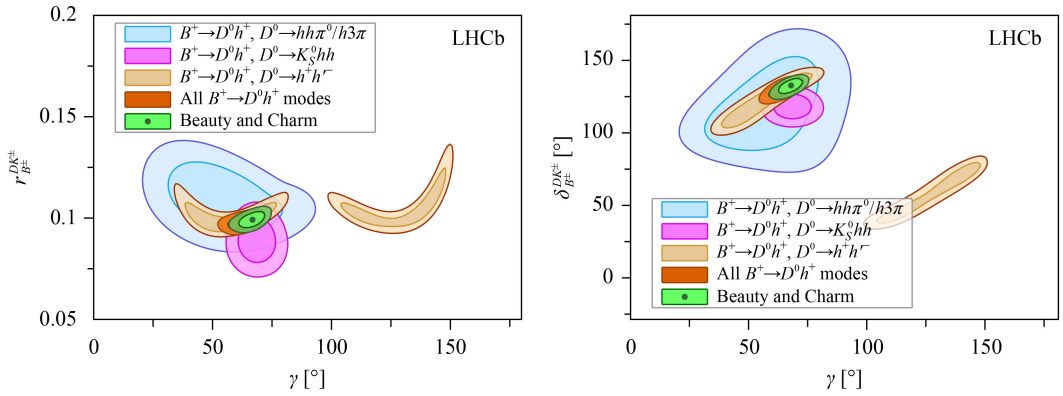

Fig. 26 Combinations of γ from all LHCb measurements, 2D contours of r_B vs. γ (left) and δ_B vs. γ (right) have been shown at 68.3% confidence level [784].

combination results, leaving those on the charm mixing parameters to be discussed later in Section 5.1.

Figure 25 shows the γ contributions from different B decays. The sensitivity on γ mainly comes from B^+ decays. For B^0 and B_s^0 decays, where multi-body decays are usually involved, only a few channels have been studied due to the complications in analysis procedures. The small sample sizes and small number of available measurements limit their sensitivity on γ. The central values of γ determination from B^0 and B_s^0 are around 20° higher, which motivates further measurements with the B^0 and B_s^0 mesons to check overall consistency between different B mesons. Special efforts to the B_s^0 meson are well worth, since the B_s^0–$\bar{B}_s^0$ mixing is involved and new physics contributions can easily enter inside.

The 1σ contour of the constraint on γ and strong parameters of B^+ decays are shown in Fig. 26. Ambiguities on determination of γ from two-body D decays can be seen as has been discussed in Section 4.1.1, however, they constrain the parameter space into a very narrow region and together with the unique determination of γ from the BPGGSZ channel, γ can be precisely obtained. The combined γ is found to be $\gamma = (65.4^{+3.8}_{-4.2})°$ and is the most precise determination from a single experiment.

4.2 CKM angle β

The angle β, defined as $\arg(-V_{cd}V_{cb}^*/V_{td}V_{tb}^*)$, is approximately the phase of V_{td}^* in the Wolfenstein parameterisation [811]. It enters the decay time distributions of B^0 and $\bar{B}^0$ meson decays due to B^0–$\bar{B}^0$ oscillation. The effective value of $\sin(2\beta)$, which could have been altered by NP contributions in B^0–$\bar{B}^0$ mixing, can be extracted from the time-dependent CP asymmetries of B^0 decays via $b\to c\bar{c}s$ transitions following the relation

$$A_{CP}(t) = \frac{\Gamma(\bar{B}^0(t)\to f_{CP}) - \Gamma(B^0(t)\to f_{CP})}{\Gamma(\bar{B}^0(t)\to f_{CP}) + \Gamma(B^0(t)\to f_{CP})} \approx \eta_f \sin(2\beta)\sin(\Delta m t)\ , \quad (23)$$

where f_{CP} is a CP eigenstate with eigenvalue η_f, and the approximation assumes no CP violation in the mixing or decay. Any significant deviation of the measured $\sin(2\beta)$ value from the indirect determination of $\sin(2\beta)$ through a global CKM fit excluding $\sin(2\beta)$ measurements is a clear sign of NP.

The $c\bar{c}$ pair could appear either in a charmonium meson or in two charmed mesons in the final state. The precision of the β is mainly driven by B^0 decays to charmonium final-states due to their large decay rates and distinct characteristics for identification. The world-average of $\sin(2\beta)$ of all the charmonium measurements is $\sin(2\beta) = 0.699 \pm 0.017$ [812]. The LHCb experiment has performed measurements of $\sin(2\beta)$ in the decays $B^0\to J/\psi(\to\mu^+\mu^-)K_S^0$ [813], $B^0\to J/\psi(\to e^+e^-)K_S^0$ and $B^0\to\psi(2S)(\to\mu^+\mu^-)K_S^0$ [814]. The combined value is $\sin(2\beta) = 0.760 \pm 0.034$, the precision of which is already comparable to that of the BaBar result $\sin(2\beta) = 0.09 \pm 0.03 \pm 0.01$ [815] and the Belle result $\sin(2\beta) = 0.67 \pm 0.02 \pm 0.01$ [816]. An improvement by a factor of two is expected from measurements including LHCb Run 2 data.

The presence of small penguin contributions in $b\to c\bar{c}s$ processes may shift the measured values of $\sin(2\beta)$ by up to few percent [817]. The decays via tree-level $b\to c\bar{u}d$ transitions, though having smaller signal yields due to the small branching fractions of D decays, are free of the penguin effects and thus theoretically clean. A recent joint analysis of the decay $\overline{B}^0\to Dh^0$ with $D\to K_S^0h^+h^-$ by the BaBar and Belle experiments measured $\sin(2\beta) = 0.80 \pm 0.14 \pm 0.04 \pm 0.03$ and $\cos(2\beta) = 0.91 \pm 0.22 \pm 0.09 \pm 0.07$, which ruled out the other solution of β at 7.3σ [818, 819]. Analysis of this decay is challenging at LHCb due to the presence of K_S^0 and π^0 mesons in the final state. On the other hand, the decay $\overline{B}^0\to D\pi^+\pi^-$ followed by $D\to K^+K^-(\pi^+\pi^-)$ only involves charged particle and thus is ideal for LHCb to pursue.

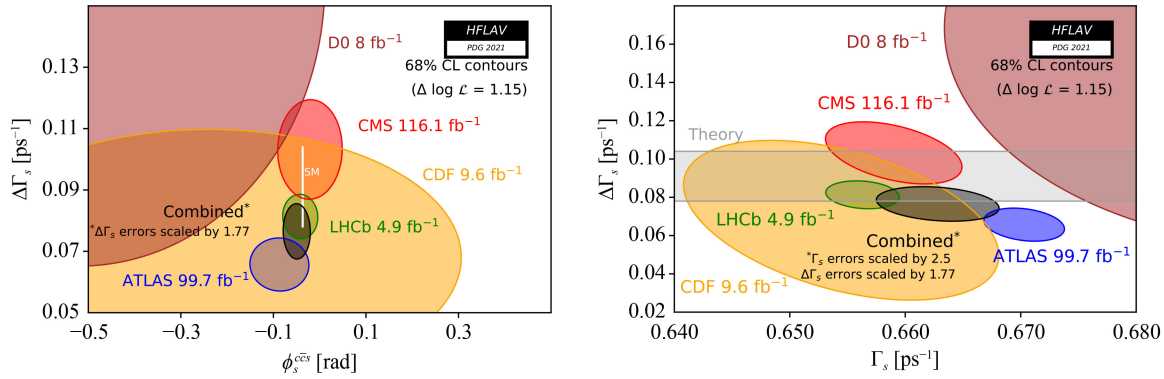

Fig. 27 Combination of $\phi_s^{c\bar{c}s}$ measurements by HFLAV [812], where 2D contours of (left) $\phi_s^{c\bar{c}s}$ vs $\Delta\Gamma_s$ and (right) Γ_s vs $\Delta\Gamma_s$ are displayed at 68% confidence level.

4.3 CKM angle β_s

The angle β_s, defined as $-\arg(-V_{cb}V_{cs}^*/V_{tb}V_{ts}^*)$, is approximately the phase of V_{ts} in the Wolfenstein parameterisation. The effective value of $-2\beta_s$ can be measured in the time-dependent CP asymmetries of B_s^0 decays to CP eigenstates via $b\to c\bar{c}s$ transitions, and is denoted $\phi_s^{c\bar{c}s}$. In contract to the angle β, β_s is very small. The SM prediction for ϕ_s is $\phi_s^{\rm SM} = -2\beta_s = -0.03696 \pm 0.0004$ [820], which is subject to small corrections due to the neglected penguin contributions in $b\to c\bar{c}s$ decays. Presence of new particles in B_s^0–$\bar{B}_s^0$ mixing diagrams may have a sizeable effect on ϕ_s, making it a sensitive probe of physics beyond the SM.

The LHCb experiment has performed measurements of $\phi_s^{c\bar{c}s}$ in the decays $B_s^0\to J/\psi(\to\mu^+\mu^-)\phi$ [821], $B_s^0\to J/\psi(\to\mu^+\mu^-)\pi^+\pi^-$ [822], $B_s^0\to J/\psi(\to\mu^+\mu^-)K^+K^-$ with $m(K^+K^-) > 1.05\,{\rm GeV}/c^2$ [823], $B_s^0\to\psi(2S)(\to\mu^+\mu^-)\phi$ [824], $B_s^0\to D_s^+D_s^-$ [825] and more recently in $B_s^0\to J/\psi(\to e^+e^-)\phi$ [826]. A combination of the measurements in $B_s^0\to J/\psi(\to\mu^+\mu^-)\phi$ and $B_s^0\to J/\psi(\to\mu^+\mu^-)\pi^+\pi^-$ obtained using data taken during 2011–2016 gives $\phi_s^{c\bar{c}s} = -0.042 \pm 0.025$ rad [821].

The average of all LHCb measurements of $\phi_s^{c\bar{c}s}$ is compared with the ATLAS [827] and CMS [828] results in Fig. 27, where 2-dimensional contours in the plane of $\phi_s^{c\bar{c}s}$ versus the B_s^0 decay width difference ($\Delta\Gamma_s$) are displayed at 68% confidence level [812]. Note ATLAS and CMS have only performed measurements in $B_s^0\to J/\psi(\to\mu^+\mu^-)\phi$ decays, due to constraints from their trigger systems,. The current world-average value is $\phi_s^{c\bar{c}s} = -0.050 \pm 0.019$ rad [812]. In Fig. 27, one can see a good agreement in the $\phi_s^{c\bar{c}s}$ measurements from different measurements. However, some tension is observed for $\Delta\Gamma_s$ and Γ_s. Factors of 2.5 and 1.77 have been applied to scale up the uncertainties of Γ_s and $\Delta\Gamma_s$ in the combination. Further investigations by the relevant experiments are needed to solve this problem. With the uncertainty of $\phi_s^{c\bar{c}s}$ well below its SM value, the study of CP violation in B_s^0 decays enter an era of precision test, and control of the penguin pollution in $\phi_s^{c\bar{c}s}$ using data-driven methods is essential for identification of NP signals in B_s^0–$\bar{B}_s^0$ mixing [829–836]. In this regard, the LHCb experiment has measured CP violation in the penguin-enhanced $b\to c\bar{c}d$ decays $B^0\to J/\psi\rho^0$ [837] and $B_s^0\to J/\psi\bar{K}^0$ [838] decays. The measurements are used to estimate the penguin shift of $\phi_s^{c\bar{c}s}$ measured in $B_s^0\to J/\psi\phi$, assuming $SU(3)$ flavour symmetry. The shift is found to be compatible with zero [838], with an uncertain well below the statistical uncertainties of the current $\phi_s^{c\bar{c}s}$ measurements.

Similar CP-violating phases can also be measured in decays of B_s^0 mesons via $b\to s\bar{s}s$ and $b\to d\bar{d}s$ transitions, denoted $\phi_s^{s\bar{s}s}$ and $\phi_s^{d\bar{d}s}$, respectively. Since these decays are dominated by penguin diagrams with internal top quarks, the phases $\phi_s^{s\bar{s}s}$ and $\phi_s^{d\bar{d}s}$ receive contributions from the decay amplitudes that cancel out the contribution of -2β from the B_s^0–$\bar{B}_s^0$ mixing, resulting vanishing values in the SM predictions. Measurements of these quantities can probe NP in these FCNC decays. LHCb has measured $\phi_s^{s\bar{s}s}$ and $\phi_s^{d\bar{d}s}$ in the $B_s^0\to\phi\phi$ and $B_s^0\to K^*(892)K^*(892)$ decays using data taken during 2011–2016, and the results are $\phi_s^{s\bar{s}s} = -0.073 \pm 0.115 \pm 0.027$ rad [839] and $\phi_s^{d\bar{d}s} = -0.10 \pm 0.13 \pm 0.14$ rad [840], respectively, where the first uncertainties are statistical and the second systematic.

4.4 CKM elements V_{ub} and V_{cb}

The amplitudes of the CKM matrix elements V_{ub} and V_{cb} are measured through semi-leptonic transitions of $b\to u\ell\nu$ and $b\to c\ell\nu$. They have been extensively studied previously in B-factories using the so-called exclusive and inclusive methods, which infer to whether a specific decay channel is used or not. The two approaches suffer from different theoretical and experimental uncertainties and offer important cross-checks between each other. In the inclusive measurements, the Heavy Quark Expansion (HQE) is used as $\Lambda_{\rm QCD}/m_b$ is small and the Operator Product Expansion (OPE) calculates non-perturbative contribu-

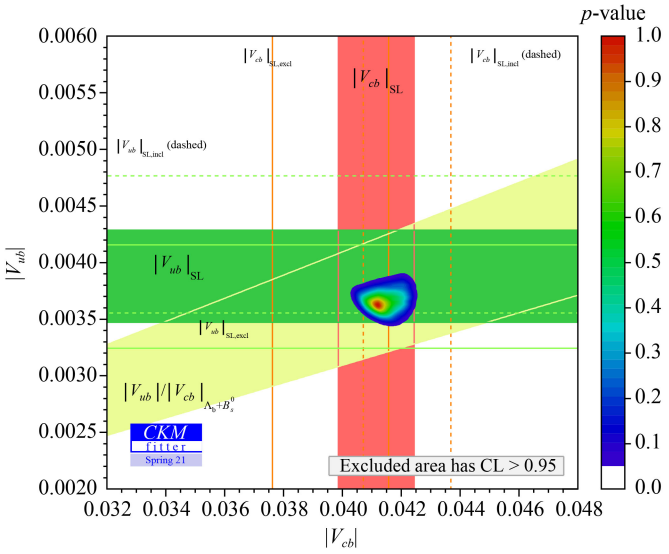

Fig. 28 Global fits of $|V_{ub}|$ and $|V_{cb}|$ from the CKMfitter group [846] where measurements using different methods have been displayed.

tions involved. For the exclusive measurements, parameterisation of the form factor of the corresponding decay is needed, where inputs are obtained from light-cone sum rules (LCSR) [669, 841–845] or from lattice QCD (LQCD). However, tensions have been found between the inclusive and exclusive results as can be seen in Fig. 28 [846]. Efforts from both experimental and theoretical sides are needed to understand the discrepancy.

Unlike B-factories, where full kinematics can be obtained, LHCb can not obtain kinematic information of neutrinos from energy-momentum conservation as it covers only forward region. In addition, background contributions from other b and c hadrons, and also huge combinatorial backgrounds randomly combined from tracks other than signal makes the analyses of semileptonic decays very complicated. Despite of these difficulties, the LHCb experiment has successfully measured the ratio of $|V_{ub}|$ and $|V_{cb}|$ using $\Lambda_b^0 \to p\mu^-\nu_\mu$ ($q^2 > 15\ \mathrm{GeV}^2/c^4$) and $\Lambda_b^0 \to \Lambda_c^+\mu^-\nu_\mu$ ($q^2 > 7\ \mathrm{GeV}^2/c^4$) [847]. The usage of the control channel $\Lambda_b^0 \to \Lambda_c^+\mu^-\nu_\mu$ not only cancels out common systematic uncertainties between the two channels, but also offers a global scale needed to determine $|V_{ub}|$ from branching fractions. Using the updated branching fraction measurement of $\Lambda_c^+ \to pK^-\pi^+$, benefiting from the $\Lambda_c^+\bar{\Lambda}_c^-$ data collected by the BESIII experiment [848], the ratio is determined to be $|V_{ub}|/|V_{cb}| = 0.079 \pm 0.009$.

Using the same approach, the ratio of $|V_{ub}|$ and $|V_{cb}|$ is also determined using $B_s^0 \to K^-\mu^+\nu_\mu$ and $B_s^0 \to D_s^-\mu^+\nu_\mu$ [849]. In the measurement, two q^2 regions are used, $q^2 > 7\ \mathrm{GeV}^2/c^4$ and $q^2 < 7\ \mathrm{GeV}^2/c^4$ where the form factors are obtained from LQCD and LCSR, respectively. However, the ratios of $|V_{ub}|$ and $|V_{cb}|$ obtained from the two methods differ significantly, $|V_{ub}|/|V_{cb}|_{q^2<7\,\mathrm{GeV}^2/c^4} = 0.0607 \pm 0.0015 \pm 0.0013 \pm 0.0008 \pm 0.0030$ and $|V_{ub}|/|V_{ub}|/|V_{cb}|_{q^2>7\,\mathrm{GeV}^2/c^4} = 0.0946 \pm 0.0030^{+0.0024}_{-0.0025} \pm 0.00013 \pm 0.0068$, where the first uncertainty of each result is statistical, the second systematic, the third due to D_s^- branching fraction, and the last one from the form factor. The discrepancy between the two results clearly indicates that more efforts from theoretical side are needed to resolve the tension on $|V_{ub}|$ and $|V_{cb}|$ measurements.

In addition to the ratio between the two CKM matrix elements, the LHCb experiment is also exploring its potential in determine the $|V_{cb}|$ alone using $B_s^0 \to D_s^{(*)-}\mu^+\nu_\mu$ [850]. The branching fraction of $B_s^0 \to D_s^{(*)-}\mu^+\nu_\mu$ is needed to set the global scale for the determination of $|V_{cb}|$. This is obtained using the control channel $B^0 \to D^{(*)-}\mu\nu_\mu$, where the ratios of

$$R = \frac{B_s^0 \to D_s^-\mu^+\nu_\mu}{B^0 \to D^-\mu\nu_\mu}, \tag{24}$$

$$R^* = \frac{B_s^0 \to D_s^{*-}\mu^+\nu_\mu}{B^0 \to D^{*-}\mu\nu_\mu}, \tag{25}$$

are determined. The data from LHCb offer q^2 dependence needed to extract $|V_{cb}|$ together with non-perturbative inputs. Using form factor parameterisations from Caprini, Lellouch and Neubert [851] or from Boyd, Grinstein and Lebed [852, 853], the measured values of $|V_{cb}|$ are $(41.4 \pm 0.6 \pm 0.9 \pm 1.2) \times 10^{-3}$ and $(42.3 \pm 0.8 \pm 0.9 \pm 1.2) \times 10^{-3}$, respectively, where the first uncertainty is statistical, the second systematic, and the last one due to external inputs such as theoretical inputs on form factors, branching fractions of D_s^- or D^- decays, B_s^0 lifetime.

4.5 Δm_d and Δm_s

The parameters Δm_d and Δm_s denote the mass differences between the heavy and light mass eigenstate of the B^0 and B_s^0 systems, and define the oscillation frequencies of B^0 mixing and B_s^0 mixing, respectively. Currently, The most precise determination of Δm_d comes from the LHCb measurements in semileptonic decays with a D^- or D^{*-} meson using 3 fb^{-1} of data. Combining the results obtained in the two decay modes yields $\Delta m_d = (0.5050 \pm 0.0021 \pm 0.0010)\ \mathrm{ps}^{-1}$ [854], where the first uncertainty is statistical and the second systematic. The world-average is $\Delta m_d = 0.5065 \pm 0.0019\ \mathrm{ps}^{-1}$ [812]. The determination of Δm_s is also led by the LHCb experiment. Combining the recent measurements in the decays $B_s^0 \to D_s^-\pi^+$ [855] and $B_s^0 \to D_s^-\pi^+\pi^-\pi^+$ [804] and earlier measurements yields $\Delta m_s = 17.7656 \pm 0.0057\ \mathrm{ps}^{-1}$.

However, the constraints on the CKM matrix elements provided by the Δm_d and Δm_s measurements rely on the decay constants and Bag parameters of the the B^0 and B_s^0 mesons, which are obtained from Lattice QCD calculations [856]. The precision of these hadronic

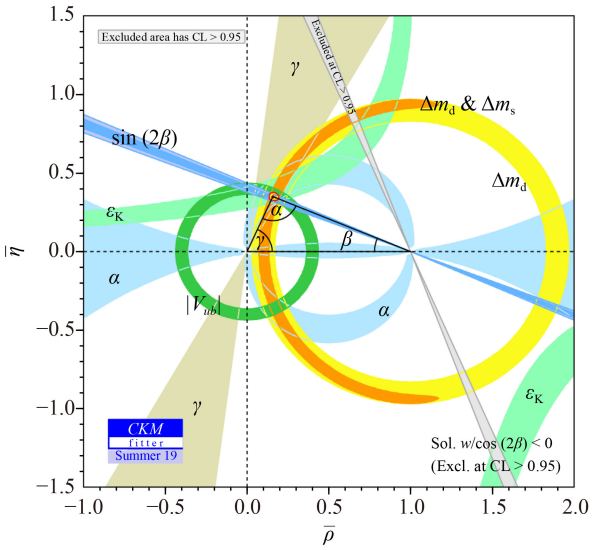

Fig. 29 Global fit results of the CKM matrix from different measurements, provided by the CKMfitter group [846]. Different colours and labels on the plot indicate constraints from measurements of different observables.

parameters is much worse than the experimental precision, thus limits the constraining power of Δm_d and Δm_s on the CKM global fit. Further improvements in Lattice QCD calculations are eagerly awaited.

4.6 Global fit

The four parameters of the CKM matrix, namely A, λ, ρ and η in the Wolfenstein parameterization [811], are measured in different processes and some of the key observables have been discussed in the above sections. A global fit is needed to get the best sensitivity and to probe NP effects. The χ^2 value of the fit provides a measure of the overall consistency between the different measurements, while the pull value for each measurement quantifies the difference between the measured value and value predicted by the fit results. Clues for new physics can be identified from large χ^2 or pull values.

The constraining of the CKM matrix is usually illustrated in complex planes using triangles defined using unitarity relations of the CKM matrix. The most commonly quoted CKM triangle corresponds to the relation $V_{ud}V_{ub}^* + V_{cd}V_{cb}^* + V_{td}V_{tb}^* = 0$, where V_{ij} is the CKM matrix element between the quarks of the flavours i and j. The results of the state-of-the-art global fit are shown in Fig. 29 provided by the CKMfitter group [820]. Inside, $\bar{\rho}$ and $\bar{\eta}$ [857] are used to ensure the relationship $\bar{\rho} + i\bar{\eta} = -(V_{ud}V_{ub}^*)/(V_{cd}V_{cb}^*)$.

Within current precision, different measurements cross on a single point and give an overall consistent picture. However, the argument of matter-antimatter asymmetry suggests that CP violation from sources beyond the CKM matrix may break the consistency. One of the main efforts of the LHCb experiment is to search for such a discrepancy by further improving measurement precision in the beauty and charm sectors.

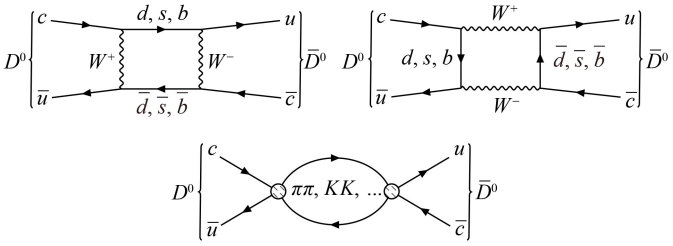

Fig. 30 Oscillation of D^0 mesons via (top) $W^{\pm}$ exchanges or (bottom) rescattering effect.

In the following decade, both the LHCb and Belle II experiments will accumulate much more data to further constrain the CKM matrix. With data collected till 2025, either experiment will be able to reduce the uncertainty of γ to around 1.5°, and further improve it to 0.3° after 2030s. Other CKM angles and matrix elements will also be significantly improved. Details on the future outlook can be found in Section 6.2. Together with improvements of other measurements and lattice calculations, NP may be observed from inconsistency between different measurements.

5 Charm mixing and CP violation

Charm physics covers the studies of hadrons containing charm quarks. CP violation in the charm sector is expected to be incredibly small in the SM, of the order $\mathcal{O}(10^{-3})$ or less [326]. However, the presence of new physics may enhance the amount of CP violation, which can be probed using the enormously large sample of charmed hadrons at LHCb. Particularly, the study of mixing and CP violation of neutral D mesons can provide unique probes of NP in FCNC transitions in the up-type quark sector, complementary to the study of mixing and CP violation in neutral B and K mesons, which are sensitive to NP in FCNC transitions of down-type quarks. For this reason, this section mainly focuses on results in mixing and CP violation of D^0 mesons from the LHCb experiment.

5.1 Neutral D meson mixing

Similar to neutral K^0 and $B^0_{(s)}$ mesons, the neutral charmed meson, D^0, can oscillate to its antiparticle partner, $\bar{D}^0$, via the short-distance $W^{\pm}$ exchange or long-distance rescattering diagrams, as shown in Fig. 30. This phenomenon of oscillation or mixing can be characterised by the normalised (dimensionless) mixing parameters x and y, defined as

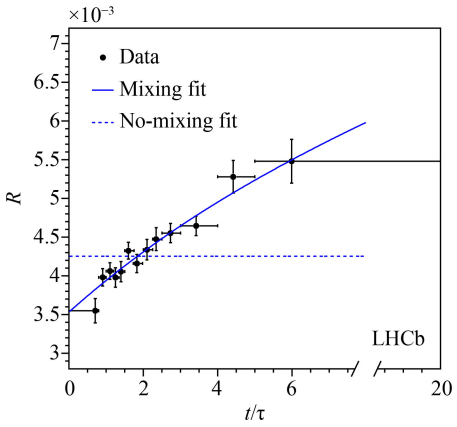

Fig. 31 Ratio of the $D^0 \to K^+\pi$ to $D^0 \to K^-\pi^+$ decay rates, R, as a function of the D^0 decay time normalised by the average D^0 lifetime [863]. The solid (dashed) line indicates the projection of the mixing (no-mixing) fits.

$$x \equiv \frac{\Delta M}{\Gamma}, \quad y \equiv \frac{\Delta\Gamma}{2\Gamma}, \tag{26}$$

where ΔM ($\Delta\Gamma$) is the mass (decay width) difference of the heavy and light mass eigenstates, and Γ is the average decay width. Unlike in the case of the K^0 or $B^0_{(s)}$ system, both x and y in the D^0 system are significantly smaller than unity, thus very large data samples are required to observe D^0 mixing and determine the tiny values of x and y.

Evidence of D^0–$\bar{D}^0$ mixing was first reported by BaBar [858] and Belle [859] in 2007, and later also seen by CDF [860] in 2008. Subsequent measurements by BaBar [861, 862] with different D^0 decay channels provided more evidences of the mixing. The combination of these measurements confirmed the existence of charm mixing with a significance more than 5σ. The first observation of D^0–$\bar{D}^0$ mixing in a single measurement was achieved by LHCb [863] in 2012 by using the data taken in 2011 to study the time-dependent ratio of $D^0 \to K^+\pi^-$ (doubly Cabibbo-suppressed, DCS) to $D^0 \to K^-\pi^+$ (Cabibbo favoured, CF) decay rates. The D^0 candidates are selected from the $D^{*+} \to D^0\pi^+$ decays, where the charge of the pion directly from each D^{*+} decay is used to determine the D^0 flavour at its production time.

The $D^{*+} \to D^0(\to K^-\pi^+)\pi^+$ process, referred to as the right-sign (RS) process, is dominated by a CF decay, contaminated with a small contribution from the D^0–$\bar{D}^0$ mixing followed by the DCS decay; the $D^{*+} \to D^0(\to K^+\pi^-)\pi^+$ process, referred to as wrong-sign (WS) process, includes contributions from both the DCS decay and the D^0–$\bar{D}^0$ mixing followed by the CF decay. Under the assumption of small mixing and negligible CP violation, the time-dependent ratio of the WS to the RS decay rates, R, is given by [864]

$$R(t) \approx R_D + \sqrt{R_D}\, y' \frac{t}{\tau} + \frac{x'^2 + y'^2}{4} \left(\frac{t}{\tau}\right)^2,$$

Table 4 Summary of the charm mixing parameters measured by LHCb using $D^0 \to K^+\pi^-$ decays. Results under the assumptions of CP invariance and CP violation are given.

Data sample	no CPV		CPV allowed	
	x'^2 ($\times 10^{-3}$)	y' ($\times 10^{-3}$)	x'^2 ($\times 10^{-3}$)	y' ($\times 10^{-3}$)
1.0 fb^{-1}, D^* tag [863]	-0.09 ± 0.13	7.2 ± 2.4	–	–
3.0 fb^{-1}, D^* tag [865]	0.055 ± 0.049	2.8 ± 1.0	D^0: 0.049 ± 0.070 $\bar{D}^0$: 0.060 ± 0.068	5.1 ± 1.4 4.5 ± 1.4
3.0 fb^{-1}, B tag [866]	0.028 ± 0.310	4.6 ± 3.7	D^0: -0.019 ± 0.447 $\bar{D}^0$: 0.079 ± 0.433	5.81 ± 5.26 3.32 ± 5.23
5.0 fb^{-1}, D^* tag [867]	0.039 ± 0.027	5.28 ± 0.52	D^0: 0.061 ± 0.037 $\bar{D}^0$: 0.016 ± 0.039	5.01 ± 0.74 5.54 ± 0.74

Table 5 Summary of the charm mixing parameters measured by LHCb using $D^0 \to K^0_S\pi^+\pi^-$ decays.

Data sample	CP-averaged parameters	
	x ($\times 10^{-3}$)	y ($\times 10^{-3}$)
1.0 fb^{-1}, D^* tag [868]	$-8.6 \pm 5.3 \pm 1.7$	$0.3 \pm 4.6 \pm 1.3$
3.0 fb^{-1}, B tag [869]	$2.7 \pm 1.6 \pm 0.4$	$7.4 \pm 3.6 \pm 1.1$
5.4 fb^{-1}, D^* tag [870]	$3.97 \pm 0.46 \pm 0.29$	$4.59 \pm 1.20 \pm 0.85$
	CP-violating parameters	
Data sample	Δx ($\times 10^{-3}$)	Δy ($\times 10^{-3}$)
3.0 fb^{-1}, B tag [869]	$-0.53 \pm 0.70 \pm 0.22$	$0.6 \pm 1.6 \pm 0.3$
5.4 fb^{-1}, D^* tag [870]	$-0.27 \pm 0.18 \pm 0.01$	$0.20 \pm 0.36 \pm 0.13$

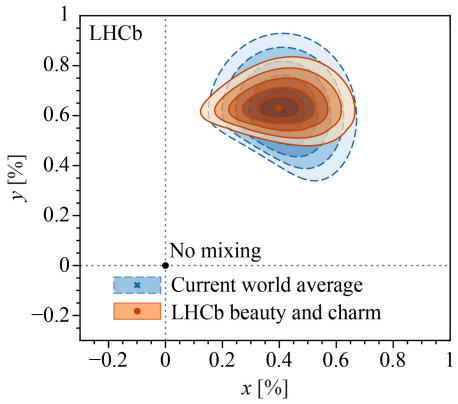

Fig. 32 Profile likelihood contours (from 1 to 5 σ) of the charm mixing parameters x and y. The solid (brown) contours are determined from the simultaneous combination [784], while the dashed (blue) indicate the current world average from Ref. [812].

where t/τ is the decay time normalised to the average D^0 lifetime, R_D is the ratio between the DCS and CF decay rates, and x' and y' are the mixing parameters "rotated" by the strong phase difference δ between the DCS and CF amplitudes: $x' = x\cos\delta + y\sin\delta$ and $y' = y\cos\delta - x\sin\delta$. The time evolution of the ratio R is shown in Fig. 31. Further studies with larger data samples have also been performed by LHCb [863, 865–867] and the results are summarized in Table 4.

The measurements in the $D^0\to K^-\pi^+$ decay are sensitive to the normalised decay-width difference y and the sum x^2+y^2 (under the assumption of negligible CP violation), but not to the sign of the normalised mass difference x. One approach to solve this problem is to study the Dalitz distributions of three-body decays. The "golden channel" at LHCb for such studies is the decay $D^0\to K^0_S\pi^+\pi^-$, where the decay to the $K^0_S\pi^+\pi^-$ final state proceed mainly via the following three processes with different intermediate resonances: i) the $K^0_S\rho^0$ process with $\rho^0\to\pi^+\pi^-$, which is common for both D^0 and $\bar{D}^0$ mesons; ii) the $K^{*-}\pi^+$ process with $K^{*-}\to K^0_S\pi^-$, which is a CF decay; and iii) the $K^{*+}\pi^-$ process with $K^{*+}\to K^0_S\pi^+$, which is either a DCS decay or $D^0-\bar{D}^0$ oscillation followed by a CF decay.

In the Dalitz phase space, the DCS and CF decay amplitudes of the $D^0\to K^0_S\pi^+\pi^-$ decay populate the same space and interfere. Therefore, the parameters x and y can be determined by measuring the strong phase difference between the contributing amplitudes in an amplitude analysis, or by importing the average strong-phase difference in regions of phase space obtained by e^+e^- experiments operating at the energy of the $\psi(3770)$ resonance. The latter approach is employed in several LHCb measurements [868–870], and the most recent measurement [870] led to the first observation of a nonzero mass difference between the two mass eigenstates in the D^0–$\bar{D}^0$ system. The results of these measurements using $D^0\to K^0_S\pi^+\pi^-$ decays are summarised in Table 5.

As mentioned in Section 4.1.5, different from the past LHCb γ combinations, the recent combination exploited the LHCb measurements that are sensitive to the CKM angle γ and to the charm mixing parameters, and the γ angle and charm mixing parameters are simultaneously determined [784]. The motivation for the simultaneous combination is as follows:

- The γ angle and the strong phase difference between the interfering B decays are now so precisely constrained by the large B-meson samples that the strong phase difference, $\delta_D^{K\pi}$, between the decays $D^0\to K^-\pi^+$ and $\bar{D}^0\to K^-\pi^+$ can achieve a precision of about a factor of two better than the previous world average [812]. This improvement can then be used to improve the precision of the charm mixing parameters x and y.
- Due to non-negligible effects originating from charm-meson mixing, a simultaneous combination is needed to obtain an unbiased determination of the γ angle and the charm mixing parameters x and y.

In the charm sector, the inputs used in the combination are obtained from the time-dependent measurements of $D^0\to h^+h^-$, $D^0\to K^+\pi^-$, $D^0\to K^\pm\pi^\mp\pi^+\pi^-$, and $D^0\to K^0_S\pi^+\pi^-$ decays performed by LHCb [790, 866–878]. Figure 32 shows the two-dimensional profile likelihood contours in the x–y plane. The values of x and y, determined in the simultaneous combination, are found to be

$$x = (0.400^{+0.052}_{-0.053})\%, \quad y = (0.630^{+0.033}_{-0.030})\%.$$

These results provide the most precise determinations of the parameters x and y. Particularly, the precision of y is improved by a factor of two with respect to the current world average [812].

5.2 CP violation

5.2.1 Time-integrated CP violation

The time-integrated CP asymmetry, $\mathcal{A}_{CP}$, in the decay $D\to f$ is dominated by the direct CP asymmetry. Its measurement follows the formula

Table 6 Summary of the $\Delta\mathcal{A}_{CP}$ results from the LHCb measurements in the charm sector.

Data sample	$\Delta\mathcal{A}_{CP}$ ($\times10^{-3}$)
0.62 fb^{-1}, D^* tag [879]	$-8.2\pm4.1\pm0.6$
1.0 fb^{-1}, B tag [880]	$4.9\pm3.0\pm1.4$
3.0 fb^{-1}, B tag [871]	$1.4\pm1.6\pm0.8$
3.0 fb^{-1}, D^* tag [872]	$-1.0\pm0.8\pm0.3$
5.9 fb^{-1}, B or D^* tag [790]	-1.54 ± 0.29

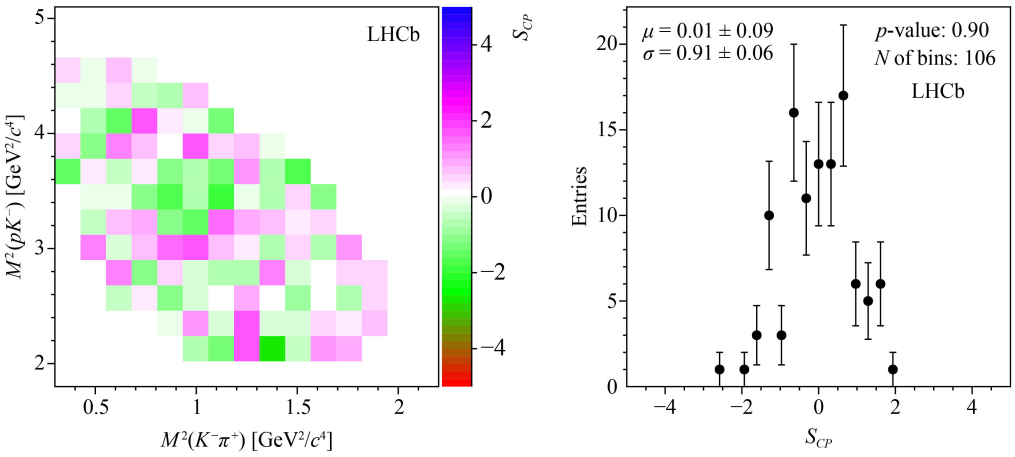

Fig. 33 (Left) Distributions of local per-bin asymmetry significance S_{CP} and (right) corresponding one-dimensional distributions obtained by the binned χ^2 method for $\Xi_c^+ \to pK^-\pi^+$ decays. Reproduced from Ref. [896].

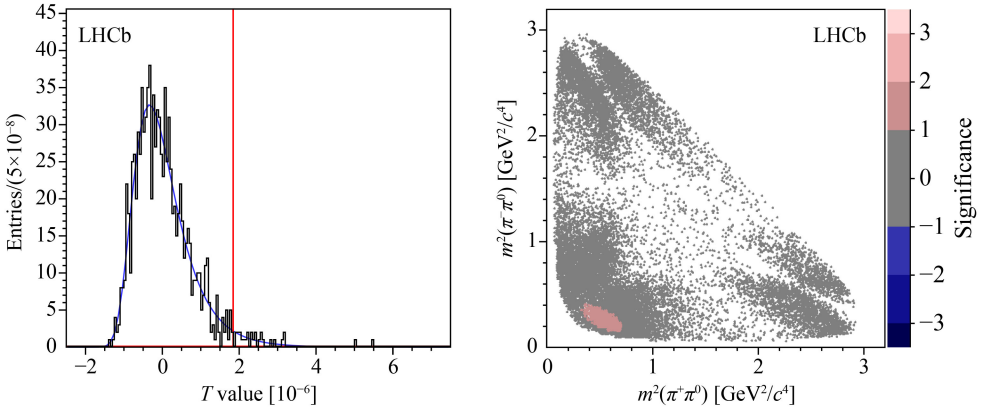

Fig. 34 (Left) The global test statistic compared with the distribution of the statistic calculated from a large number of random permutations obtained from the energy test applied in the CP violation searches in $D^0 \to \pi^-\pi^+\pi^0$ decays. (Right) Dalitz plot distribution of significance of local test statistics. Reproduced from Ref. [897].

$$\mathcal{A}_{CP} = \mathcal{A}_{raw} - \mathcal{A}_{prod} - \mathcal{A}_{det}, \tag{27}$$

where $\mathcal{A}_{prod}$ denotes the meson production asymmetry between the c-hadron and its antiparticle, $\mathcal{A}_{det}$ represents the detection asymmetry, and $\mathcal{A}_{raw}$ is the raw asymmetry between the yields of $D \to f$ and $\overline{D} \to \overline{f}$ decays. Often the difference of CP asymmetries between two different decay processes are measured, which is defined as

$$\Delta\mathcal{A}_{CP} \equiv \mathcal{A}_{CP}(D \to f_1) - \mathcal{A}_{CP}(D \to f_2), \tag{28}$$

where f_1 and f_2 are two different final states with similar topologies. The effects of production asymmetry and CP asymmetries in mixing as well as part of the detection asymmetries on $\Delta\mathcal{A}_{CP}$ are largely cancelled.

Two-body decays of D mesons are particularly interesting due to their super large sample sizes, which are crucial for probing the tiny CP violating effects. The first observation of CP violation in the charm sector was reported by LHCb in 2019 using the Run 2 data [790]. The difference of $\mathcal{A}_{CP}$ between the $D^0 \to K^+K^-$ and $D^0 \to \pi^+\pi^-$ decays, $\Delta\mathcal{A}_{CP} \equiv \mathcal{A}_{CP}(K^+K^-) - \mathcal{A}_{CP}(\pi^+\pi^-)$, was measured with a deviation from zero corresponding to a significance of $5.3\,\sigma$. Table 6 summarises the $\Delta\mathcal{A}_{CP}$ results of a series of LHCb measurements [790, 871, 872, 879, 880].

Several $\mathcal{A}_{CP}$ measurements using two-body decays have been performed by LHCb as well [881–890], and the first evidence of direct CP violation in a specific charm hadron decay was reported in Ref. [890].

While multi-body charm decays often have much smaller sample sizes compared to two-body charm decays, they can provide excellent opportunities for CP violation measurements. The presence of intermediate resonances can lead to large variation of the strong phase difference between the interfering amplitudes, which can lead to sizeable local CP asymmetries. Besides the $\Delta\mathcal{A}_{CP}$ method, several techniques to search

Table 7 Summary of LHCb direct CP violation searches in phase space of charm decays.

Decay channel	Data sample	Method
$D^+ \to K^-K^+\pi^+$ [892]	35 pb^{-1}	binned χ^2
$D^0 \to K^-K^+\pi^-\pi^+$ [893]	1.0 fb^{-1}, D^* tag	binned χ^2
$D^0 \to \pi^-\pi^+\pi^-\pi^+$ [893]	1.0 fb^{-1}, D^* tag	binned χ^2
$D^+ \to \pi^-\pi^+\pi^+$ [894]	1.0 fb^{-1}	binned χ^2
$D^0 \to K^-K^+\pi^-\pi^+$ [895]	3.0 fb^{-1}, B tag	binned χ^2
$D^0 \to \pi^-\pi^+\pi^0$ [897]	2.0 fb^{-1}, D^* tag	energy test
$D^0 \to \pi^-\pi^+\pi^-\pi^+$ [898]	3.0 fb^{-1}, D^* tag	energy test
$\Lambda_c^+ \to ph^-h^+$ [901]	3.0 fb^{-1}	$\Delta\mathcal{A}_{CP}$
$D^0 \to K^-K^+\pi^-\pi^+$ [891]	3.0 fb^{-1}, B tag	amplitude analysis
$\Xi_c^+ \to pK^-\pi^+$ [896]	3.0 fb^{-1}	binned χ^2

for CP violation in multi-body charm decays are exploited by LHCb, including amplitude analysis [891], the binned χ^2 technique [892–896], and an unbinned technique called the energy test [897, 898]. For the latter two methods, model-dependent analyses are eventually required to pin down the source in case significant CP violation were observed.

The binned χ^2 technique computes the distribution of local asymmetries and compare it with a normal distribution to judge if CP violation were observed. An example of binned χ^2 distribution in a Dalitz plot is shown in Fig. 33. This method relies on the optimal choice of the binning scheme. Wide bins across resonances can lead to the cancellation of real CP asymmetries within a bin.

The LHCb collaboration has developed a novel unbinned method, energy test [899, 900], to perform model-independent search for CP violation in many-body decays. With this method, a test statistic, T, is defined. For a given data sample, a p-value for the hypothesis of CP invariance is assigned by comparing the observed value of T to the distribution of T obtained from many random permutations of the data. This method has been applied to search for CP violation in decays of charm mesons and beauty baryons. As an example, Fig. 34 shows the global test statistic compared with the distribution of the statistic from many random permutations, and the Dalitz plot distribution of significance of local test statistics in $D^0 \to \pi^-\pi^+\pi^0$ decays. Despite the many efforts made by LHCb and the significant improvements in the measurement precision, no evidence of CP violation in multi-body charm decays has ever been found to date. Table 7 summarises the searches for direct CP violation in phase space of charm decays by LHCb.

5.2.2 y_{CP} and A_Γ measurements

The amplitudes of the direct decay of D^0 to a CP eigenstate and the decay after mixing can interfere and lead to indirect CP asymmetry. Its contribution to the time-integrated CP asymmetry is denoted $\mathcal{A}_{CP}^{ind}$.

Due to the D^0–$\bar{D}^0$ mixing, the effective decay width of D^0 decays to a CP-even final state (e.g., f=K^+K^- or $\pi^+\pi^-$), Γ_{CP+}, differs from the average decay width Γ. We can define the parameter $y_{CP} \equiv \Gamma_{CP+}/\Gamma - 1$ to represent the amount of CP-violation in mixing. The quantity y_{CP} is related to x and y, $|q/p|$, and $\phi \equiv arg(q\bar{A}/pA)$,

$$y_{CP} \approx \frac{1}{2}\left(\left|\frac{q}{p}\right| + \left|\frac{p}{q}\right|\right) y\cos\phi - \frac{1}{2}\left(\left|\frac{q}{p}\right| - \left|\frac{p}{q}\right|\right) x\sin\phi\,.$$

Only if CP is conserved, y_{CP} is equal to y. The decay rate asymmetry is defined as

$$A_\Gamma \approx \frac{1}{2}\left(\left|\frac{q}{p}\right| - \left|\frac{p}{q}\right|\right) y\cos\phi - \frac{1}{2}\left(\left|\frac{q}{p}\right| + \left|\frac{p}{q}\right|\right) x\sin\phi\,.$$

The asymmetry A_Γ is related to the indirect CP asymmetry $\mathcal{A}_{CP}^{ind}$ through $\mathcal{A}_{CP}^{ind} = -A_\Gamma$.

The quantities y_{CP} and A_Γ can be determined by measuring the ratio of the effective lifetimes of D^0 and $\bar{D}^0$ decays to the same CP eigenstate:

$$y_{CP} = \frac{2\tau(D^0 \to f_{\not CP})}{\tau(\bar{D}^0 \to f_{CP}) + \tau(D^0 \to f_{CP})} - 1, \tag{29}$$

$$A_\Gamma = \frac{\tau(D^0 \to f_{CP}) - \tau(D^0 \to f_{CP})}{\tau(\bar{D}^0 \to f_{CP}) + \tau(D^0 \to f_{CP})}, \tag{30}$$

where $f_{\not CP}$ denotes a non-CP-eigenstate, such as $K^-\pi^+$.

In recent years, LHCb has preformed several measurements of y_{CP} and A_Γ, which are summarized in Table 8 [873–876, 902–904]. A recent study shows that using the average decay width of $D^0 \to K^-\pi^+$ and $\overline{D}^0 \to K^+\pi^-$ decays as a proxy to the average decay width of the neutral charm meson mass eigenstates D_1 and D_2 does not give direct access to y_{CP} but rather corresponds to $y_{CP} - y_{CP}^{K\pi}$ [905], where $y_{CP}^{K\pi}$ is approximately equal to -0.4×10^{-3} [904]. In Ref. [877], an LHCb legacy result of A_Γ combined with both D^* and B flavour tag using 2011–2012 and 2015–2018 data sample is obtained. None of these measurements shows any indication of CP violation in D^0–$\overline{D}^0$ mixing or in the interference between mixing and decay. Figure 35 compares the y_{CP} and A_Γ measurements performed by different experiments, and the averages provided by the Heavy Flavour Averaging Group [812]. The world averages are dominated by the measurements by the LHCb experiment.

6 Prospects and summary

6.1 Upgrade plan of LHCb

The physics output discussed in this review shows that LHCb has successfully deepened our understanding of

Table 8 Summary of LHCb y_{CP} and A_Γ measurements.

Data sample	Final state(s)	y_{CP} [%]	A_Γ ($\times 10^{-3}$)
29 pb^{-1}, D^* tag [902]	K^+K^-	$0.55 \pm 0.63 \pm 0.41$	$-5.9 \pm 5.9 \pm 2.1$
1.0 fb^{-1}, D^* tag [903]	$\pi^+\pi^-$	–	$0.33 \pm 1.06 \pm 0.14$
1.0 fb^{-1}, D^* tag [903]	K^+K^-	–	$-0.35 \pm 0.62 \pm 0.12$
3.0 fb^{-1}, B tag [874]	$\pi^+\pi^-$	–	$-0.92 \pm 2.6^{+0.25}_{-0.33}$
3.0 fb^{-1}, B tag [874]	K^+K^-	–	$-1.34 \pm 0.77^{+0.26}_{-0.34}$
3.0 fb^{-1}, B tag [874]	$\pi^+\pi^-$ & K^+K^-	–	-1.25 ± 0.73
3.0 fb^{-1}, B tag [873]	$\pi^+\pi^-$ & K^+K^-	$0.57 \pm 0.13 \pm 0.09$	–
3.0 fb^{-1}, D^* tag [875]	$\pi^+\pi^-$	–	$0.46 \pm 0, 58 \pm 0.12$
3.0 fb^{-1}, D^* tag [875]	K^+K^-	–	$-0.30 \pm 0.32 \pm 0.10$
3.0 fb^{-1}, D^* tag [875]	$\pi^+\pi^-$ & K^+K^-	–	$-0.13 \pm 2.0 \pm 0.7$
5.4 fb^{-1}, B tag [876]	$\pi^+\pi^-$	–	$0.22 \pm 0.70 \pm 0.08$
5.4 fb^{-1}, B tag [876]	K^+K^-	–	$-0.43 \pm 0.36 \pm 0.05$
6 fb^{-1}, D^* tag [877]	$\pi^+\pi^-$	–	$0.4 \pm 0.28 \pm 0.04$
6 fb^{-1}, D^* tag [877]	K^+K^-	–	$0.23 \pm 0.15 \pm 0.03$
8.4 fb^{-1}, D^* or B tag [877]	$\pi^+\pi^-$	–	$0.36 \pm 0.24 \pm 0.04$
8.4 fb^{-1}, D^* or B tag [877]	K^+K^-	–	$0.03 \pm 0.13 \pm 0.03$
8.4 fb^{-1}, D^* or B tag [877]	$\pi^+\pi^-$ & K^+K^-	–	$0.10 \pm 0.11 \pm 0.03$
6 fb^{-1}, D^* tag [904]	$\pi^+\pi^-$	$0.657 \pm 0.053 \pm 0.016$ [1)]	–
6 fb^{-1}, D^* tag [904]	K^+K^-	$0.708 \pm 0.030 \pm 0.014$ [2)]	–
6 fb^{-1}, D^* tag [904]	$\pi^+\pi^-$ & K^+K^-	$0.696 \pm 0.026 \pm 0.013$ [3)]	–

[1)] $y_{CP}^{\pi\pi} - y_{CP}^{K\pi}$ is measured in this analysis.
[2)] $y_{CP}^{KK} - y_{CP}^{K\pi}$ is measured in this analysis.
[3)] $y_{CP} - y_{CP}^{K\pi}$ is measured in this analysis.

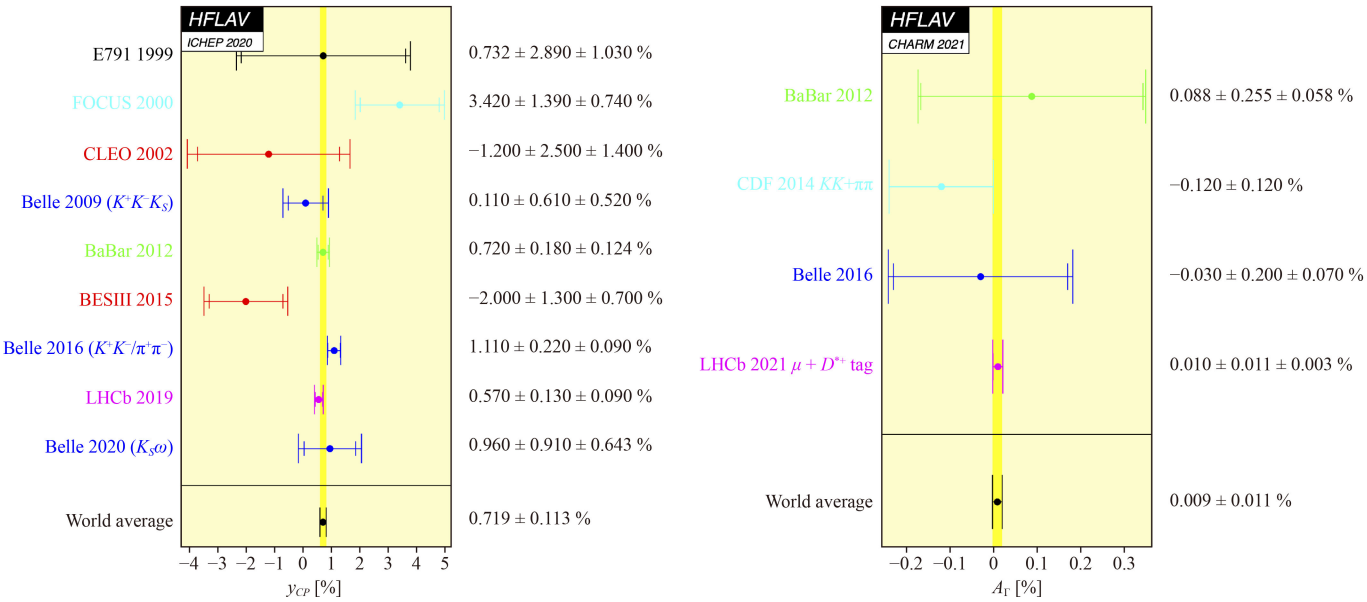

Fig. 35 The world averages of y_{CP} and A_Γ. Reproduced from Ref. [812].

flavour physics with experimental data taken up to the year of 2018. Most of the the key flavour observables are measured to an unprecedented precision, yet it is generally true that the uncertainties are still dominated by statistical fluctuation. To further increase the availability of high-quality collision data, the LHCb detector is currently under a major upgrade [906], known as Upgrade Ia or simply Upgrade I. The installation has almost completed

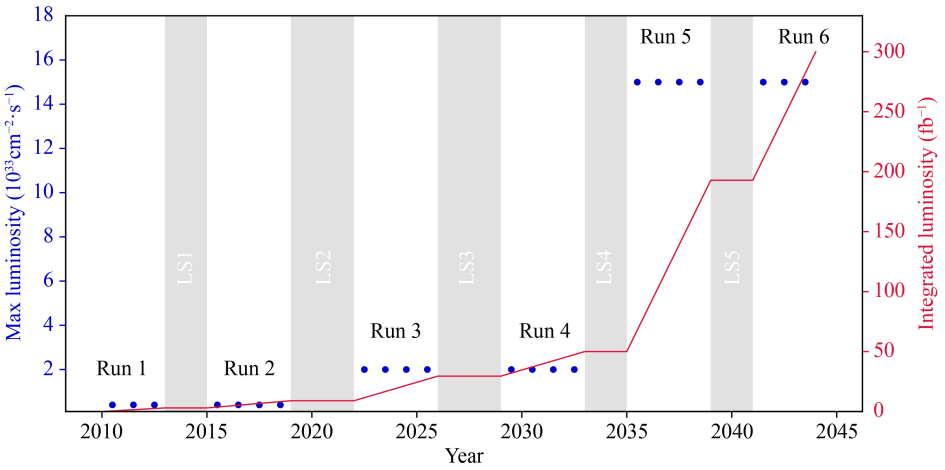

Fig. 36 Instantaneous and integrated luminosities of LHCb as functions of year.

by the end of the second Long Shutdown (LS2) of the LHC, and the upgraded detector is starting to take data in 2022 with an instantaneous luminosity of $2 \times 10^{33}\,\mathrm{cm}^{-2}\mathrm{s}^{-1}$, five times the value achieved so far. Fig. 36 shows the plan for LHCb operation after upgrade. LHCb aims to accumulate an integrated luminosity of approximately 23 fb^{-1} by the end of Run 3 around 2025, and a total of 50 fb^{-1} by the end of Run 4. Note that during the Long Shutdown 3 (LS3) between Run 3 and 4, intensive work will be done on the machine configuration to prepare the High Luminosity Large Hadron Collider (HL-LHC) [907]. During this period consolidation work (Upgrade Ib) will be carried out at LHCb with only minor change on the detector configuration or performance. In order to fully exploit the HL-LHC potential in flavour physics, the collaboration plans another major upgrade, Upgrade II [908], to enable the detector to operate at luminosity as high as $1.5 \times 10^{34}\,\mathrm{cm}^{-2}\cdot\mathrm{s}^{-1}$. This will allow for an integrated luminosity of ~300 fb^{-1} to be achieved in the lifetime of the (HL-)LHC.

To put the LHCb prospects in context, other players in the field of flavour physics study have to be mentioned. The Belle II experiment [909], the B-factory at the superKEKB [910], has started to take collision data of $e^+e^- \to \Upsilon(4S) \to B\bar{B}$ since 2018, aiming to collect an integrated luminosity of $50\,\mathrm{ab}^{-1}$ by 2025. Belle II and LHCb are expected to be competitive in pushing the measurement precision, though with very different systematic uncertainties, of a number of key flavour observables such as the CKM unitarity angles, the Wilson coefficients and the tests on lepton flavour universality. Given the difference in production mechanism and corresponding detector features, their complementarity should be more appreciated. With the beam energy constraints Belle II will be generally good at treating final states with neutral particles (γ, π^0) or missing energy (neutrinos); it has unique advantage in studying the τ leptons through $e^+e^- \to \tau^+\tau^-$ process. With the huge cross section of heavy hadrons, LHCb will have larger yield in most of the final states especially those with charged tracks. The beauty hadrons produced at high-energy pp collisions are highly boosted, hence their decay vertices could be well separated from the primary vertices. With an excellent vertex detector LHCb fully exploits this phenomenon to suppress background for most B signatures to an extremely low level. In addition to B mesons, the studies at LHCb extend to all type of heavy hadrons like B_s^0, B_c^+ and beauty baryons. Future electron positron colliders proposed primarily for Higgs study, such as CEPC [911] and FCC-ee [912], also plan to operate at Z pole. With yields of B-mesons comparable or higher than Belle II depending on the machine design, future Z factories produce all spectrum of beauty hadrons with large boost and efficient trigger, hence will also contribute to heavy flavour physics with unique advantages. At the HL-LHC era ATLAS and CMS will keep pushing the high-energy frontier by studying the Higgs and searching for signature of new physics beyond the Standard Model, meanwhile the yield of beauty hadrons will be so considerable that measurement of a few key flavour observables can be made precisely, especially those with a pair of muons in their final state. They are designed to perform well at high p_T and central rapidity, perfectly complementing the kinematic range of LHCb. The BESIII experiment [913] will continue to operate for another 10 years [914] and accumulate a sample of charm mesons corresponding to ~20 fb^{-1}, which will not only allow more mixing and CP violation study in the charm sector but also help to reduce the uncertainties related to the charm strong phase in measurement of the CKM γ angle [915]. Even larger $D\bar{D}$ samples at the order of $\sim$ ab^{-1} are expected at proposed future tau-charm factories SCTF [916] and STCF [917].

6.1.1 Upgrade I

The ongoing Upgrade I aims to increase the instantaneous luminosity of LHCb from the current value of $4 \times 10^{32}\,\mathrm{cm}^{-2}\cdot\mathrm{s}^{-1}$ to $2 \times 10^{33}\,\mathrm{cm}^{-2}\cdot\mathrm{s}^{-1}$. Naïvely it would mean a five-fold increase in all signal yield, which will be roughly true for final states with muons. Actually the gain for all-hadronic final state will be more than that due to a major change in the trigger system [918]. The hardware trigger L0, which reduces the data rate from 40 MHz to 1 MHz, will be completely removed after Upgrade I, allowing a more flexible full software trigger. Generally the trigger efficiencies for all-hadronic final states are expected to be doubled, as taken in simulation study of upgrade performances, however this number could vary depending on the individual channel.

The increased pile-up causes much higher combinatorial background and more challenging track reconstruction, therefore the tracking systems [919, 920] have been completely redesigned with higher granularity and better radiation tolerance so as to provide uncompromised tracking performance at higher pile-up. Components of the particle identification systems [921] will be reused as much as possible, yet the readout electronics will be replaced in accordance with the 40 MHz readout rate. As a result of higher luminosity, improved trigger rate and larger number of output channels, the data volume to be treated either in real time or offline will be substantially higher, hence new software infrastructure and computing models have been developed correspondingly [922–924] to ensure physics data to be processed and stored in a timely manner. A new subsystem has been installed to enhance the detector's capability in fixed target and heavy-ion studies without disturbing the main physics program [925]. The simulation study shows that detector performance after upgrade will be at least as good as before, with improvement at some areas.

6.1.2 Upgrade II

By the end of Run 4 LHCb will have accumulated 50 fb^{-1} pp collision data, with many subdetectors reaching end of lifetime. Operation at the same condition beyond that point would be less attractive. To fully exploit the HL-LHC potential in flavour physics study, the collaboration proposed Upgrade II towards an integrated luminosity of 300 fb^{-1} [908]. The physics cases with the luminosity an order of magnitude higher than before HL-

Table 9 Sensitivity of selected key flavour observables for LHCb, ATLAS and CMS, reproduced from Ref. [664] with updates when available, and Belle II sensitivities from Ref. [930].

Observable	LHCb current	LHCb (23 fb^{-1})	LHCb (300 fb^{-1})	Belle II (50 ab^{-1})	ATLAS & CMS
CKM tests					
γ (all modes)	4° [784, 931]	1.5°	0.35°	1.5°	–
γ ($B_s^0 \to D_s^+ K^-$)	$(^{+17}_{-22})°$	4°	1°	–	–
$\sin 2\beta$	0.04 [932]	0.011	0.003	0.005	–
ϕ_s ($B_s^0 \to J/\psi\phi$)	49 mrad [933]	14 mrad	4 mrad	–	22 mrad [934] 5–6 mrad [935]
ϕ_s ($B_s^0 \to D_s^+ D_s^-$)	170 mrad [825]	35 mrad	9 mrad	–	–
$\phi_s^{s\bar{s}s}$ ($B_s^0 \to \phi\phi$)	154 mrad [936]	39 mrad	11 mrad	–	feasible [937]
a_{sl}^s	33×10^{-4} [938]	10×10^{-4}	3×10^{-4}	–	–
$\lvert V_{ub}\rvert/\lvert V_{cb}\rvert$	6% [847]	3%	1%	1%	–
Charm					
$\Delta\mathcal{A}^{CP}$	2.9×10^{-4} [790]	1.7×10^{-4}	3.0×10^{-5}	5.4×10^{-4}	–
A_Γ	1.3×10^{-4} [877]	4.2×10^{-5}	1.0×10^{-5}	3.5×10^{-4}	–
$B_{(s)}^0 \to \mu^+\mu^-$					
$\frac{\mathcal{B}(B^0\to\mu^+\mu^-)}{\mathcal{B}(B_s^0\to\mu^+\mu^-)}$	71% [661, 662]	34%	10%	–	21% [939, 940]
$\tau_{B_s^0\to\mu^+\mu^-}$	14% [661, 662]	8%	2%	–	–
EW penguins					
R_K ($B^+ \to K^+\ell^+\ell^-$)	0.044 [703]	0.025	0.007	0.036	–
R_{K^*} ($B^0 \to K^{*0}\ell^+\ell^-$)	0.10 [709]	0.031	0.008	0.032	–
LFU tests					
R_{D^*} ($B^0 \to D^{*-}\ell^+\nu$)	0.026 [941, 942]	0.007	0.002	0.005	–
$R_{J/\psi}$ ($B_c^+ \to J/\psi\ell^+\nu$)	0.24 [943]	0.07	0.02	–	–

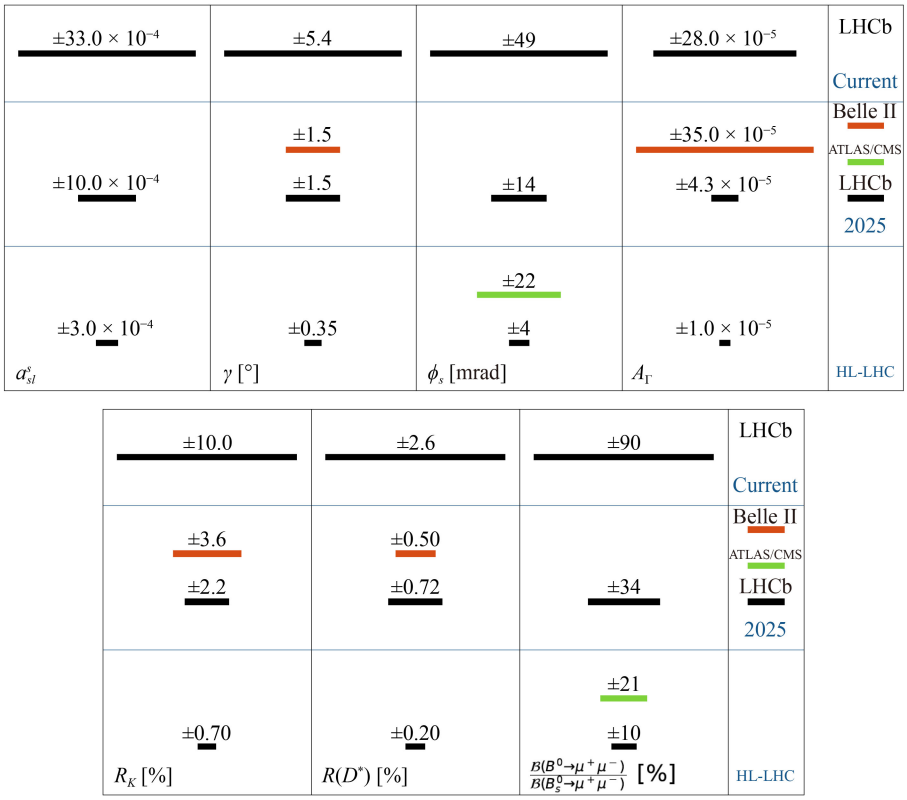

Fig. 37 Sensitivity to probe key CP violating variables, rare decay and lepton flavour universality tests expected from LHCb upgrades. Anticipated results from Belle II, ATLAS or CMS are listed when available. Reproduced from Ref. [664].

LHC time have been studied extensively by the collaboration and summarised in a document in 2018 [664]. A few benchmarks will be discussed below. Note that the HL-LHC baseline design assumes LHCb running condition to be the same as in Run 3, the HL-LHC experts recently released a report on the upgrade feasibility from the machine side [926] showing that possible solution of operating at a luminosity of $1.5\times10^{34}\,\mathrm{cm^{-2}s^{-1}}$ will allow the target of 300 $\mathrm{fb^{-1}}$ to be met.

The seven-fold increase of luminosity will again impose more technical challenges for the experiment. The expected number of interactions per crossing is around 40, twenty times of current situation (or a hundred times of the LHCb initial design). Fast timing resolution will be required in most subsystems to fight against the combinatorial backgrounds caused by the pile-up. Finer granularity in all tracking detectors is compulsory under much higher multiplicity. Radiation hardness will be more of concern especially for areas close to the beampipe. A daunting amount of 200 Tb of data will be produced every second, and has to be reduced by four orders of magnitude before stored permanently. New subsystems are being proposed in order to extend geometrical acceptance for low-momentum tracks, and to improve K/π separation at lower momentum. A lot of development activities have been launched driven by these requirements, while exploiting new technologies in detector and computing. A framework Technical Design Report summarising these activities was released recently [927].

6.2 Physics prospects

Before the HL-LHC or by the end of Run 3, LHCb will have taken 23 $\mathrm{fb^{-1}}$ data, drastically reducing the statistical uncertainties for most of channels compared with current measurements. The expected projections are studied in detail [906] and updated with inputs from experiences in Run I [928, 929]. The physics opportunities in Upgrade II with 300 $\mathrm{fb^{-1}}$ have also been studied [664], which concludes that the energy scale probed by flavour observables will be doubled with respect to pre-HL-LHC era. The sensitivity of a selection of key flavour observables after LHCb upgrades are listed in Table 9 and illustrated in Fig. 37, mostly from Ref. [664] with minor updates when available. Note that Belle II will have completed data taking when LHCb collects 23 $\mathrm{fb^{-1}}$ data. Expected projection from Belle II, ATLAS and CMS are listed for comparison when applicable. A few highlights will be briefly mentioned here.

Rare decays. The decay of $B^0\to\mu^+\mu^-$ is not very far from being observed with imminent Upgrade I data, and its branching fraction with respect to $B^0_s\to\mu^+\mu^-$ will be measured with 10% uncertainty giving a powerful test of

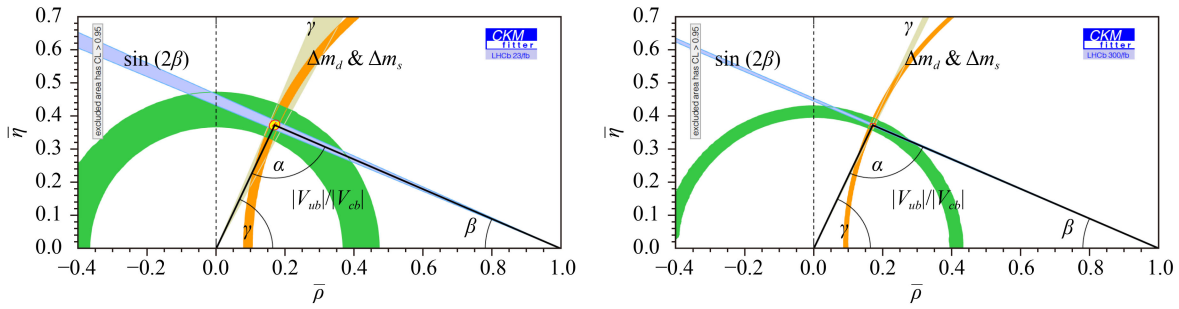

Fig. 38 LHCb constraints to the unitarity triangle with anticipated improvement from (left) Upgrade I and (right) Upgrade II. Reproduced from Ref. [664].

minimal flavour violation. A wide range of studies will be performed in $b\to s\ell^+\ell^-$ or $b\to d\ell^+\ell^-$ decays with improved precision, so the current hint of discrepancy in $R_{K^{(*)}}$ with SM predictions will be confirmed or excluded with confidence. A series of tests on lepton flavour universality can be carried out in $b\to c\ell^-\nu$ decays. The precision of R_{D^*} will reach per mille level.

CKM tests. The CKM unitarity triangle will be so precisely determined in the future that discrepancies between various measurement caused by physics beyond Standard Model will be extremely difficult to hide, as shown in Fig. 38. The angle γ, currently still the least well-known, will be determined with an uncertainty of 1.5° after Run 3, similar as the precision expected from Belle II; the uncertainty will be further reduced to 0.35° after Upgrade II. The expected precision on B_s weak mixing angle ϕ_s will be pushed to a few mrad, the same level as the current precision determined indirectly from CKM fit using tree-level measurements.

CP violation in charm. After Upgrade II LHCb will be able to probe CP violation in charm with a sensitivity of $\mathcal{O}(10^{-5})$, the only future facility promising in observing indirect CP violation in charm which is predicted to be $\mathcal{O}(10^{-4})$ or less in the SM.

Heavy-flavour spectroscopy. LHCb has demonstrated its capability as a general purpose detector in the forward region, and it will be better equipped in this respect after Upgrades. With data sample over an order of magnitude large than currently available, LHCb will systematically update our knowledge on heavy hadron spectroscopy, including less-studied conventional hadrons, such as doubly heavy baryons, and those labelled as exotic nowadays, such as pentaquark and tetraquark states.

Beyond flavour physics. In the high $p_{\rm T}$ range LHCb could also make contribution complementary to ATLAS and CMS, for instance to the precision determination of the effective weak mixing angle $\sin\theta^2_W$ and the W mass. Measurements of top pair and gauge boson production at LHCb are also crucial to study the poorly known gluon parton distribution functions at high-x range. This is an important study in the QCD, which help to understand the ubiquitous background for any new high-mass states in ATLAS or CMS. LHCb will also push sensitivity in search for dark-photon and long-lived particles predicted in several NP scenarios.

6.3 Summary

This manuscript briefly reviews the recent experimental highlights using data collected with the LHCb detector in its first 10-year operation. They are not only from the flavour physics benchmarks that the experiment was designed for, but also include unexpected discoveries revealing LHCb's capability as a general purpose detector in the forward region:

- A large variety of new particles are discovered, either filling gaps in conventional heavy hadron spectroscopy or establishing new types of their own, like pentaquarks or tetraquarks;
- Some processes predicted to be extremely rare in the SM are observed, such as the $B^0_s\to\mu^+\mu^-$ decay. Precise measurements are performed on semileptonic and radiative FCNC beauty decays, where NP at high energy scale can be probed with promising sensitivity, and tensions with the SM are found in some cases;
- The CKM parameters are determined precisely using multiple approaches in a wide range of final states. The angle γ, which was the least known in the unitarity triangle, has been determined with an unprecedented precision of about 4°;
- Heavy flavour study in the charm sector witnesses a couple of milestones, such as the observation of D^0–$\bar{D}^0$ mixing in a single measurement and observation of non-zero mass difference between the two mass eigenstates in the $D^0-\bar{D}^0$ system. Precision in probing the CP violation in charm keeps pushing forward.

This is by far not a complete list [4], and many interesting topics studied at LHCb are not covered due to limited space. With the Upgrade I detector in place, the LHCb experiment has resumed operation in 2022 and will continue to take data at a higher luminosity while preparing for the future Upgrade II. New exciting

physics results are expected, which will continue to shape the landscape of heavy flavour physics and beyond.

Acknowledgements This work was partially supported by the National Key Research and Development Program of China under Grant Nos. 2017YFA0402100 and 2022YFA1601900, the National Natural Science Foundation of China (NSFC) under Grant Nos. 11435003, 11575091, 11575094, 11925504, 11975015, 12175245, 12175005, 11705209, 12205312, 12275100, 11961141015 and 12061141007, Chinese Academy of Sciences, Fundamental Research Funds for the Central Universities, Peking University Funds for the New Faculty Startup program. We thank Franz Muheim and Niels Tuning for suggestions in improving the draft.

References and notes

1. O. S. Brüning, et al., LHC Design Report, CERN Yellow Reports: Monographs, CERN, Geneva, 2004
2. ATLAS Collaboration, G. Aad, et al., Observation of a new particle in the search for the standard model Higgs boson with the ATLAS detector at the LHC, *Phys. Lett. B* 716, 1 (2012), arXiv: 1207.7214
3. CMS Collaboration, S. Chatrchyan, et al., Observation of a new boson at a mass of 125 GeV with the CMS experiment at the LHC, *Phys. Lett. B* 716, 30 (2012), arXiv: 1207.7235
4. Webpage: lhcbproject.web.cern.ch/Publications/LHCbProjectPublic/Summary_all.html
5. LHCb Collaboration, A. A. Alves Jr., et al., The LHCb detector at the LHC, *J. Instrument.* 3, S08005 (2008)
6. LHCb Collaboration, R. Aaij, et al., Measurement of $\sigma(pp\to b\bar{b}X)$ at $\sqrt{s}=7$ TeV in the forward region, *Phys. Lett. B* 694 (2010) 209, arXiv: 1009.2731
7. LHCb Collaboration, R. Aaij, et al., Measurement of J/ψ production in pp collisions at $\sqrt{s}=7$ TeV, *Eur. Phys. J. C* 71 (2011) 1645, arXiv: 1103.0423
8. LHCb Collaboration, R. Aaij, et al., Production of J/ψ and Υ mesons in pp collisions at $\sqrt{s}=8$ TeV, *J. High Energy Phys.* 06, 064 (2013), arXiv: 1304.6977
9. LHCb Collaboration, R. Aaij, et al., Prompt charm production in pp collisions at $\sqrt{s}=7$ TeV, *Nucl. Phys. B* 871 (2013) 1, arXiv: 1302.2864
10. LHCb Collaboration, R. Aaij, et al., Measurement of forward J/ψ production cross-sections in pp collisions at $\sqrt{s}=13$ TeV, *J. High Energy Phys.* 10, 172 (2015), Erratum: *J. High Energy Phys.* 05, 063 (2017), arXiv: 1509.00771
11. LHCb Collaboration, R. Aaij, et al., Measurements of prompt charm production cross-sections in pp collisions at $\sqrt{s}=13$ TeV, *J. High Energy Phys.* 03, 159 (2016), Erratum: *J. High Energy Phys.* 09, 013 (2016), Erratum: *J. High Energy Phys.* 05, 074 (2017), arXiv: 1510.01707
12. LHCb Collaboration, R. Aaij, et al., Measurement of the b-quark production cross-section in 7 and 13 TeV pp collisions, *Phys. Rev. Lett.* 118, 052002 (2017), Erratum: *Phys. Rev. Lett.* 119, 169901 (2017), arXiv: 1612.05140
13. M. Cacciari, et al., Theoretical predictions for charm and bottom production at the LHC, *J. High Energy Phys.* 10, 137(2012), arXiv: 1205.6344
14. A. Andronic, et al., Heavy-avour and quarkonium production in the LHC era: From proton-proton to heavy-ion collisions, *Eur. Phys. J. C* 76 (2016) 107, arXiv: 1506.03981
15. X.-H. Zhang, F.-H. Liu, and K. K. Olimov, A systematic analysis of transverse momentum spectra of J/ψ mesons in high energy collisions, *Int. J. Mod. Phys. E* 30, 2150051 (2021), arXiv: 2105.14700
16. C.-H. Chen, et al., A study on the exotic state $P_c(4312)$, $P_c(4440)$, $P_c(4457)$ in pp collisions at $\sqrt{s}=7$, 13 GeV, arXiv: 2111.03241 (2021)
17. A.-P. Chen, Y.-Q. Ma, and H. Zhang, A short theoretical review of charmonium production, arXiv: 2109.04028 (2021)
18. Q. Wang and F.-H. Liu, Excitation function of initial temperature of heavy avor quarkonium emission source in high energy collisions, *Adv. High Energy Phys.* 2020, 5031494 (2020), arXiv: 2005.04940
19. Y.-H. Chen, Y.-G. Ma, G.-L. Ma, and J.-H. Chen, Transverse momentum spectra of J/ψ produced in collisions over an energy range from 17.4 GeV to 13 TeV, *J. Phys. G* 47, 045111 (2020)
20. Y. Yang, S. Cai, Y. Cai, and W. Xiang, Inclusive diffractive heavy quarkonium photoproduction in pp, pA and AA collisions, *Nucl. Phys. A* 990, 17 (2019), arXiv: 1907.09036
21. Z.-G. He, B. A. Kniehl, M. A. Nefedov, and V. A. Saleev, Double prompt J/ψ hadroproduction in the parton Reggeization approach with high-energy resummation, *Phys. Rev. Lett.* 123, 162002 (2019), arXiv: 1906.08979
22. M. Butenschoen and B. A. Kniehl, World data of J/ψ production consolidate NRQCD factorization at NLO, *Phys. Rev. D* 84, 051501 (2011), arXiv: 1105.0820
23. J.-P. Lansberg and H.-S. Shao, Towards an automated tool to evaluate the impact of the nuclear modification of the gluon density on quarkonium, D and B meson production in proton–nucleus collisions, *Eur. Phys. J. C* 77, 1 (2017), arXiv: 1610.05382
24. H.-F. Zhang, Z. Sun, W.-L. Sang, and R. Li, Impact of η_c hadroproduction data on charmonium production and polarization within NRQCD framework, *Phys. Rev. Lett.* 114, 092006 (2015), arXiv: 1412.0508
25. J. P. Ma, J. X. Wang, and S. Zhao, Transverse momentum dependent factorization for quarkonium production at low transverse momentum, *Phys. Rev. D* 88, 014027 (2013), arXiv: 1211.7144
26. Y. Feng, B. Gong, C.-H. Chang, and J.-X. Wang, Remaining parts of the long-standing J/ψ polarization puzzle, *Phys. Rev. D* 99, 014044(2019), arXiv: 1810.08989
27. J.-X. Wang and H.-F. Zhang, h_c production at hadron colliders, *J. Phys. G* 42, 025004 (2015), arXiv: 1403.5944
28. Z. Tang, N. Xu, K. Zhou, and P. Zhuang, Charmonium transverse momentum distribution in high energy nuclear collisions, *J. Phys. G* 41, 124006 (2014), arXiv: 1409.5559

29. Q.-F. Sun, Y. Jia, X. Liu, and R. Zhu, Inclusive h_c production and energy spectrum from e^+e^- annihilation at a super B factory, *Phys. Rev. D* 98, 014039 (2018), arXiv: 1801.10137
30. B.-C. Li, T. Bai, Y.-Y. Guo, and F.-H. Liu, On J/ψ and Υ transverse momentum distributions in high energy collisions, *Adv. High Energy Phys.* 2017, 9383540 (2017), arXiv: 1701.04689
31. H. Han, et al., η_c production at LHC and indications on the understanding of J/ψ production, *Phys. Rev. Lett.* 114, 092005(2015), arXiv: 1411.7350
32. H. Han, et al., $\Upsilon(nS)$ and $\chi_b(nP)$ production at hadron colliders in nonrelativistic QCD, *Phys. Rev. D* 94, 014028 (2016), arXiv: 1410.8537
33. P. Zhang, C. Meng, Y.-Q. Ma, and K.-T. Chao, Gluon fragmentation into ${}^3P_J^{[1,8]}$ quark pair and test of NRQCD factorization at two-loop level, *J. High Energy Phys.* 08, 111(2021), arXiv: 2011.04905
34. H.-Y. Liu, Y.-Q. Ma, and K.-T. Chao, Improvement for color glass condensate factorization: Single hadron production in pA collisions at next-to-leading order, *Phys. Rev. D* 100, 071503 (2019), arXiv: 1909.02370
35. Y. -Q. Ma and K.-T. Chao, New factorization theory for heavy quarkonium production and decay, *Phys. Rev. D* 100, 094007 (2019), arXiv: 1703.08402
36. L.-P. Sun, H. Han, and K.-T. Chao, Impact of J/ψ pair production at the LHC and predictions in nonrelativistic QCD, *Phys. Rev. D* 94, 074033(2016), arXiv: 1404.4042
37. Y.-Q. Ma, K. Wang, and K.-T. Chao, A complete NLO calculation of the J/ψ and ψ' production at hadron colliders, *Phys. Rev. D* 84, 114001(2011), arXiv: 1012.1030
38. Y.-Q. Ma, K. Wang, and K.-T. Chao, $J/\psi(\psi')$ production at the Tevatron and LHC at $\mathcal{O}(\alpha_s^4 v^4)$ in nonrelativistic QCD, *Phys. Rev. Lett.* 106, 042002(2011), arXiv: 1009.3655
39. B.-Q. Li and K.-T. Chao, Higher charmonia and X, Y, Z states with screened potential, *Phys. Rev. D* 79, 094004 (2009), arXiv: 0903.5506
40. Y.-Q. Ma, K. Wang, and K.-T. Chao, QCD radiative corrections to χ_{cJ} production at hadron colliders, *Phys. Rev. D* 83, 111503 (2011), arXiv: 1002.3987
41. Y.-J. Zhang, Y.-Q. Ma, K. Wang, and K.-T. Chao, QCD radiative correction to color-octet J/ψ inclusive production at B factories, *Phys. Rev. D* 81, 034015 (2010), arXiv: 0911.2166
42. H.-S. Shao, HELAC-Onia: An automatic matrix element generator for heavy quarkonium physics, *Comput. Phys. Commun.* 184, 2562 (2013), arXiv: 1212.5293
43. C.-H. Chang and X.-G. Wu, Uncertainties in estimating B_c hadronic production and comparisons of the production at TEVATRON and LHC, *Eur. Phys. J. C* 38, 267 (2004), arXiv: hep-ph/0309121
44. J.-J. Niu, L. Guo, H.-H. Ma, and S.-M. Wang, Heavy quarkonium production through the top quark rare decays via the channels involving flavor changing neutral currents, *Eur. Phys. J. C* 78, 657 (2018), arXiv: 1808.01231
45. K. He, et al., P-wave excited B_c^{**} meson photoproduction at the LHeC, *J. Phys. G* 45, 055005 (2018), arXiv: 1710.11508
46. G. Zhang and B.-Q. Ma, Searching for lepton number violating Λ baryon decays mediated by a GeV-scale Majorana neutrino with LHCb, *Phys. Rev. D* 103, 033004 (2021), arXiv: 2101.05566
47. G. Chen, X.-G. Wu, and S. Xu, Impacts of the intrinsic charm content of the proton on the Ξ_{cc} hadroproduction at a fixed target experiment at the LHC, *Phys. Rev. D* 100, 054022 (2019), arXiv: 1903.00722
48. Y. Hu, et al., The production of doubly charmed exotic hadrons in heavy ion collisions, arXiv: 2109.07733 (2021)
49. S. Jia, X. Zhou, and C. Shen, Experimental review of the $\Upsilon(1S, 2S, 3S)$ physics at e^+e^- colliders and the LHC, *Front. Phys.* 15, 64301 (2020), arXiv: 2005.05892
50. N. Brambilla, et al., The XYZ states: Experimental and theoretical status and perspectives, *Phys. Rep.* 873, 1 (2020), arXiv: 1907.07583
51. H.-X. Chen, W. Chen, X. Liu, and S.-L. Zhu, The hidden-charm pentaquark and tetraquark states, *Phys. Rep.* 639, 1 (2016), arXiv: 1601.02092
52. F.-K. Guo, et al., Hadronic molecules, *Rev. Mod. Phys.* 90, 015004 (2018), arXiv: 1705.00141
53. E. S. Swanson, The new heavy mesons: A status report, *Phys. Rep.* 429 (2006) 243, arXiv: hep-ph/0601110
54. S. L. Olsen, T. Skwarnicki, and D. Zieminska, Nonstandard heavy mesons and baryons: Experimental evidence, *Rev. Mod. Phys.* 90, 015003 (2018), arXiv: 1708.04012
55. Y.-R. Liu, et al., Pentaquark and tetraquark states, *Prog. Part. Nucl. Phys.* 107, 237 (2019), arXiv: 1903.11976
56. H.-X. Chen, et al., A review of the open charm and open bottom systems, *Rep. Prog. Phys.* 80, 076201 (2017), arXiv: 1609.08928
57. X. Liu, An overview of XYZ new particles, *Chin. Sci. Bull.* 59, 3815 (2014), arXiv: 1312.7408
58. F.-K. Guo, X.-H. Liu, and S. Sakai, Threshold cusps and triangle singularities in hadronic reactions, *Prog. Part. Nucl. Phys.* 112, 103757 (2020), arXiv: 1912.07030
59. C.-Z. Yuan, The XYZ states revisited, *Int. J. Mod. Phys. A* 33, 1830018 (2018), arXiv: 1808.01570
60. X. Liu, Z.-G. Luo, Y.-R. Liu, and S.-L. Zhu, $X(3872)$ and other possible heavy molecular states, *Eur. Phys. J. C* 61, 411 (2009), arXiv: 0808.0073
61. X.-K. Dong, F.-K. Guo, and B.-S. Zou, A survey of heavy-heavy hadronic molecules, *Commun. Theor. Phys.* 73, 125201 (2021), arXiv: 2108.02673
62. R.-X. Shi, Y. Xiao, and L.-S. Geng, Magnetic moments of the spin-1/2 singly charmed baryons in covariant baryon chiral perturbation theory, *Phys. Rev. D* 100, 054019 (2019), arXiv: 1812.07833
63. A. Ali, J. S. Lange, and S. Stone, Exotics: Heavy pentaquarks and tetraquarks, *Prog. Part. Nucl. Phys.* 97, 123 (2017), arXiv: 1706.00610
64. A. Esposito, et al., Four-quark hadrons: An updated review, *Int. J. Mod. Phys. A* 30, 1530002 (2015), arXiv: 1411.5997
65. L. Maiani, F. Piccinini, A. D. Polosa, and V. Riquer,

The $Z(4430)$ and a new paradigm for spin interactions in tetraquarks, *Phys. Rev. D* 89, 114010 (2014), arXiv: 1405.1551

66. F.-Z. Peng, M.-Z. Liu, M. S. Sánchez, and M. P. Valderrama, Heavy-hadron molecules from light-meson-exchange saturation, *Phys. Rev. D* 102, 114020 (2020), arXiv: 2004.05658
67. G. Yang, J. Ping, and J. Segovia, Tetra- and penta-quark structures in the constituent quark model, *Symmetry* 12, 1869 (2020), arXiv: 2009.00238
68. J.-M. Richard, Fully-heavy tetraquarks and other heavy multiquarks, *Nucl. Part. Phys. Proc.* 312–317, 15295 (2021), arXiv: 2105.02503
69. M. Karliner, J. L. Rosner, and T. Skwarnicki, Multiquark states, *Ann. Rev. Nucl. Part. Sci.* 68, 17 (2018), arXiv: 1711.10626
70. J.-M. Richard, Exotic hadrons: Review and perspectives, *Few Body Syst.* 57, 1185 (2016), arXiv: 1606.08593
71. R.-H. Wu, et al., NLO effects for QQQ baryons in QCD sum rules, *Chin. Phys. C* 45, 093103 (2021), arXiv: 2104.07384
72. S. Wicks, W. Horowitz, M. Djordjevic, and M. Gyulassy, Elastic, inelastic, and path length fluctuations in jet tomography, *Nucl. Phys. A* 784, 426 (2007), arXiv: nucl-th/0512076
73. K. Zhou, N. Xu, Z. Xu, and P. Zhuang, Medium effects on charmonium production at ultrarelativistic energies available at the CERN Large Hadron Collider, *Phys. Rev. C* 89, 054911 (2014), arXiv: 1401.5845
74. LHCb Collaboration, Study of prompt D^0 meson production in pPb at $\sqrt{s_{NN}} = 8.16$ TeV at LHCb, LHCb-CONF-2019-004, 2019
75. LHCb Collaboration, R. Aaij, et al., Observation of J/ψ-pair production in pp collisions at $\sqrt{s} = 7$ TeV, *Phys. Lett. B* 707, 52 (2012), arXiv: 1109.0963
76. LHCb collaboration, R. Aaij, et al., Measurement of the cross-section ratio $\sigma(\chi_{c2})/\sigma(\chi_{c1})$ for prompt χ_c production at $\sqrt{s} = 7$ TeV, *Phys. Lett. B* 714, 215 (2012), arXiv: 1202.1080
77. LHCb Collaboration, R. Aaij, et al., Measurement of the ratio of prompt χ_c to J/ψ production in pp collisions at $\sqrt{s} = 7$ TeV, *Phys. Lett. B* 718, 431 (2012), arXiv: 1204.1462
78. LHCb Collaboration, R. Aaij, et al., Observation of $X(3872)$ production in pp collisions at $\sqrt{s} = 7$ TeV, *Eur. Phys. J. C* 72, 1972 (2012), arXiv: 1112.5310
79. LHCb Collaboration, R. Aaij, et al., Measurement of Υ production in pp collisions at $\sqrt{s} = 7$ TeV, *Eur. Phys. J. C* 72, 2025 (2012), arXiv: 1202.6579
80. LHCb Collaboration, R. Aaij, et al., Measurement of the $B^{\pm}$ production cross-section in pp collisions at $\sqrt{s} = 7$ TeV, *J. High Energy Phys.* 04, 093 (2012), arXiv: 1202.4812
81. LHCb Collaboration, R. Aaij, et al., Measurement of $\psi(2S)$ meson production in pp collisions at $\sqrt{s} = 7$ TeV, *Eur. Phys. J. C* 72, 2100 (2012), Erratum: *Eur. Phys. J. C* 80, 49 (2020), arXiv: 1204.1258
82. LHCb Collaboration, R. Aaij, et al., Observation of double charm production involving open charm in pp collisions at $\sqrt{s} = 7$ TeV, *J. High Energy Phys.* 06, 141 (2012), Addendum: *J. High Energy Phys.* 03, 108 (2014), arXiv: 1205.0975
83. LHCb Collaboration, R. Aaij, et al., Measurements of B_c^+ production and mass with the $B_c^+ \to J/\psi\pi^+$ decay, *Phys. Rev. Lett.* 109, 232001 (2012), arXiv: 1209.5634
84. LHCb Collaboration, R. Aaij, et al., Measurement of J/ψ production in pp collisions at $\sqrt{s} = 2.76$ TeV, *J. High Energy Phys.* 02, 041 (2013), arXiv: 1212.1045
85. LHCb Collaboration, R. Aaij, et al., Measurement of B meson production cross-sections in proton–proton collisions at $\sqrt{s} = 7$ TeV, *J. High Energy Phys.* 08, 117 (2013), arXiv: 1306.3663
86. LHCb Collaboration, R. Aaij, et al., Measurement of the relative rate of prompt χ_{c0}, χ_{c1} and χ_{c2} production at $\sqrt{s} = 7$ TeV, *J. High Energy Phys.* 10, 115 (2013), arXiv: 1307.4285
87. LHCb Collaboration, R. Aaij, et al., Study of J/ψ production and cold nuclear matter effects in pPb collisions at $\sqrt{s_{NN}} = 5$ TeV, *J. High Energy Phys.* 02, 072 (2014), arXiv: 1308.6729
88. LHCb Collaboration, R. Aaij, et al., Measurement of Υ production in pp collisions at $\sqrt{s} = 2.76$TeV, *Eur. Phys. J. C* 74, 2835(2014), arXiv: 1402.2539
89. LHCb Collaboration, R. Aaij, et al., Study of the kinematic dependences of Λ_b^0 production in pp collisions and a measurement of the $\Lambda_b^0 \to \Lambda_c^0\pi^-$ branching fraction, *J. High Energy Phys.* 08, 143 (2014), arXiv: 1405.6842
90. LHCb Collaboration, R. Aaij, et al., Study of Υ production and cold nuclear matter effects in pPb collisions at $\sqrt{s_{NN}} = 5$ TeV, *J. High Energy Phys.* 07, 094 (2014), arXiv: 1405.5152
91. LHCb Collaboration, R. Aaij, et al., Measurement of the $\eta_c(1S)$ production cross-section in proton–proton collisions via the decay $\eta_c(1S) \to p\bar{p}$, *Eur. Phys. J. C* 75, 311 (2015), arXiv: 1409.3612
92. LHCb Collaboration, R. Aaij, et al., Study of χ_b meson production in pp collisions at $\sqrt{s} = 7$ and 8 TeV and observation of the decay $\chi_b \to \Upsilon(3S)\gamma$, *Eur. Phys. J. C* 74 (2014) 3092, arXiv: 1407.7734
93. LHCb Collaboration, R. Aaij, et al., Measurement of the $\chi_b(3P)$ mass and of the relative rate of $\chi_{b1}(1P)$ and $\chi_{b2}(1P)$ production, *J. High Energy Phys.* 10, 088 (2014), arXiv: 1409.1408
94. LHCb Collaboration, R. Aaij, et al., Measurement of B_c^+ production in proton–proton collisions at $\sqrt{s} = 8$ TeV, *Phys. Rev. Lett.* 114, 132001 (2015), arXiv: 1411.2943
95. LHCb Collaboration, R. Aaij, et al., Identification of beauty and charm quark jets at LHCb, *J. Instrument.* 10, P06013 (2015), arXiv: 1504.07670
96. LHCb Collaboration, R. Aaij, et al., Study of the productions of Λ_b^0 and $\overline{B}^0$ hadrons in pp collisions and first measurement of the $\Lambda_b^0 \to J/\psi p K^-$ branching fraction, *Chin. Phys. C* 40, 011001 (2016), arXiv: 1509.00292
97. LHCb Collaboration, R. Aaij, et al., Forward production of Υ mesons in pp collisions at $\sqrt{s} = 7$ and 8 TeV, *J. High Energy Phys.* 11, 103 (2015), arXiv: 1509.02372
98. LHCb Collaboration, R. Aaij, et al., Production of associated Υ and open charm hadrons in pp collisions at $\sqrt{s} = 7$ and 8 TeV via double parton scattering, *J.*

High Energy Phys. 07, 052 (2016), arXiv: 1510.05949
99. LHCb Collaboration, R. Aaij, et al., Study of $\psi(2S)$ production cross-sections and cold nuclear matter effects in pPb collisions at $\sqrt{s_{NN}} = 5$ TeV, *J. High Energy Phys.* 03, 133 (2016), arXiv: 1601.07878
100. LHCb Collaboration, R. Aaij, et al., Measurements of prompt charm production cross-sections in pp collisions at $\sqrt{s} = 5$ TeV, *J. High Energy Phys.* 06, 147 (2017), arXiv: 1610.02230
101. LHCb Collaboration, R. Aaij, et al., Measurement of the J/ψ pair production cross-section in pp collisions at $\sqrt{s} = 13$ TeV, *J. High Energy Phys.* 06 (2017) 047, Erratum: *J. High Energy Phys.* 10, 068 (2017), arXiv: 1612.07451
102. LHCb Collaboration, R. Aaij, et al., Study of J/ψ production in jets, *Phys. Rev. Lett.* 118, 192001 (2017), arXiv: 1701.05116
103. LHCb Collaboration, R. Aaij, et al., Prompt and nonprompt J/ψ production and nuclear modification in pPb collisions at $\sqrt{s_{NN}} = 8.16$ TeV, *Phys. Lett. B* 774 (2017) 159, arXiv: 1706.07122
104. LHCb Collaboration, R. Aaij, et al., Study of prompt D^0 meson production in pPb collisions at $\sqrt{s_{NN}} = 5$ TeV, *J. High Energy Phys.* 10, 090 (2017), arXiv: 1707.02750
105. LHCb Collaboration, R. Aaij, et al., Measurement of the $B^{\pm}$ production cross-section in pp collisions at $\sqrt{s} =$ 7 and 13 TeV, *J. High Energy Phys.* 12, 026 (2017), arXiv: 1710.04921
106. LHCb Collaboration, R. Aaij, et al., Measurement of Υ production cross-section in pp collisions at $\sqrt{s} = 13$ TeV, *J. High Energy Phys.* 07, 134 (2018), arXiv: 1804.09214
107. LHCb Collaboration, R. Aaij, et al., Prompt Λ_c^+ production in pPb collisions at $\sqrt{s_{NN}} = 5.02$ TeV, *J. High Energy Phys.* 02, 102 (2019), arXiv: 1809.01404
108. LHCb Collaboration, R. Aaij, et al., Study of Υ production in pPb collisions at $\sqrt{s_{NN}} = 8.16$ TeV, *J. High Energy Phys.* 11, 194 (2018), arXiv: 1810.07655
109. LHCb Collaboration, R. Aaij, et al., Measurement of the mass and production rate of Ξ_b^- baryons, *Phys. Rev. D* 99, 052006 (2019), arXiv: 1901.07075
110. LHCb Collaboration, R. Aaij, et al., Measurement of B^+, B^0 and Λ_b^0 production in pPb collisions at $\sqrt{s_{NN}} =$ 8.16 TeV, *Phys. Rev. D* 99, 052011 (2019), arXiv: 1902.05599
111. LHCb Collaboration, R. Aaij, et al., Measurement of $\psi(2S)$ production cross-sections in proton–proton collisions at $\sqrt{s} = 7$ and 13 TeV, *Eur. Phys. J. C* 80, 185 (2020), arXiv: 1908.03099
112. LHCb Collaboration, R. Aaij, et al., Measurement of the $\eta_c(1S)$ production cross-section in pp collisions at $\sqrt{s} = 13$ TeV, *Eur. Phys. J. C* 80, 191 (2020), arXiv: 1911.03326
113. LHCb Collaboration, R. Aaij, et al., Measurement of the B_c^- production fraction and asymmetry in 7 and 13 TeV pp collisions, *Phys. Rev. D* 100, 112006 (2019), arXiv: 1910.13404
114. LHCb Collaboration, R. Aaij, et al., Measurement of Ξ_{cc}^{++} production in pp collisions at $\sqrt{s} = 13$ TeV, *Chin. Phys. C* 44, 022001 (2020), arXiv: 1910.11316
115. LHCb Collaboration, R. Aaij, et al., Observation of enhanced double parton scattering in proton-lead collisions at $\sqrt{s_{NN}} = 8.16$ TeV, *Phys. Rev. Lett.* 125, 212001 (2020), arXiv: 2007.06945
116. LHCb Collaboration, R. Aaij, et al., Observation of multiplicity-dependent $\chi_{c1}(3872)$ and $\psi(2S)$ production in pp collisions, *Phys. Rev. Lett.* 126, 092001 (2021), arXiv: 2009.06619
117. LHCb Collaboration, R. Aaij, et al., Precise measurement of the f_s/f_d ratio of fragmentation fractions and of B_s^0 decay branching fractions, *Phys. Rev. D* 104, 032005 (2021), arXiv: 2103.06810
118. LHCb Collaboration, R. Aaij, et al., Measurement of prompt-cross-section ratio $\sigma(\chi_{c2})/\sigma(\chi_{c1})$ in pPb collisions at $\sqrt{s_{NN}} = 8.16$ TeV, *Phys. Rev. C* 103 (2021) 064905, arXiv: 2103.07349
119. LHCb Collaboration, R. Aaij, et al., Measurement of $\chi_{c1}(3872)$ production in proton–proton collisions at $\sqrt{s} =$ 8 and 13 TeV, *J. High Energy Phys.* 01, 131 (2022), arXiv: 2109.07360
120. J. Pumplin, et al., New generation of parton distributions with uncertainties from global QCD analysis, *J. High Energy Phys.* 07, 012 (2002), arXiv: hep-ph/0201195
121. M. Cacciari, M. Greco, and P. Nason, The $p_{\rm T}$ spectrum in heavy-flavor hadroproduction, *J. High Energy Phys.* 05, 007 (1998), arXiv: hep-ph/9803400
122. R. Gauld and J. Rojo, Precision determination of the small-x gluon from charm production at LHCb, *Phys. Rev. Lett.* 118, 072001 (2017), arXiv: 1610.09373
123. LHCb Collaboration, R. Aaij, et al., Measurement of J/ψ polarization in pp collisions at $\sqrt{s} = 7$ TeV, *Eur. Phys. J. C* 73, 2631 (2013), arXiv: 1307.6379
124. K.-T. Chao, et al., J/ψ polarization at hadron colliders in nonrelativistic QCD, *Phys. Rev. Lett.* 108, 242004 (2012), arXiv: 1201.2675
125. M. Butenschoen and B. A. Kniehl, J/ψ production in NRQCD: A global analysis of yield and polarization, *Nucl. Phys. B Proc. Suppl.* 222–224, 151 (2012), arXiv: 1201.3862
126. B. Gong, L.-P. Wan, J.-X. Wang, and H.-F. Zhang, Polarization for prompt J/ψ and $\psi(2S)$ production at the Tevatron and LHC, *Phys. Rev. Lett.* 110, 042002 (2013), arXiv: 1205.6682
127. Y.-Q. Ma and R. Venugopalan, Comprehensive description of J/ψ production in proton–proton collisions at collider energies, *Phys. Rev. Lett.* 113, 192301 (2014), arXiv: 1408.4075
128. Y. Zhang, Measurement of charmonium polarization with the LHCb detector, PhD thesis, Tsinghua University, Beijing, 2013
129. N. Brambilla, et al., Heavy quarkonium: Progress, puzzles, and opportunities, *Eur. Phys. J. C* 71, 1534 (2011), arXiv: 1010.5827
130. N. Brambilla, A. Pineda, J. Soto, and A. Vairo, Effective field theories for heavy quarkonium, *Rev. Mod. Phys.* 77, 1423 (2005), arXiv: hep-ph/0410047
131. G. T. Bodwin, E. Braaten, and G. P. Lepage, Rigorous QCD analysis of inclusive annihilation and production of heavy quarkonium, *Phys. Rev. D* 51, 1125 (1995), Erratum: *Phys. Rev. D* 55, 5853 (1997), arXiv: hep-ph/9407339

132. Y.-Q. Ma and R. Vogt, Quarkonium production in an improved color evaporation model, *Phys. Rev. D* 94, 114029 (2016), arXiv: 1609.06042
133. LHCb Collaboration, R. Aaij, et al., Measurement of the $\Upsilon(nS)$ polarizations in pp collisions at $\sqrt{s} = 7$ and 8 TeV, *J. High Energy Phys.* 12, 110 (2017), arXiv: 1709.01301
134. LHCb Collaboration, R. Aaij, et al., Measurement of $\psi(2S)$ polarisation in pp collisions at $\sqrt{s} = 7$ TeV, *Eur. Phys. J. C* 74, 2872 (2014), arXiv: 1403.1339
135. H. S. Shao, et al., Yields and polarizations of prompt J/ψ and $\psi(2S)$ production in hadronic collisions, *J. High Energy Phys.* 05, 103 (2015), arXiv: 1411.3300
136. H.-S. Shao, Probing heavy quarkonium production mechanism: χ_c polarization, *AIP Conf. Proc.* 1701, 050006 (2016), arXiv: 1412.2576
137. M. Butenschoen and B. A. Kniehl, J/ψ polarization at Tevatron and LHC: Nonrelativistic-QCD factorization at the crossroads, *Phys. Rev. Lett.* 108, 172002 (2012), arXiv: 1201.1872
138. Y.-Q. Ma, T. Stebel, and R. Venugopalan, J/ψ polarization in the CGC+NRQCD approach, *J. High Energy Phys.* 12, 057 (2018), arXiv: 1809.03573
139. H.-S. Shao, Y.-Q. Ma, K. Wang, and K.-T. Chao, Polarizations of χ_{c1} and χ_{c2} in prompt production at the LHC, *Phys. Rev. Lett.* 112, 182003 (2014), arXiv: 1402.2913
140. H.-S. Shao and K.-T. Chao, Spin correlations in polarizations of P-wave charmonia χ_{cJ} and impact on J/ψ polarization, *Phys. Rev. D* 90, 014002 (2014), arXiv: 1209.4610
141. E. Chapon, et al., Prospects for quarkonium studies at the high-luminosity LHC, *Prog. Part. Nucl. Phys.* 122, 103906 (2022), arXiv: 2012.14161
142. C. H. Kom, A. Kulesza, and W. J. Stirling, Pair production of J/ψ as a probe of double parton scattering at LHCb, *Phys. Rev. Lett.* 107, 082002 (2011), arXiv: 1105.4186
143. H.-S. Shao and Y.-J. Zhang, Triple prompt J/ψ hadroproduction as a hard probe of multiple-parton scatterings, *Phys. Rev. Lett.* 122, 192002 (2019), arXiv: 1902.04949
144. Z.-G. He, Y. Fan, and K.-T. Chao, Relativistic corrections to J/ψ exclusive and inclusive double charm production at B factories, *Phys. Rev. D* 75, 074011 (2007), arXiv: hep-ph/0702239
145. J.-P. Lansberg and H.-S. Shao, Production of $J/\psi + \eta_c$ versus $J/\psi + J/\psi$ at the LHC: Importance of real α_s^5 corrections, *Phys. Rev. Lett.* 111, 122001 (2013), arXiv: 1308.0474
146. H.-S. Shao, J/ψ meson production in association with an open charm hadron at the LHC: A reappraisal, *Phys. Rev. D* 102, 034023 (2020), arXiv: 2005.12967
147. CDF Collaboration, F. Abe, et al., Double parton scattering in $\bar{p}p$ collisions at $\sqrt{s} = 1.8$ TeV, *Phys. Rev. D* 56, 3811 (1997)
148. ATLAS Collaboration, M. Aaboud, et al., Measurement of the prompt J/ψ pair production cross-section in pp collisions at $\sqrt{s} = 8$ TeV with the ATLAS detector, *Eur. Phys. J. C* 77, 76 (2017), arXiv: 1612.02950
149. D0 Collaboration, V. M. Abazov, et al., Evidence for simultaneous production of J/ψ and Υ mesons, *Phys. Rev. Lett.* 116, 082002 (2016), arXiv: 1511.02428
150. J.-P. Lansberg and H.-S. Shao, J/ψ-pair production at large momenta: Indications for double parton scatterings and large α_s^5 contributions, *Phys. Lett. B* 751, 479 (2015), arXiv: 1410.8822
151. S. P. Baranov, A. M. Snigirev, and N. P. Zotov, Double heavy meson production through double parton scattering in hadronic collisions, *Phys. Lett. B* 705, 116 (2011), arXiv: 1105.6276
152. D. d'Enterria and A. M. Snigirev, Same-sign WW production in proton–nucleus collisions at the LHC as a signal for double parton scattering, *Phys. Lett. B* 718, 1395 (2013), arXiv: 1211.0197
153. E. G. Ferreiro and J.-P. Lansberg, Is bottomonium suppression in proton–nucleus and nucleus–nucleus collisions at LHC energies due to the same effects? *J. High Energy Phys.* 10, 094 (2018), Erratum: *J. High Energy Phys.* 03, 063 (2019), arXiv: 1804.04474
154. S. Gavin and J. Milana, Energy loss at large x_F in nuclear collisions, *Phys. Rev. Lett.* 68, 1834 (1992)
155. N. Armesto, Nuclear shadowing, *J. Phys. G* 32, R367 (2006), arXiv: hep-ph/0604108
156. F. Arleo and S. Peigne, Heavy-quarkonium suppression in p–A collisions from parton energy loss in cold QCD matter, *J. High Energy Phys.* 03, 122 (2013), arXiv: 1212.0434
157. A. Kusina, J.-P. Lansberg, I. Schienbein, and H.-S. Shao, Gluon shadowing in heavy-flavor production at the LHC, *Phys. Rev. Lett.* 121, 052004 (2018), arXiv: 1712.07024
158. F. Arleo, G. Jackson, and S. Peigné, Impact of fully coherent energy loss on heavy meson production in pA collisions, arXiv: 2107.05871 (2021)
159. E. Braaten, L.-P. He, K. Ingles, and J. Jiang, Production of $X(3872)$ at high multiplicity, *Phys. Rev. D* 103, L071901 (2021), arXiv: 2012.13499
160. A. Esposito, et al., The nature of $X(3872)$ from high-multiplicity pp collisions, *Eur. Phys. J. C* 81, 669 (2021), arXiv: 2006.15044
161. M. Gell-Mann, A schematic model of baryons and mesons, *Phys. Lett.* 8, 214 (1964)
162. G. Zweig, An SU_3 Model for Strong Interaction Symmetry and Its Breaking, Version 2, 1964
163. S.-L. Zhu, Understanding pentaquark states in QCD, *Phys. Rev. Lett.* 91, 232002 (2003), arXiv: hep-ph/0307345
164. Z.-F. Sun, et al., $Z_b(10610)^{\pm}$ and $Z_b(10650)^{\pm}$ as the $B^*\overline{B}$ and $B^*\overline{B}^*$ molecular states, *Phys. Rev. D* 84, 054002 (2011), arXiv: 1106.2968
165. X. Liu and S.-L. Zhu, $Y(4143)$ is probably a molecular partner of $Y(3930)$, *Phys. Rev. D* 80, 017502 (2009), Erratum: *Phys. Rev. D* 85, 019902 (2012), arXiv: 0903.2529
166. Y.-R. Liu, X. Liu, W.-Z. Deng, and S.-L. Zhu, Is $X(3872)$ really a molecular state? *Eur. Phys. J. C* 56, 63 (2008), arXiv: 0801.3540
167. S.-L. Zhu, New hadron states, *Int. J. Mod. Phys. E* 17, 283 (2008), arXiv: hep-ph/0703225
168. R. Chen, Z.-F. Sun, X. Liu, and S.-L. Zhu, Strong LHCb evidence supporting the existence of the hidden-

charm molecular pentaquarks, *Phys. Rev. D* 100, 011502 (2019), arXiv: 1903.11013
169. X. Liu, Y.-R. Liu, W.-Z. Deng, and S.-L. Zhu, Is $Z^+(4430)$ a loosely bound molecular state? *Phys. Rev. D* 77, 034003 (2008), arXiv: 0711.0494
170. Webpage: www.nikhef.nl/%7Epkoppenb/particles.html
171. LHCb Collaboration, R. Aaij, et al., Precise measurements of the properties of the $B_1(5721)^{0,+}$ and $B_2^*(5747)^{0,+}$ states and observation of structure at higher invariant mass in the $B^+\pi^-$ and $B^0\pi^+$ spectra, *J. High Energy Phys.* 04, 024 (2015), arXiv: 1502.02638
172. LHCb Collaboration, R. Aaij, et al., Observation of new excited B_s^0 states, *Eur. Phys. J. C* 81, 601 (2021), arXiv: 2010.15931
173. LHCb Collaboration, R. Aaij, et al., Study of D_J meson decays to $D^+\pi^-$, $D^0\pi^+$ and $D^{*+}\pi^-$ final states in pp collisions, *J. High Energy Phys.* 09, 145 (2013), arXiv: 1307.4556
174. LHCb Collaboration, R. Aaij, et al., Observation of overlapping spin-1 and spin-3 $\bar{D}^0K^-$ resonances at mass 2.86 GeV/c^2, *Phys. Rev. Lett.* 113, 162001 (2014), arXiv: 1407.7574
175. LHCb Collaboration, R. Aaij, et al., Amplitude analysis of $B^-\to D^+\pi^-\pi^-$ decays, *Phys. Rev. D* 94, 072001 (2016), arXiv: 1608.01289
176. LHCb Collaboration, R. Aaij, et al., Observation of a new excited D_s^+ state in $B^0\to D^-D^+K^+\pi^-$ decays, *Phys. Rev. Lett.* 126, 122002 (2021), arXiv: 2011.09112
177. S.-Q. Luo, B. Chen, X. Liu, and T. Matsuki, Predicting a new resonance as charmed-strange baryonic analog of D_{s0}^* (2317), *Phys. Rev. D* 103, 074027 (2021), arXiv: 2102.00679
178. R.-H. Ni, Q. Li, and X.-H. Zhong, Mass spectra and strong decays of charmed and charmed-strange mesons, arXiv: 2110.05024 (2021)
179. J.-M. Xie, M.-Z. Liu, and L.-S. Geng, $D_{s0}(2590)$ as a dominant $c\bar{s}$ state with a small D^*K component, arXiv: 2108.12993 (2021)
180. Z. Yang, et al., Novel coupled channel framework connecting quark model and lattice QCD: An investigation on near-threshold D_s states, arXiv: 2107.04860 (2021)
181. G.-L. Wang, et al., The newly observed state $D_{s0}(2590)^+$ and width of $D^*(2007)^0$, arXiv: 2107.01751 (2021)
182. Z.-H. Wang, G.-L. Wang, J.-M. Zhang, and T.-H. Wang, The productions and strong decays of $D_q(2S)$ and $B_q(2S)$, *J. Phys. G* 39, 085006 (2012), arXiv: 1207.2528
183. X. Liu, et al., Bottom baryons, *Phys. Rev. D* 77, 014031 (2008), arXiv: 0710.0123
184. G.-L. Yu, Z.-G. Wang, and X.-W. Wang, The $1D$, $2D$ Ξ_b and Λ_b baryons, arXiv: 2109.02217 (2021)
185. K.-L. Wang and X.-H. Zhong, Toward establishing the low-lying P-wave excited Σ_c baryon states, arXiv: 2110.12443 (2021)
186. T. Matsuki, et al., Regge-like relation and universal description of heavy-light systems, *PoS Hadron* 2017, 071 (2018)
187. K.-L. Wang, Y.-X. Yao, X.-H. Zhong, and Q. Zhao, Strong and radiative decays of the low-lying S- and P-wave singly heavy baryons, *Phys. Rev. D* 96, 116016 (2017), arXiv: 1709.04268
188. Q. Mao, et al., D-wave heavy baryons of the $SU(3)$ flavor $\mathbf{6}_F$, *Phys. Rev. D* 96, 074021 (2017), arXiv: 1707.03712
189. H.-Y. Cheng and C.-W. Chiang, Quantum numbers of Ω_c states and other charmed baryons, *Phys. Rev. D* 95, 094018 (2017), arXiv: 1704.00396
190. H.-M. Yang and H.-X. Chen, P-wave bottom baryons of the $SU(3)$ flavor $\mathbf{6}_F$, *Phys. Rev. D* 101, 114013 (2020), Erratum: *Phys. Rev. D* 102, 079901 (2020), arXiv: 2003.07488
191. B. Chen, K.-W. Wei, X. Liu, and A. Zhang, Role of newly discovered $\Xi_b(6227)^-$ for constructing excited bottom baryon family, *Phys. Rev. D* 98, 031502 (2018), arXiv: 1805.10826
192. Z.-Y. Wang, J.-J. Qi, X.-H. Guo, and K.-W. Wei, Spectra of charmed and bottom baryons with hyperfine interaction, *Chin. Phys. C* 41, 093103 (2017), arXiv: 1701.04524
193. K.-W. Wei, et al., Spectroscopy of singly, doubly, and triply bottom baryons, *Phys. Rev. D* 95, 116005 (2017), arXiv: 1609.02512
194. J.-X. Lu, et al., $\Lambda_c(2595)$ resonance as a dynamically generated state: The compositeness condition and the large N_c evolution, *Phys. Rev. D* 93, 114028 (2016), arXiv: 1603.05388
195. H.-Z. He, W. Liang, Q.-F. Lü, and Y.-B. Dong, Strong decays of the low-lying bottom strange baryons, *Sci. China Phys. Mech. Astron.* 64, 261012 (2021), arXiv: 2102.07391
196. J.-R. Zhang and M.-Q. Huang, Heavy baryon spectroscopy in QCD, *Phys. Rev. D* 78, 094015 (2008), arXiv: 0811.3266
197. J.-R. Zhang and M.-Q. Huang, Mass spectra of the heavy baryons Λ_Q and $\Sigma_Q^{(*)}$ From QCD sum rules, *Phys. Rev. D* 77, 094002 (2008), arXiv: 0805.0479
198. K.-W. Wei and X.-H. Guo, Mass spectra of doubly heavy mesons in Regge phenomenology, *Phys. Rev. D* 81, 076005 (2010)
199. F.-K. Guo, C. Hanhart, and U.-G. Meissner, Mass splittings within heavy baryon isospin multiplets in chiral perturbation theory, *J. High Energy Phys.* 09, 136 (2008), arXiv: 0809.2359
200. LHCb Collaboration, R. Aaij, et al., Observation of five new narrow $\Omega^0{}_c$ states decaying to $\Xi_c^+K^-$, *Phys. Rev. Lett.* 118, 182001 (2017), arXiv: 1703.04639
201. Belle Collaboration, J. Yelton, et al., Observation of excited Ω_c charmed baryons in e^+e^- collisions, *Phys. Rev. D* 97, 051102 (2018), arXiv: 1711.07927
202. LHCb Collaboration, R. Aaij, et al., Observation of excited Ω_c^0 baryons in $\Omega_b^-\to\Xi_c^+K^-\pi^+$ decays, *Phys. Rev. D* 104, L091102 (2021), arXiv: 2107.03419
203. M. Karliner and J. L. Rosner, Very narrow excited c baryons, *Phys. Rev. D* 95, 114012 (2017), arXiv: 1703.07774
204. K.-L. Wang, L.-Y. Xiao, X.-H. Zhong, and Q. Zhao, Understanding the newly observed Ω_c states through their decays, *Phys. Rev. D* 95, 116010 (2017), arXiv: 1703.09130
205. H.-G. Xu, et al., Investigation of Ω_c^0 states decaying to

$\Xi_c^+ K^-$ in pp collisions at $\sqrt{s} = 7.13$ TeV, *Phys. Rev. C* 102, 054319 (2020), arXiv: 1912.12905

206. B. Chen and X. Liu, New Ω_c^0 baryons discovered by LHCb as the members of $1P$ and $2S$ states, *Phys. Rev. D* 96, 094015 (2017), arXiv: 1704.02583
207. W. Wang and R.-L. Zhu, Interpretation of the newly observed Ω_c^0 resonances, *Phys. Rev. D* 96, 014024 (2017), arXiv: 1704.00179
208. H.-X. Chen, et al., Decay properties of P-wave charmed baryons from light-cone QCD sum rules, *Phys. Rev. D* 95, 094008 (2017), arXiv: 1703.07703
209. G. Yang and J. Ping, Dynamical study of Ω_c^0 in the chiral quark model, *Phys. Rev. D* 97, 034023 (2018), arXiv: 1703.08845
210. H.-J. Wang, Z.-Y. Di, and Z.-G. Wang, Analysis of the excited Ω_c states as the $(1/2)^{\pm}$ pentaquark states with QCD sum rules, *Commun. Theor. Phys.* 73, 035201 (2021)
211. Z.-G. Wang and J.-X. Zhang, Possible pentaquark candidates: New excited Ω_c states, *Eur. Phys. J. C* 78, 503 (2018), arXiv: 1804.06195
212. R. Chen, A. Hosaka, and X. Liu, Searching for possible Ω_c-like molecular states from meson–baryon interaction, *Phys. Rev. D* 97, 036016 (2018), arXiv: 1711.07650
213. C. Wang et al., Possible open-charmed pentaquark molecule $\Omega_c(3188)$ — the $D\Xi$ bound state — in the Bethe–Salpeter formalism, *Eur. Phys. J. C* 78, 407 (2018), arXiv: 1710.10850
214. Z.-G. Wang, X.-N. Wei, and Z.-H. Yan, Revisit assignments of the new excited Ω_c states with QCD sum rules, *Eur. Phys. J. C* 77, 832 (2017), arXiv: 1706.09401
215. LHCb Collaboration, R. Aaij, et al., Observation of new Ξ_c^0 baryons decaying to $\Lambda_c^+ K^-$, *Phys. Rev. Lett.* 124, 222001 (2020), arXiv: 2003.13649
216. Belle collaboration, Y. B. Li, et al., Observation of $\Xi_c(2930)^0$ and updated measurement of $B^- \to K^- \Lambda_c^+ \overline{\Lambda}_c^-$ at Belle, *Eur. Phys. J. C* 78, 252 (2018), arXiv: 1712.03612
217. LHCb Collaboration, R. Aaij, et al., Study of the $B^+ \to \Lambda_c^+ \overline{\Lambda}_c^- K^+$ decay, arXiv: 2211.00812 (submitted to *Phys. Rev. D*)
218. D. Ebert, R. N. Faustov, and V. O. Galkin, Masses of excited heavy baryons in the relativistic quark model, *Phys. Lett. B* 659, 612 (2008), arXiv: 0705.2957
219. W. Roberts and M. Pervin, Heavy baryons in a quark model, *Int. J. Mod. Phys. A* 23, 2817 (2008), arXiv: 0711.2492
220. S. Migura, D. Merten, B. Metsch, and H.-R. Petry, Charmed baryons in a relativistic quark model, *Eur. Phys. J. A* 28, 41 (2006), arXiv: hep-ph/0602153
221. H.-M. Yang and H.-X. Chen, P-wave charmed baryons of the $SU(3)$ flavor $\mathbf{6}_F$, *Phys. Rev. D* 104, 034037 (2021), arXiv: 2106.15488
222. B. Chen, S.-Q. Luo, and X. Liu, Universal behavior of mass gaps existing in the single heavy baryon family, *Eur. Phys. J. C* 81, 474 (2021), arXiv: 2101.10806
223. J. Nieves, R. Pavao, and L. Tolos, Ξ_c and Ξ_b excited states within a $SU(6)_{\rm lsf}\times$HQSS model, *Eur. Phys. J. C* 80, 22 (2020), arXiv: 1911.06089
224. Y.-J. Xu, Y.-L. Liu, C.-Y. Cui, and M.-Q. Huang, P-wave Ω_b states: Masses and pole residues, arXiv: 2010.10697 (2020)
225. M. Karliner and J. L. Rosner, Interpretation of excited Ω_b signals, *Phys. Rev. D* 102, 014027 (2020), arXiv: 2005.12424
226. L.-Y. Xiao and X.-H. Zhong, Toward establishing the low-lying P-wave Σ_b states, *Phys. Rev. D* 102, 014009 (2020), arXiv: 2004.11106
227. H.-M. Yang, H.-X. Chen, and Q. Mao, Excited Ξ_c^0 baryons within the QCD rum rule approach, *Phys. Rev. D* 102, 114009 (2020), arXiv: 2004.00531
228. L.-Y. Xiao, K.-L. Wang, M.-S. Liu, and X.-H. Zhong, Possible interpretation of the newly observed Ω_b states, *Eur. Phys. J. C* 80, 279 (2020), arXiv: 2001.05110
229. Z.-G. Wang, Analysis of the $\Omega_b(6316)$, $\Omega_b(6330)$, $\Omega_b(6340)$ and $\Omega_b(6350)$ with QCD sum rules, *Int. J. Mod. Phys. A* 35, 2050043 (2020), arXiv: 2001.02961
230. W.-H. Liang and E. Oset, Observed Ω_b spectrum and meson–baryon molecular states, *Phys. Rev. D* 101, 054033 (2020), arXiv: 2001.02929
231. H.-X. Chen, et al., Excited Ω_b baryons and fine structure of strong interaction, *Eur. Phys. J. C* 80, 256 (2020), arXiv: 2001.02147
232. W. Liang and Q.-F. Lü, Strong decays of the newly observed narrow Ω_b structures, *Eur. Phys. J. C* 80, 198 (2020), arXiv: 2001.02221
233. Q.-F. Lü and X.-H. Zhong, Strong decays of the higher excited Λ_Q and Σ_Q baryons, *Phys. Rev. D* 101, 014017 (2020), arXiv: 1910.06126
234. B. Chen and X. Liu, Assigning the newly reported $\Sigma_b(6097)$ as a P-wave excited state and predicting its partners, *Phys. Rev. D* 98, 074032 (2018), arXiv: 1810.00389
235. H.-J. Wang, Z.-Y. Di, and Z.-G. Wang, Analysis of the $\Xi_b(6227)$ as the $(1/2)^{\pm}$ pentaquark molecular states with QCD sum rules, *Int. J. Theor. Phys.* 59, 3124 (2020)
236. Q. Mao, et al., QCD sum rule calculation for P-wave bottom baryons, *Phys. Rev. D* 92, 114007 (2015), arXiv: 1510.05267
237. J.-X. Lu, et al., Dynamically generated $J^P = 1/2^-$ $(3/2^-)$ singly charmed and bottom heavy baryons, *Phys. Rev. D* 92, 014036 (2015), arXiv: 1409.3133
238. P. Yang, J.-J. Guo, and A. Zhang, Identification of the newly observed $\Sigma_b(6097)^{\pm}$ baryons from their strong decays, *Phys. Rev. D* 99, 034018 (2019), arXiv: 1810.06947
239. Y. Huang, C.-j. Xiao, L.-S. Geng, and J. He, Strong decays of the $\Xi_b(6227)$ as a $\Sigma_b \overline{K}$ molecule, *Phys. Rev. D* 99, 014008 (2019), arXiv: 1811.10769
240. LHCb Collaboration, R. Aaij, et al., Observation of excited Λ_b^0 baryons, *Phys. Rev. Lett.* 109, 172003 (2012), arXiv: 1205.3452
241. LHCb Collaboration, R. Aaij, et al., Observation of new resonances in the $\Lambda_b^0 \pi^+ \pi^-$ system, *Phys. Rev. Lett.* 123, 152001 (2019), arXiv: 1907.13598
242. LHCb Collaboration, R. Aaij, et al., Observation of a new baryon state in the $\Lambda_b^0 \pi^+ \pi^-$ mass spectrum, JHEP 06 (2020) 136, arXiv: 2002.05112
243. B. Chen, S.-Q. Luo, X. Liu, and T. Matsuki, Interpretation of the observed $\Lambda_b(6146)^0$ and $\Lambda_b(6152)^0$ states

as 1D bottom baryons, *Phys. Rev. D* 100, 094032 (2019), arXiv: 1910.03318
244. H.-M. Yang, et al., Decay properties of *P*-wave bottom baryons within light-cone sum rules, *Eur. Phys. J. C* 80, 80 (2020), arXiv: 1909.13575
245. K.-L. Wang, Q.-F. Lü, and X.-H. Zhong, Interpretation of the newly observed $\Lambda_b(6146)^0$ and $\Lambda_b(6152)^0$ states in a chiral quark model, *Phys. Rev. D* 100, 114035 (2019), arXiv: 1908.04622
246. K.-L. Wang, Q.-F. Lü, and X.-H. Zhong, Interpretation of the newly observed $\Sigma_b(6097)^{\pm}$ and $\Xi_b(6227)^-$ states as the *P*-wave bottom baryons, *Phys. Rev. D* 99, 014011 (2019), arXiv: 1810.02205
247. Q. Mao, H.-X. Chen, and H.-M. Yang, Identifying the $\Lambda_b(6146)^0$ and $\Lambda_b(6152)^0$ as *D*-wave bottom baryons, *Universe* 6, 86 (2020), arXiv: 2002.11435
248. CDF Collaboration, T. Aaltonen, et al., Observation of the heavy baryons Σ_b and Σ_b^*, *Phys. Rev. Lett.* 99, 202001 (2007), arXiv: 0706.3868
249. LHCb Collaboration, R. Aaij, et al., Observation of two resonances in the $\Lambda_b^0\pi^{\pm}$ systems and precise measurement of $\Sigma_b^{\pm}$ and $\Sigma_b^{*\pm}$ properties, *Phys. Rev. Lett.* 122, 012001 (2019), arXiv: 1809.07752
250. CMS Collaboration, S. Chatrchyan, et al., Observation of a new Ξ_b baryon, *Phys. Rev. Lett.* 108, 252002 (2012), arXiv: 1204.5955
251. LHCb Collaboration, R. Aaij, et al., Observation of two new Ξ_b^- baryon resonances, *Phys. Rev. Lett.* 114, 062004 (2015), arXiv: 1411.4849
252. LHCb Collaboration, R. Aaij, et al., Observation of a new Ξ_b^- resonance, *Phys. Rev. Lett.* 121, 072002 (2018), arXiv: 1805.09418
253. LHCb Collaboration, R. Aaij, et al., Observation of a new Ξ_b^0 state, *Phys. Rev. D* 103, 012004 (2021), arXiv: 2010.14485
254. LHCb Collaboration, R. Aaij, et al., Observation of two new excited Ξ_b^0 states decaying to $\Lambda_b^0K^-\pi^+$, *Phys. Rev. Lett.* 128, 162001 (2022), arXiv: 2110.04497
255. CMS Collaboration, A. M. Sirunyan, et al., Observation of a new excited beauty strange baryon decaying to $\Xi_b^-\pi^+\pi^-$, *Phys. Rev. Lett.* 126, 252003 (2021), arXiv: 2102.04524
256. LHCb Collaboration, R. Aaij, et al., First observation of excited Ω_b^- states, *Phys. Rev. Lett.* 124, 082002 (2020), arXiv: 2001.00851
257. LHCb Collaboration, R. Aaij, et al., Observation of an excited B_c^+ state, *Phys. Rev. Lett.* 122, 232001 (2019), arXiv: 1904.00081
258. LHCb Collaboration, R. Aaij, et al., Observation of the doubly charmed baryon Ξ_{cc}^{++}, *Phys. Rev. Lett.* 119, 112001 (2017), arXiv: 1707.01621
259. LHCb Collaboration, R. Aaij, et al., Near-threshold $D\overline{D}$ spectroscopy and observation of a new charmonium state, *J. High Energy Phys.* 07, 035 (2019), arXiv: 1903.12240
260. T. Barnes, S. Godfrey, and E. S. Swanson, Higher charmonia, *Phys. Rev. D* 72, 054026 (2005), arXiv: hep-ph/0505002
261. CMS Collaboration, A. M. Sirunyan, et al., Observation of two excited B_c^+ states and measurement of the $B_c^+(2S)$ mass in pp collisions at $\sqrt{s}$= 13 TeV, *Phys. Rev. Lett.* 122, 132001 (2019), arXiv: 1902.00571
262. S. N. Gupta and J. M. Johnson, B_c spectroscopy in a quantum chromodynamic potential model, *Phys. Rev. D* 53, 312 (1996), arXiv: hep-ph/9511267
263. Y. -Q. Chen and Y. -P. Kuang, Improved QCD motivated heavy quark potentials with explicit $\Lambda_{\overline{\rm MS}}$ dependence, *Phys. Rev. D* 46, 1165 (1992), Erratum: *Phys. Rev. D* 47, 350 (1993)
264. R. Ding, et al., Finding $B_c(3S)$ states via their strong decays, *Phys. Lett. B* 816, 136277 (2021), arXiv: 2101.01958
265. M. Chen, L. Chang, and Y.-X. Liu, B_c meson spectrum via Dyson–Schwinger equation and Bethe–Salpeter equation approach, *Phys. Rev. D* 101, 056002 (2020), arXiv: 2001.00161
266. L. Chang, et al., Can the hyperfine mass splitting formula in heavy quarkonia be applied to the B_c system? *Few Body Syst.* 62, 4 (2021), arXiv: 1912.08339
267. L. Chang, M. Chen, and Y.-X. Liu, Excited B_c states via the Dyson–Schwinger equation approach of QCD, *Phys. Rev. D* 102, 074010 (2020), arXiv: 1904.00399
268. C.-H. Chang, C. Driouichi, P. Eerola, and X. G. Wu, BCVEGPY: An event generator for hadronic production of the B_c meson, *Comput. Phys. Commun.* 159, 192 (2004), arXiv: hep-ph/0309120
269. C.-H. Chang, J.-X. Wang, and X.-G. Wu, BCVEGPY2.0: An upgraded version of the generator BCVEGPY with an addition of hadroproduction of the *P*-wave B_c states, *Comput. Phys. Commun.* 174, 241 (2006), arXiv: hep-ph/0504017
270. F.-S. Yu, Role of decay in the search for double-charm baryons, *Sci. China Phys. Mech. Astron.* 63, 221065 (2020), arXiv: 1912.10253
271. X.-H. Hu and Y.-J. Shi, Light-cone sum rules analysis of $\Xi_{QQ'} \to \Sigma_{Q'}$ weak decays, *Eur. Phys. J. C* 80, 56 (2020), arXiv: 1910.07909
272. LHCb Collaboration, R. Aaij, et al., First observation of the doubly charmed baryon decay $\Xi_{cc}^{++} \to \Xi_c^+\pi^+$, *Phys. Rev. Lett.* 121, 162002 (2018), arXiv: 1807.01919
273. LHCb Collaboration, R. Aaij, et al., Precision measurement of the Ξ_{cc}^{++} mass, *J. High Energy Phys.* 02, 049 (2020), arXiv: 1911.08594
274. LHCb Collaboration, R. Aaij, et al., Search for the doubly charmed baryon Ξ_{cc}^+, *Sci. China Phys. Mech. Astron.* 63, 221062 (2020), arXiv: 1909.12273
275. LHCb Collaboration, R. Aaij, et al., Search for the doubly charmed baryon Ω_{cc}^+, *Sci. China Phys. Mech. Astron.* 64, 101062 (2021), arXiv: 2105.06841
276. LHCb Collaboration, R. Aaij, et al., Search for the doubly charmed baryon Ξ_{cc}^{++} in the $\Xi_c^+\pi^-\pi^+$ final state, *J. High Energy Phys.* 12, 107 (2021), arXiv: 2109.07292
277. H.-Z. Tong and H.-S. Li, The chiral corrections to the masses of the doubly heavy baryons, arXiv: 2110.01380 (2021)
278. H.-S. Li and W.-L. Yang, Spin-3/2 doubly charmed baryon contribution to the magnetic moments of the spin-1/2 doubly charmed baryons, *Phys. Rev. D* 103, 056024 (2021), arXiv: 2012.14596
279. J.-B. Wang, et al., Ω_{cc} resonances with negative parity

in the chiral constituent quark model, *Phys. Rev. D* 104, 094008 (2021), arXiv: 2110.06408
280. M.-S. Liu, Q.-F. Lü, and X.-H. Zhong, Triply charmed and bottom baryons in a constituent quark model, *Phys. Rev. D* 101, 074031 (2020), arXiv: 1912.11805
281. J. M. Dias, et al., Ξ_{bb} and Ξ_{bbb} molecular states, *Chin. Phys. C* 44 (2020) 064101, arXiv: 1912.04517
282. Q.-X. Yu, J. M. Dias, W.-H. Liang, and E. Oset, Molecular Ξ_{bc} states from meson–baryon interaction, *Eur. Phys. J. C* 79, 1025 (2019), arXiv: 1909.13449
283. Q. Li, C.-H. Chang, S.-X. Qin, and G.-L. Wang, Mass spectra and wave functions of the doubly heavy baryons with $J^P = 1^+$ heavy diquark cores, *Chin. Phys. C* 44, 013102 (2020), arXiv: 1903.02282
284. H.-X. Chen, et al., Establishing low-lying doubly charmed baryons, *Phys. Rev. D* 96, 031501 (2017), Erratum: *Phys. Rev. D* 96, 119902 (2017), arXiv: 1707.01779
285. C.-Y. Wang, C. Meng, Y.-Q. Ma, and K.-T. Chao, NLO effects for doubly heavy baryons in QCD sum rules, *Phys. Rev. D* 99, 014018 (2019), arXiv: 1708.04563
286. T. Guo, J. Li, J. Zhao, and L. He, Mass spectra of doubly heavy tetraquarks in an improved chromomagnetic interaction model, arXiv: 2108.10462 (2021)
287. Q. Qin, et al., Inclusive approach to hunt for the beauty-charmed baryons Ξ_{bc}, *Phys. Rev. D* 105, L031902 (2022), arXiv: 2108.06716
288. D. Gao, et al., Masses of doubly heavy tetraquark states with isospin = 1/2 and 1 and spin-parity $1^{+\pm}$, arXiv: 2007.15213 (2020)
289. X.-Z. Weng, X.-L. Chen, and W.-Z. Deng, Masses of doubly heavy-quark baryons in an extended chromomagnetic model, *Phys. Rev. D* 97, 054008 (2018), arXiv: 1801.08644
290. J.-J. Han, et al., Weak decays of bottom-charm baryons: $\mathcal{B}_{bc} \to \mathcal{B}_b P$, *Eur. Phys. J. C* 81, 539 (2021), arXiv: 2102.00961
291. D.-M. Li, X.-R. Zhang, Y. Xing, and J. Xu, Weak decays of doubly heavy baryons: Four-body nonleptonic decay channels, *Eur. Phys. J. Plus* 136, 772 (2021), arXiv: 2101.12574
292. J.-J. Han, et al., Rescattering mechanism of weak decays of double-charm baryons, *Chin. Phys. C* 45, 053105 (2021), arXiv: 2101.12019
293. Z.-G. Wang, Analysis of the triply-heavy baryon states with the QCD sum rules, *AAPPS Bull.* 31, 5 (2021), arXiv: 2010.08939
294. L.-Y. Xiao, Q.-F. Lü, and S.-L. Zhu, Strong decays of the $1P$ and $2D$ doubly charmed states, *Phys. Rev. D* 97, 074005 (2018), arXiv: 1712.07295
295. Y.-J. Shi, W. Wang, and Z.-X. Zhao, QCD sum rules analysis of weak decays of doubly-heavy baryons, *Eur. Phys. J. C* 80, 568 (2020), arXiv: 1902.01092
296. H.-Y. Cheng and F. Xu, Lifetimes of doubly heavy baryons $\mathcal{B}_{bb}$ and $\mathcal{B}_{bc}$, *Phys. Rev. D* 99, 073006 (2019), arXiv: 1903.08148
297. Q.-A. Zhang, Weak decays of doubly heavy baryons: W-exchange, *Eur. Phys. J. C* 78, 1024 (2018), arXiv: 1811.02199
298. L.-J. Jiang, B. He, and R.-H. Li, Weak decays of doubly heavy baryons: $\mathcal{B}_{cc} \to \mathcal{B}_c V$, *Eur. Phys. J. C* 78, 961 (2018), arXiv: 1810.00541
299. Z.-X. Zhao, Weak decays of heavy baryons in the light-front approach, *Chin. Phys. C* 42, 093101 (2018), arXiv: 1803.02292
300. W. Wang and J. Xu, Weak decays of triply heavy baryons, *Phys. Rev. D* 97, 093007 (2018), arXiv: 1803.01476
301. E.-L. Cui, et al., Suggested search for doubly charmed baryons of $J^P = 3/2^+$ via their electromagnetic transitions, *Phys. Rev. D* 97, 034018 (2018), arXiv: 1712.03615
302. Y.-J. Shi, W. Wang, Y. Xing, and J. Xu, Weak decays of doubly heavy baryons: Multi-body decay channels, *Eur. Phys. J. C* 78, 56 (2018), arXiv: 1712.03830
303. L. Meng, H.-S. Li, Z.-W. Liu, and S.-L. Zhu, Magnetic moments of the spin-3/2 doubly heavy baryons, *Eur. Phys. J. C* 77, 869 (2017), arXiv: 1710.08283
304. C. Q. Geng, Y. K. Hsiao, C.-W. Liu, and T.-H. Tsai, Charmed baryon weak decays with $SU(3)$ flavor symmetry, *J. High Energy Phys.* 11, 147 (2017), arXiv: 1709.00808
305. Q.-F. Lü, K.-L. Wang, L.-Y. Xiao, and X.-H. Zhong, Mass spectra and radiative transitions of doubly heavy baryons in a relativized quark model, *Phys. Rev. D* 96, 114006 (2017), arXiv: 1708.04468
306. L.-Y. Xiao, et al., Strong and radiative decays of the doubly charmed baryons, *Phys. Rev. D* 96, 094005 (2017), arXiv: 1708.04384
307. H.-S. Li, L. Meng, Z.-W. Liu, and S.-L. Zhu, Radiative decays of the doubly charmed baryons in chiral perturbation theory, *Phys. Lett. B* 777, 169 (2018), arXiv: 1708.03620
308. W. Wang, Z.-P. Xing, and J. Xu, Weak decays of doubly heavy baryons: $SU(3)$ analysis, *Eur. Phys. J. C* 77, 800 (2017), arXiv: 1707.06570
309. W. Wang, F.-S. Yu, and Z.-X. Zhao, Weak decays of doubly heavy baryons: The $1/2 \to 1/2$ case, *Eur. Phys. J. C* 77, 781 (2017), arXiv: 1707.02834
310. F.-S. Yu, et al., Discovery potentials of doubly charmed baryons, *Chin. Phys. C* 42, 051001 (2018), arXiv: 1703.09086
311. G.-Y. Chen, W.-S. Huo, and Q. Zhao, Identifying the structure of near-threshold states from the line shape, *Chin. Phys. C* 39, 093101 (2015), arXiv: 1309.2859
312. Z.-Y. Wang, J.-J. Qi, X.-H. Guo, and C. Wang, $X(3872)$ as a molecular $D\overline{D}^*$ state in the Bethe–Salpeter equation approach, *Phys. Rev. D* 97, 016015 (2018), arXiv: 1710.07424
313. J.-B. Cheng, et al., Double-heavy tetraquark states with heavy diquark–antiquark symmetry, *Chin. Phys. C* 45, 043102 (2021), arXiv: 2008.00737
314. Q.-F. Lü, D.-Y. Chen, and Y.-B. Dong, Masses of doubly heavy tetraquarks $T_{QQ'}$ in a relativized quark model, *Phys. Rev. D* 102, 034012 (2020), arXiv: 2006.08087
315. Y.-J. Shi, W. Wang, Z.-X. Zhao, and U.-G. Meiβner, Towards a heavy diquark effective theory for weak decays of doubly heavy baryons, *Eur. Phys. J. C* 80, 398 (2020), arXiv: 2002.02785
316. H.-T. An, et al., Exotic pentaquark states with the

$qqQQ\overline{Q}$ configuration, *Phys. Rev. D* 100, 056004 (2019), arXiv: 1905.07858

317. L. Meng and S.-L. Zhu, Light pseudoscalar meson and doubly charmed baryon scattering lengths with heavy diquark-antiquark symmetry, *Phys. Rev. D* 100, 014006 (2019), arXiv: 1811.07320
318. Q.-S. Zhou, et al., Surveying exotic pentaquarks with the typical $QQq\bar{q}$ configuration, *Phys. Rev. C* 98, 045204 (2018), arXiv: 1801.04557
319. K. Chen, et al., Triply heavy tetraquark states with the $QQ\overline{Qq}$ configuration, *Eur. Phys. J. A* 53, 5 (2017), arXiv: 1609.06117
320. X.-K. Dong, F.-K. Guo, and B. S. Zou, Near threshold structures and hadronic molecules, *Few Body Syst.* 62, 61 (2021)
321. Z.-M. Ding, H.-Y. Jiang, D. Song, and J. He, Hidden and doubly heavy molecular states from interactions $D_{(s)}^{(*)}\bar{D}_s^{(*)}/B_{(s)}^{(*)}\bar{B}_s^{(*)}$ and $D_{(s)}^{(*)}D_s^{(*)}/B_{(s)}^{(*)}B_s^{(*)}$, *Eur. Phys. J. C* 81, 732 (2021), arXiv: 2107.00855
322. X. Chen, The genuine resonance of full-charm tetraquarks, *Universe* 7, 155 (2021)
323. G. Yang, J. Ping, and J. Segovia, QQ tetraquarks in the chiral quark model, *Phys. Rev. D* 102, 054023 (2020), arXiv: 2007.05190
324. Belle Collaboration, S. K. Choi, et al., Observation of a narrow charmoniumlike state in exclusive $B^{\pm}\to K^{\pm}\pi^+\pi^- J/\psi$ decays, *Phys. Rev. Lett.* 91, 262001 (2003), arXiv: hep-ex/0309032
325. LHCb Collaboration, R. Aaij, et al., Quantum numbers of the $X(3872)$ state and orbital angular momentum in its ρ^0 J/ψ decays, *Phys. Rev. D* 92, 011102(R) (2015), arXiv: 1504.06339
326. Particle Data Group, P. A. Zyla, et al., Review of particle physics, *Prog. Theor. Exp. Phys.* 2020, 083C01 (2020)
327. LHCb Collaboration, R. Aaij, et al., Study of the line shape of the $\chi_{c1}(3872)$ state, *Phys. Rev. D* 102, 092005 (2020), arXiv: 2005.13419
328. LHCb Collaboration, R. Aaij, et al., Study of the $\psi_2(3823)$ and $\chi_{c1}(3872)$ states in $B^+\to(J/\psi\pi^+\pi^-)$ K^+ decays, *J. High Energy Phys.* 08, 123 (2020), arXiv: 2005.13422
329. LHCb Collaboration, R. Aaij, et al., Evidence for the decay $X(3872)\to\psi(2S)\gamma$, *Nucl. Phys. B* 886, 665 (2014), arXiv: 1404.0275
330. LHCb Collaboration, R. Aaij, et al., Observation of sizeable ω contribution to $\chi_{c1}\to\pi^+\pi^- J/\psi$ decays, arXiv: 2204.12597 (submitted to *Phys. Rev. Lett.*)
331. Z.-H. Zhang and F.-K. Guo, $D^{\pm}D^{*\mp}$ hadronic atom as a key to revealing the $X(3872)$ mystery, *Phys. Rev. Lett.* 127, 012002 (2021), arXiv: 2012.08281
332. L. Meng, G.-J. Wang, B. Wang, and S.-L. Zhu, Revisit the isospin violating decays of $X(3872)$, *Phys. Rev. D* 104, 094003 (2021), arXiv: 2109.01333
333. L. He, K. Ingles, E. Braaten, and J. Jiang, Triangle singularities in the production of $X(3872)$, *PoS CHARM* 2020, 027 (2021)
334. L. Maiani, F. Piccinini, A. D. Polosa, and V. Riquer, Diquark–antidiquarks with hidden or open charm and the nature of $X(3872)$, *Phys. Rev. D* 71, 014028 (2005), arXiv: hep-ph/0412098
335. Z.-G. Wang and T. Huang, Analysis of the $X(3872)$, $Z_c(3900)$ and $Z_c(3885)$ as axial-vector tetraquark states with QCD sum rules, *Phys. Rev. D* 89, 054019 (2014), arXiv: 1310.2422
336. W. Chen and S.-L. Zhu, Vector and axial-vector charmoniumlike states, *Phys. Rev. D* 83, 034010 (2011), arXiv: 1010.3397
337. B. A. Li, Is $X(3872)$ a possible candidate of as a hybrid meson, *Phys. Lett. B* 605, 306 (2005), arXiv: hep-ph/0410264
338. F.-K. Guo, C. Hanhart, Q. Wang, and Q. Zhao, Could the near-threshold XYZ states be simply kinematic effects? *Phys. Rev. D* 91, 051504 (2015), arXiv: 1411.5584
339. F.-K. Guo, et al., Production of the $X(3872)$ in charmonia radiative decays, *Phys. Lett. B* 725, 127 (2013), arXiv: 1306.3096
340. C. Meng and K.-T. Chao, Decays of the $X(3872)$ and $\chi_{c1}(2P)$ charmonium state, *Phys. Rev. D* 75, 114002 (2007), arXiv: hep-ph/0703205
341. F.-K. Guo, et al., Interplay of quark and meson degrees of freedom in near-threshold states: A practical parametrization for line shapes, *Phys. Rev. D* 93 (2016) 074031, arXiv: 1602.00940
342. S.-Q. Luo, et al., Exotic tetraquark states with the $qq\overline{QQ}$ configuration, *Eur. Phys. J. C* 77, 709 (2017), arXiv: 1707.01180
343. X.-W. Kang and J. A. Oller, Different pole structures in line shapes of the $X(3872)$, *Eur. Phys. J. C* 77, 399 (2017), arXiv: 1612.08420
344. C. Z. Yuan, P. Wang, and X. H. Mo, The $Y(4260)$ as an $\omega\chi_{c1}$ molecular state, *Phys. Lett. B* 634, 399 (2006), arXiv: hep-ph/0511107
345. Y. Cui, X.-L. Chen, W.-Z. Deng, and S.-L. Zhu, Possible heavy tetraquarks $qQ\bar{q}\bar{Q}, qq\overline{QQ}$ and $qQ\overline{QQ}^*$, *High Energy Phys. Nucl. Phys.* 31, 7 (2007), arXiv: hep-ph/0607226
346. C. Meng, Y.-J. Gao, and K.-T. Chao, $B\to\chi_{c1}(1P, 2P)K$ decays in QCD factorization and $X(3872)$, *Phys. Rev. D* 87, 074035 (2013), arXiv: hep-ph/0506222
347. J.-R. Zhang and M.-Q. Huang, $\{Q\bar{q}\}\left\{\bar{Q}^{(\prime)}q\right\}$ molecular states, *Phys. Rev. D* 80, 056004 (2009), arXiv: 0906.0090
348. O. Zhang, C. Meng, and H. Q. Zheng, Ambiversion of $X(3872)$, *Phys. Lett. B* 680, 453 (2009), arXiv: 0901.1553
349. C. Meng, H. Han, and K.-T. Chao, $X(3872)$ and its production at hadron colliders, *Phys. Rev. D* 96, 074014 (2017), arXiv: 1304.6710
350. G.-J. Ding, J.-F. Liu, and M.-L. Yan, Dynamics of hadronic molecule in one-boson exchange approach and possible heavy flavor molecules, *Phys. Rev. D* 79, 054005 (2009), arXiv: 0901.0426
351. H.-X. Chen, et al., QCD sum rule study of hidden-charm pentaquarks, *Eur. Phys. J. C* 76, 572 (2016), arXiv: 1602.02433
352. N. Li and S.-L. Zhu, Isospin breaking, coupled-channel effects and diagnosis of $X(3872)$, *Phys. Rev. D* 86, 074022 (2012), arXiv: 1207.3954
353. M.-Z. Liu, et al., Heavy-quark spin and avor symmetry partners of the $X(3872)$ revisited: What can we learn from the one boson exchange model? *Phys. Rev. D* 99,

094018 (2019), arXiv: 1902.03044
354. W. Chen, et al., QCD sum-rule interpretation of X(3872) with $J^{PC}=1^{++}$ mixtures of hybrid charmonium and $\bar{D}D^*$ molecular currents, Phys. Rev. D 88 (2013) 045027, arXiv: 1305.0244
355. X.-K. Dong, F.-K. Guo, and B.-S. Zou, A survey of heavy-antiheavy hadronic molecules, *Prog. Phys.* 41 (2021) 65, arXiv: 2101.01021
356. F.-K. Guo, et al., What can radiative decays of the $X(3872)$ teach us about its nature? *Phys. Lett. B* 742, 394 (2015), arXiv: 1410.6712
357. F.-K. Guo, Novel method for precisely measuring the $X(3872)$ mass, *Phys. Rev. Lett.* 122, 202002 (2019), arXiv: 1902.11221
358. L. Zhao, L. Ma, and S.-L. Zhu, Spin-orbit force, recoil corrections, and possible $B\bar{B}^*$ and $D\bar{D}^*$ molecular states, *Phys. Rev. D* 89, 094026 (2014), arXiv: 1403.4043
359. Y.-R. Liu and Z.-Y. Zhang, X(3872) and the bound state problem of $D^0\bar{D}^{*0}$ ($\bar{D}^0D^{*0}$) in a chiral quark model, *Phys. Rev. C* 79, 035206 (2009), arXiv: 0805.1616
360. H.-W. Ke, et al., Is $Z_b(10610)$ a molecular state? *J. High Energy Phys.* 04, 056 (2012), arXiv: 1202.2178
361. L. Geng, J. Lu, and M. P. Valderrama, Scale invariance in heavy hadron molecules, *Phys. Rev. D* 97, 094036 (2018), arXiv: 1704.06123
362. C. Meng, et al., Refined analysis on the $X(3872)$ resonance, *Phys.* Rev. D 92, 034020 (2015), arXiv: 1411.3106
363. R. Chen, A. Hosaka, and X. Liu, Heavy molecules and one-σ/ω-exchange model, *Phys. Rev. D* 96, 116012 (2017), arXiv: 1707.08306
364. L.-L. Shen, et al., The molecular systems composed of the charmed mesons in the $H\overline{S}$ + *h.c.* doublet, *Eur. Phys. J. C* 70, 183 (2010), arXiv: 1005.0994
365. H. X. Zhang, M. Zhang, and Z. Y. Zhang, $Qq\bar{Q}\bar{q}'$ states in chiral $SU(3)$ quark model, *Chin. Phys. Lett.* 24, 2533 (2007), arXiv: 0705.2470
366. T. Wang, G.-L. Wang, Y. Jiang, and W.-L. Ju, Electromagnetic decay of $X(3872)$ as the $1^1D_2(2^{-+})$ charmonium, *J. Phys. G* 40, 035003 (2013), arXiv: 1205.5725
367. W. Wang and Q. Zhao, Decipher the short-distance component of $X(3872)$ in B_c decays, *Phys. Lett. B* 755, 261 (2016), arXiv: 1512.03123
368. Y.-C. Yang, Z.-Y. Tan, J. Ping, and H.-S. Zong, Possible $D^{(*)}\bar{D}^{(*)}$ and $B^{(*)}\bar{B}^{(*)}$ molecular states in the extended constituent quark models, *Eur. Phys. J. C* 77, 575 (2017), arXiv: 1703.09718
369. Z.-R. Liang, X.-Y. Wu, and D.-L. Yao, Hunting for states in the recent LHCb di-J/ψ invariant mass spectrum, *Phys. Rev. D* 104, 034034 (2021), arXiv: 2104.08589
370. B.-X. Sun, D.-M. Wan, and S.-Y. Zhao, The $D\bar{D}^*$ interaction with isospin zero in an extended hidden gauge symmetry approach, *Chin. Phys. C* 42, 053105 (2018), arXiv: 1709.07263
371. S.-H. Yu, B.-K. Wang, X.-L. Chen, and W.-Z. Deng, Study the Heavy molecular states in quark model with meson exchange interaction, *Chin. Phys. C* 36, 25 (2012), arXiv: 1104.4535
372. H.-Y. Cao and H.-Q. Zhou, Decay widths of ^3P_J charmonium to DD, DD^*, D^*D^* and corresponding mass shifts of ^3P_J charmonium, *Eur. Phys. J. C* 80, 975 (2020), arXiv: 2008.11324
373. C.-F. Qiao and L. Tang, Molecular states with hidden charm and strange in QCD sum rules, *Europhys. Lett.* 107, 31001 (2014), arXiv: 1309.7596
374. Belle Collaboration, S. K. Choi, et al., Observation of a resonance-like structure in the $\pi^{\pm}\psi'$ mass distribution in exclusive $B\to K\pi^{\pm}\psi'$ decays, *Phys. Rev. Lett.* 100, 142001 (2008), arXiv: 0708.1790
375. LHCb Collaboration, T. Gershon, Exotic hadron naming convention, arXiv: 2206.15233 (2022)
376. LHCb Collaboration, R. Aaij, et al., Observation of the resonant character of the $Z(4430)^-$ state, *Phys. Rev. Lett.* 112, 222002 (2014), arXiv: 1404.1903
377. BESIII collaboration, M. Ablikim et al., Observation of a charged charmoniumlike structure in $e^+e^-\to \pi^+\pi^- J/\psi$ at $\sqrt{s}=4.26$ GeV, *Phys. Rev. Lett.* 110, 252001 (2013), arXiv: 1303.5949
378. Q. Wu and D.-Y. Chen, Exploration of the hidden charm decays of $Z_{cs}(3985)$, *Phys. Rev. D* 104, 074011 (2021), arXiv: 2108.06700
379. F.-L. Wang, X.-D. Yang, R. Chen, and X. Liu, Correlation of the hidden-charm molecular tetraquarks and the charmoniumlike structures existing in the $B\to XYZ+K$ process, *Phys. Rev. D* 104, 094010 (2021), arXiv: 2103.04698
380. Y. Zhang, E. Wang, D.-M. Li, and Y.-X. Li, Search for the $D^*\bar{D}^*$ molecular state $Z_c(4000)$ in the reaction $B^-\to J/\psi\rho^0K^-$, *Chin. Phys. C* 44, 093107 (2020), arXiv: 2001.06624
381. L.-Y. Xiao, G.-J. Wang, and S.-L. Zhu, Hidden-charm strong decays of the Z_c states, *Phys. Rev. D* 101, 054001 (2020), arXiv: 1912.12781
382. J. He and D.-Y. Chen, Interpretation of $Y(4390)$ as an isoscalar partner of $Z(4430)$ from $D^*(2010)\bar{D}_1(2420)$ interaction, *Eur. Phys. J. C* 77, 398 (2017), arXiv: 1704.08776
383. W. Chen, T. G. Steele, H.-X. Chen, and S.-L. Zhu, Mass spectra of Z_c and Z_b exotic states as hadron molecules, *Phys. Rev. D* 92, 054002 (2015), arXiv: 1505.05619
384. W. Chen, T. G. Steele, H.-X. Chen, and S.-L. Zhu, $Z_c(4200)^+$ decay width as a charmonium-like tetraquark state, *Eur. Phys. J. C* 75, 358 (2015), arXiv: 1501.03863
385. X.-H. Liu, et al., Resolving the puzzling decay patterns of charged Z_c and Z_b states, *Phys. Rev. D* 90, 074020 (2014), arXiv: 1407.3684
386. L. Ma, X.-H. Liu, X. Liu, and S.-L. Zhu, Strong decays of the XYZ states, *Phys. Rev. D* 91, 034032 (2015), arXiv: 1406.6879
387. Z.-G. Wang, Analysis of the $Z(4430)$ as the first radial excitation of the $Z_c(3900)$, *Commun. Theor. Phys.* 63, 325 (2015), arXiv: 1405.3581
388. L. Ma, X.-H. Liu, X. Liu, and S.-L. Zhu, Exotic four quark matter: $Z_1(4475)$, *Phys. Rev. D* 90, 037502 (2014), arXiv: 1404.3450
389. H.-W. Ke, Z.-T. Wei, and X.-Q. Li, Is $Z_c(3900)$ a molecular state, *Eur. Phys. J. C* 73, 2561 (2013), arXiv: 1307.2414
390. L. Zhao, W.-Z. Deng, and S.-L. Zhu, Hidden-Charm

Tetraquarks and charged Z_c states, *Phys. Rev. D* 90, 094031 (2014), arXiv: 1408.3924
391. Q.-R. Gong, et al., $Z_c(3900)$ as a $D\overline{D}^*$ molecule from the pole counting rule, *Phys. Rev. D* 94, 114019 (2016), arXiv: 1604.08836
392. L.-C. Gui, et al., Strong decays of higher charmonium states into open-charm meson pairs, *Phys. Rev. D* 98, 016010 (2018), arXiv: 1801.08791
393. Z.-G. Wang, Analysis of the hidden-charm tetraquark mass spectrum with the QCD sum rules, *Phys. Rev. D* 102, 014018 (2020), arXiv: 1908.07914
394. J. He and P.-L. Lü, $D^*\overline{D}_1(2420)$ and $D\overline{D}'^*(2600)$ interactions and the charged charmonium-like state $Z(4430)$, *Chin. Phys. C* 40, 043101 (2016), arXiv: 1410.8645
395. Y.-R. Liu and Z.-Y. Zhang, A chiral quark model study of $Z^+(4430)$ in the molecular picture, arXiv: 0908.1734 (2009)
396. CDF Collaboration, T. Aaltonen, et al., Evidence for a narrow near-threshold structure in the $J/\psi\phi$ mass spectrum in $B^+ \to J/\psi\phi K^+$ decays, *Phys. Rev. Lett.* 102, 242002 (2009), arXiv: 0903.2229
397. CDF Collaboration, T. Aaltonen, et al., Observation of the $Y(4140)$ structure in the $J/\psi\phi$ mass spectrum in $B^\pm \to J/\psi\phi K^\pm$ decays, *Mod. Phys. Lett. A* 32, 1750139 (2017), arXiv: 1101.6058
398. CMS Collaboration, S. Chatrchyan, et al., Observation of a peaking structure in the $J/\psi\phi$ mass spectrum from $B^\pm \to J/\psi\phi K^\pm$ decays, *Phys. Lett. B* 734, 261 (2014), arXiv: 1309.6920
399. B. Hu, et al., Possible heavy molecular states composed of a pair of excited charm-strange mesons, *Chin. Phys. C* 35, 113 (2011), arXiv: 1004.4032
400. Q. Meng, et al., Compact *sssc* pentaquark states predicted by a quark model, *Phys. Lett. B* 798, 135028 (2019), arXiv: 1907.00144
401. LHCb Collaboration, R. Aaij, et al., Observation of exotic $J/\psi\phi$ structures from amplitude analysis of $B^\pm \to J/\psi\phi K^\pm$ decays, *Phys. Rev. Lett.* 118, 022003 (2017), arXiv: 1606.07895
402. Q.-F. Cao, H.-R. Qi, Y.-F. Wang, and H.-Q. Zheng, Discussions on the line-shape of the $X(4660)$ resonance, *Phys. Rev. D* 100, 054040 (2019), arXiv: 1906.00356
403. W. Hao, et al., Canonical interpretation of the $X(4140)$ state within the $^3P_0$ model, *Eur. Phys. J. C* 80, 626 (2020), arXiv: 1909.13099
404. F.-L. Wang and X. Liu, Exotic double-charm molecular states with hidden or open strangeness and around 4.5–4.7 GeV, *Phys. Rev. D* 102, 094006 (2020), arXiv: 2008.13484
405. D.-Y. Chen and C.-J. Xiao, Strong two-body decays of the S-wave $D_s^+ D_s^-$ molecule state, *Nucl. Phys. A* 947, 26 (2016)
406. Q.-F. Lü and Y.-B. Dong, $X(4140)$, $X(4274)$, $X(4500)$, and $X(4700)$ in the relativized quark model, *Phys. Rev. D* 94, 074007 (2016), arXiv: 1607.05570
407. J. Wu, et al., $X(4140)$, $X(4270)$, $X(4500)$ and $X(4700)$ and their $cs\overline{cs}$ tetraquark partners, *Phys. Rev. D* 94, 094031 (2016), arXiv: 1608.07900
408. X.-H. Liu, How to understand the underlying structures of $X(4140)$, $X(4274)$, $X(4500)$ and $X(4700)$, *Phys. Lett. B* 766, 117 (2017), arXiv: 1607.01385
409. Z.-G. Wang, Reanalysis of the $X(3915)$, $X(4500)$ and $X(4700)$ with QCD sum rules, *Eur. Phys. J. A* 53, 19 (2017), arXiv: 1607.04840
410. Z.-G. Wang, Reanalysis of the $Y(3940)$, $Y(4140)$, $Z_c(4020)$, $Z_c(4025)$ and $Z_b(10650)$ as molecular states with QCD sum rules, *Eur. Phys. J. C* 74, 2963 (2014), arXiv: 1403.0810
411. J.-R. Zhang and M.-Q. Huang, $(Q\bar{s})^{(*)}(\bar{Q}s)^{(*)}$ molecular states from QCD sum rules: A view on $Y(4140)$, *J. Phys. G* 37, 025005 (2010), arXiv: 0905.4178
412. X. Liu, The hidden charm decay of $Y(4140)$ by the rescattering mechanism, *Phys. Lett. B* 680, 137 (2009), arXiv: 0904.0136
413. H.-X. Chen, et al., Understanding the internal structures of the $X(4140)$, $X(4274)$, $X(4500)$ and $X(4700)$, *Eur. Phys. J. C* 77, 160 (2017), arXiv: 1606.03179
414. Z.-G. Wang, Analysis of the $X(4350)$ as a scalar $\bar{c}c$ and $D_s^*\bar{D}_s^*$ mixing state with QCD sum rules, *Phys. Lett. B* 690, 403 (2010), arXiv: 0912.4626
415. E. Wang, J.-J. Xie, L.-S. Geng, and E. Oset, Analysis of the $B^+ \to J/\psi\phi K^+$ data at low $J/\psi\phi$ invariant masses and the $X(4140)$ and $X(4160)$ resonances, *Phys. Rev. D* 97, 014017 (2018), arXiv: 1710.02061
416. J. He and P.-L. Lü, Understanding $Y(4274)$ and $X(4320)$ in the $J/\psi\phi$ invariant mass spectrum, *Nucl. Phys. A* 919, 1 (2013), arXiv: 1309.6718
417. J. Ferretti, E. Santopinto, M. N. Anwar, and Y. Lu, Quark structure of the $\chi_c(3P)$ and $X(4274)$ resonances and their strong and radiative decays, *Eur. Phys. J. C* 80, 464 (2020), arXiv: 2002.09401
418. C. Deng, H. Chen, and J. Ping, Can the state $Y(4626)$ be a P-wave tetraquark state $[cs][\bar{c}\bar{s}]$? *Phys. Rev. D* 101, 054039 (2020), arXiv: 1912.07174
419. Z.-G. Wang, X.-S. Yang, and Q. Xin, Tetraquark molecular states in the $D_s\bar{D}_{s1}$ and $D_s^*\bar{D}_{s0}^*$ mass spectrum, *Int. J. Mod. Phys. A* 36, 2150202 (2021), arXiv: 2106.12400
420. P.-P. Shi, F. Huang, and W.-L. Wang, Hidden charm tetraquark states in a diquark model, *Phys. Rev. D* 103, 094038 (2021), arXiv: 2105.02397
421. X. Liu, et al., The explanation of some exotic states in the *cs* tetraquark system, *Eur. Phys. J. C* 81, 950 (2021), arXiv: 2103.12425
422. Y.-H. Ge, X.-H. Liu, and H.-W. Ke, Threshold effects as the origin of $Z_{cs}(4000)$, $Z_{cs}(4220)$ and $X(4700)$ observed in $B^+ \to J/\psi\phi K^+$, *Eur. Phys. J. C* 81, 854 (2021), arXiv: 2103.05282
423. X.-D. Yang, F.-L. Wang, Z.-W. Liu, and X. Liu, Newly observed $X(4630)$: A new charmoniumlike molecule, *Eur. Phys. J. C* 81, 807 (2021), arXiv: 2103.03127
424. Z. Yang, et al., Strange molecular partners of the $Z_c(3900)$ and $Z_c(4020)$, *Phys. Rev. D* 103, 074029 (2021), arXiv: 2011.08725
425. Q.-N. Wang, W. Chen, and H.-X. Chen, Exotic $\bar{D}_s^{(*)}D^{(*)}$ molecular states and $sc\overline{qc}$ tetraquark states with $J^P = 0^+, 1^+, 2^+$, *Chin. Phys. C* 45, 093102 (2021), arXiv: 2011.10495
426. D.-Y. Chen, X. Liu, and T. Matsuki, Predictions of charged charmoniumlike structures with hidden-charm and open-strange channels, *Phys. Rev. Lett.* 110,

232001 (2013), arXiv: 1303.6842
427. X. Jin, et al., Strange hidden-charm tetraquarks in constituent quark models, arXiv: 2011.12230 (2020)
428. Z. Liu, Four-quark matter — a new era of spectroscopy, *AAPPS Bull.* 31, 8 (2021)
429. LHCb Collaboration, R. Aaij, et al., Observation of new resonances decaying to $J/\psi K^+$ and $J/\psi\phi$, *Phys. Rev. Lett.* 127, 082001 (2021), arXiv: 2103.01803
430. BESIII Collaboration, M. Ablikim, et al., Observation of a near-threshold structure in the K^+ recoil-mass spectra in $e^+e^- \to K^+\left(D_s^- D^{*0} + D_s^{*-} D^0\right)$, *Phys. Rev. Lett.* 126, 102001 (2021), arXiv: 2011.07855
431. LHCb Collaboration, R. Aaij, et al., TBD, LHCb-PAPER-2022-040 (in preparation)
432. X. Cao and Z. Yang, Hunting for the heavy quark spin symmetry partner of Z_{cs}, arXiv: 2110.09760 (2021)
433. M.-Y. Duan, et al., Revisiting the $Z_c(4025)$ structure observed by BESIII in $e^+e^- \to (D^*\bar{D}^*)^{\pm,0}\pi^{\mp,0}$ at $\sqrt{s} =$ 4.26 GeV, *Phys. Rev. D* 104, 074030 (2021), arXiv: 2109.00731
434. LHCb Collaboration, R. Aaij, et al., Model-independent study of structure in $B^+ \to D^+D^-K^+$ decays, *Phys. Rev. Lett.* 125, 242001 (2020), arXiv: 2009.00025
435. LHCb collaboration, R. Aaij et al., Amplitude analysis of the $B^+ \to D^+D^-K^+$ decay, *Phys. Rev. D* 102, 112003 (2020), arXiv: 2009.00026
436. Y.-K. Chen, et al., Branching fractions of $B^- \to D^- X_{0,\,1}(2900)$ and their implications, *Eur. Phys. J. C* 81, 71 (2021), arXiv: 2009.01182
437. LHCb Collaboration, R. Aaij, et al., TBD, LHCb-PAPER-2022-026, arXiv: 2212.02716 (submitted to *Phys. Rev. Lett.*)
438. LHCb Collaboration, R. Aaij, et al., TBD, LHCb-PAPER-2022-027, arXiv: 2212.02717 (submitted to *Phys. Rev. D*)
439. Q. -F. Lü, D.-Y. Chen, and Y.-B. Dong, Open charm and bottom tetraquarks in an extended relativized quark model, *Phys. Rev. D* 102, 074021 (2020), arXiv: 2008.07340
440. M.-Z. Liu, J.-J. Xie, and L.-S. Geng, $X_0(2866)$ as a $D^*\bar{K}^*$ molecular state, *Phys. Rev. D* 102, 091502 (2020), arXiv: 2008.07389
441. M.-W. Hu, X.-Y. Lao, P. Ling, and Q. Wang, $X_0(2900)$ and its heavy quark spin partners in molecular picture, *Chin. Phys. C* 45, 021003 (2021), arXiv: 2008.06894
442. Y. Tan and J. Ping, $X(2900)$ in a chiral quark model, *Chin. Phys. C* 45, 093104 (2021), arXiv: 2010.04045
443. X.-K. Dong and B.-S. Zou, Prediction of possible DK1 bound states, *Eur. Phys. J. A* 57, 139 (2021), arXiv: 2009.11619
444. L. R. Dai, J.-J. Xie, and E. Oset, $B^0 \to D^0\bar{D}^0K^0$, $B^+ \to D^0\bar{D}^0K^+$, and the scalar $D\overline{D}$ bound state, *Eur. Phys. J. C* 76, 121 (2016), arXiv: 1512.04048
445. J.-B. Cheng, et al., Spectrum and rearrangement decays of tetraquark states with four different flavors, *Phys. Rev. D* 101, 114017 (2020), arXiv: 2001.05287
446. B.Wang and S.-L. Zhu, How to understand the X(2900)? arXiv: 2107.09275 (2021)
447. Z.-G. Wang, Analysis of the $X_0(2900)$ as the scalar tetraquark state via the QCD sum rules, *Int. J. Mod. Phys. A* 35, 2050187 (2020), arXiv: 2008.07833
448. Y. Huang, J.-X. Lu, J.-J. Xie, and L.-S. Geng, Strong decays of $\bar{D}^*K^*$ molecules and the newly observed $X_{0,1}$ states, *Eur. Phys. J. C* 80, 973 (2020), arXiv: 2008.07959
449. X.-G. He, W. Wang, and R. Zhu, Open-charm tetraquark X_c and open-bottom tetraquark X_b, *Eur. Phys. J. C* 80, 1026 (2020), arXiv: 2008.07145
450. H.-X. Chen, W. Chen, R.-R. Dong, and N. Su, $X_0(2900)$ and $X_1(2900)$: Hadronic molecules or compact tetraquarks, *Chin. Phys. Lett.* 37, 101201 (2020), arXiv: 2008.07516
451. J.-R. Zhang, Open-charm tetraquark candidate: Note on $X_0(2900)$, *Phys. Rev. D* 103, 054019 (2021), arXiv: 2008.07295
452. X.-H. Liu, et al., Triangle singularity as the origin of $X_0(2900)$ and $X_1(2900)$ observed in $B^+ \to D^+D^-K^+$, *Eur. Phys. J. C* 80, 1178 (2020), arXiv: 2008.07190
453. LHCb Collaboration, R. Aaij, et al., Observation of a resonant structure near the $D_s^+D_s^-$ threshold in the $B^+ \to D_s^+D_s^-K^+$ decay, arXiv: 2210.15153 (submitted to *Phys. Rev. Lett.*)
454. LHCb Collaboration, R. Aaij, et al., First observation of the $B^+ \to D_s^+D_s^-K^+$ decay, arXiv: 2211.05034 (submitted to *Phys. Rev. D*)
455. Y. Yang, C. Deng, J. Ping, and T. Goldman, S-wave $QQ\bar{q}\bar{q}$ state in the constituent quark model, *Phys. Rev. D* 80, 114023 (2009)
456. LHCb Collaboration, R. Aaij, et al., Observation of an exotic narrow doubly charmed tetraquark, *Nat. Phys.* 18, 751 (2022), arXiv: 2109.01038
457. LHCb Collaboration, R. Aaij, et al., Study of the doubly charmed tetraquark T_{cc}^+, *Nat. Commun.* 13, 3351 (2022), arXiv: 2109.01056
458. X.-Z. Ling, et al., Can we understand the decay width of the T_{cc}^+ state? arXiv: 2108.00947 (2021)
459. L. Meng, G.-J. Wang, B. Wang, and S.-L. Zhu, Probing the long-range structure of the $T^+{}_{cc}$ with the strong and electromagnetic decays, *Phys. Rev. D* 104, 051502 (2021), arXiv: 2107.14784
460. L.-Y. Dai, et al., Pole analysis on the doubly charmed meson in $D^0D^0\pi^+$ mass spectrum, *Phys. Rev. D* 105, L051507 (2022), arXiv: 2108.06002
461. N. Li, Z.-F. Sun, X. Liu, and S.-L. Zhu, Perfect DD^* molecular prediction matching the T_{cc} observation at LHCb, *Chin. Phys. Lett.* 38, 092001 (2021), arXiv: 2107.13748
462. T. Guo, J. Li, J. Zhao, and L. He, Mass spectra and decays of open-heavy tetraquark states, *Phys. Rev. D* 105, 054018 (2022), arXiv: 2108.06222
463. R. Chen, et al., Doubly charmed molecular pentaquarks, *Phys. Lett. B* 822, 136693 (2021), arXiv: 2108.12730
464. Y. Xing and Y. Niu, The study of doubly charmed pentaquark $cc\bar{q}qq$ with the $SU(3)$ symmetry, *Eur. Phys. J. C* 81, 978 (2021), arXiv: 2106.09939
465. H.-T. An, K. Chen, Z.-W. Liu, and X. Liu, Heavy flavor pentaquarks with four heavy quarks, *Phys. Rev. D* 103, 114027 (2021), arXiv: 2106.02837
466. C. Deng, H. Chen, and J. Ping, Systematical investigation on the stability of doubly heavy tetraquark states, *Eur.*

Phys. J. A 56, 9 (2020), arXiv: 1811.06462
467. Z.-G. Wang and Z.-H. Yan, Analysis of the scalar, axialvector, vector, tensor doubly charmed tetraquark states with QCD sum rules, *Eur. Phys. J. C* 78, 19 (2018), arXiv: 1710.02810
468. M. Karliner and J. L. Rosner, Discovery of the doubly-charmed Ξ_{cc} baryon implies a stable $bb\bar{u}\bar{d}$ tetraquark, *Phys. Rev. Lett.* 119, 202001 (2017), arXiv: 1707.07666
469. E. J. Eichten and C. Quigg, Heavy-quark symmetry implies stable heavy tetraquark mesons $Q_iQ_j\bar{q}_k\bar{q}_l$, *Phys. Rev. Lett.* 119, 202002 (2017), arXiv: 1707.09575
470. R. Zhu, Hidden charm octet tetraquarks from a diquark–antidiquark model, *Phys. Rev. D* 94, 054009 (2016), arXiv: 1607.02799
471. G. Yang, J. Ping, and J. Segovia, Doubly-heavy tetraquarks, *Phys. Rev. D* 101, 014001 (2020), arXiv: 1911.00215
472. X. Yan, B. Zhong, and R. Zhu, Doubly charmed tetraquarks in a diquark–antidiquark model, *Int. J. Mod. Phys. A* 33, 1850096 (2018), arXiv: 1804.06761
473. Y. Tan, W. Lu, and J. Ping, Systematics of $QQ\bar{q}\,\bar{q}$ in a chiral constituent quark model, *Eur. Phys. J. Plus* 135, 716 (2020), arXiv: 2004.02106
474. S.-Y. Kong, J.-T. Zhu, D. Song, and J. He, Heavy-strange meson molecules and possible candidates $D_{s0}^*(2317)$, $D_{s1}(2460)$, and $X_0(2900)$, *Phys. Rev. D* 104, 094012 (2021), arXiv: 2106.07272
475. Y.-K. Hsiao and Y. Yu, New $X_{0,1}(2900)$-like exotic states in b-baryon decays, *Phys. Rev. D* 104, 034008 (2021), arXiv: 2104.01296
476. H.-X. Chen, Hadronic molecules in B decays, *Phys. Rev. D* 105, 094003 (2022), arXiv: 2103.08586
477. X.-K. Dong, et al., Is the existence of a $J/\psi J/\psi$ bound state plausible? *Sci. Bull.* 66, 2462 (2021), arXiv: 2107.03946
478. Z.-G. He, B. A. Kniehl, M. A. Nefedov, and V. A. Saleev, Double prompt J/ψ production at hadron colliders, *Mod. Phys. Lett. A* 36, 2130018 (2021)
479. A. J. Majarshin, Y.-A. Luo, F. Pan, and J. Segovia, Bosonic algebraic approach applied to the $[QQ][\overline{Q}\,\overline{Q}]$ tetraquarks, *Phys. Rev. D* 105, 054024 (2022), arXiv: 2106.01179
480. F.-L. Wang, R. Chen, and X. Liu, A new group of doubly charmed molecule with T-doublet charmed meson pair, *Phys. Lett. B* 835, 137502 (2022), arXiv: 2111.00208
481. M.-L. Du, et al., Coupled-channel approach to T_{cc}^+ including three-body effects, *Phys. Rev. D* 105, 014024 (2022), arXiv: 2110.13765
482. X.-Z. Ling, M.-Z. Liu, and L.-S. Geng, Masses and strong decays of open charm hexaquark states $\Sigma_c^{(*)}\Sigma_c^{(*)}$, *Eur. Phys. J. C* 81, 1090 (2021), arXiv: 2110.13792
483. V. Baru, et al., Effective range expansion for narrow near-threshold resonances, *Phys. Lett. B* 833, 137290 (2022), arXiv: 2110.07484
484. H. Ren, F. Wu, and R. Zhu, Hadronic molecule interpretation of T_{cc}^+ and its beauty partners, *Adv. High Energy Phys.* 2022, 9103031 (2022), arXiv: 2109.02531
485. Z.-G. Wang, Analysis of the axialvector doubly heavy tetraquark states with QCD sum rules, *Acta Phys. Polon. B* 49, 1781 (2018), arXiv: 1708.04545
486. K. Chen, B. Wang, and S.-L. Zhu, Exploration of the doubly charmed molecular pentaquarks, *Phys. Rev. D* 103, 116017 (2021), arXiv: 2102.05868
487. LHCb Collaboration, R. Aaij, et al., Observation of structure in the J/ψ-pair mass spectrum, *Sci. Bull.* 65, 1983 (2020), arXiv: 2006.16957
488. Y. Iwasaki, Is a state $c\bar{c}c\bar{c}$ found at 6.0 GeV, *Phys. Rev. Lett.* 36, 1266 (1976)
489. K.-T. Chao, The $cc-\bar{c}\,\bar{c}$(diquark–antidiquark) states in e^+e^- annihilation, *Z. Phys. C* 7, 317 (1981)
490. J.-P. Ader, J.-M. Richard, and P. Taxil, Do narrow heavy multiquark states exist, *Phys. Rev. D* 25, 2370 (1982)
491. B.-A. Li and K.-F. Liu, J/ψ pair production in hadronic collisions, *Phys. Rev. D* 29, 426 (1984)
492. A. M. Badalian, B. L. Ioffe, and A. V. Smilga, Four quark states in heavy quark systems, *Nucl. Phys.* 281, B85 (1987)
493. A. V. Berezhnoy, A. V. Luchinsky, and A. A. Novoselov, Heavy tetraquarks production at the LHC, *Phys. Rev. D* 86, 034004 (2012), arXiv: 1111.1867
494. J. Wu, et al., Heavy-flavored tetraquark states with the $QQ\overline{Q}\,\overline{Q}$ configuration, *Phys. Rev. D* 97, 094015 (2018), arXiv: 1605.01134
495. M. Karliner, S. Nussinov, and J. L. Rosner, $QQ\overline{Q}\,\overline{Q}$ states: Masses, production, and decays, *Phys. Rev. D* 95, 034011 (2017), arXiv: 1611.00348
496. N. Barnea, J. Vijande, and A. Valcarce, Four-quark spectroscopy within the hyper-spherical formalism, *Phys. Rev. D* 73, 054004 (2006), arXiv: hep-ph/0604010
497. V. R. Debastiani and F. S. Navarra, A non-relativistic model for the $[cc][\bar{c}\bar{c}]$ tetraquark, *Chin. Phys. C* 43, 013105 (2019), arXiv: 1706.07553
498. M.-S. Liu, Q.-F. Lü, X.-H. Zhong, and Q. Zhao, All-heavy tetraquarks, *Phys. Rev. D* 100, 016006 (2019), arXiv: 1901.02564
499. W. Chen, et al., Hunting for exotic doubly hidden-charm/bottom tetraquark states, *Phys. Lett. B* 773, 247 (2017), arXiv: 1605.01647
500. G.-J. Wang, L. Meng, and S.-L. Zhu, Spectrum of the fully-heavy tetraquark state $QQ\bar{Q}'\bar{Q}'$, *Phys. Rev. D* 100, 096013 (2019), arXiv: 1907.05177
501. M. A. Bedolla, J. Ferretti, C. D. Roberts, and E. Santopinto, Spectrum of fully-heavy tetraquarks from a diquark+antidiquark perspective, *Eur. Phys. J. C* 80, 1004 (2020), arXiv: 1911.00960
502. R. J. Lloyd and J. P. Vary, All-charm tetraquarks, *Phys. Rev. D* 70, 014009 (2004), arXiv: hep-ph/0311179
503. X. Chen, Fully-charm tetraquarks: $cc\bar{c}\bar{c}$, arXiv: 2001.06755 (2020)
504. Z.-G. Wang and Z.-Y. Di, Analysis of the vector and axialvector $QQ\overline{Q}\,\overline{Q}$ tetraquark states with QCD sum rules, *Acta Phys. Polon. B* 50, 1335 (2019), arXiv: 1807.08520
505. M. N. Anwar, et al., Spectroscopy and decays of the fully-heavy tetraquarks, *Eur. Phys. J. C* 78, 647 (2018), arXiv: 1710.02540
506. A. Esposito and A. D. Polosa, A $bb\bar{b}\bar{b}$ di-bottomonium at the LHC? *Eur. Phys. J. C* 78, 782 (2018), arXiv:

1807.06040
507. C. Becchi, A. Giachino, L. Maiani, and E. Santopinto, Search for $bb\bar{b}\bar{b}$ tetraquark decays in 4 muons, B^+B^-, $B^0\bar{B}^0$ and $B_s^0\bar{B}_s^0$ channels at LHC, *Phys. Lett. B* 806, 135495 (2020), arXiv: 2002.11077
508. Y. Bai, S. Lu, and J. Osborne, Beauty-full tetraquarks, *Phys. Lett. B* 798, 134930 (2019), arXiv: 1612.00012
509. J.-M. Richard, A. Valcarce, and J. Vijande, String dynamics and metastability of all-heavy tetraquarks, *Phys. Rev. D* 95, 054019 (2017), arXiv: 1703.00783
510. Y. Chen and R. Vega-Morales, Golden probe of the di-Υ threshold, arXiv: 1710.02738 (2017)
511. X. Chen, Fully-heavy tetraquarks: $bb\bar{c}\bar{c}$ and $bc\bar{b}\bar{c}$, *Phys. Rev. D* 100, 094009 (2019), arXiv: 1908.08811
512. A. V. Berezhnoy, A. K. Likhoded, and A. A. Novoselov, Υ-meson pair production at the LHC, *Phys. Rev. D* 87, 054023 (2013), arXiv: 1210.5754
513. CMS Collaboration, Observation of new structures in the $J/\psi J/\psi$ mass spectrum in pp collisions at $\sqrt{s} = 13$ TeV
514. ATLAS Collaboration, Observation of an excess of di-charmonium events in the four-muon final state with the ATLAS detector
515. K.-T. Chao and S.-L. Zhu, The possible tetraquark states $cc\bar{c}\bar{c}$ observed by the LHCb experiment, *Sci. Bull.* 65, 1952 (2020), arXiv: 2008.07670
516. X.-Z. Weng, X.-L. Chen, W.-Z. Deng, and S.-L. Zhu, Systematics of fully heavy tetraquarks, *Phys. Rev. D* 103, 034001 (2021), arXiv: 2010.05163
517. H.-T. An, K. Chen, and X. Liu, Exotic pentaquark states and chromomagnetic interaction, arXiv: 2010.05014 (2020)
518. Q.-F. Lü, D.-Y. Chen, and Y.-B. Dong, Masses of fully heavy tetraquarks $QQ\bar{Q}\bar{Q}$ in an extended relativized quark model, *Eur. Phys. J. C* 80, 871 (2020), arXiv: 2006.14445
519. N. Lee, Z.-G. Luo, X.-L. Chen, and S.-L. Zhu, Possible deuteronlike molecular states composed of heavy baryons, *Phys. Rev. D* 84, 014031 (2011), arXiv: 1104.4257
520. X. Jin, Y. Xue, H. Huang, and J. Ping, Full-heavy tetraquarks in constituent quark models, *Eur. Phys. J. C* 80, 1083 (2020), arXiv: 2006.13745
521. J.-X. Lu, L.-S. Geng, and M. P. Valderrama, Heavy baryon-antibaryon molecules in effective field theory, *Phys. Rev. D* 99, 074026 (2019), arXiv: 1706.02588
522. L. Meng, N. Li, and S.-L. Zhu, Deuteron-like states composed of two doubly charmed baryons, *Phys. Rev. D* 95, 114019 (2017), arXiv: 1704.01009
523. Z.-G. Wang, Revisit the tetraquark candidates in the J/ψ J/ψ mass spectrum, Int. *J. Mod. Phys. A* 36, 2150014 (2021), arXiv: 2009.05371
524. L. Tang, B.-D. Wan, K. Maltman, and C.-F. Qiao, Doubly heavy tetraquarks in QCD sum rules, *Phys. Rev. D* 101, 094032 (2020), arXiv: 1911.10951
525. B.-D. Wan and C.-F. Qiao, Gluonic tetracharm configuration of $X(6900)$, *Phys. Lett. B* 817, 136339 (2021), arXiv: 2012.00454
526. B.-C. Yang, L. Tang, and C.-F. Qiao, Scalar fully-heavy tetraquark states $QQ'\bar{Q}\bar{Q}'$ in QCD sum rules, *Eur. Phys. J. C* 81, 324 (2021), arXiv: 2012.04463
527. G. Li, X.-F. Wang, and Y. Xing, Fully heavy tetraquark $bb\bar{c}\bar{c}$: Lifetimes and weak decays, *Eur. Phys. J. C* 79, 645 (2019), arXiv: 1902.05805
528. M.-Z. Liu and L.-S. Geng, Is $X(7200)$ the heavy anti-quark diquark symmetry partner of $X(3872)$? *Eur. Phys. J. C* 81, 179 (2021), arXiv: 2012.05096
529. Z. Zhao, et al., Study of charmoniumlike and fully-charm tetraquark spectroscopy, *Phys. Rev. D* 103, 116027 (2021), arXiv: 2012.15554
530. Y. Yan, et al., Fully heavy pentaquarks in quark models, arXiv: 2110.10853 (2021)
531. F.-X. Liu, M.-S. Liu, X.-H. Zhong, and Q. Zhao, Higher mass spectra of the fully-charmed and fully-bottom tetraquarks, arXiv: 2110.09052 (2021)
532. Q.-N. Wang, Z.-Y. Yang, and W. Chen, Exotic fully-heavy $Q\bar{Q}Q\bar{Q}$ tetraquark states in $8_{[Q\bar{Q}]} \otimes 8_{[Q\bar{Q}]}$ color configuration, arXiv: 2109.08091 (2021)
533. Q. Li, C.-H. Chang, G.-L. Wang, and T. Wang, Mass spectra and wave functions of $T_{QQ\bar{Q}\bar{Q}}$ tetraquarks, *Phys. Rev. D* 104, 014018 (2021), arXiv: 2104.12372
534. H.-W. Ke, X. Han, X.-H. Liu, and Y.-L. Shi, Tetraquark state $X(6900)$ and the interaction between diquark and antidiquark, *Eur. Phys. J. C* 81, 427 (2021), arXiv: 2103.13140
535. G. Huang, J. Zhao, and P. Zhuang, Pair structure of heavy tetraquark systems, *Phys. Rev. D* 103, 054014 (2021), arXiv: 2012.14845
536. H.-T. An, K. Chen, Z.-W. Liu, and X. Liu, Fully heavy pentaquarks, *Phys. Rev. D* 103, 074006 (2021), arXiv: 2012.12459
537. C. Gong, et al., Nature of $X(6900)$ and its production mechanism at LHCb, arXiv: 2011.11374 (2020)
538. J.-W. Zhu, et al., A possible interpretation for $X(6900)$ observed in four-muon final state by LHCb - A light Higgs-like boson? arXiv: 2011.07799 (2020)
539. J.-R. Zhang, Fully-heavy pentaquark states, *Phys. Rev. D* 103, 074016 (2021), arXiv: 2011.04594
540. Q.-F. Cao, H. Chen, H.-R. Qi, and H.-Q. Zheng, Some remarks on $X(6900)$, *Chin. Phys. C* 45, 103102 (2021), arXiv: 2011.04347
541. Z.-H. Guo and J. A. Oller, Insights into the inner structures of the fully charmed tetraquark state $X(6900)$, *Phys. Rev. D* 103, 034024 (2021), arXiv: 2011.00978
542. R. Zhu, Fully-heavy tetraquark spectra and production at hadron colliders, *Nucl. Phys. B* 966, 115393 (2021), arXiv: 2010.09082
543. J.-R. Zhang, 0^+ fully-charmed tetraquark states, *Phys. Rev. D* 103, 014018 (2021), arXiv: 2010.07719
544. R. N. Faustov, V. O. Galkin, and E. M. Savchenko, Masses of the $QQ\bar{Q}\bar{Q}$ tetraquarks in the relativistic diquark–antidiquark picture, *Phys. Rev. D* 102, 114030 (2020), arXiv: 2009.13237
545. F. Feng, et al., Fragmentation production of fully-charmed tetraquarks at LHC, arXiv: 2009.08450 (2020)
546. Y.-Q. Ma and H.-F. Zhang, Exploring the di-J/ψ resonances around 6.9 GeV based on *ab initio* perturbative QCD, arXiv: 2009.08376 (2020)
547. X.-K. Dong, et al., Coupled-channel interpretation of the LHCb double-J/ψ spectrum and hints of a new state near the $J/\psi J/\psi$ threshold, *Phys. Rev. Lett.* 126,

132001 (2021), Erratum: *Phys. Rev. Lett.* 127, 119901 (2021), arXiv: 2009.07795
548. M. Karliner and J. L. Rosner, Interpretation of structure in the di-J/ψ spectrum, *Phys. Rev. D* 102, 114039 (2020), arXiv: 2009.04429
549. J.-Z. Wang, D.-Y. Chen, X. Liu, and T. Matsuki, Producing fully charm structures in the J/ψ-pair invariant mass spectrum, *Phys. Rev. D* 103, 071503 (2021), arXiv: 2008.07430
550. G. Yang, J. Ping, L. He, and Q. Wang, Potential model prediction of fully-heavy tetraquarks $QQ\bar{Q}\bar{Q}$ ($Q = c$, b), arXiv: 2006.13756 (2020)
551. C. Deng, H. Chen, and J. Ping, Towards the understanding of fully-heavy tetraquark states from various models, *Phys. Rev. D* 103, 014001 (2021), arXiv: 2003.05154
552. Z.-C. Yang, et al., Possible hidden-charm molecular baryons composed of an anti-charmed meson and a charmed baryon, *Chin. Phys. C* 36, 6 (2012), arXiv: 1105.2901
553. R. Zhu and C.-F. Qiao, Pentaquark states in a diquark–triquark model, *Phys. Lett. B* 756, 259 (2016), arXiv: 1510.08693
554. N. Li and S.-L. Zhu, Hadronic molecular states composed of heavy flavor baryons, *Phys. Rev. D* 86, 014020 (2012), arXiv: 1204.3364
555. M.-Z. Liu, et al., $D\Xi$ and $D^*\Xi$ molecular states from one boson exchange, *Phys. Rev. D* 98, 014014 (2018), arXiv: 1805.08384
556. LHCb Collaboration, R. Aaij, et al., Observation of $J/\psi p$ resonances consistent with pentaquark states in $\Lambda_b^0 \to J/\psi p K^-$ decays, *Phys. Rev. Lett.* 115, 072001 (2015), arXiv: 1507.03414
557. LHCb Collaboration, R. Aaij, et al., Evidence for exotic hadron contributions to $\Lambda_b^0 \to J/\psi p \pi^-$ decays, *Phys. Rev. Lett.* 117, 082003 (2016), arXiv: 1606.06999
558. LHCb Collaboration, R. Aaij, et al., Model-independent evidence for $J/\psi p$ contributions to $\Lambda_b^0 \to J/\psi p K^-$ decays, *Phys. Rev. Lett.* 117, 082002 (2016), arXiv: 1604.05708
559. LHCb Collaboration, R. Aaij, et al., Observation of a narrow pentaquark state, $P_c(4312)^+$, and of two-peak structure of the $P_c(4450)^+$, *Phys. Rev. Lett.* 122, 222001 (2019), arXiv: 1904.03947
560. LHCb Collaboration, R. Aaij, et al., Evidence for a new structure in the $J/\psi p$ and $J/\psi \bar{p}$ systems in $B_s^0 \to J/\psi p \bar{p}$ decays, *Phys. Rev. Lett.* 128, 062001 (2022), arXiv: 2108.04720
561. B. Wang, L. Meng, and S.-L. Zhu, Spectrum of the strange hidden charm molecular pentaquarks in chiral effective field theory, *Phys. Rev. D* 101, 034018 (2020), arXiv: 1912.12592
562. H.-X. Chen, et al., Looking for a hidden-charm pentaquark state with strangeness $S = -1$ from Ξ_b^- decay into $J/\psi K^- \Lambda$, *Phys. Rev. C* 93, 065203 (2016), arXiv: 1510.01803
563. LHCb Collaboration, R. Aaij, et al., Evidence of a $J/\psi\Lambda$ structure and observation of excited Ξ^- states in the $\Xi_b^- \to J/\psi \Lambda K^-$ decay, *Sci. Bull.* 66, 1278 (2021), arXiv: 2012.10380
564. LHCb Collaboration, R. Aaij, et al., Observation of a $J/\psi\Lambda$ resonance consistent with a strange pentaquark candidate in $B^- \to J/\psi \Lambda \bar{p}$ decays, arXiv: 2210.10346 (submitted to *Phys. Rev. Lett.*)
565. F.-L. Wang, R. Chen, Z. -W. Liu, and X. Liu, Probing new types of P_c states inspired by the interaction between S-wave charmed baryon and anti-charmed meson in a doublet, *Phys. Rev. C* 101, 025201 (2020), arXiv: 1905.03636
566. M.-L. Du, et al., Interpretation of the LHCb P_c states as hadronic molecules and hints of a narrow $P_c(4380)$, *Phys. Rev. Lett.* 124, 072001 (2020), arXiv: 1910.11846
567. L. Meng, B. Wang, G.-J. Wang, and S.-L. Zhu, Hidden charm pentaquark states and $\Sigma_c \bar{D}^{(*)}$ interaction in chiral perturbation theory, *Phys. Rev. D* 100, 014031 (2019), arXiv: 1905.04113
568. X.-Z. Weng, X.-L. Chen, W.-Z. Deng, and S.-L. Zhu, Hidden-charm pentaquarks and P_c states, *Phys. Rev. D* 100, 016014 (2019), arXiv: 1904.09891
569. Y.-J. Xu, C.-Y. Cui, Y.-L. Liu, and M.-Q. Huang, Partial decay widths of $P_c(4312)$ as a $\bar{D}\Sigma_c$ molecular state, *Phys. Rev. D* 102, 034028 (2020), arXiv: 1907.05097
570. U. Ozdem and K. Azizi, Magnetic dipole moment of $Z_b(10610)$ in light-cone QCD, *Phys. Rev. D* 97, 014010 (2018), arXiv: 1709.09714
571. H. Huang, C. Deng, J. Ping, and F. Wang, Possible pentaquarks with heavy quarks, *Eur. Phys. J. C* 76, 624 (2016), arXiv: 1510.04648
572. M.-L. Du, Z.-H. Guo, and J. A. Oller, Insights into the nature of the $P_{cs}(4459)$, arXiv: 2109.14237 (2021)
573. K. Chen, et al., Systematics of the heavy flavor hadronic molecules, *Eur. Phys. J. C* 82, 581 (2022), arXiv: 2109.13057
574. X. Hu and J. Ping, Investigation of hidden-charm pentaquarks with strangeness $S = -1$, *Eur. Phys. J. C* 82, 118 (2022), arXiv: 2109.09972
575. N. Yalikun, et al., Coupled channel effects of the $\Sigma_c^{(*)}\bar{D}^{(*)}$-$\Lambda_c(2595)D^*$ system and molecular nature of the P_c pentaquark states from one-boson exchange model, *Phys. Rev. D* 104, 094039 (2021), arXiv: 2109.03504
576. J.-X. Lu, M.-Z. Liu, R.-X. Shi, and L.-S. Geng, Understanding $P_{cs}(4459)$ as a hadronic molecule in the $\Xi_b^- \to J/\psi \Lambda K^-$ decay, *Phys. Rev. D* 104, 034022 (2021), arXiv: 2104.10303
577. M.-L. Du, et al., Revisiting the nature of the P_c pentaquarks, *J. High Energy Phys.* 08, 157 (2021), arXiv: 2102.07159
578. J.-T. Zhu, L.-Q. Song, and J. He, $P_{cs}(4459)$ and other possible molecular states from $\Xi_c^{(*)}\bar{D}^{(*)}$ and $\Xi_c'\bar{D}^{(*)}$ interactions, *Phys. Rev. D* 103, 074007 (2021), arXiv: 2101.12441
579. S. X. Nakamura, A. Hosaka, and Y. Yamaguchi, $P_c(4312)^+$ and $P_c(4337)^+$ as interfering $\Sigma_c\bar{D}$ and $\Lambda_c\bar{D}^*$ (anomalous) threshold cusps, arXiv: 2109.15235 (2021)
580. P.-P. Shi, F. Huang, and W.-L. Wang, Hidden charm pentaquark states in a diquark model, *Eur. Phys. J. A* 57, 237 (2021), arXiv: 2107.08680
581. K. Phumphan, et al., P_c resonances in molecular picture, arXiv: 2105.03150 (2021)
582. S. X. Nakamura, $P_c(4312)^+$, $P_c(4380)^+$, and $P_c(4457)^+$ as double triangle cusps, *Phys. Rev. D* 103, 111503

(2021), arXiv: 2103.06817
583. C. W. Xiao, J. J. Wu, and B. S. Zou, Molecular nature of $P_{cs}(4459)$ and its heavy quark spin partners, *Phys. Rev. D* 103, 054016 (2021), arXiv: 2102.02607
584. R. Chen, Can the newly reported $P_{cs}(4459)$ be a strange hidden-charm $\Xi_c\bar{D}^*$ molecular pentaquark? *Phys. Rev. D* 103 (2021) 054007, arXiv: 2011.07214
585. Z.-G. Wang, Analysis of the $P_{cs}(4459)$ as the hidden-charm pentaquark state with QCD sum rules, *Int. J. Mod. Phys. A* 36, 2150071 (2021), arXiv: 2011.05102
586. F.-Z. Peng, et al., Peaks within peaks and the possible two-peak structure of the $P_c(4457)$: The effective field theory perspective, *Phys. Rev. D* 103, 014023 (2021), arXiv: 2007.01198
587. H. Xu, Q. Li, C.-H. Chang, and G.-L. Wang, Recently observed P_c as molecular states and possible mixture of $P_c(4457)$, *Phys. Rev. D* 101, 054037 (2020), arXiv: 2001.02980
588. A. Giachino, et al., Hidden-charm and bottom meson-baryon molecules coupled with five-quark states, *Springer Proc. Phys.* 238, 621 (2020)
589. C.-Y. Chen, M. Chen, and Y.-X. Liu, Quantum numbers of the pentaquark states P_c^+ via symmetry analysis, *Commun. Theor. Phys.* 72, 125202 (2020), arXiv: 1912.01931
590. B. Wang, L. Meng, and S.-L. Zhu, Hidden-charm and hidden-bottom molecular pentaquarks in chiral effective field theory, *J. High Energy Phys.* 11, 108 (2019), arXiv: 1909.13054
591. A. Pimikov, H.-J. Lee, and P. Zhang, Hidden-charm pentaquarks with color-octet sub-structure in QCD sum rules, *Phys. Rev. D* 101, 014002 (2020), arXiv: 1908.04459
592. Z.-G. Wang and X. Wang, Analysis of the strong decays of the $P_c(4312)$ as a pentaquark molecular state with QCD sum rules, *Chin. Phys. C* 44, 103102 (2020), arXiv: 1907.04582
593. Y. Yamaguchi, et al., P_c pentaquarks with chiral tensor and quark dynamics, *Phys. Rev. D* 101, 091502 (2020), arXiv: 1907.04684
594. J.-B. Cheng and Y.-R. Liu, $P_c(4457)^+$, $P_c(4440)^+$, and $P_c(4312)^+$: Molecules or compact pentaquarks? *Phys. Rev. D* 100, 054002 (2019), arXiv: 1905.08605
595. Z.-G. Wang, Analysis of the $P_c(4312)$, $P_c(4440)$, $P_c(4457)$ and related hidden-charm pentaquark states with QCD sum rules, *Int. J. Mod. Phys. A* 35, 2050003 (2020), arXiv: 1905.02892
596. JPAC Collaboration, C. Fernández-Ramírez, et al., Interpretation of the LHCb $P_c(4312)^+$ signal, *Phys. Rev. Lett.* 123, 092001 (2019), arXiv: 1904.10021
597. C.-J. Xiao, et al., Exploring the molecular scenario of $P_c(4312)$, $P_c(4440)$, and $P_c(4457)$, *Phys. Rev. D* 100, 014022 (2019), arXiv: 1904.00872
598. Z.-H. Guo and J. A. Oller, Anatomy of the newly observed hidden-charm pen-taquark states: $P_c(4312)$, $P_c(4440)$ and $P_c(4457)$, *Phys. Lett. B* 793, 144 (2019), arXiv: 1904.00851
599. J. He, Study of $P_c(4457)$, $P_c(4440)$, and $P_c(4312)$ in a quasipotential Bethe–Salpeter equation approach, *Eur. Phys. J. C* 79, 393 (2019), arXiv: 1903.11872
600. F.-K. Guo, H.-J. Jing, U.-G. Meiβner, and S. Sakai, Isospin breaking decays as a diagnosis of the hadronic molecular structure of the $P_c(4457)$, *Phys. Rev. D* 99, 091501 (2019), arXiv: 1903.11503
601. H.-X. Chen, W. Chen, and S.-L. Zhu, *Possible interpretations* of the $P_c(4312)$, $P_c(4440)$, and $Pc(4457)$, *Phys. Rev. D* 100, 051501 (2019), arXiv: 1903.11001
602. X. Liu, H. Huang, and J. Ping, Hidden strange pentaquark states in constituent quark models, *Phys. Rev. C* 98, 055203 (2018), arXiv: 1807.03195.
603. J. Ferretti, E. Santopinto, M. Naeem Anwar, and M. A. Bedolla, The baryo-quarkonium picture for hidden-charm and bottom pentaquarks and LHCb $P_c(4380)$ and $P_c(4450)$ states, *Phys. Lett. B* 789, 562 (2019), arXiv: 1807.01207
604. E. Hiyama, A. Hosaka, M. Oka, and J. -M. Richard, Quark model estimate of hidden-charm pentaquark resonances, *Phys. Rev. C* 98, 045208 (2018), arXiv: 1803.11369
605. S.-X. Qin, C. D. Roberts, and S. M. Schmidt, Poincaré-covariant analysis of heavy-quark baryons, *Phys. Rev. D* 97, 114017 (2018), arXiv: 1801.09697
606. J.-M. Richard, A. Valcarce, and J. Vijande, Stable heavy pentaquarks in constituent models, *Phys. Lett. B* 774, 710 (2017), arXiv: 1710.08239. 100
607. J. He, Understanding spin parity of $P_c(4450)$ and Y (4274) in a hadronic molecular state picture, *Phys. Rev. D* 95, 074004 (2017), arXiv: 1607.03223
608. M. I. Eides, V. Y. Petrov, and M. V. Polyakov, Pentaquarks with hidden charm as hadroquarkonia, *Eur. Phys. J. C* 78, 36 (2018), arXiv: 1709.09523
609. Y. Yamaguchi, et al., Hidden-charm and bottom meson-baryon molecules coupled with five-quark states, *Phys. Rev. D* 96, 114031 (2017), arXiv: 1709.00819
610. Y. Dong, A. Faessler, and V. E. Lyubovitskij, Description of heavy exotic resonances as molecular states using phenomenological Lagrangians, *Prog. Part. Nucl. Phys.* 94, 282 (2017)
611. Y.-H. Lin, C.-W. Shen, F.-K. Guo, and B.-S. Zou, Decay behaviors of the Pc hadronic molecules, *Phys. Rev. D* 95, 114017 (2017), arXiv: 1703.01045
612. R. Chen, J. He, and X. Liu, Possible strange hidden-charm pentaquarks from $\Sigma_c^{(*)}\bar{D}_s^*$ and $\Xi_c^{(',*)}\bar{D}^*$ interactions, *Chin. Phys. C* 41, 103105 (2017), arXiv: 1609.03235
613. F.-K. Guo, U. G. Meißner, J. Nieves, and Z. Yang, Remarks on the P_c structures and triangle singularities, *Eur. Phys. J. A* 52, 318 (2016), arXiv: 1605.05113
614. E. Santopinto and A. Giachino, Compact pentaquark structures, *Phys. Rev. D* 96, 014014 (2017), arXiv: 1604.03769
615. C.-W. Shen, F.-K. Guo, J.-J. Xie, and B.-S. Zou, Disentangling the hadronic molecule nature of the $Pc(4380)$ pentaquark-like structure, *Nucl. Phys. A* 954, 393 (2016), arXiv: 1603.04672
616. Y. Shimizu, D. Suenaga, and M. Harada, Coupled channel analysis of molecule picture of $P_c(4380)$, *Phys. Rev. D* 93, 114003 (2016), arXiv: 1603.02376
617. Q.-F. Lü and Y.-B. Dong, Strong decay mode $J/\psi p$ of hidden charm pentaquark states P_c (4380) and $P_c^+(4450)$ in Σ_c^* molecular scenario, *Phys. Rev. D* 93, 074020 (2016), arXiv: 1603.00559

618. E. Oset, et al., Weak decays of heavy hadrons into dynamically generated resonances, *Int. J. Mod. Phys. E* 25, 1630001 (2016), arXiv: 1601.03972
619. R. Chen, X. Liu, and S.-L. Zhu, Hidden-charm molecular pentaquarks and their charm-strange partners, *Nucl. Phys. A* 954, 406 (2016), arXiv: 1601.03233
620. Z.-G. Wang, Analysis of the $\frac{3}{2}^{\pm}$ pentaquark states in the diquark–diquark–antiquark model with QCD sum rules, *Nucl. Phys. B* 913, 163 (2016), arXiv: 1512.04763
621. G. Yang and J. Ping, Structure of pentaquarks P_c^+ in the chiral quark model, *Phys. Rev. D* 95, 014010 (2017), arXiv: 1511.09053
622. T. J. Burns, Phenomenology of $P_c(4380)^+$, $P_c(4450)^+$ and related states, *Eur. Phys. J. A* 51, 152(2015), arXiv: 1509.02460
623. N. N. Scoccola, D. O. Riska, and M. Rho, Pentaquark candidates $P_c^+(4380)$ and $P_c^+(4450)$ within the soliton picture of baryons, *Phys. Rev. D* 92, 051501 (2015), arXiv: 1508.01172
624. Z.-G. Wang, Analysis of $P_c(4380)$ and $P_c(4450)$ as pentaquark states in the diquark model with QCD sum rules, *Eur. Phys. J. C* 76, 70 (2016), arXiv: 1508.01468
625. R. Ghosh, A. Bhattacharya, and B. Chakrabarti, A study on $P_c^*(4380)$ and $P_c^*(4450)$ mass in the quasi particle diquark model, *Phys. Part. Nucl. Lett.* 14, 550 (2017), arXiv: 1508.00356
626. G.-N. Li, X.-G. He, and M. He, Some predictions of diquark model for hidden charm pentaquark discovered at the LHCb, *J. High Energy Phys.* 12, 128 (2015), arXiv: 1507.08252
627. V. V. Anisovich, et al., Pentaquarks and resonances in the pJ/ψ spectrum, arXiv: 1507.07652 (2015)
628. M. Mikhasenko, A triangle singularity and the LHCb pentaquarks, arXiv: 1507.06552 (2015)
629. R. F. Lebed, The pentaquark candidates in the dynamical diquark picture, *Phys. Lett. B* 749, 454 (2015), arXiv: 1507.05867
630. X.-H. Liu, Q. Wang, and Q. Zhao, Understanding the newly observed heavy pentaquark candidates, *Phys. Lett. B* 757, 231 (2016), arXiv: 1507.05359
631. J. He, $\bar{D}\Sigma_c^*$ and $\bar{D}^*\Sigma_c$ interactions and the LHCb hidden-charmed pentaquarks, *Phys. Lett. B* 753, 547 (2016), arXiv: 1507.05200
632. L. Maiani, A. D. Polosa, and V. Riquer, The new pentaquarks in the diquark model, *Phys. Lett. B* 749, 289 (2015), arXiv: 1507.04980
633. F.-K. Guo, U.-G. Meißner, W. Wang, and Z. Yang, How to reveal the exotic nature of the $P_c(4450)$, *Phys. Rev. D* 92, 071502 (2015), arXiv: 1507.04950
634. A. Mironov and A. Morozov, Is the pentaquark doublet a hadronic molecule? *JETP Lett.* 102, 271 (2015), arXiv: 1507.04694
635. L. Roca, J. Nieves, and E. Oset, LHCb pentaquark as a $\bar{D}^*\Sigma_c$–$\bar{D}^*\Sigma_c^*$ molecular state, *Phys. Rev. D* 92, 094003 (2015), arXiv: 1507.04249
636. H.-X. Chen, et al., Towards exotic hidden-charm pentaquarks in QCD, *Phys. Rev. Lett.* 115, 172001 (2015), arXiv: 1507.03717
637. R. Chen, X. Liu, X.-Q. Li, and S.-L. Zhu, Identifying exotic hidden-charm pentaquarks, *Phys. Rev. Lett.* 115 (2015) 132002, arXiv: 1507.03704
638. M. Karliner and J. L. Rosner, New exotic meson and baryon resonances from doubly heavy hadronic molecules, *Phys. Rev. Lett.* 115, 122001 (2015), arXiv: 1506.06386
639. X.-K. Dong, F.-K. Guo, and B.-S. Zou, Explaining the many threshold structures in the heavy-quark hadron spectrum, *Phys. Rev. Lett.* 126, 152001 (2021), arXiv: 2011.14517
640. TWQCD Collaboration, T.-W. Chiu and T.-H. Hsieh, $X(3872)$ in lattice QCD with exact chiral symmetry, *Phys. Lett. B* 646, 95 (2007), arXiv: hep-ph/0603207
641. F.-K. Guo, L. Liu, U.-G. Meissner, and P. Wang, Tetraquarks, hadronic molecules, meson–meson scattering and disconnected contributions in lattice QCD, *Phys. Rev. D* 88, 074506 (2013), arXiv: 1308.2545
642. Y. Bi, et al., Diquark mass differences from unquenched lattice QCD, *Chin. Phys. C* 40, 073106(2016), arXiv: 1510.07354
643. C. Liu, Review on hadron spectroscopy, *PoS LATTICE2016*, 006(2017), arXiv: 1612.00103
644. L. Leskovec, S. Prelovsek, C. B. Lang, and D. Mohler, Study of the Z_c^+ channel in lattice QCD, *PoS LATTICE* 2014, 118 (2015), arXiv: 1410.8828
645. Hadron Spectrum Collaboration, L. Gayer, et al., Isospin-1/2 $D\pi$ scattering and the lightest D_0^* resonance from lattice QCD, *J. High Energy Phys.* 07, 123 (2021), arXiv: 2102.04973
646. Hadron Spectrum Collaboration, G. K. C. Cheung, et al., DK $I = 0$, $D\bar{K}I = 0$, 1 scattering and the ${D_{s0}}^*(2317)$ from lattice QCD, *J. High Energy Phys.* 02, 100 (2021), arXiv: 2008.06432
647. S. L. Glashow, J. Iliopoulos, and L. Maiani, Weak interactions with lepton–hadron symmetry, *Phys. Rev. D* 2, 1285 (1970)
648. A. J. Buras and M. Munz, Effective Hamiltonian for $B \to X_s e^+ e^-$ beyond leading logarithms in the naive dimensional regularization and 't Hooft-Veltman schemes, *Phys. Rev. D* 52, 186 (1995), arXiv: hep-ph/9501281
649. A. J. Buras, Weak Hamiltonian, *CP* violation and rare decays, in Les Houches summer school in theoretical physics, session 68: Probing the standard model of particle interactions, 1998, arXiv: hep-ph/9806471
650. G. Buchalla, A. J. Buras, and M. E. Lautenbacher, Weak decays beyond leading logarithms, *Rev. Mod. Phys.* 68, 1125 (1996), arXiv: hep-ph/9512380
651. W. Altmannshofer, et al., Symmetries and asymmetries of $B \to K^*\mu^+\mu^-$ decays in the standard model and beyond, *J. High Energy Phys.* 01, 019 (2009), arXiv: 0811.1214.
652. F. Kruger and J. Matias, Probing new physics via the transverse amplitudes of $B^0 \to K^{*0}(\to K^-\pi^+)l^+l^-$ at large recoil, *Phys. Rev. D* 71 (2005) 094009, arXiv: hep-ph/0502060
653. S. Descotes-Genon, D. Ghosh, J. Matias, and M. Ramon, Exploring new physics in the C_7–C_7' plane, *J. High Energy Phys.* 06, 099 (2011), arXiv: 1104.3342
654. E. Lunghi and J. Matias, Huge right-handed current effects in $B \to K^*(K\pi)\ell^+\ell^-$ in supersymmetry, *J. High Energy Phys.* 04, 058 (2007), arXiv: hep-ph/0612166
655. M. Beneke, C. Bobeth, and R. Szafron, Power-

enhanced leading-logarithmic QED corrections to $B_q \to \mu^+\mu^-$, *J. High Energy Phys.* 10, 232 (2019), arXiv: 1908.07011

656. CMS and LHCb Collaborations, V. Khachatryan, et al., Observation of the rare $B_s^0 \to \mu^+\mu^-$ decay from the combined analysis of CMS and LHCb data, *Nature* 522, 68 (2015), arXiv: 1411.4413
657. LHCb Collaboration, R. Aaij, et al., Measurement of the $B_s^0 \to \mu^+\mu^-$ branching fraction and effective lifetime and search for $B^0 \to \mu^+\mu^-$ decays, *Phys. Rev. Lett.* 118 (2017) 191801, arXiv: 1703.05747
658. CMS Collaboration, A. M. Sirunyan, et al., Measurement of properties of $B_s^0 \to \mu^+\mu^-$ decays and search for $B^0 \to \mu^+\mu^-$ with the CMS experiment, *J. High Energy Phys.* 04, 188 (2020), arXiv: 1910.12127
659. ATLAS Collaboration, M. Aaboud et al., Study of the rare decays of B_s^0 and B^0 mesons into muon pairs using data collected during 2015 and 2016 with the ATLAS detector, *J. High Energy Phys.* 04, 098 (2019), arXiv: 1812.03017
660. LHCb Collaboration, Combination of the ATLAS, CMS and LHCb results on the $B_{(s)}^0 \to \mu^+\mu^-$ decays, LHCb-CONF-2020-002, 2020, ATLAS-CONF-2020-049, CMS PAS BPH-20-003, LHCb-CONF-2020-002
661. LHCb Collaboration, R. Aaij, et al., Analysis of neutral B-meson decays into two muons, *Phys. Rev. Lett.* 128, 041801 (2022), arXiv: 2108.09284
662. LHCb Collaboration, R. Aaij, et al., Measurement of the $B_s^0 \to \mu^+\mu^-$ decay properties and search for the $B_s^0 \to \mu^+\mu^-$ and $B_s^0 \to \mu^+\mu^-\gamma$ decays, *Phys. Rev. D*105, 012010 (2022), arXiv: 2108.09283
663. K. De Bruyn et al., Probing new physics via the $B_s^0 \to \mu^+\mu^-$ effective lifetime, *Phys. Rev. Lett.* 109, 041801 (2012), arXiv: 1204.1737
664. LHCb Collaboration, Physics case for an LHCb Upgrade II - Opportunities in flavour physics, and beyond, in the HL-LHC era, arXiv: 1808.08865
665. LHCb Collaboration, R. Aaij, et al., Search for the rare decays $B_s^0 \to e^+e^-$ and $B^0 \to e^+e^-$, *Phys. Rev. Lett.* 124, 211802 (2020), arXiv: 2003.03999
666. LHCb Collaboration, R. Aaij et al., Search for rare $B_{(s)}^0 \to \mu^+\mu^-\mu^+\mu^-$ decays, *J. High Energy Phys.* 03, 109 (2022), arXiv: 2111.11339
667. A. Bharucha, D. M. Straub, and R. Zwicky, $B \to V\ell^+\ell^-$ in the standard model from light-cone sum rules, *J. High Energy Phys.* 08, 098 (2016), arXiv: 1503.05534
668. A. Khodjamirian, T. Mannel, A. A. Pivovarov, and Y. -M. Wang, Charm-loop effect in $B \to K^{(*)}\ell^+\ell^-$ and $B \to K^*\gamma$, *J. High Energy Phys.* 09, 089 (2010), arXiv: 1006.4945
669. J. Gao, et al., Precision calculations of $B \to V$ form factors from soft-collinear effective theory sum rules on the light-cone, *Phys.* Rev. D 101, 074035 (2020), arXiv: 1907.11092
670. R. R. Horgan, Z. Liu, S. Meinel, and M. Wingate, Lattice QCD calculation of form factors describing the rare decays $B \to K^*\ell^+\ell^-$ and $B_s \to \phi\ell^+\ell^-$, *Phys. Rev. D* 89, 094501 (2014), arXiv: 1310.3722
671. R. R. Horgan, Z. Liu, S. Meinel, and M. Wingate, Rare B decays using lattice QCD form factors, *PoS Lattice* 2014, 372 (2015), arXiv: 1501.00367
672. LHCb Collaboration, R. Aaij, et al., Angular analysis and differential branching fraction of the decay $B_s^0 \to \phi\mu^+\mu^-$, *J. High Energy Phys.* 09, 179 (2015), arXiv: 1506.08777
673. LHCb Collaboration, R. Aaij, et al., Branching fraction measurements of the rare $B_s^0 \to \phi\mu^+\mu^-$ and $B_s^0 \to f_2'(1525)\mu^+\mu^-$ decays, *Phys. Rev. Lett.* 127, 151801 (2021), arXiv: 2105.14007
674. LHCb Collaboration, R. Aaij, et al., Differential branching fraction and angular analysis of $\Lambda_b^0 \to \Lambda\mu^+\mu^-$ decays, *J. High Energy Phys.* 06, 115 (2015), Erratum *JHEP* 09, 145 (2018), arXiv: 1503.07138
675. LHCb Collaboration, R. Aaij, et al., Measurements of the S-wave fraction in $B^0 \to K^+\pi^-\mu^+\mu^-$ decays and the $B^0 \to K^*(892)^0\mu^+\mu^-$ differential branching fraction, *J. High Energy Phys.* 11, 047 (2016), Erratum: *J. High Energy Phys.* 04, 142 (2017), arXiv: 1606.04731
676. LHCb Collaboration, R. Aaij, et al., Differential branching fractions and isospin asymmetries of $B \to K^{(*)}\mu^+\mu^-$ decays, *J. High Energy Phys.* 06, 133 (2014), arXiv: 1403.8044
677. W. Altmannshofer and D. M. Straub, New physics in $b \to s$ transitions after LHC Run 1, *Eur. Phys. J. C* 75, 382 (2015), arXiv: 1411.3161
678. W. Altmannshofer and D. M. Straub, Implications of $b \to s$ measurements, in 50th Rencontres de Moriond on EW Interactions and Unified Theories, 333–338, 2015, arXiv: 1503.06199
679. W. Detmold, C. -J. D. Lin, S. Meinel, and M. Wingate, $\Lambda_b^0 \to \Lambda\ell^+\ell^-$ form factors and differential branching fraction from lattice QCD, *Phys. Rev. D* 87, 074502 (2013), arXiv: 1212.4827
680. C. Bobeth, G. Hiller, and D. van Dyk, More benefits of semileptonic rare B decays at low recoil: CP violation, *J. High Energy Phys.* 07, 067 (2011), arXiv: 1105.0376
681. C. Bobeth, G. Hiller, D. van Dyk, and C. Wacker, The decay $B \to \ell^+\ell^-$ at low hadronic recoil and model-independent $\Delta B = 1$ constraints, *J. High Energy Phys.* 01, 107 (2012), arXiv: 1111.2558
682. BaBar Collaboration, B. Aubert, et al., Measurements of branching fractions, rate asymmetries, and angular distributions in the rare decays $B \to K\ell^+\ell^-$ and $B \to K^*\ell^+\ell^-$, *Phys. Rev. D* 73, 092001 (2006), arXiv: hep-ex/0604007
683. Belle Collaboration, S. Wehle, et al., Lepton-flavor-dependent angular analysis of $B \to K^*\ell^+\ell^-$, *Phys. Rev. Lett.* 118, 111801 (2017), arXiv: 1612.05014
684. ATLAS Collaboration, M. Aaboud, et al., Angular analysis of $B_d^0 \to K^*\mu^+\mu^-$ decays in pp collisions at $\sqrt{s} =$ 8 TeV with the ATLAS detector, *J. High Energy Phys.* 10 (2018) 047, arXiv: 1805.04000
685. CMS Collaboration, A. M. Sirunyan, et al., Measurement of angular parameters from the decay $B^0 \to K^{*0}\mu^+\mu^-$ in proton–proton collisions at $\sqrt{s} = 8$ TeV, *Phys. Lett. B* 781, 517 (2018), arXiv: 1710.02846
686. LHCb Collaboration, R. Aaij, et al., Differential branching fraction and angular analysis of the decay $B^0 \to K^{*0}\mu^+\mu^-$, *Phys. Rev. Lett.* 108, 181806 (2012), arXiv: 1112.3515
687. LHCb Collaboration, R. Aaij, et al., Differential

branching fraction and angular analysis of the decay $B^0 \to K^{*0}\mu^+\mu^-$, *JHEP* 08, 131 (2013), arXiv: 1304.6325
688. LHCb Collaboration, R. Aaij, et al., Angular analysis of the $B^0 \to K^{*0}\mu^+\mu^-$ decay using 3 fb^{-1} of integrated luminosity, *J. High Energy Phys.* 02, 104 (2016), arXiv: 1512.04442
689. LHCb Collaboration, R. Aaij, et al., Measurement of *CP*-averaged observables in the $B^0 \to K^{*0}\mu^+\mu^-$ decay, *Phys. Rev. Lett.* 125, 011802 (2020), arXiv: 2003.04831
690. S. Descotes-Genon, L. Hofer, J. Matias, and J. Virto, On the impact of power corrections in the prediction of $B \to K^*\mu^+\mu^-$ observables, *J. High Energy Phys.* 12, 125 (2014), arXiv: 1407.8526
691. D. M. Straub, flavio: A Python package for flavour and precision phenomenology in the standard model and beyond, arXiv: 1810.08132
692. LHCb Collaboration, R. Aaij et al., Angular analysis of the $B^+ \to K^{*+}\mu^+\mu^-$ decay, *Phys. Rev. Lett.* 126, 161802 (2021), arXiv: 2012.13241
693. LHCb Collaboration, R. Aaij, et al., Angular analysis of the rare decay $B_s^0 \to \phi\mu^+\mu^-$, *J. High Energy Phys.* 11, 043 (2021), arXiv: 2107.13428
694. C. Bobeth, G. Hiller, and G. Piranishvili, *CP* asymmetries in $\overline{B} \to \overline{K}^*(\to \overline{K}\pi)\overline{\ell}\ell$ and untagged $\overline{B}_s$, $\overline{B}_s \to \phi(\to K^+K^-)\overline{\ell}\ell$ decays at NLO, *J. High Energy Phys.* 07, 106 (2008), arXiv: 0805.2525
695. S. Descotes-Genon and J. Virto, Time dependence in $B \to V\ell\ell$ decays, *J. High Energy Phys.* 04, 045 (2015), Erratum: *J. High Energy Phys.* 07, 049 (2015), arXiv: 1502.05509
696. LHCb Collaboration, R. Aaij, et al., Angular analysis of charged and neutral $B \to K\mu^+\mu^-$ decays, *J. High Energy Phys.* 05, 082 (2014), arXiv: 1403.8045
697. CMS Collaboration, A. M. Sirunyan et al., Angular analysis of the decay $B^+ \to K^+\mu^+\mu^-$ in proton-proton collisions at $\sqrt{s} = 8$ TeV, *Phys. Rev. D* 98, 112011 (2018), arXiv: 1806.00636
698. LHCb Collaboration, R. Aaij, et al., Angular moments of the decay $\Lambda_b^0 \to \Lambda\mu^+\mu^-$ at low hadronic recoil, *J. High Energy Phys.* 09, 146 (2018), arXiv: 1808.00264
699. G. Hiller and F. Kruger, More model-independent analysis of $b \to s$ processes, *Phys. Rev. D* 69, 074020 (2004), arXiv: hep-ph/0310219
700. M. Bordone, G. Isidori, and A. Pattori, On the standard model predictions for R_K and R_{K^*}, *Eur. Phys. J. C* 76, 440 (2016), arXiv: 1605.07633
701. G. Isidori, S. Nabeebaccus, and R. Zwicky, QED corrections in $\overline{B} \to \overline{K}\ell^+\ell^-$ at the double-differential level, *J. High Energy Phys.* 12, 104 (2020), arXiv: 2009.00929
702. LHCb Collaboration, R. Aaij et al., Search for lepton-universality violation in $B^+ \to K^+\ell^+\ell^-$ decays, *Phys. Rev. Lett.* 122, 191801 (2019), arXiv: 1903.09252
703. LHCb Collaboration, R. Aaij, et al., Test of lepton universality in beauty-quark decays, *Nat. Phys.* 18, 277 (2022), arXiv: 2103.11769
704. S. Descotes-Genon, L. Hofer, J. Matias, and J. Virto, Global analysis of $b \to s\ell\ell$ anomalies, *J. High Energy Phys.* 06, 092 (2016), arXiv: 1510.04239
705. C. Bobeth, G. Hiller, and G. Piranishvili, Angular distributions of $\overline{B} \to \overline{K}\,\ell\,\overline{\ell}$ decays, *J. High Energy Phys.* 12, 040 (2007), arXiv: 0709.4174
706. D. van Dyk, F. Beaujean, and C. Bobeth, Eos ("delta456" release), 2016, Zenodo, doi: 10.5281/zenodo.159680
707. BaBar Collaboration, J. P. Lees, et al., Measurement of branching fractions and rate asymmetries in the rare decays $B \to K^{(*)}\ell^+\ell^-$, *Phys. Rev. D* 86, 032012 (2012), arXiv: 1204.3933
708. Belle Collaboration, J.-T. Wei, et al., Measurement of the differential branching fraction and forward-backward asymmetry for $B \to K^{(*)}\ell^+\ell^-$, *Phys. Rev. Lett.* 103, 171801 (2009), arXiv: 0904.0770
709. LHCb Collaboration, R. Aaij, et al., Test of lepton universality with $B^0 \to K^{*0}\ell^+\ell^-$ decays, *J. High Energy Phys.* 08, 055(2017), arXiv: 1705.05802
710. B. Capdevila, S. Descotes-Genon, J. Matias, and J. Virto, Assessing lepton-flavour non-universality from $B \to K^*\ell^+\ell^-$ angular analyses, *J. High Energy Phys.* 10, 075 (2016), arXiv: 1605.03156
711. B. Capdevila, S. Descotes-Genon, L. Hofer, and J. Matias, Hadronic uncertainties in $B \to K^*\mu^+\mu^-$: A state-of-the-art analysis, *J. High Energy Phys.* 04, 016 (2017), arXiv: 1701.08672
712. N. Serra, R. Silva Coutinho, and D. van Dyk, Measuring the breaking of lepton flavor universality in $B \to K^*\ell^+\ell^-$, *Phys. Rev. D* 95, 035029 (2017), arXiv: 1610.08761
713. S. Jäger and J. M. Camalich, Reassessing the discovery potential of the $B \to K^*\ell^+\ell^-$ decays in the large-recoil region: SM challenges and BSM opportunities, *Phys. Rev. D* 93, 014028 (2016), arXiv: 1412.3183
714. LHCb Collaboration, R. Aaij, et al., Test of lepton universality using $\Lambda_b^0 \to pK^-\ell^+\ell^-$ decays, *J. High Energy Phys.* 05, 040 (2020), arXiv: 1912.08139
715. LHCb Collaboration, R. Aaij, et al., Tests of lepton universality using $B^0 \to K_S^0\ell^+\ell^-$ and $B^+ \to K^{*+}\ell^+\ell^-$ decays, *Phys. Rev. Lett.* 128, 191802 (2022), arXiv: 2110.09501
716. M. Algueró, et al., Emerging patterns of new physics with and without lepton flavour universal contributions, *Eur. Phys. J. C* 79, 714 (2019), Addendum *Eur. Phys. J. C* 80, 511(2020), arXiv: 1903.09578
717. M. Ciuchini, et al., Lessons from the $B^{0,+} \to K^{*0,+}\,\mu^+\mu^-$ angular analyses, *Phys. Rev. D* 103, 015030 (2021), arXiv: 2011.01212
718. J. Aebischer, et al., B-decay discrepancies after Moriond 2019, *Eur. Phys. J. C* 80, 252 (2020), arXiv: 1903.10434
719. M. Algueró, et al., $b \to s\ell\ell$ global fits after Moriond 2021 results, in: 55th Rencontres de Moriond on QCD and High Energy Interactions, 2021, arXiv: 2104.08921
720. W. Altmannshofer and P. Stangl, New physics in rare B decays after Moriond 2021, *Eur. Phys. J. C* 81, 952 (2021), arXiv: 2103.13370
721. L.-S. Geng, et al., Implications of new evidence for lepton-universality violation in $b \to s\ell^+\ell^-$ decays, *Phys. Rev. D* 104, 035029 (2021), arXiv: 2103.12738
722. C. Cornella, et al., Reading the footprints of the B-meson flavor anomalies, *J. High Energy Phys.* 08, 050 (2021), arXiv: 2103.16558
723. G. Isidori, D. Lancierini, P. Owen, and N. Serra, On

the significance of new physics in $b \to s\ell^+\ell^-$ decays, *Phys. Lett. B* 822, 136644 (2021), arXiv: 2104.05631

724. G. Isidori, et al., A general effective field theory description of $b \to s\ell^+\ell^-$ lepton universality ratios, *Phys. Lett. B* 830, 137151 (2022), arXiv: 2110.09882
725. T. Hurth, F. Mahmoudi, D. M. Santos, and S. Neshatpour, More indications for lepton nonuniversality in $b \to s\ell^+\ell^-$, *Phys. Lett. B* 824, 136838 (2022), arXiv: 2104.10058
726. S. Descotes-Genon, M. Novoa-Brunet, and K. K. Vos, The time-dependent angular analysis of $B_d \to K_S\ell\ell$, a new benchmark for new physics, *J. High Energy Phys.* 02, 129 (2021), arXiv: 2008.08000
727. N. Košnik and A. Smolkovič, LFU and *CP* violation with $S3$, arXiv: 2108.11929
728. M. Bordone, C. Cornella, G. Isidori, and M. König, The LFU ratio R_π in the standard model and beyond, *Eur. Phys. J. C* 81, 850 (2021), arXiv: 2101.11626
729. A. V. Rusov, Probing new physics in $b \to d$ transitions, *J. High Energy Phys.* 07 (2020) 158, arXiv: 1911.12819
730. N. R. Soni, et al., Rare $b \to d$ decays in covariant confined quark model, arXiv: 2008.07202 (2020)
731. B. Kindra and N. Mahajan, Predictions of angular observables for $\overline{B}_s \to K^*\ell\ell$ and $\overline{B} \to \rho\ell\ell$ in the standard model, *Phys. Rev. D* 98, 094012 (2018), arXiv: 1803.05876
732. D. Atwood, M. Gronau, and A. Soni, Mixing induced *CP* asymmetries in radiative B decays in and beyond the standard model, *Phys. Rev. Lett.* 79, 185 (1997), arXiv: hep-ph/9704272
733. L. L. Everett, et al., Alternative approach to $b \to s\gamma$ in the uMSSM, *J. High Energy Phys.* 01, 022 (2002), arXiv: hep-ph/0112126
734. B. Grinstein, Y. Grossman, Z. Ligeti, and D. Pirjol, Photon polarization in $B \to X\gamma$ in the standard model, *Phys. Rev. D* 71, 011504 (2005), arXiv: hep-ph/0412019
735. D. Becirevic, E. Kou, A. Le Yaouanc, and A. Tayduganov, Future prospects for the determination of the Wilson coefficient $C_{7\gamma}'$, *J. High Energy Phys.* 08, 090 (2012), arXiv: 1206.1502
736. E. Kou, C.-D. Lü, and F.-S. Yu, Photon polarization in the $b \to s\gamma$ processes in the left-right symmetric model, *J. High Energy Phys.* 12, 102 (2013), arXiv: 1305.3173
737. N. Haba, et al., Search for new physics via photon polarization of $b \to s\gamma$, *J. High Energy Phys.* 03, 160 (2015), arXiv: 1501.00668
738. A. Paul and D. M. Straub, Constraints on new physics from radiative B decays, *J. High Energy Phys.* 04, 027 (2017), arXiv: 1608.02556
739. D. Atwood, T. Gershon, M. Hazumi, and A. Soni, Mixing-induced *CP* violation in $B \to P_1P_2\gamma$ in search of clean new physics signals, *Phys. Rev. D* 71, 076003 (2005), arXiv: hep-ph/0410036
740. F. Muheim, Y. Xie, and R. Zwicky, Exploiting the width difference in $B_s \to \phi\gamma$, *Phys. Lett. B* 664, 174 (2008), arXiv: 0802.0876
741. BaBar Collaboration, J. P. Lees, et al., Precision measurement of the $B \to X_s\gamma$ photon energy spectrum, branching fraction, and direct *CP* asymmetry $A_{CP}(B \to X_{s+d}\gamma)$, *Phys. Rev. Lett.* 109, 191801 (2012), arXiv: 1207.2690
742. Belle Collaboration, T. Horiguchi, et al., Evidence for isospin violation and measurement of *CP* asymmetries in $B \to K^*(892)\ \gamma$, *Phys. Rev. Lett.* 119, 191802 (2017), arXiv: 1707.00394
743. LHCb Collaboration, R. Aaij, et al., Measurement of the ratio of branching fractions $\mathcal{B}(B^0 \to K^{*0}\gamma)/\mathcal{B}(B_s^0 \to \phi\gamma)$ and the direct *CP* asymmetry in $B^0 \to K^{*0}\gamma$, *Nucl. Phys. B* 867, 1 (2013), arXiv: 1209.0313
744. Belle Collaboration, Y. Ushiroda, et al., Time-dependent *CP* asymmetries in $B_s^0 \to K_S^0\pi^0\gamma$ transitions, *Phys. Rev. D* 74, 111104 (2006), arXiv: hep-ex/0608017
745. BaBar Collaboration, B. Aubert, et al., Measurement of time-dependent *CP* asymmetry in $B^0 \to K_S^0\pi^0\gamma$ decays, *Phys. Rev. D* 78, 071102 (2008), arXiv: 0807.3103
746. LHCb Collaboration, R. Aaij, et al., Measurement of *CP*-violating and mixing-induced observables in $B_s^0 \to \phi\gamma$ decays, *Phys. Rev. Lett.* 123, 081802 (2019), arXiv: 1905.06284
747. D. Becirevic and E. Schneider, On transverse asymmetries in $B \to K^*\ell^+\ell^-$, *Nucl. Phys. B* 854, 321 (2012), arXiv: 1106.3283
748. LHCb Collaboration, R. Aaij, et al., Strong constraints on the $b \to s\gamma$ photon polarisation from $B^0 \to K^{*0}e^+e^-$ decays, *J. High Energy Phys.* 12, 081 (2020), arXiv: 2010.06011
749. M. Gronau and D. Pirjol, Photon polarization in radiative B decays, *Phys. Rev. D* 66, 054008 (2002), arXiv: hep-ph/0205065
750. E. Kou, A. Le Yaouanc, and A. Tayduganov, Determining the photon polarization of the $b \to s\gamma$ using the $B \to K_1(1270) \to (K\pi\pi)\gamma$ decay, *Phys. Rev. D* 83, 094007 (2011), arXiv: 1011.6593
751. LHCb Collaboration, R. Aaij, et al., Observation of photon polarization in the $b \to s\gamma$ transition, *Phys. Rev. Lett.* 112, 161801 (2014), arXiv: 1402.6852
752. W. Wang, F.-S. Yu, and Z.-X. Zhao, Novel method to reliably determine the photon helicity in $B \to K1\gamma$, *Phys. Rev. Lett.* 125, 051802 (2020), arXiv: 1909.13083
753. H.-Y. Cheng, X.-R. Lyu, and Z.-Z. Xing, Charm physics in the high-luminosity super τ-charm factory, in: 2022 Snowmass Summer Study, 2022, arXiv: 2203.03211
754. LHCb Collaboration, R. Aaij, et al., First observation of the radiative $\Lambda_b^0 \to \Lambda\gamma$ decay, *Phys. Rev. Lett.* 123, 031801 (2019), arXiv: 1904.06697
755. M. Gremm, F. Kruger, and L. M. Sehgal, Angular distribution and polarization of photons in the inclusive decay $\Lambda_b \to Xs\gamma$, *Phys. Lett. B* 355, 579 (1995), arXiv: hep-ph/9505354
756. T. Mannel and S. Recksiegel, Flavor changing neutral current decays of heavy baryons: The case $\Lambda_b \to \Lambda\gamma$, *J. Phys. G* 24, 979 (1998), arXiv: hep-ph/9701399
757. G. Hiller and A. Kagan, Probing for new physics in polarized Λ_b decays at the Z, *Phys. Rev. D* 65, 074038 (2002), arXiv: hep-ph/0108074
758. LHCb Collaboration, R. Aaij, et al., Measurement of the photon polarization in $\Lambda_b^0 \to \Lambda\gamma$ decays, arXiv: 2111.10194, submitted to *PRL*

759. BESIII Collaboration, M. Ablikim, et al., Polarization and entanglement in baryon-antibaryon pair production in electron-positron annihilation, *Nature Phys.* 15, 631 (2019), arXiv: 1808.08917
760. Y.-M. Wang, Y. Li, and C.-D. Lü, Rare decays of $\Lambda_b \to \Lambda + \gamma$ and $\Lambda_b \to \Lambda + l^+l^-$ in the light-cone sum rules, *Eur. Phys. J. C* 59, 861 (2009), arXiv: 0804.0648
761. T. Mannel and Y.-M. Wang, Heavy-to-light baryonic form factors at large recoil, *J. High Energy Phys.* 12, 067 (2011), arXiv: 1111.1849
762. T. Gutsche, et al., Rare baryon decays $\Lambda_b \to \Lambda\ell^+\ell^-$ ($\ell = e, \mu, \tau$) and $\Lambda_b \to \Lambda\gamma$: Differential and total rates, lepton- and hadron-side forward-backward asymmetries, *Phys. Rev. D* 87, 074031 (2013), arXiv: 1301.3737
763. LHCb Collaboration, R. Aaij, et al., Search for the radiative $\Xi_b^- \to \Xi^-\gamma$ decay, *J. High Energy Phys.* 01, 069 (2022), arXiv: 2108.07678
764. LHCb Collaboration, R. Aaij, et al., Search for the lepton flavour violating decay $B^0 \to K^{*0}\tau^\pm\mu^\mp$, arXiv: 2209.09846 (submitted to *J. High Energy Phys.*)
765. LHCb Collaboration, R. Aaij, et al., Search for the lepton-flavour violating decays $B^0 \to K^{*0}\mu^\pm e^\mp$ and $B_s^0 \to \phi\mu^\pm e^\mp$, arXiv: 2207.04005 (submitted to *J. High Energy Phys.*)
766. LHCb Collaboration, R. Aaij, et al., Search for the lepton flavour violating decay $B^+ \to K^+\mu^-\tau^+$ using B_{s2}^{*0} decays, *J. High Energy Phys.* 06, 129(2020), arXiv: 2003.04352
767. LHCb Collaboration, R. Aaij, et al., Search for the lepton-flavour violating decays $B^+ \to K^+\mu^\pm e^\mp$, *Phys. Rev. Lett.* 123, 231802 (2019), arXiv: 1909.01010
768. LHCb Collaboration, R. Aaij, et al., Search for the lepton-flavour-violating decays $B_s^0 \to \tau^\pm\mu^\mp$ and $B^0 \to \tau^\pm\mu^\mp$, *Phys. Rev. Lett.* 123, 211801 (2019), arXiv: 1905.06614
769. LHCb Collaboration, R. Aaij, et al., Search for the lepton-flavour violating decays $B_{(s)}^0 \to e^\pm\mu^\mp$, *J. High Energy Phys.* 03, 078 (2018), arXiv: 1710.04111
770. LHCb Collaboration, R. Aaij, et al., Search for the baryon- and lepton-number violating decays $B^0 \to p\mu^-$ and $B_s^0 \to p\mu^-$, arXiv: 2210.10412 (submitted to *Phys. Rev. D*)
771. LHCb Collaboration, R. Aaij, et al., Evidence for the decay $B_s^0 \to \overline{K}^{*0}\mu^+\mu^-$, *J. High Energy Phys.* 07, 020 (2018), arXiv: 1804.07167
772. LHCb Collaboration, R. Aaij, et al., Observation of the suppressed decay $\Lambda_b^0 \to p\pi^-\mu^+\mu^-$, *J. High Energy Phys.* 04, 029 (2017), arXiv: 1701.08705
773. LHCb Collaboration, R. Aaij, et al., First observation of the decay $B^+ \to \pi^+\mu^+\mu^-$, *J. High Energy Phys.* 12, 125 (2012), arXiv: 1210.2645
774. LHCb Collaboration, R. Aaij, et al., Search for the decay $B^0 \to \phi\mu^+\mu^-$, *J. High Energy Phys.* 05, 067 (2022), arXiv: 2201.10167
775. LHCb Collaboration, R. Aaij, et al., Search for the rare decay $B^0 \to J/\psi\phi$, *Chin. Phys. C* 45, 043001 (2021), arXiv: 2011.06847
776. J. Brod, A. Lenz, G. Tetlalmatzi-Xolocotzi, and M. Wiebusch, New physics effects in tree-level decays and the precision in the determination of the quark mixing angle γ, *Phys. Rev. D* 92, 033002 (2015), arXiv: 1412.1446
777. J. Brod and J. Zupan, The ultimate theoretical error on γ from $B \to DK$ decays, *JHEP* 01, 051 (2014), arXiv: 1308.5663
778. M. Gronau and D. Wyler, On determining a weak phase from *CP* asymmetries in charged *B* decays, *Phys. Lett. B* 265, 172 (1991)
779. M. Gronau and D. London, How to determine all the angles of the unitarity triangle from $B_d^0 \to DK_s$ and $B_s^0 \to D\phi$, *Phys. Lett. B* 253, 483 (1991)
780. D. Atwood, I. Dunietz, and A. Soni, Enhanced *CP* violation with $B \to KD^0(\overline{D}^0)$ modes and extraction of the Cabibbo–Kobayashi–Maskawa angle γ, *Phys. Rev. Lett.* 78, 3257 (1997), arXiv: hep-ph/9612433
781. A. Giri, Y. Grossman, A. Soffer, and J. Zupan, Determining γ using $B^\pm \to DK^\pm$ with multibody *D* decays, *Phys. Rev. D* 68, 054018 (2003), arXiv: hep-ph/0303187
782. A. Bondar and A. Poluektov, Feasibility study of model-independent approach to φ_3 measurement using Dalitz plot analysis, *Eur. Phys. J. C* 47, 347 (2006), arXiv: hep-ph/0510246
783. A. Bondar and A. Poluektov, The use of quantum-correlated D^0 decays for φ_3 measurement, *Eur. Phys. J. C* 55, 51 (2008), arXiv: 0801.0840
784. LHCb Collaboration, R. Aaij, et al., Simultaneous determination of CKM angle γ and charm mixing parameters, *J. High Energy Phys.* 12, 141 (2021), arXiv: 2110.02350
785. S. Malde et al., First determination of the *CP* content of $D \to \pi^+\pi^-\pi^+\pi^-$ and updated determination of the *CP* contents of $D \to \pi^+\pi^-\pi^0$ and $D \to K^+K^-\pi^0$, *Phys. Lett. B* 747, 9 (2015), arXiv: 1504.05878
786. BaBar Collaboration, B. Aubert, et al., Measurement of *CP* violation parameters with a Dalitz plot analysis of $B^\pm \to D(\pi^+\pi^-\pi^0)K^\pm$, *Phys. Rev. Lett.* 99, 251801 (2007), arXiv: hep-ex/0703037
787. CLEO Collaboration, D. Cronin-Hennessy, et al., Searches for *CP* violation and $\pi\pi$ S-wave in the dalitz-Plot of $D^0 \to \pi^+\pi^-\pi^0$, *Phys. Rev. D* 72, 031102 (2005), Erratum: *Phys. Rev. D* 75, 119904 (2007), arXiv: hep-ex/0503052
788. BaBar Collaboration, B. Aubert, et al., Amplitude analysis of the decay $D^0 \to K^+K^-\pi^0$, *Phys. Rev. D* 76, 011102 (2007), arXiv: 0704.3593
789. CLEO Collaboration, C. Cawlfield, et al., Measurement of interfering $K^{*+}K^-$ and $K^{*-}K^+$ amplitudes in the decay $D^0 \to K^+K^-\pi^0$, *Phys. Rev. D* 74, 031108 (2006), arXiv: hep-ex/0606045
790. LHCb Collaboration, R. Aaij, et al., Observation of *CP* violation in charm decays, *Phys. Rev. Lett.* 122, 211803 (2019), arXiv: 1903.08726
791. W. Wang, CP violation effects on the measurement of the Cabibbo–Kobayashi–Maskawa angle γ from $B \to DK$, *Phys. Rev. Lett.* 110, 061802 (2013), arXiv: 1211.4539
792. LHCb Collaboration, R. Aaij, et al., Measurement of *CP* observables in $B^\pm \to D^{(*)}K^\pm$ and $B^\pm \to D^{(*)}\pi^\pm$ decays using two-body *D* final states, *J. High Energy Phys.* 04, 081 (2021), arXiv: 2012.09903
793. T. Evans, et al., Improved determination of the $D \to$

$K^-\pi^+\pi^+\pi^-$ coherence factor and associated hadronic parameters from a combination of $e^+e^- \to \psi(3770) \to c\bar{c}$ and $pp \to c\bar{c}X$ data, *Phys. Lett. B* 757, 520 (2016), Erratum: *Phys. Lett. B* 765, 402 (2017), arXiv: 1602.07430

794. T. Evans, J. Libby, S. Malde, and G. Wilkinson, Improved sensitivity to the CKM phase γ through binning phase space in $B^- \to DK^-$, $D \to K^+\pi^-\pi^-\pi^+$ decays, *Phys. Lett. B* 802, 135188 (2020), arXiv: 1909.10196. 112
795. LHCb Collaboration, R. Aaij, et al., Measurement of the CKM angle γ with $B^\mp \to D[K^\pm\pi^\mp\pi^\mp\pi^\pm]h^\mp$ decays using a binned phase-space approach, arXiv: 2209.03692 (submitted to *J. High Energy Phys.*)
796. LHCb Collaboration, R. Aaij, et al., Constraints on the CKM angle γ from $B^\pm \to Dh^\pm$ decays using $D \to h^\pm h'^\mp\pi^0$ final states, *J. High Energy Phys.* 07, 099 (2022), arXiv: 2112.10617
797. CLEO Collaboration, J. Libby, et al., Model-independent determination of the strong-phase difference between D^0 and $\overline{D}^0 \to K^0_{S,L}h^+h^-$ ($h = \pi$, K) and its impact on the measurement of the CKM angle γ/ϕ_3, *Phys. Rev. D* 82, 112006 (2010), arXiv: 1010.2817
798. BESIII Collaboration, M. Ablikim, et al., Determination of strong-phase parameters in $D \to K^0_{S,L}\pi^+\pi^-$, *Phys. Rev. Lett.* 124, 241802 (2020), arXiv: 2002.12791
799. BESIII Collaboration, M. Ablikim, et al., Model-independent determination of the relative strong-phase difference between D^0 and $\overline{D}^0 \to K^0_{S,L}\pi^+\pi^-$ and its impact on the measurement of the CKM angle γ/ϕ_3, *Phys. Rev. D* 101, 112002 (2020), arXiv: 2003.00091
800. BESIII Collaboration, M. Ablikim, et al., Improved model-independent determination of the strong-phase difference between D^0 and $\overline{D}^0 \to K^0_{S,L}K^+K^-$ decays, *Phys. Rev. D* 102, 052008 (2020), arXiv: 2007.07959
801. LHCb Collaboration, R. Aaij, et al., Measurement of the CKM angle γ using $B^\pm \to DK^\pm$ with $D \to K^0_S\pi^+\pi^-$, $K^0_SK^+K^-$ decays, *J. High Energy Phys.* 08, 176 (2018), Erratum *JHEP* 10, 107 (2018), arXiv: 1806.01202
802. LHCb Collaboration, R. Aaij, et al., Measurement of the CKM angle γ in $B^\pm \to DK^\pm$ and $B^\pm \to D\pi^\pm$ decays with $D \to K^0_Sh^+h^-$, *J. High Energy Phys.* 02 (2021) 0169, arXiv: 2010.08483
803. LHCb Collaboration, R. Aaij, et al., Constraints on the unitarity triangle angle γ from Dalitz plot analysis of $B^0 \to DK^+\pi^-$ decays, *Phys. Rev. D* 93, 112018 (2016), Erratum: *Phys. Rev. D* 94, 079902 (2016), arXiv: 1602.03455
804. LHCb Collaboration, R. Aaij, et al., Measurement of the CKM angle γ and B_s^0–$\overline{B}_s^0$ mixing frequency with $B_s^0 \to D_s^\mp h^\pm\pi^\pm\pi^\mp$ decays, *J. High Energy Phys.* 03, 137 (2021), arXiv: 2011.12041
805. LHCb Collaboration, R. Aaij, et al., Measurement of *CP* asymmetry in $B_s^0 \to D_s^\mp K^\pm$ decays, J. *High Energy Phys.* 03, 059 (2018), arXiv: 1712.07428
806. LHCb Collaboration, R. Aaij, et al., Observation of the decay $B_s^0 \to \overline{D}^0\phi$, *Phys. Lett. B* 727, 403 (2013), arXiv: 1308.4583
807. LHCb Collaboration, R. Aaij, et al., Observation of the decay $B_s^0 \to \overline{D}^{0*}\phi$ and search for the mode $B^0 \to \overline{D}^0\phi$, *Phys. Rev. D* 98, 071103(R) (2018), arXiv: 1807.01892
808. LHCb Collaboration, R. Aaij, et al., Measurement of *CP* asymmetry in $B_s^0 \to D_s^\mp K^\pm$ decays, *J. High Energy Phys.* 11, 060 (2014), arXiv: 1407.6127
809. D. Ao et al., Study of CKM angle γ sensitivity using flavor untagged $B_s^0 \to \tilde{D}^{(*)0}\phi$ decays, *Chin. Phys. C* 45, 023003 (2021), arXiv: 2008.00668
810. W. Wang, Determining *CP* violation angle γ with *B* decays into a scalar/tensor meson, *Phys. Rev. D* 85, 051301 (2012), arXiv: 1110.5194
811. L. Wolfenstein, Parametrization of the Kobayashi-Maskawa matrix, *Phys. Rev. Lett.* 51, 1945 (1983)
812. Heavy Flavor Averaging Group, Y. Amhis, et al., Averages of *b*-hadron, *c*-hadron, and τ-lepton properties as of 2018, *Eur. Phys. J. C* 81, 226 (2021), arXiv: 1909.12524, updated results and plots available at https://hflav.web.cern.ch
813. LHCb Collaboration, R. Aaij, et al., Measurement of CP violation in $B^0 \to J/\psi K^0_S$ decays, *Phys. Rev. Lett.* 115, 031601 (2015), arXiv: 1503.07089
814. LHCb Collaboration, R. Aaij, et al., Measurement of CP violation in $B^0 \to J/\psi K^0_S$ and $B^0 \to \psi(2S)K^0_S$ decays, *J. High Energy Phys.* 11, 170 (2017), arXiv: 1709.03944
815. BaBar Collaboration, B. Aubert, et al., Measurement of time-dependent *CP* asymmetry in $B^0 \to c\bar{c}K^{(*)0}$ Decays, *Phys. Rev. D* 79, 072009 (2009), arXiv: 0902.1708
816. Belle Collaboration, I. Adachi, et al., Precise measurement of the *CP* violation parameter $\sin(2\phi_1)$ in $B^0 \to (c\bar{c})K^0$ decays, *Phys. Rev. Lett.* 108, 171802 (2012), arXiv: 1201.4643
817. M. Ciuchini, M. Pierini, and L. Silvestrini, Effect of penguin operators in the $B^0 \to J/\psi K^0$ *CP* asymmetry, *Phys. Rev. Lett.* 95, 221804 (2005), arXiv: hep-ph/0507290
818. BaBar, Belle Collaboration, I. Adachi, et al., First evidence for $\cos(2\beta) > 0$ and resolution of the Cabibbo–Kobayashi–Maskawa quark-mixing unitarity triangle ambiguity, *Phys. Rev. Lett.* 121, 261801 (2018), arXiv: 1804.06152
819. BaBar, Belle Collaboration, I. Adachi, et al., Measurement of $\cos(2\beta)$ in $B^0 \to D^{(*)}h^0$ with $D \to K_S^0\pi^+\pi^-$ decays by a combined time-dependent Dalitz plot analysis of BaBar and Belle data, *Phys. Rev. D* 98, 112012 (2018), arXiv: 1804.06153
820. CKMfitter Group, J. Charles, et al., Current status of the standard model CKM fit and constraints on $\Delta F = 2$ new physics, *Phys. Rev. D* 91, 073007 (2015), arXiv: 1501.05013, updated results and plots available at http://ckmfitter.in2p3.fr/
821. LHCb Collaboration, R. Aaij, et al., Updated measurement of time-dependent *CP*-violating observables in $B_s^0 \to J/\psi K^+K^-$ decays, *Eur. Phys. J. C* 79, 706 (2019), Erratum: *Eur. Phys. J. C* 80, 601 (2020), arXiv: 1906.08356
822. LHCb Collaboration, R. Aaij, et al., Measurement of the CP-violating phase ϕ_s from $B_s^0 \to J/\psi\pi^+\pi^-$ decays in 13 TeV *pp* collisions, *Phys. Lett. B* 797, 134789 (2019), arXiv: 1903.05530
823. LHCb Collaboration, R. Aaij, et al., Resonances and

CP-violation in $B^0{}_s$ and $\overline{B}^0{}_s \to J/\psi K^+K^-$ decays in the mass region above the $\phi(1020)$, *J. High Energy Phys.* 08, 037 (2017), arXiv: 1704.08217

824. LHCb Collaboration, R. Aaij, et al., Measurement of the *CP* violating phase and decay-width difference in $B_s{}^0 \to \psi(2S)\phi$ decays, *Phys.* Lett. B 762, 253 (2016), arXiv: 1608.04855
825. LHCb Collaboration, R. Aaij, et al., Measurement of the *CP*-violating phase ϕ_s in $\overline{B}_s^0 \to D_s^+ D_s^-$ decays, *Phys. Rev. Lett.* 113, 211801 (2014), arXiv: 1409.4619
826. LHCb Collaboration, R. Aaij, et al., First measurement of the *CP*-violating phase in $B_s^0 \to J/\psi(e^+e^-)\phi$ decays, arXiv: 2105.14738 (2021)
827. ATLAS Collaboration, G. Aad, et al., Measurement of the *CP*-violating phase ϕ_s in $B_s^0 \to J/\psi\phi$ decays in ATLAS at 13 TeV, *Eur. Phys. J. C* 81, 342(2021), arXiv: 2001.07115
828. CMS Collaboration, A. M. Sirunyan, et al., Measurement of the *CP*-violating phase ϕ_s in the $B_s^0 \to J/\psi\phi(1020) \to \mu^+\mu^- K^+K^-$ channel in proton–proton collisions at $\sqrt{s} =$ 13 TeV, *Phys. Lett. B* 816, 136188 (2021), arXiv: 2007.02434
829. X. Liu, W. Wang, and Y. Xie, Penguin pollution in $B \to J/\psi V$ decays and impact on the extraction of the B_s–$\overline{B}_s^0$ mixing phase, *Phys. Rev. D* 89, 094010 (2014), arXiv: 1309.0313
830. S. Faller, M. Jung, R. Fleischer, and T. Mannel, The golden modes $B^0 \to J/\psi K_{S,L}$ in the era of precision flavour physics, *Phys. Rev. D* 79, 014030 (2009), arXiv: 0809.0842
831. H. Nagahiro, L. Roca, A. Hosaka, and E. Oset, Hidden gauge formalism for the radiative decays of axial-vector mesons, *Phys. Rev. D* 79, 014015 (2009), arXiv: 0809.0943
832. K. De Bruyn, R. Fleischer, and P. Koppenburg, Extracting γ and penguin topologies through CP violation in $B_s^0 \to J/\psi K_S^0$, *Eur. Phys. J. C* 70, 1025 (2010), arXiv: 1010.0089
833. M. Jung, Determining weak phases from $B \to J/\psi P$ decays, *Phys. Rev. D* 86, 053008 (2012), arXiv: 1206.2050
834. K. De Bruyn and R. Fleischer, A roadmap to control penguin effects in $B_d^0 \to J/\psi K_S^0$ and $B_s^0 \to J/\psi\phi$, *J. High Energy Phys.* 03, 145 (2015), arXiv: 1412.6834
835. P. Frings, U. Nierste, and M. Wiebusch, Penguin contributions to *CP* phases in $B_{d,s}$ decays to charmonium, *Phys. Rev. Lett.* 115, 061802 (2015), arXiv: 1503.00859
836. M. Z. Barel, K. De Bruyn, R. Fleischer, and E. Malami, In pursuit of new physics with $B_d^0 \to J/\psi K^0$ and $B_s^0 \to J/\psi\phi$ decays at the high-precision frontier, *J. Phys. G* 48, 065002 (2021), arXiv: 2010.14423
837. LHCb Collaboration, R. Aaij, et al., Measurement of the *CP*-violating phase β in $\overline{B}^0 \to J/\psi\pi^+\pi^-$ decays and limits on penguin effects, *Phys. Lett. B* 742, 38 (2015), arXiv: 1411.1634
838. LHCb Collaboration, R. Aaij, et al., Measurement of *CP* violation parameters and polarisation fractions in $B_s^0 \to J/\psi\overline{K}^{*0}$ decays, *J. High Energy Phys.* 11, 082 (2015), arXiv: 1509.00400
839. LHCb Collaboration, R. Aaij, et al., Measurement of *CP* violation in the $B_s^0 \to \phi\phi$ decay and search for the $B^0 \to \phi\phi$ decay, *J. High Energy Phys.* 12, 155 (2019), arXiv: 1907.10003.
840. LHCb Collaboration, R. Aaij, et al., First measurement of the *CP*-violating phase ϕ_s^d in $B_s^0 \to (K^+\pi^-)(K^-\pi^+)$ decays, *J. High Energy Phys.* 03, 140 (2018), arXiv: 1712.08683
841. H.-n. Li, Y.-L. Shen, and Y.-M. Wang, Next-to-leading-order corrections to $B \to \pi$ form factors in kT factorization, *Phys. Rev. D* 85, 074004 (2012), arXiv: 1201.5066
842. Y.-M. Wang and Y.-L. Shen, QCD corrections to $B \to \pi$ form factors from light-cone sum rules, *Nucl. Phys. B* 898, 563 (2015), arXiv: 1506.00667
843. Y.-M. Wang, Y.-B. Wei, Y.-L. Shen, and C.-D. Lü, Perturbative corrections to $B \to D$ form factors in QCD, *JHEP* 06, 062 (2017), arXiv: 1701.06810
844. C.-D. Lü, Y.-L. Shen, Y.-M. Wang, and Y.-B. Wei, QCD calculations of $B \to \pi$, K form factors with higher-twist corrections, *J. High Energy Phys.* 01, 024 (2019), arXiv: 1810.00819
845. A. Khodjamirian, C. Klein, T. Mannel, and Y.-M. Wang, Form factors and strong couplings of heavy baryons from QCD light-cone sum rules, *J. High Energy Phys.* 09, 106 (2011), arXiv: 1108.2971
846. CKMfitter group, J. Charles, et al., *CP* violation and the CKM matrix: Assessing the impact of the asymmetric B factories, *Eur. Phys. J. C* 41, 1 (2005), arXiv: hep-ph/0406184
847. LHCb Collaboration, R. Aaij, et al., Determination of the quark coupling strength $|V_{ub}|$ using baryonic decays, *Nat. Phys.* 11, 743 (2015), arXiv: 1504.01568
848. BESIII Collaboration, M. Ablikim, et al., Measurements of absolute hadronic branching fractions of Λ_c^+ baryon, *Phys. Rev. Lett.* 116, 052001 (2016), arXiv: 1511.08380
849. LHCb Collaboration, R. Aaij, et al., First observation of the decay $B_s^0 \to K^-\mu^+\nu_\mu$ and measurement of $|V_{ub}| / |V_{cb}|$, *Phys. Rev. Lett.* 126, 081804 (2021), arXiv: 2012.05143
850. LHCb Collaboration, R. Aaij, et al., Measurement of $|Vcb|$ with $B^0 \to D(*)s^-\mu^+\nu$ decays, *Phys.* Rev. D 101, 072004 (2020), arXiv: 2001.03225
851. I. Caprini, L. Lellouch, and M. Neubert, Dispersive bounds on the shape of $B \to D^{(*)}\ell\nu$ form factors, *Nucl. Phys. B* 530, 153 (1998), arXiv: hep-ph/9712417
852. C. G. Boyd, B. Grinstein, and R. F. Lebed, Constraints on form factors for exclusive semileptonic heavy to light meson decays, *Phys. Rev. Lett.* 74, 4603 (1995), arXiv: hep-ph/9412324
853. C. G. Boyd, B. Grinstein, and R. F. Lebed, Precision corrections to dispersive bounds on form factors, *Phys. Rev. D* 56, 6895 (1997), arXiv: hep-ph/9705252
854. LHCb Collaboration, R. Aaij, et al., A precise measurement of the B^0 meson oscillation frequency, *Eur. Phys. J. C* 76, 412 (2016), arXiv: 1604.03475
855. LHCb Collaboration, R. Aaij, et al., Precise determination of the B_s^0–$\overline{B}_s^0$ oscillation frequency, *Nat. Phys.* 18, 1 (2022), arXiv: 2104.04421
856. Flavour Lattice Averaging Group, S. Aoki, et al., FLAG review 2019, *Eur. Phys. J. C* 80, 113 (2020), arXiv: 1902.08191

857. A. J. Buras, M. E. Lautenbacher, and G. Ostermaier, Waiting for the top quark mass, $K^+ \to \pi^+ v\bar{v}$, B_s^0–$\overline{B}_s^0$ mixing and *CP* asymmetries in *B*-decays, *Phys. Rev. D* 50, 3433 (1994), arXiv: hep-ph/9403384
858. BaBar Collaboration, B. Aubert, et al., Evidence for D^0–$\overline{D}^0$ mixing, *Phys. Rev. Lett.* 98, 211802 (2007), arXiv: hep-ex/0703020
859. BELLE Collaboration, M. Staric, et al., Evidence for D^0–$\overline{D}^0$ mixing, *Phys. Rev. Lett.* 98, 211803 (2007), arXiv: hep-ex/0703036
860. CDF Collaboration, T. Aaltonen, et al., Evidence for D^0–$\overline{D}^0$ mixing using the CDF II detector, *Phys. Rev. Lett.* 100, 121802 (2008), arXiv: 0712.1567
861. BaBar Collaboration, B. Aubert, et al., Measurement of D^0–$\overline{D}^0$ mixing from a time-dependent amplitude analysis of $D^0 \to K^+\pi^-\pi^0$ decays, *Phys. Rev. Lett.* 103, 211801 (2009), arXiv: 0807.4544
862. BaBar Collaboration, B. Aubert et al., Measurement of D^0–$\overline{D}^0$ mixing using the ratio of lifetimes for the decays $D^0 \to K^-\pi^+$ and K^+K^-, *Phys. Rev. D* 80, 071103 (2009), arXiv: 0908.0761
863. LHCb Collaboration, R. Aaij, et al., Observation of D^0–$\overline{D}^0$ oscillations, *Phys. Rev. Lett.* 110, 101802 (2013), arXiv: 1211.1230
864. S. Bianco, F. L. Fabbri, D. Benson, and I. Bigi, A Cicerone for the physics of charm, *Riv. Nuovo Cim.* 26, 1 (2003), arXiv: hep-ex/0309021
865. LHCb Collaboration, R. Aaij, et al., Measurement of D^0–$\overline{D}^0$ mixing parameters and search for *CP* violation using $D^0 \to K^+\pi^-$ decays, *Phys. Rev. Lett.* 111, 251801 (2013), arXiv: 1309.6534
866. LHCb Collaboration, R. Aaij, et al., Measurements of charm mixing and *CP* violation using $D^0 \to K^\pm\pi^\mp$ decays, *Phys. Rev. D* 95, 052004 (2017), Erratum: *Phys. Rev.* D 96, 099907 (2017), arXiv: 1611.06143
867. LHCb Collaboration, R. Aaij, et al., Updated determination of D^0–$\overline{D}^0$ mixing and *CP* violation parameters with $D^0 \to K^+\pi^-$ decays, *Phys. Rev. D* 97, 031101 (2018), arXiv: 1712.03220
868. LHCb Collaboration, R. Aaij et al., Model-independent measurement of mixing parameters in $D^0 \to K_S^0\pi^+\pi^-$ decays, *J. High Energy Phys.* 04, 033 (2016), arXiv: 1510.01664
869. LHCb Collaboration, R. Aaij, et al., Measurement of the mass difference between neutral charm-meson eigenstates, *Phys. Rev. Lett.* 122, 231802 (2019), arXiv: 1903.03074
870. LHCb Collaboration, R. Aaij, et al., Observation of the mass difference between neutral charm-meson eigenstates, *Phys. Rev. Lett.* 127, 111801 (2021), arXiv: 2106.03744
871. LHCb Collaboration, R. Aaij, et al., Measurement of *CP* asymmetry in $D^0 \to K^-K^+$ and $D^0 \to \pi^-\pi^+$ decays, *J. High Energy Phys.* 07, 041 (2014), arXiv: 1405.2797
872. LHCb Collaboration, R. Aaij, et al., Measurement of the difference of time-integrated *CP* asymmetries in $D^0 \to K^-K^+$ and $D^0 \to \pi^-\pi^+$ decays, *Phys. Rev. Lett.* 116, 191601 (2016), arXiv: 1602.03160
873. LHCb Collaboration, R. Aaij, et al., Measurement of the charm-mixing parameter y_{CP}, *Phys. Rev. Lett.* 122, 011802 (2019), arXiv: 1810.06874
874. LHCb Collaboration, R. Aaij, et al., Measurement of indirect *CP* asymmetries in $D^0 \to K^-K^+$ and $D^0 \to \pi^-\pi^+$ decays using semileptonic *B* decays, *J. High Energy Phys.* 04, 043 (2015), arXiv: 1501.06777
875. LHCb Collaboration, R. Aaij, et al., Measurement of the *CP* violation parameter A_Γ in $D^0 \to K^+K^-$ and $D^0 \to \pi^+\pi^-$ decays, *Phys. Rev. Lett.* 118, 261803 (2017), arXiv: 1702.06490
876. LHCb Collaboration, R. Aaij, et al., Updated measurement of decay-time-dependent *CP* asymmetries in $D^0 \to K^+K^-$ and $D^0 \to \pi^+\pi^-$ decays, *Phys. Rev. D* 101, 012005 (2020), arXiv: 1911.01114
877. LHCb Collaboration, R. Aaij, et al., Search for time-dependent CP violation in $D^0 \to K^+K^-$ and $D^0 \to \pi^+\pi^-$ decays, *Phys. Rev. D* 104, 072010 (2021), arXiv: 2105.09889
878. LHCb Collaboration, R. Aaij, et al., First observation of $D^0 \to \overline{D}^0$ oscillations in $D^0 \to K^+\pi^+\pi^-\pi^-$decays and a measurement of the associated coherence parameters, *Phys. Rev. Lett.* 116, 241801 (2016), arXiv: 1602.07224
879. LHCb Collaboration, R. Aaij, et al., Evidence for *CP* violation in time-integrated $D^0 \to h^-h^+$ decay rates, *Phys. Rev. Lett.* 108, 111602 (2012), arXiv: 1112.0938
880. LHCb Collaboration, R. Aaij, et al., Search for direct *CP* violation in $D^0 \to h^-h^+$ modes using semileptonic *B* decays, *Phys. Lett. B* 723, 33 (2013), arXiv: 1303.2614
881. LHCb Collaboration, R. Aaij, et al., Search for *CP* violation in $D^+ \to \phi\pi^+$ and $D_s^+ \to K_S^0\pi^+$ decays, *J. High Energy Phys.* 06, 112 (2013), arXiv: 1303.4906
882. LHCb Collaboration, R. Aaij et al., Search for *CP* violation in $D^\pm \to K_S^0K^\pm$ and $D_s^\pm \to K_S^0\pi^\pm$ decays, *J. High Energy Phys.* 10, 025 (2014), arXiv: 1406.2624
883. LHCb Collaboration, R. Aaij, et al., Measurement of the time-integrated *CP* asymmetry in $D^0 \to K_S^0K_S^0$ decays, *J. High Energy Phys.* 10, 055 (2015), arXiv: 1508.06087
884. LHCb Collaboration, R. Aaij, et al., Measurement of *CP* asymmetries in $D^\pm \to \eta'\pi^\pm$ and $D_s^\pm \to \eta'\pi^\pm$ decays, *Phys. Lett. B* 771, 21 (2017), arXiv: 1701.01871
885. LHCb Collaboration, R. Aaij, et al., Measurement of the time-integrated *CP* asymmetry in $D^0 \to K_S^0K_S^0$ decays, *J. High Energy Phys.* 11, 048 (2018), arXiv: 1806.01642
886. LHCb Collaboration, R. Aaij, et al., Search for *CP* violation in $D_s^+ \to K_S^0\pi^+$, $D^+ \to K_S^0K^+$ and $D^+ \to \phi\pi^+$ decays, *Phys. Rev. Lett.* 122, 191803 (2019), arXiv: 1903.01150
887. LHCb Collaboration, R. Aaij, et al., Measurement of *CP* asymmetry in $D^0 \to K_S^0K_S^0$ decays, *Phys. Rev. D* 104, L031102 (2021), arXiv: 2105.01565
888. LHCb Collaboration, R. Aaij, et al., Search for *CP* violation in $D_{(s)}^+ \to h^+\pi^0$ and $D_{(s)}^+ \to h^+\eta$ decays, *J. High Energy Phys.* 06, 019 (2021), arXiv: 2103.11058
889. LHCb Collaboration, R. Aaij, et al., Measurement of *CP* asymmetries in $D_{(s)}^+ \to \eta'\pi^+$ and $D_{(s)}^+ \to \eta'\pi^+$ decays, arXiv: 2204.12228 (to be published in *J. High Energy Phys.*)
890. LHCb Collaboration, R. Aaij, et al., Measurement of the time-integrated *CP* asymmetry in $D^0 \to K^-K^+$ decays, arXiv: 2209.03179 (submitted to *Phys. Rev. Lett.)*

891. LHCb Collaboration, R. Aaij, et al., Search for *CP* violation through an amplitude analysis of $D^0 \to K^+K^-\pi^+\pi^-$ decays, *J. High Energy Phys.* 02, 126 (2019), arXiv: 1811.08304
892. LHCb Collaboration, R. Aaij, et al., Search for *CP* violation in $D^+ \to K^-K^+\pi^+$ decays, *Phys. Rev. D* 84, 112008 (2011), arXiv: 1110.3970
893. LHCb Collaboration, R. Aaij, et al., Model-independent search for *CP* violation in $D^0 \to K^-K^+\pi^+\pi^-$ and $D^0 \to \pi^-\pi^+\pi^-\pi^+$ decays, *Phys. Lett. B* 726, 623 (2013), arXiv: 1308.3189
894. LHCb Collaboration, R. Aaij, et al., Search for *CP* violation in the decay $D^+ \to \pi^-\pi^+\pi^+$, *Phys. Lett. B* 728, 585 (2014), arXiv: 1310.7953
895. LHCb Collaboration, R. Aaij, et al., Search for *CP* violation using *T*-odd correlations in $D^0 \to K^+K^-\pi^+\pi^-$ decays, *J. High Energy Phys.* 10, 005 (2014), arXiv: 1408.1299
896. LHCb Collaboration, R. Aaij, et al., Search for *CP* violation in $\Xi_c^+ \to pK^-\pi^+$ decays with model-independent techniques, *Eur. Phys. J. C* 80, 986 (2020), arXiv: 2006.03145
897. LHCb Collaboration, R. Aaij, et al., Search for *CP* violation in $D^0 \to \pi^-\pi^+\pi^0$ decays with the energy test, *Phys. Lett. B* 740, 158 (2015), arXiv: 1410.4170
898. LHCb Collaboration, R. Aaij, et al., Search for *CP* violation in the phase space of $D^0 \to \pi^+\pi^-\pi^+\pi^-$decays, *Phys. Lett. B* 769, 345 (2017), arXiv: 1612.03207
899. M. Williams, Observing *CP* violation in many-body decays, *Phys. Rev. D* 84, 054015 (2011), arXiv: 1105.5338
900. C. Parkes, et al., On model-independent searches for direct *CP* violation in multi-body decays, *J. Phys. G* 44, 085001 (2017), arXiv: 1612.04705
901. LHCb Collaboration, R. Aaij, et al., Search for *CP* violation in $\Lambda_c^+ \to pK^-K^+$ and $\Lambda_c^+ \to p\pi^-\pi^+$decays, *J. High Energy Phys.* 03, 182 (2018), arXiv: 1712.07051
902. LHCb Collaboration, R. Aaij, et al., Measurement of mixing and *CP* violation parameters in two-body charm decays, *J. High Energy Phys.* 04, 129 (2012), arXiv: 1112.4698
903. LHCb Collaboration, R. Aaij, et al., Measurements of indirect *CP* asymmetries in $D^0 \to K^-K^+$ and $D^0 \to \pi^-\pi^+$ decays, *Phys. Rev. Lett.* 112, 041801 (2014), arXiv: 1310.7201
904. LHCb Collaboration, R. Aaij, et al., Measurement of the charm mixing parameter $y_{\rm CP}$–$y_{CP}^{K\pi}$ using two-body D^0 meson decays, *Phys. Rev. D* 105, 092013 (2022), arXiv: 2202.09106
905. T. Pajero and M. J. Morello, Mixing and CP violation in $D^0 \to K^-\pi^+$ decays, *J. High Energy Phys.* 03, 162 (2022), arXiv: 2106.02014
906. LHCb Collaboration, Framework TDR for the LHCb Upgrade: Technical Design Report, CERN-LHCC-2012-007, 2012
907. O. Aberle, et al., High-Luminosity Large Hadron Collider (HL-LHC): Technical design report, *CERN* Yellow Reports: Monographs, CERN, Geneva, 10 (2020)
908. LHCb Collaboration, Expression of Interest for a Phase-II LHCb Upgrade: Opportunities in flavour physics, and beyond, in the HL-LHC era, CERN-LHCC-2017-003, 2017
909. S. Hashimoto, et al., Letter of intent for KEK super B factory KEK-REPORT-2004-4, 2004
910. Y. Ohnishi, et al., Accelerator design at SuperKEKB, *Prog. Theor. Exp. Phys.* 2013, 03A011 (2013)
911. CEPC Study Group, M. Dong, et al., CEPC Conceptual Design Report: Volume 2, Physics & Detector, arXiv: 1811.10545 (2018)
912. FCC Collaboration, A. Abada, et al., FCC-ee: The Lepton Collider: Future Circular Collider Conceptual Design Report Volume 2, *Eur. Phys. J. ST* 228, 261 (2019)
913. BESIII Collaboration, M. Ablikim, et al., Design and construction of the BESIII Detector, *Nucl. Instrum. Meth. A* 614, 345 (2010), arXiv: 0911.4960
914. BESIII Collaboration, M. Ablikim et al., Future physics programme of BESIII, *Chin. Phys. C* 44, 040001 (2020), arXiv: 1912.05983
915. G. Wilkinson, Charming synergies: The role of charm-threshold studies in the search for physics beyond the Standard Model, *Sci. Bull.* 66, 2251 (2021), arXiv: 2107.08414
916. SCTF Collaboration, D. A. Epifanov, Project of super charm-tau factory, *Phys. Atom. Nucl.* 83, 944 (2020)
917. H. P. Peng, Y. H. Zheng, and X. R. Zhou, Super tau-charm facility of China, *Physics* 49, 513 (2020)
918. LHCb Collaboration, LHCb Trigger and Online Upgrade Technical Design Report, CERN-LHCC-2014-016, 2014
919. LHCb Collaboration, LHCb VELO Upgrade Technical Design Report, CERN-LHCC-2013-021, 2013
920. LHCb Collaboration, LHCb Tracker Upgrade Technical Design Report, CERNLHCC-2014-001, 2014
921. LHCb Collaboration, LHCb PID Upgrade Technical Design Report, CERN-LHCC-2013-022, 2013
922. LHCb Collaboration, LHCb Upgrade Software and Computing, CERN-LHCC-2018-007, 2018
923. LHCb Collaboration, Computing Model of the Upgrade LHCb experiment, CERNLHCC-2018-014, 2018
924. LHCb Collaboration, LHCb Upgrade GPU High Level Trigger Technical Design Report, CERN-LHCC-2020-006, 2020
925. LHCb Collaboration, LHCb SMOG Upgrade, CERN-LHCC-2019-005, 2019
926. I. Efthymiopoulos, et al., LHCb Upgrades and operation at 1034 $\rm cm^{-2}{\cdot}s^{-1}$ luminosity — a first study, CERN-ACC-NOTE-2018-0038, 2018
927. LHCb Collaboration, LHCb Framework TDR for the LHCb Upgrade II Opportunities in flavour physics, and beyond, in the HL-LHC era, CERN-LHCC-2021-012, 2022
928. LHCb Collaboration, R. Aaij, et al., and A. Bharucha et al., Implications of LHCb measurements and future prospects, *Eur. Phys. J. C* 73, 2373 (2013), arXiv: 1208.3355
929. LHCb Collaboration, Updated sensitivity projections for the LHCb Upgrade, LHCb-PUB-2013-015, CERN-LHCb-PUB-2013-015, CERN, Geneva, 2013

930. Belle-II Collaboration, W. Altmannshofer, et al., The Belle II physics book, *Prog. Theor. Exp. Phys.* 2019, 123C01 (2019), Erratum: *Prog. Theor. Exp. Phys.* 2020, 029201 (2020), arXiv: 1808.10567
931. LHCb Collaboration, Updated LHCb combination of the CKM angle γ, LHCb- CONF-2020-003, 2020
932. LHCb Collaboration, R. Aaij, et al., Measurement of *CP* violation in $B^0 \to J/\psi K_S^0$ and $B^0 \to \psi(2S)K_S^0$ decays, *J. High Energy Phys.* 11, 170 (2017), arXiv: 1709.03944
933. LHCb Collaboration, R. Aaij *et al.*, Precision measurement of *CP* violation in $B_s^0 \to J/\psi K^+K^-$ decays, *Phys. Rev. Lett.* 114, 041801 (2015), arXiv: 1411.3104
934. ATLAS Collaboration, ATLAS B-physics studies at increased LHC luminosity, potential for CP-violation measurement in the $B_s^0 \to J/\psi\phi$ decay, ATL-PHYS-PUB-2013-010, 2013
935. CMS Collaboration, CP-violation studies at the HL-LHC with CMS using B_s^0 decays to $J/\psi\phi$ (1020), CMS-PAS-FTR-18-041, 2018
936. LHCb Collaboration, R. Aaij et al., Measurement of CP violation in $B_s^0 \to \phi\phi$ decays, *Phys. Rev. D* 90, 052011 (2014), arXiv: 1407.2222
937. CMS Collaboration, ECFA 2016: Prospects for selected standard model measurements with the CMS experiment at the High-Luminosity LHC, CMS-PAS-FTR-16-006, 2017
938. LHCb Collaboration, R. Aaij, et al., Measurement of the CP asymmetry in B_s^0–$\overline{B}_s^0$ mising, *Phys. Rev. Lett.* 117, 061803 (2016), arXiv: 1605.09768
939. CMS Collaboration, B Physics analyses for the Phase-II Upgrade Technical Proposal, CMS-PAS-FTR-14-015, 2015
940. CMS Collaboration, Measurement of rare $B \to \mu^+\mu^-$decays with the Phase-2 upgraded CMS detector at the HL-LHC, CMS-PAS-FTR-18-013, 2018
941. LHCb Collaboration, R. Aaij, et al., Measurement of the ratio of branching fractions $\mathcal{B}(\overline{B}^0 \to D^{*+}\tau^-\overline{\nu}_\tau)/\mathcal{B}(\overline{B}^0 \to D^{*+}\mu^-\overline{\nu}_\mu)$, *Phys. Rev. Lett.* 115, 111803 (2015) Publisher's Note, *Phys. Rev. Lett.* 115, 159901, (2015), arXiv: 1506.08614
942. LHCb Collaboration, R. Aaij, et al., Test of lepton flavor universality by the measurement of the $B^0 \to D^{*-}\tau^+\nu_\tau$ branching fraction using three-prong τ decays, *Phys. Rev. D* 97, 072013 (2018), arXiv: 1711.02505
943. LHCb Collaboration, R. Aaij, et al., Measurement of the ratio of branching fractions $\mathcal{B}(B_c^+ \to J/\psi\tau^+\nu_\tau)/\mathcal{B}(B_c^+ \to J/\psi\mu^+\nu_\mu)$, *Phys. Rev. Lett* 120**,** 121801 (2018), arXiv: 1711.05623